Sustainable way of producing biodiesel using oleaginous *Tetradesmus obliquus* KMC24

A Thesis

Submitted in Partial Fulfillment of the Requirements for the Degree of

DOCTOR OF PHILOSOPHY

by

Madonna Roy

(156151002)

School of Energy Science and Engineering

Indian Institute of Technology Guwahati

Guwahati - 781039, Assam (India)

January-2022

This thesis is dedicated to my Parents who have inspired me and made me strong enough to achieve my goal

SCHOOL OF ENERGY SCIENCE AND ENGINEERING

INDIAN INSTITUTE OF TECHNOLOGY GUWAHATI

STATEMENT

I do hereby declare that the content embodied in this thesis entitled "***Sustainable way of producing biodiesel using oleaginous Tetradesmus obliquus KMC24***" is the result of investigations carried out by me at the School of Energy Science and Engineering, Indian Institute of Technology Guwahati, Guwahati, India, under the guidance of **Prof. Kaustubha Mohanty**.

In keeping with the general practice of reporting scientific observations, due acknowledgements have been made wherever the work described is based on the findings of other investigators.

January, 2022 **Madonna Roy**

SCHOOL OF ENERGY SCIENCE AND ENGINEERING

INDIAN INSTITUTE OF TECHNOLOGY GUWAHATI

CERTIFICATE

This is to certify that **Miss Madonna Roy** has been working under my supervision since July 2015. I hereby forward her thesis entitled **"*Sustainable way of producing biodiesel using oleaginous Tetradesmus obliquus KMC24*"** to be submitted for the award of the degree of Doctor of Philosophy to IIT Guwahati. I certify that she has fulfilled all the requirements according to the rules of this institute and the investigations embodied in her thesis have not been submitted elsewhere for a degree or diploma.

Date:

IIT Guwahati

Dr. Kaustubha Mohanty

Professor of Chemical Engineering and Head,

School of Energy Science and Engineering,

Indian Institute of Technology Guwahati

Acknowledgement

I would like to take this opportunity to express my heart-felt gratitude to them, whose contribution has made this thesis possible. With immense gratitude, I would like to acknowledge my thesis supervisor Prof. Kaustubha Mohanty for mentoring me throughout this research period and helping me explore and understand the fascinating field of science and technology with innovative ideas. His esteemed guidance, advice, and encouragement at every step have enabled me to propel my research in a fruitful direction. I would also like to thank him for providing a well-equipped laboratory, vast resources, and dedicated work culture that has enabled my working in his laboratory a pleasant experience. Thank you so much, Sir.

I will always be obliged to my doctoral committee members, Prof. Kannan Pakshirajan, Prof. Vishal Trivedi, and Dr. Prabu Vairakannu, for their insightful advice and suggestions throughout the research. I would like to thank the former and present Heads for School of Energy Science and Engineering, Prof. Pranab Goswami, Prof. Vijay S. Moholkar, and Prof. Kaustubha Mohanty, for providing me with all the necessary facilities.

I would also like to thank Dr. Pankaj Kalita, Dr. Lepakshi Barbora, and all the staff members of School of Energy Science and Engineering for their incessant motivation and support. I am thankful to School of Energy Science and Engineering, Department of Biosciences and Bioengineering, Department of Chemical Engineering, Central Instruments Facility (IIT Guwahati), Department of Civil Engineering and Biotech Park for providing with the instrumental facilities. I would like to gratefully acknowledge Ministry of Human Resource Development (MHRD) for providing fellowship.

I am indebted to the selfless help and co-operation of my research group members Dr. Himadri Sahu, Dr. Sanjukta Bhoi, Dr. Madhusmita Dash, Dr. Kulbhushan Samal, Dr. Ranjeet Kumar Mishra, Dr. Rahul Maurya, Dr. Saran Sarangapany, Dr. Sounak Bera, Dr. Sanjeev Mishra, Dr. Bikashbindu Das, Barasa Malakar, Pranab Jyoti Sarma,

Sachankar Buragohain, Munmi Bhattacharya, Deepesh Singh Chohan, Saptaswa Biswas, Ankit Agarwal, Naveenkumar A Yaranal, Aanisha Akhtar, Harsh Vardhan, Om Prakash, Ananya Bardhan, Janaki Komandur, Santosh Kumar Hotta, Pooja Singh, and Anindita Das. I would also like to acknowledge Trishna Anand and Harrison Hihu Muigai, Tasrin Shahnaz, and Heena Kauser for their unconditional help and support.

I cannot find words to express my gratitude towards my friends Anupama, Himali, Susmita, Shashi, Jon, Philip, and Pilik with whom I shared the most precious moments in IIT Guwahati with lots of happiness, laughter, parties, and trips. They always filled my heart with positivity and motivation during challenging phases. I am grateful to my friends Vegonia and Ashim for their constant support and encouragement. Thank you all for making my Ph.D. an unforgettable experience. Last but not the least, I extend my sincere thanks to my best friend for life Sounak for his reassurance in my tough times, and standing by me with a cheerful positive attitude in all the circumstances. My sincere apology goes to them whom I forgot to mention but helped me at any phase of the research work.

No words would suffice to express my deepest sense of gratitude to my parents for their blessings, love, patience, support, trust and inspiration towards the completion of my Ph.D. thesis. My PhD endeavour would not have been possible without them. Above all, I offer my gentle reverence to the Almighty God who made everything possible and feel blessed to have this opportunity of working in one of the esteemed institutes.

Madonna Roy
January 2022

ABSTRACT

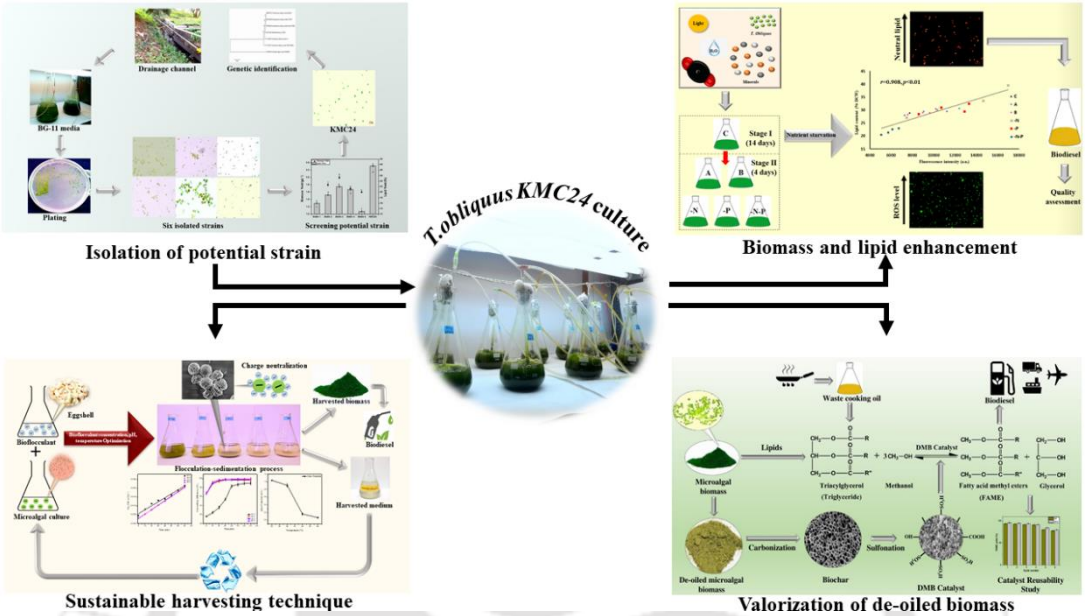

Oleaginous microalgae are deemed as cell bio-factories for biodiesel production. However, the lower biomass and lipid productivity, along with the high cost of downstream processing such as harvesting, lipid extraction and conversion to biodiesel makes microalgae-based biodiesel production system economically unviable. To address this challenge, the present study aims to develop a sustainable biodiesel production system by employing various strategies such as selection of potential microalgal strain, modification of cultivation mode, optimization of culture conditions, development of low-cost harvesting and lipid to biodiesel conversion techniques. In the present study, a novel microalgae, *Tetradesmus obliquus* KMC24 was isolated and exposed to nutrient stress (nitrogen and/or phosphorus) for a short period via two-stage cultivation to obtain maximum biomass and lipid. The effect of nutrient starvation on the morphology, biomass concentration, photosynthetic activity, and biochemical composition of *Tetradesmus obliquus* KMC24 was investigated. Two days nitrogen-starved cells (-N2) were able to accumulate the maximum amount of lipid (39.93 ± 0.44%) without affecting the biomass concentration (2.15 ± 0.04 g L^{-1}). During nitrogen (-N) and phosphorus (-P) starvation, photosynthetically fixed carbon pool was diverted to lipid biosynthesis.

Pearson's correlation analysis suggested that stress-induced lipid accumulation is associated with an increased intracellular reactive oxygen species (ROS) level. The ROS fluorescence intensity was highest in –N2 cultures (17051.49 ± 93.15 a.u.), suggesting highly oxidative stress-tolerant cells. A high degree of fatty acid saturation was obtained under nitrogen starvation as compared to other culture conditions. Biodiesel properties such as cetane number, saponification number, and iodine value were improved under nitrogen starvation.

High-energy requirement for harvesting microalgal biomass poses a major challenge during downstream processing. Addressing this challenge, the present study developed a sustainable and efficient harvesting technique by valorizing waste eggshell. Herein, waste eggshell-derived bioflocculant was used for harvesting *T. obliquus* in a circular bioeconomy approach. It was found that 120 mg L^{-1} bioflocculant can flocculate 98.62 ± 0.43% of *T. obliquus* cells within 25 min at optimal pH 4.0 and temperature 35 °C. The influence of bioflocculant concentration, pH and temperature on zeta potential was evaluated to understand the flocculation mechanism. Microscopic and FESEM-EDX images were analyzed to evaluate the microalgal structural changes. Adsorption mechanism of bioflocculant over the microalgal cells was determined by performing adsorption kinetic studies. Pseudo-second order kinetic model was a suitable fit for the data obtained from the experiments, which indicated chemisorption as the probable mechanism. The spent medium recovered after harvesting process was successfully recycled for subsequent cultivation of *T. obliquus* KMC24, thus reducing the dependency on fresh medium. The FAME composition of the biomass treated with bioflocculant was not altered.

The last study was focused on developing and characterizing low-cost and eco-friendly catalyst for microalgal lipid transesterification to biodiesel. Herein, a novel carbon-based solid acid catalyst was synthesized by carbonization of de-oiled microalgal biomass followed by sulfonation. The effect of catalyst synthesis conditions such as carbonization temperature, sulfonation time, and H_2SO_4 concentration on the surface acidity of the catalyst and free fatty acid conversion was determined. The de-oiled microalgal biomass-based (DMB) solid acid catalyst was predominantly composed of carboxylic, phenolic, and sulfonic

groups as indicated by the FTIR analysis and supported by the XPS analysis. The catalyst was further characterized by various methods to determine its physiochemical properties. A maximum fatty acid methyl ester (FAME) yield of 94.23% for microalgal oil (AO) and 96.25% for waste cooking oil (WCO) was obtained under optimized transesterification conditions. The catalyst exhibited high catalytic activity (FAME yield >90%) until the fourth cycle. Most of the biodiesel properties were within the permissible limit of EN 14,212 and ASTM D6751 standards.

Keywords: Microalgae; Biodiesel; Biorefinery; Circular Bioeconomy; Catalyst

CONTENTS

LIST OF TABLES

LIST OF FIGURES

Abbreviations

ANOVA	Analysis of variance
APX	Ascorbate peroxidase
AO	Microalgal oil
AC	Activated carbon
ASTM	American Society for Testing and Materials
BLAST	Basic local alignment search tool
BET	Brunauer-Emmett-Teller
CAT	Catalyst
CAT	Catalase
CFPP	Cold filter plugging property
CHNS analyzer	Carbon hydrogen nitrogen and sulphur analyzer
CN	Cetane number
Caro	Carotenoid
Chl	Chlorophyll
DCW	Dry cell weight
DU	Degree of unsaturation
DMB	De-oiled microalgal biomass-based
DCFH-DA	2′, 7′-dichlorodihydrofluoresceine diacetate
DMSO	Dimethyl sulfoxide
EDTA	Ethylenediamine tetraacetic acid
ETC	Electron transport chain
ER	Endoplasmic reticulum
EDX	Energy dispersive spectroscopy
EU	European Union
FESEM	Field emission scanning electron microscopic
F_v/F_m	Maximum quantum yield

FW	Fresh weight
FAME	Fatty acid methyl esters
FAEE	Fatty acid ethyl esters
FFA	Free fatty acid
FT-IR	Fourier transform-infrared
GL	Glycolipids
HE	Harvesting efficiency
HV	Highest heating value
H_2O_2	Hydrogen peroxide
IV	Iodine value
LSD	Least significant difference
LCSF	Long-chain saturation factor
ME	Malic enzyme
MUFA	Monounsaturated fatty acid
MDA	Malondialdehyde
NCBI	National center for biotechnology information
NL	Neutral lipids
NADPH	Nicotinamide adenine dinucleotide phosphate
OD	Optical density
OPP	Oxidative pentose phosphate
PBS	Phosphate buffer saline
PS II	Photosystem II
PAM	Pulse amplitude modulated
PL	Phospholipids
PUFA	Polyunsaturated fatty acid
ROS	Reactive oxygen species
SFA	Saturated fatty acid
SV	Saponification value
TAG	Triacylglycerol

TBA	Thiobarbituric acid
TCA	Trichloroacetic acid
TGA	Thermogravimetric analysis
TG	Triglyceride
TPD	Temperature programmed desorption
UFA	Unsaturated fatty acid
WCO	Waste cooking oil
XRD	X-ray diffraction
XPS	X-ray photoelectron spectroscopy

Symbols and Units

g L^{-1}	Gram per liter
µm	Micrometer
g L^{-1} day^{-1}	Gram per liter per day
ΔX	Difference in biomass concentration
Δt	Cultivation period
v/v	Volume/volume
µL	Microliter
mg mL^{-1}	Milligram per milliliter
°C	Degree Celsius
g-force	Gravitational force
min	Minutes
$L_{content}$	Lipid content
W_{lipid}	Lipid weight
W_{sample}	Sample weight
w/v	Weight/volume
mL	Milliliter
h	Hour
µg mL^{-1}	Microgram per milliliter
µM	Micromolar
rpm	Rotation per minute
µmol g^{-1} FW	Micromole per gram of fresh weight
nm	Nanometer
wt.%	Weight percent
mg g^{-1}	Milligram per gram
a.u.	Arbitrary unit
U mg^{-1} protein	Units per milligram of protein

µg g^{-1} FW	Microgram per gram of fresh weight
mm^2 s^{-1}	Square millimeter per second
mg KOH g^{-1}	Quantity of base expressed in milligrams of potassium hydroxide that is required to neutralize the acidic constituents in 1 g of sample
g I_2 100 g^{-1} oil	Grams of iodine absorbed by 100 g of oil
MJ Kg^{-1}	Megajoules per kg
mol L^{-1}	Mole per liter
GW	Gigawatt
µg $mL^{-1}day^{-1}$	Microgram per millilitre per day
mV	Millivolt
ppm	Parts per million
g mg^{-1} min^{-1}	Gram per milligram per minute
K	Kelvin
kJ mol^{-1}	Kilojoule per mole
kJ mol^{-1} K^{-1}	Kilojoule per mole per kelvin
kWh kg^{-1}	Kilowatt hour per kilogram
kg^{-1}	Per kilogram
L^{-1}	Per liter
kWh m^{-3}	Kilowatt hour per cubic meter
g	Gram
mL	Millilitre
°C min^{-1}	Degree Celsius per minute
mL min^{-1}	Millilitre per minute
Å	Angstrom
mmol g^{-1}	Millimole per gram
cm^{-1}	Per centimetre
eV	Electronvolt
m^2 g^{-1}	Meter square per gram

KToe	Kilotonne of oil equivalent

Chapter 1

Introduction

1.1 Current World Energy Scenario

An upsurge in global energy demand is directly reflected in the ever increasing cost of fuels [1]. Moreover, this energy demand must be satiated for technological developments. At present, more than 80% of the global energy needs are met by the combustion of fossil fuels, i.e., oil, natural gas, and coal (Figure 1.1). The industrial and transportation sector consumes more than half of the global energy, whereas the rest is being consumed by residential buildings (21%), non-energy use (9%), commercial and public services (8%), agriculture (2%) and non-specified sectors (2%) (Figure 1.1). The increased use of fossil fuels has further resulted in about 35 Gt global carbon dioxide (CO_2) emission, which has grown at a rate of 2% (British Petroleum (BP) Statistical Review of World Energy 2019). According to the Organisation for Economic Co-operation and Development (OECD) Environmental Outlook to 2050, global greenhouse gas (GHG) emissions are projected to increase by 50%, primarily due to 70% growth in energy-related CO_2 emissions.

According to Energy Statistics India 2021, coal and oil are India's primary energy sources, accounting for 64.20% and 27.99% of total energy supply in 2019-20 (provisional), respectively. Coal production in India was recorded to be 730.87 million tonnes (MT) during 2019-20 (provisional), compared to 728.72 MT during 2018-19, growing at the rate of 0.30%. Similarly, crude oil production was 32.17 MT during 2019-20 (provisional), compared to 34.2 MT in the previous year, which is a fall of 5.95% (Energy Statistics India 2021). In 2019-20 (provisional), final Energy Consumption was 5,87,371 KToe. The industrial sector was the country's largest energy consumer, accounting for more than half of the total final energy consumption, i.e., 55.85%. India being a developing country with more than 1.3 billion population, the consumption of coal and oil in 2017-18 has increased at a Compound Annual Growth Rate (CAGR) of

5.01% (896.34 MT) and 4.59% (251.93 MMT), respectively. Besides, India imported 208.27 MT of coal and 220.43 MTs of crude oil (2017-18) due to a significant depletion of fossil fuel reserves and high ash content in Indian coal. As conventional energy resources cause global warming and are on the verge of extinction, therefore the global energy consumption pattern needs to shift towards renewable energy resources to resolve this energy crisis [2].

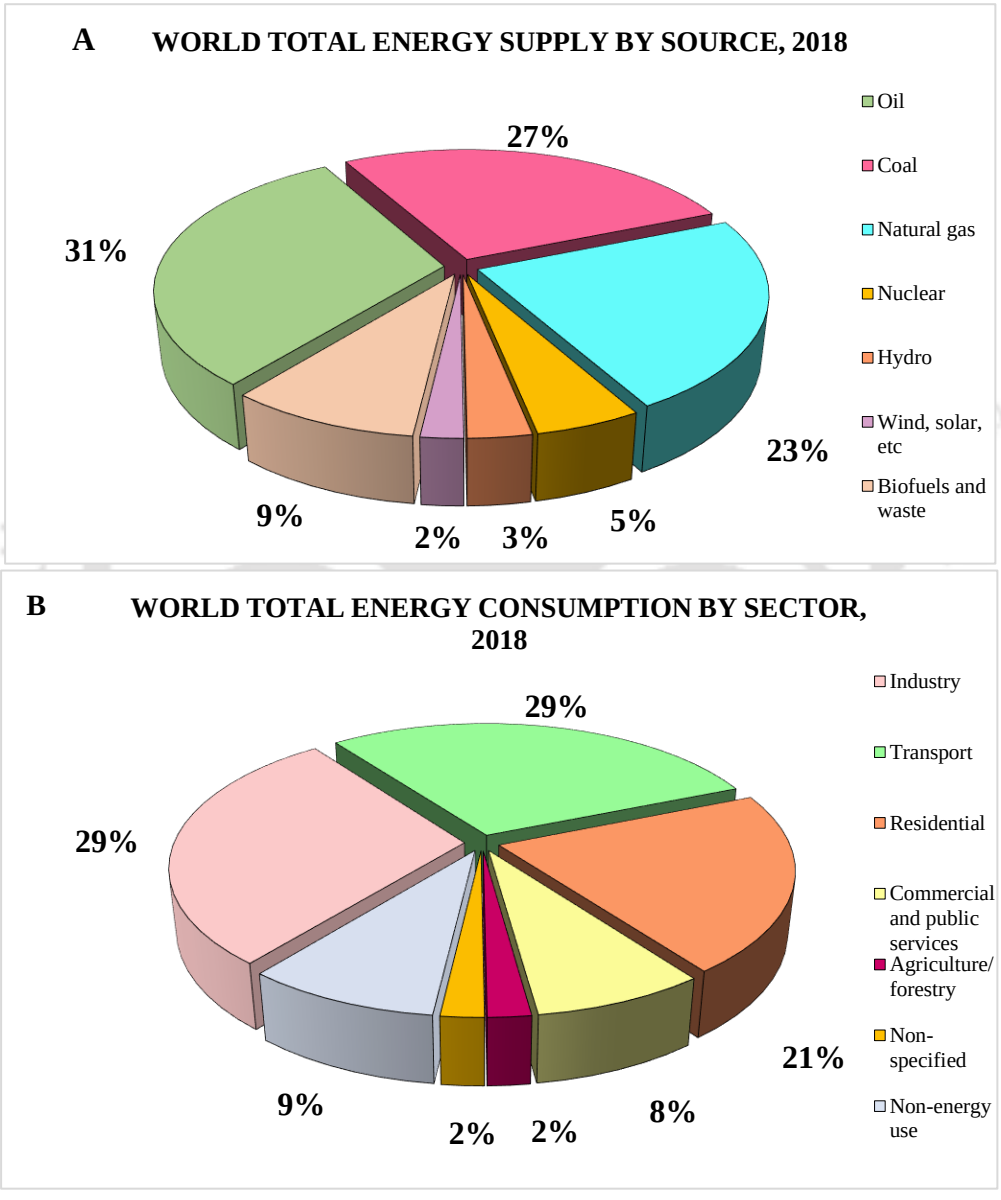

Figure 1.1. Energy scenario in the world by (A) sector and (B) source in 2018 (data source: International Energy agency, 2021).

1.2 Renewable Energy

Sustainable development of the nation necessitates secure access to affordable, reliable, sustainable, and modern energy services while reducing GHG emissions as well as the carbon footprint of the energy sector. Renewable energy is derived from natural resources that are constantly replenished, such as sunlight, wind, hydropower, geothermal, ocean, and biomass [3]. Harvesting energy from renewable resources generates almost zero pollutants and GHG. According to International Renewable Energy Agency (IRENA), in 2020, renewable energy generating capacity increased significantly, outpacing the long-term trend. At the end of 2020, global renewable energy generation capacity increased by 260 GW, amounting to 2799 GW. Solar and wind energy jointly accounted for 91% of all net renewable additions in 2020. The growth in renewable energy is dominated by countries like China and the United States of America (IRENA 2020). China and the United States of America added 136 GW and 29 GW of renewable energy, respectively, in 2020.

According to the Ministry of New and Renewable Energy (MNRE), India has set a target of installing 175 GW of renewable energy by 2022, with 100 GW from solar (Rooftop and utility solar), 60 GW from wind, and 15 GW from remaining renewable energy sources. India has already achieved to install 92.55 GW of renewable energy in January 2021, with wind and hydropower dominating. The goal of the National Energy Policy in 2017 was to cut oil imports by 10% by 2022 compared to the baseline 2014–2015 while reducing emissions by 33%–35% by 2030 compared to the baseline 2005. Currently, biomass-derived transportation fuel meets around 8%–15% of global energy demand [4]. The International Energy Agency (IEA) has set a goal for biofuels to meet more than a quarter of the world's transportation fuel demand by 2050 to reduce our dependence on petroleum and coal. In India, diesel is predominantly used for transportation and industrial applications as compared to gasoline. Hence, to reduce the dominating consumption of diesel, biomass derived biodiesel has emerged as a remarkable fuel.

1.3 Biodiesel

Rudolf Diesel first used vegetable oil as engine fuel in 1900 [5]. It, however, triggered the problems of cold-weather starting, injector coking, gumming of injectors,

lines, and filters, engine knocking, etc., due to its high viscosity and low volatility. Transesterification of vegetable oil with alcohol has emerged as a promising process for overcoming these problems. This process produces fatty acid alkyl esters with glycerol as a co-product. These alkyl esters display diesel-like fuel properties, commonly known as biodiesel. Biodiesel, also known as "green diesel", further reduces the emission of CO, CH_4, and particulate matter compared to diesel [6]. The methyl and ethyl esters of fatty acids are quite commonly known as biodiesel. The ethyl ester has a lower cloud/pour point, higher oxidative stability, better lubricity, and higher cetane number compared to methyl ester. However, methanol is cheaper than ethanol and can be easily separated from the reaction mixture. Methanol is thus widely used in this process.

Biodiesel is the only alternative biofuel that can be used alone or blended with petroleum diesel in different concentrations for a conventional engine without any further modification [7]. The B20 blend comprising of biodiesel and petroleum diesel in the ratio of 20:80 is widely used around the world. The B20 blend is implemented in nearly all diesel-fueled equipment as it represents a good balance of cost, emissions, cold-weather performance, and materials compatibility [8]. Biodiesel quality specifications are dynamic, and so they are periodically reviewed by organizations such as the European Committee of Standardization, the International Organization for the Standardization (ISO), and the American Society for Testing and Materials (ASTM).

Owing to its numerous advantages, the global consumption of biodiesel had increased from 0.25 billion gallons in 2006 to ~2.0 billion gallons in 2018, and the trend has been projected to be linear in the future years [9]. India produced 190 million litres of biodiesel in the year 2019, with installed production capacity varying between 11 million litres to 280 million litres [10]. According to U.S. Energy Information Administration, in 2019, the United States produced about 41 million barrels (1.7 billion gallons) of pure biodiesel, imported about 4 million barrels (168 million gallons), exported about 2.7 million barrels (114 million gallons), and consumed about 43 million barrels (1.8 billion gallons) nearly all as blends with petroleum diesel.

1.3.1 Classification of biodiesel feedstock

Biodiesel is produced from natural and organic resources. The selection of biodiesel feedstock is region-specific since agricultural activities and climatic conditions in different countries provide wide-ranging potential feedstock for biodiesel production [11]. Around 75% of the biodiesel production cost is contributed by the feedstock cost alone [12]. Therefore, the selection of a potential feedstock is necessary for the reduction of overall biodiesel production cost. The potential biodiesel feedstock available in major countries is shown in Figure 1.2. Biodiesel feedstock is broadly classified as first, second, and third generation feedstocks [13].

Initially (in 1930) biodiesel was produced from food crops [14]. Thus, feedstock for biodiesel extracted from food crops such as rapeseed, palm, sunflower, corn, sugar beet, wheat and soybean are considered as first generation feedstocks. However, the extensive use of first generation feedstocks resulted in food-versus-fuel conflicts and also disturbed the agricultural farmland allocation [15]. In Malaysia, the cost of edible palm oil was increased by 70% because of its wide application in biodiesel production [12]. According to Worldometer statistics till February 21, 2021, and the GHI index report, India has a population of 1.38 billion and ranks 94th out of 107 nations in terms of global hunger index (GHI). Therefore, first generation feedstock is not feasible in the Indian context to address the food-versus-fuel conflicts. Thus, to mitigate the problems associated with first generation feedstocks, second generation feedstocks were explored. Non-edible oils with higher free fatty acids substituted edible oils for biodiesel production and are considered as second generation feedstock. Non-edible oils derived from waste cooking oil, non-edible plant oil, grease, and waste animal fats are explored as second generation feedstock for biodiesel production [16]. South Asia has non-edible oilplants of more than 300 species. India has a rich source of non-edible oils (approximately 1 million tons per year). The government of India has identified *Pongamia pinnata* (karanja) and *Jatropha curcas* oils (JCO) as the most promising feedstocks for biodiesel [12]. The emphasis then shifted to third generation feedstocks, i.e., micro- and macroalgae in order to minimize the potential shortage of land and fodder.

Figure 1.2. Potential biodiesel feedstocks in major countries (data source: Alagumalai et al., 2021).

1.3.2 Microalgae as 3rd generation biodiesel feedstock

Microalgae are unicellular photosynthetic microorganisms that grow very fast and has a thirst for carbon dioxide. Microalgae are naturally found in fresh water and marine environment. Microalgae have more than 300,000 species, with a diversity far greater than plants [17]. The three key elements required for microalgal growth are the light source (obtained from the sun), nutrients (mainly nitrogen, phosphorus, and trace metals), and a carbon source (derived from CO_2) [18]. Microalgae are generally more efficient converters of solar energy compared to higher plants. Research on microalgae as a feedstock for biodiesel production continues to increase because of the inherent advantages it holds over other traditional feedstock. From a bioenergy perspective, microalgae possess the potential to generate a considerable amount of oil per acre as compared to other biofuel feedstock. Moreover, microalgal biomass being rich in biochemical composition favors the production of a broad spectrum of marketable value-added products. The presence of triglycerides in microalgal lipids favors biodiesel production [19]. Following are some of the advantages of microalgae that validate its potential as a third generation biodiesel feedstock:

- The oil production rate of microalgae is between 60,000-240,000 L/hectare/year, which is much higher than that of other oil producing feedstocks [17]. Generally, the total lipid content of microalgae ranges from 20% to 80% dry cell weight [20].
- Microalgae have better CO_2 sequestration ability. It is estimated that 1.83 kg of CO_2 is consumed in order to produce 1 kg of algal biomass [21].
- Freshwater and arable lands are not required for growing microalgae as it has the adaptability to grow in extreme environmental conditions [22].
- The cell doubling time of microalgae is as short as 3.4 h [21].
- The water footprint of microalgal biodiesel is lower than that of other biodiesel feedstocks. Microalgal biodiesel water footprint varies from 3.5 to 3726 kg of water per kg of biodiesel [23].
- Microalgae cultivation does not require the application of herbicides or pesticides [24].
- Microalgal biomass contains carbohydrates, proteins, and pigments in addition to lipids for biodiesel production, making the de-oiled biomass a potential feedstock for the production of biofuels and other value-added products [25].

Despite several advantages, microalgal biodiesel production suffers from several limitations at different stages of the upstream and downstream processes [26]. Some of the challenges are as follows:

- Potential strain with high lipid content and inherent adaptability to the local climatic conditions must be selected [21].
- Microalgal cultivation is a water-intensive process that requires almost 1000 kg of water per kg of biomass [27].
- Oil synthesis needs to be decoupled from the arrest of cell division. The amount of oil produced by a microalga is dependent on species and cultivation conditions. However, substantial oil accumulation in microalgae requires stress culture conditions. Under such stress culture conditions, microalgae can accumulate considerable amount of oil, explaining the potential of microalgae as a biodiesel feedstock. However, stress culture conditions limits the overall biomass productivity of the system [28].

- Harvesting of microalgal biomass is one of the major bottlenecks during downstream processing, as it involves high energy input [29]. Harvesting is estimated to account for 20%–30% of the total production cost [30].
- Almost 80%–90% of the equipment cost is utilized for harvesting microalgal biomass from open ponds [31].

1.3.3 Microalgal lipid enhancement strategies

Microalgae have the potential to produce a considerable amount (20%-60%) of triacylglycerol (TAG) when their cells are under stress [32]. Stress is defined as a deviation from normal growth conditions as long as homeostasis permits [33,34]. Stress can be either physical stimuli such as variations in temperature, light intensity, photoperiod, or chemical stimuli such as nutrient deprivation (nitrogen and phosphorous), salinity stress, pH of the medium, etc. [35]. These physical and chemical stimuli, be it adverse or favorable, influences the biochemical composition of microalgae severely [36].

Among the various stress stimuli, nutrient starvation is one of the most promising approaches, which is being widely employed by researchers for lipid enhancement in microalgae. Nitrogen (N) and phosphorus (P) are the primary sources of microalgal nutrients influencing carbon flux and cellular energy reorientation [37]. Nitrogen is a major component of essential biological molecules such as nucleic acids, proteins, and chlorophylls, which influences cell division and growth. Whereas phosphorus is a major component of nucleic acids and phospholipids. Moreover, modulation of nutrient levels has been reported to influence lipid accumulation and composition [38]. On the other hand, nitrogen boosts neutral lipid accumulation, whereas phosphorus limitation stimulates intra- and interspecific variability in metabolic responses. During nutrient limitation, surplus energy and carbon pool accumulated due to the inhibition of amino acids synthesis are diverted to lipid synthesis. However, this condition results in low biomass productivity and poor enzyme activity as the protein synthesis is impaired [39]. To overcome this problem, two-stage cultivation strategies is being employed widely. In the first stage of cultivation, a nutrient rich medium is used to grow microalgal cells to

obtain a high density of cells. Subsequently, these cells are shifted to a nutrient-deficient medium to enhance the accumulation of cellular lipids [19,40–42].

1.3.4 Stress-induced reactive oxygen species (ROS) generation and its putative role in lipid accumulation

Since stress-induced lipid enhancement strategies in microalgae are extensively used as an environmentally benign approach, it is of industrial and biotechnological importance to understand the relationship between different stress factors and lipid accumulation. Proteomic and genomic analysis showed that under stress conditions, the metabolic network shifts towards lipid accumulation [43,44]. However, the relationship between extracellular stress signals and intracellular lipid synthesis is poorly understood. Under various stress conditions, potential signal transduction mechanisms might be involved in triggering carbon partitioning and lipid accumulation [45]. In recent years, researchers suggested that ROS might be an important mediator for lipid accumulation under stress conditions [46,47].

Aerobic organisms gain significant energetic advantages by using molecular oxygen as a terminal oxidant in respiration. Although oxygen is a harmless molecule, however, its presence in the cellular environment causes an oxidative threat to cellular structure and processes [48]. Molecular oxygen has the potential to be partially reduced and form toxic ROS [49]. In aerobic organisms, ROS are formed by the inevitable leakage of electrons onto molecular oxygen from the electron transport activities of chloroplasts, mitochondria, and the plasma membrane [50]. The cellular ROS level remains at equilibrium under a normal physiological state [45]. However, under stress conditions, the balance between cellular ROS production and elimination gets disturbed, leading to an increased accumulation of ROS [51]. An elevated level of intracellular ROS triggers oxidative stress, which causes damage of proteins, lipids and DNA. However, ROS accumulated in the cells due to stress is counteracted by cellular defense mechanisms such as non-enzymatic antioxidants (e.g., pigments, polysaccharides, polyphenols, proline, carotenoids, and flavonoids) and enzymatic antioxidants (e.g., superoxide dismutase, catalase, ascorbate peroxidase) [19]. These antioxidants scavenge the excess oxidants and prevent the cells from harmful impacts of ROS. Thus, ROS acts as a

messenger to cellular signals and facilitates the cells to adapt to adverse growth conditions [34].

1.4 Harvesting

Harvesting is a process of separating microalgal biomass from the growth medium. The strategy employed for harvesting and dewatering the microalgae generally accounts for approximately 3%-30% of total biomass cost [21,52]. Thus, the economy of microalgal production is significantly influenced by harvesting technology [53]. Several factors such as the cell age, shape, type, density and size of the target microalgae and the significance of the end product influence the selection of harvesting technology [21]. Typically a harvesting method that yields algal biomass with minimum moisture content is preferred as the high moisture content of harvested biomass may increase the cost of further processing [29]. It has been reported that 90% of the equipment cost is utilized for harvesting microalgal biomass from open ponds [31]. An ideal harvesting method should: (a) have a high sedimentation rate; (b) have high biomass recovery; (c) not alter the quality of the biomass; (d) be eco-friendly; (e) be economical and non-toxic so that it can be applied in large scale; (f) permit the reusability of the culture medium [54].

1.4.1 Microalgal harvesting strategies and its challenges

The selection of an appropriate harvesting technique depends on the end product requirement and features of microalgal species. At present microalgal biomass is recovered either by physical, chemical, electrical, biological, or magnet-based methods [26]. Each of these harvesting techniques performs on its principle, and hence, has its advantages and disadvantages. Physical based harvesting techniques comprise of sedimentation, centrifugation, flotation, and filtration with varying efficiencies and operational cost. The main drawback of sedimentation, flotation, and filtration is that the processes are species-specific [55]. On the other hand, though centrifugation is the most extensively applied harvesting process because of its high harvesting efficiency, the process involves a high operational cost [56]. Chemical based harvesting techniques, which consist of inorganic and organic flocculants, are expensive and leads to unwanted byproducts causing a detrimental impact on the cells [26]. Electrical and magnet-based methods are strain-independent and chemical-free processes, but they have limited

application potential due to high capital expenditure and operating costs. Whereas biological harvesting methods are energy-efficient and are based on natural and chemical free organic flocculants such as cationic biopolymers, proteins extracted from microorganisms, modified soil, fungal spores, and pellet, seed extract from *Moringa oleifera*, vegetable tannin, etc. [26,55]. However, flocculants extracted from microorganisms show inconsistent results and cause microbial contamination. Therefore, flocculants extracted from natural and biodegradable resources such as cationic starches, seeds, vegetable tannins, etc., that have a low impact on cell structure are considered as a superior alternative to flocculate microalgal cells [57].

1.4.2 Flocculation

Flocculation is a promising solid-liquid separation method that has been used for harvesting microalgae since the 1980s [58]. In this process, the flocculant added to the culture medium facilitates the microalgal cells to form large aggregates known as flocs for speedy sedimentation and separation from the bulk medium [59]. There are four mechanisms by which microalgal cells flocculate (Table 1.1). Since the microalgal cell surface is negatively charged, cationic flocculants are required to either reduce or neutralize the negative charge [60]. The flocculation process is categorized into chemical, auto, bio, electrolytic, and organoclay flocculation depending on the types of flocculants used for microalgal harvesting [61]. The efficiency of flocculation depends on surface properties of microalgae, cell concentration, the charge density of flocculant, flocculant dose, pH of the culture medium, and mixing extent [59]. An ideal flocculant should: (a) not alter the quality of the biomass; (b) be eco-friendly; (c) be inexpensive and non-toxic so that it can be applied in large scale; (d) permit the reusability of the culture medium [29].

Table 1.1. Mechanisms of microalgal cell flocculation.

Mechanism	Description	Illustration
Charge neutralization	When positively charged ions, polymers or colloids strongly adsorb onto the negatively charged surface of an algal cell, eventually canceling the negative surface charge, the phenomenon is known as charge neutralization. This results in the loss of electrostatic repulsion between the algal cells, which consequently forces them to flocculate.	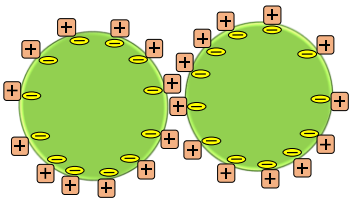
Electrostatic patching	The positively charged polymer binds to the algal cell surface and locally reverses the charge on the algal surface. Thus, algal cells attract patches of opposite charge, resulting in flocculation of the suspended algal cells.	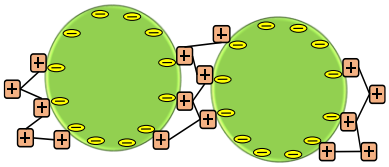
Bridging	Cationic polymers simultaneously bind to the surface of two or more algal cells, resulting in bridge formation between the algal cells.	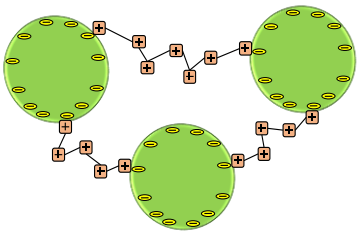
Sweeping	Algal cells are flocculated by entrapping the cells in a massive polymeric precipitation.	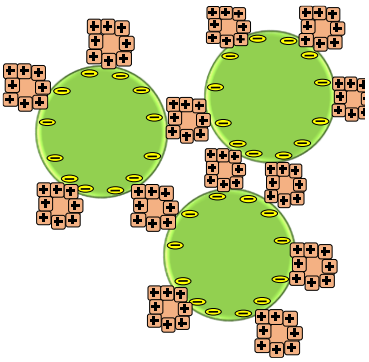

1.4.3 Bioflocculation

The flocculation process induced by microorganisms (self-flocculating algae, bacteria, fungi, or yeast), extracellular polymer substances, or bioflocculants extracted from algae, bacteria, waste biomass, plants, seeds etc. is termed as bioflocculation [59,62,63]. In this harvesting process, cells forms ionic bridges with the microorganisms (algae, bacteria, fungi) or the bioflocculants to form large flocs and finally settle down by gravimetric force without the addition of any chemical flocculants. Bioflocculation is an energy-efficient, eco-friendly and chemical-free process that maintains cell integrity.

1.5 Microalgal Biomass to Biodiesel Conversion

1.5.1 Transesterification

Microalgal biomass is conventionally converted to biodiesel through the transesterification process. Transesterification reaction converts the triglycerides extracted from biomass into long chains fatty acid alkyl esters (FAAEs) and glycerol in the presence of alcohol and catalyst [64]. The transesterification reaction is shown in Figure 1.3. Transesterification reaction involves three reversible steps: (i) in the first step; triglycerides are converted to diglycerides, (ii) in the second step; diglycerides are converted to lower glycerides, i.e., monoglycerides, (iii) finally, monoglycerides are converted to esters (biodiesel) and glycerol [65]. An ester is formed in each conversion step; thus, one triglyceride (TG) molecule produces three ester molecules. Various types of alcohols such as methanol, ethanol, propanol and butanol can be used for biodiesel production. During this transesterification process, when methanol is used as the reactant, it results in the formation of fatty acid methyl esters (FAME) whereas when ethanol is used as the reactant, fatty acid ethyl esters (FAEE) are formed as the reaction product. However, methanol due to its low-cost and availability is the most widely used alcohol during the transesterification process [66]. The high free fatty acid (FFA) in microalgal lipid reacts with the alkali catalyst resulting in an unfavorable saponification process. This process leads to the formation of by-products, such as soaps and gels that compromises the transesterification reaction's efficiency and hinders the separation of ester and glycerol phases [67]. To overcome this problem, a two-step acid-base catalytic process is widely being applied. The first step involves the acid pretreatment process, known as the esterification of FFA. In the esterification process an acid catalyst is employed to reduce

the FFA content to a safer level (<1%) and convert FFA into esters. Whereas in the second step transesterification reaction occurs, where an alkali catalyst is employed to convert the esters into FAAEs [8]. The efficacy of FAAE conversion depends on reaction temperature, retention time, lipid-alcohol ratio, and catalyst loading [68–70].

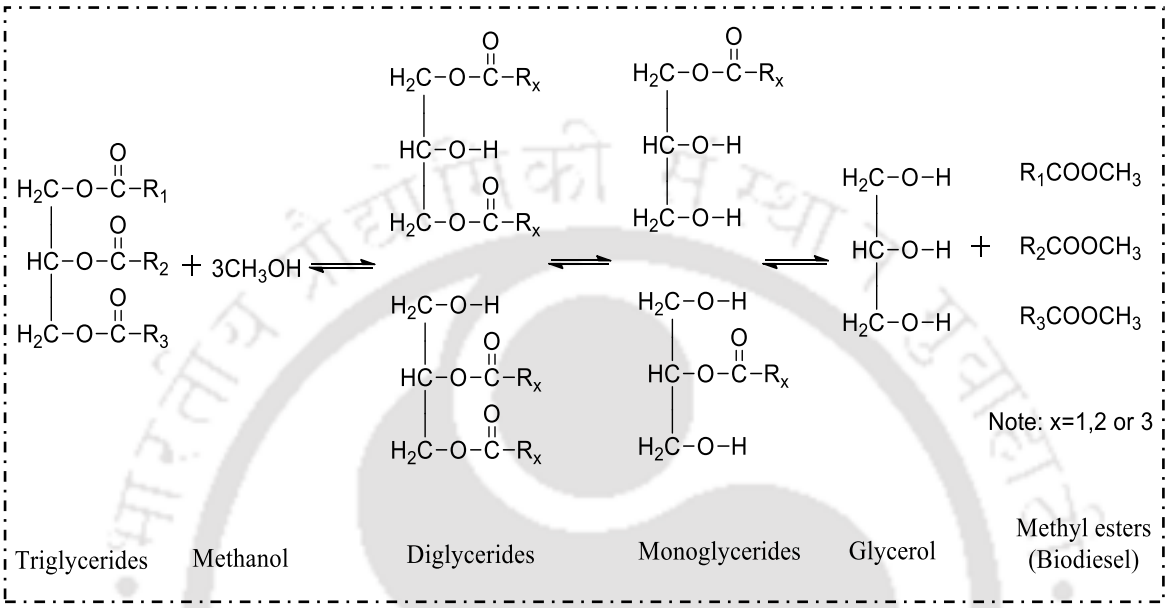

Figure 1.3. Transesterification of triglyceride into fatty acid methyl ester and glycerol.

1.5.2 Catalyst for transesterification

A catalyst expedite the transesterification reaction rate and yield [65]. Catalyst employed for transesterification reaction can be categorized into three types: acid, base, and enzyme (biocatalyst) catalyst [13] (Figure 1.4). Acid and base catalyst can be further classified based on their homogeneity and heterogeneity. A homogeneous catalyst exists in the same phase (gas or liquid) as the reactants. While, a heterogeneous catalyst does not exist in the same phase as the reactants. A heterogeneous catalyst forms either a suspension or visible physical phases with other reactants. The most significant difference between a homogeneous and heterogeneous catalyst is that a heterogeneous catalyst can be mechanically separated from reaction mixture at the end of the transesterification reaction via filtration or centrifugation, whereas a homogeneous catalyst cannot be

recovered. This property allows heterogeneous catalysts to be reused and, to some extent, unaffected by a feedstock's high FFA content [66].

Sodium hydroxide, potassium hydroxide, sodium methoxide, and potassium methoxide are some of the examples of widely used homogeneous base catalysts [71]. Homogeneous basic catalyst requires short reaction time but suffers from some significant drawbacks, such as emulsification, generation of a huge quantity of alkaline wastewater, and hurdle in separating catalyst at the end of the reaction [72]. To overcome these problems, various surface modified heterogeneous basic catalyst such as CaO, $CaTiO_3$, $CaZrO_3$, $CaO\text{-}CeO_2$, $CaMnO_3$, $Ca_2Fe_2O_5$, KOH/Al_2O_3, KOH/NaY. Al_2O_3/KI, ETS-10 zeolite, and alumina/silica supported K_2CO_3 have been developed [64]. However, the active sites of the heterogeneous basic catalyst get easily deactivated when exposed to air. As compared to the heterogeneous basic catalyst, the homogeneous acid catalyst is suitable for simultaneously esterification and transesterification reaction of oils with high free fatty acids [73]. Sulfuric acid is the most widely used homogeneous acid catalyst for transesterification. However, a homogeneous acid catalyst has a lower reaction rate and requires a large quantity of solvent for oil extraction. Moreover, the high solubility of the homogeneous acid catalyst makes its reusability complex, as the energy required for the catalyst separation and product purification is high, thus increasing the cost of product [74]. Heterogeneous solid acid catalyst such as ZnO/I_2, ZrO_2/SO_2^{-4}, TiO_2/SO_2^{-4}, niobic acid, sulfated zirconia, Amberlyst-15, and Nafion-NR50 are considered as a promising alternative for reducing the energy and production cost of biodiesel [13]. These solid acid catalysts have high reactivity and can be easily recovered. However, the low thermal stability and high production cost of commercially available heterogeneous acid catalysts limit their widespread applicability. Enzyme catalyst also known as biocatalyst is conventionally produced through microbial fermentation to overcome the shortcomings of acid and base catalyst [75]. Extracellular lipases, intracellular lipases, and free enzymes are the three types of enzyme catalyst used for transesterification reaction [13]. Enzyme based transesterification process can tolerate free fatty acid and water without soap formation, thereby making separation of biodiesel and glycerol easier. However, the high production cost of enzyme, long reaction time, and high susceptibility to alcohol denaturation makes enzyme catalyst unsustainable [76]. Hence, researchers are trying to

develop reusable heterogeneous catalysts from waste biomass resources such as woody biomass, rice husk, peanut hull, sugarcane bagasse, vegetable oil asphalt, waste shells for minimizing the production cost [77]. These green catalysts can be produced in a less energy-intensive and environmentally benign way through carbonization and sulfonation method [78].

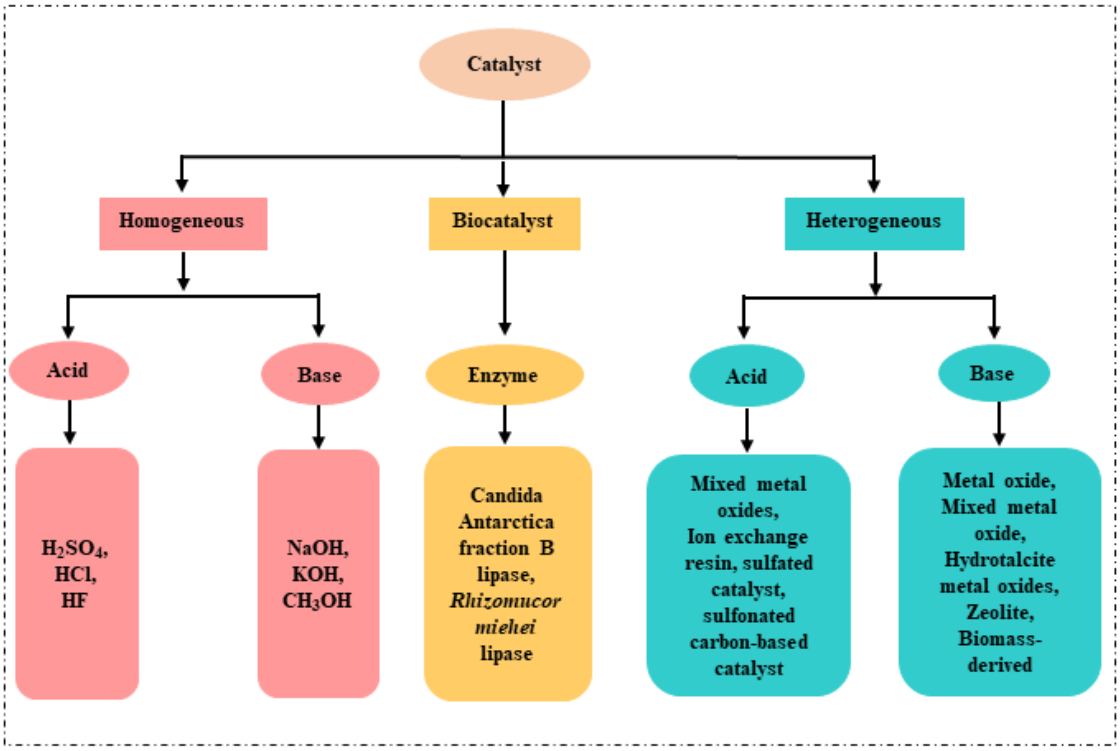

Figure 1.4. Catalyst classification for biodiesel synthesis.

1.5.3 Carbon based catalyst

The activated carbon also known as activated charcoal, is a highly porous material which is most commonly used as a carbon catalyst [79]. Activated carbon is an amorphous carbon with uniform distribution of micropores and macropores, thereby providing a large surface area for the chemical reactions to take place [80]. Activated carbon provide numerous advantages such as high thermal stability, high surface area, and hydrophobic surface that makes it favorable for anchoring desirable functional groups [81]. Activated carbon is generally produced from high carbon containing materials such as woody biomass, peat, coal, shells, and petroleum residues [82]. The carbonaceous materials can

be synthesized by different methods based on the desired product properties and end product application. Activated carbon can be prepared through direct carbonization (pyrolysis), hydrothermal carbonization (HTC), and carbon nanostructure synthesis processes that include Ordered Mesoporous Carbon (OMC), Carbon nanotube (CNT), and Metal Organic Framework (OMF). However, pyrolysis (direct carbonization) and HTC are the two most commonly used methods for producing carbonaceous materials from biomass [83].

Carbon based catalysts are divided into two types: (a) functionalized catalysts, and (b) supported catalysts. Based on the catalytic application, the surface of the carbonaceous material can be impregnated with different functionalized groups, usually by in-situ or post-synthetic methods [79]. Functionalized catalysts are sub-divided into two categories: (a) acid functionalized, in which different acid or acidic functional groups are covalently attached with carbon material, and (b) base functionalized, in which different base or basic functional groups are covalently attached with carbon material. Apart from the functionalized catalyst, the porous carbonaceous material is also being used as a support for active catalysts like CaO, KOH, 12-tungstophosphoric acid (TPA), etc. [82].

1.5.3.1 Direct carbonization

The pyrolysis process is a well-known direct carbonization method that is performed in an inert atmosphere. A reaction temperature between 200 °C and 700 °C under atmospheric pressure typically produces biochar yield between 10% and 39% of the biomass [79,84]. During pyrolysis, biomolecules in the microalgal biomass undergo cracking and depolymerization due to continuous heating. Thermal decomposition results in the production of bio-oil, chars, and non-condensable gases such as CO, CO_2, CH_4, H_2 [79]. Pyrolysis of organic materials results in the formation of products containing –OH and –COOH groups [85]. The pyrolysis treatment in the carbonization process is highly efficient and flexible, but it is not appropriate for raw materials with high moisture content [86]. The carbonization temperature influences the structure and acid density of the carbonaceous material [85]. In comparison to hydrothermal carbonization, the pyrolysis process requires a relatively longer reaction time.

1.5.3.2 Hydrothermal carbonization

Hydrothermal carbonization is a thermochemical conversion process that is performed in the presence of water at different temperature ranges. The process is generally conducted at high pressures so that the water molecules can be suppressed and prevented from escaping during the reaction [87]. HTC process generally involves a series of reactions such as hydrolysis, dehydration, decarboxylation, condensation, and aromatization to disintegrate the biomass bonds [79]. The water plays the role of both reactant and reaction medium, thereby enhancing the carbonization process by hydrolyzing biomass to form a new molecular fragment [88]. The solid hydrochar, liquid bio-oil, and gaseous products are the three primary products of the HTC process [87]. The type of feedstock, temperature, reaction time and biomass to water ratio influences the product distribution ratio between solid, liquid and gas product. HTC process performed at a lower temperature (<200 °C) generates hydrochar as a primary product, whereas HTC performed between 200 °C - 400 °C produces liquid hydrocarbon as its main product. HTC process carried out at the supercritical state for water produces gases as its primary product [79].

1.5.3.3 Sulfonated carbon based catalyst

All the reported acid functionalized carbon based catalysts are sulfonated activated carbon. These sulfonated activated carbons catalyzes the process of biodiesel production either by catalyzing the esterification of FFAs present in the oil or by simultaneously catalyzing esterification and transesterification reactions similar to concentrated H_2SO_4 [82]. Sulfonated carbon-based catalysts are notable for their excellent stability, ease of synthesis, low-cost, and presence of strong protonic acid sites. Numerous studies have reported the use of sulfonated carbon based catalyst with high density of sulfonic acid groups ($–SO_3H$) as a noble alternative to H_2SO_4 in reactions such as hydrolysis, esterification, and nitration [89–91]. Sulfonated carbon based catalyst are synthesized by two methods: (a) direct sulfonation and, (b) sulfonation through reductive alkylation/arylation [77]. Direct sulfonation is generally carried out by heating the mixture of catalyst support and sulfonating agent to synthesize the catalyst (Figure 1.5). H_2SO_4 is the most commonly used sulfonating agent for synthesizing sulfonated carbon

catalyst. Reaction parameters such as sulfonating agent, sulfonation time and carbon precursor influences the catalytic activity of the catalyst [82]. Sulfonation of carbonaceous material by reductive alkylation/arylation of sulfonic acid-containing aryl radical has been used to synthesis sulfonated activated carbon using various carbon sources such as ordered mesoporous carbon (OMC), nanotubes, graphite, and graphene.

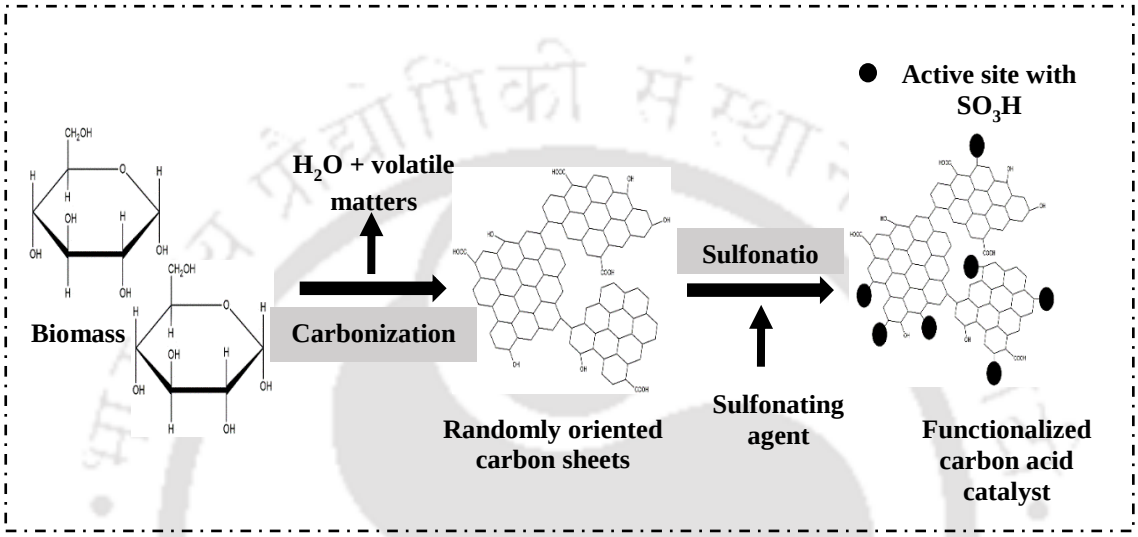

Figure 1.5. Synthesis pathway of solid acid catalyst from biomass (data source: Tang et al., 2018).

भारतीय प्रौद्योगिकी संस्थान गुवाहाटी
Indian Institute of Technology Guwahati

Chapter 2

Literature Review and Objectives

2.1 Microalgae Strain Selection

Isolation and screening of new microalgal strains with potential for biofuel production is an essential first step for commercial-scale biofuel production using microalgae. Microalgal diversity offers both an opportunity and a challenge in the process of potential strain selection. For commercial-scale biofuel production, the microalgal strains must meet a range of criteria for efficient high-productivity cultivation (e.g., their temperature and salinity tolerance, efficiency and mechanisms of uptake of inorganic carbon, photosynthetic capacity, lipid content and quality, shear tolerance, etc.), harvestability (e.g., cells size and morphology), and extractability (e.g., cell covering) [92]. In 1983, the Solar Energy Research Laboratory (SERI) in the United States started the isolation and screening process of a wide range of microalgae from the saline environment. The researchers achieved a significant improvement in productivity due to the selection of potential strain. Zhang et al. (2014) isolated 101 microalgal strains from partial waters in Hainan province, of which eight strains were selected based on their biomass productivity, lipid content, and ease of cultivation. Among all the isolates, *Desmodesmus* sp. WC08 was found to be the potential candidate for biodiesel production, based on its higher biomass concentration (2.32 g L^{-1}), lipid content (31.30%), lipid productivity (115.73 mg L^{-1} d^{-1}), and oleic acid content (>50% of the total fatty acids) [93]. In another study, Minhas et al. (2016) screened four microalgal strains out of twenty-two isolates with the potential to produce significant quantities of multiple products such as lipids, lutein, astaxanthin, and carotenoid [94]. Thus, selecting a potential strain with high productivity of the desired product and an inherent ability to grow in the environmental conditions under which it will be grown in large scale cuts the production cost to a great extent.

2.2 Cultivation Strategies for Improved Biomass and Lipid Content

The economic feasibility of a microalgae-based biodiesel production system is determined by two mutually exclusive parameters: biomass content and lipid content. In general, the nutrien starvation strategy is extensively employed to increase the lipid content of the microalgal cells but at the cost of reduced biomass content [39]. Nutrient starvation reduces cell division and growth as nitrogen, phosphorous, sulfur, carbon, and trace mineral nutrients are essential components of biological molecules such as nucleic acids, proteins, and chlorophylls [19,95]. To deal with these problems, various cultivation strategies have been widely employed. Microalgal cultivation strategies are primarily categorized as batch, fed-batch, continuous, semi-continuous, and two-stage cultivation strategies (Figure 2.1).

In the batch cultivation process, all the nutrients are added at the beginning of the cultivation, and no additional nutrients are added in the subsequent process. However, in batch cultivation mode, cell growth is accompanied by insufficient nutrient uptake due to the gradual depletion of nutrients in the medium, leading to lower biomass concentration. Due to this limitation, researchers have developed various batch culture-based cultivation systems such as continuous, semi-continuous, and fed-batch processes [96]. Initially, continuous and semi-continuous cultivation processes are performed in batch cultures. In a continuous cultivation mode, the fresh culture medium is continuously added to the culture vessel while effluent and product are simultaneously withdrawn. While in a semi-continuous mode, a portion of the culture containing cells is periodically withdrawn, and the remaining culture is replenished with a fresh medium. In a fed-batch process, nutrients are fed to the culture vessel intermittently [97]. In this cultivation process, optimum nutrient concentration is maintained by adjusting the feed rates. Continuous and fed-batch processes are generally performed under nutrient-rich conditions, which leads to a low level of lipid accumulation.

Two-stage cultivation strategies are being widely employed to obtain high biomass concentration and lipid yield. In the first stage of the cultivation process, a nutrient-rich medium is used to grow microalgal cells to obtain a high density of cells. Subsequently, in the second stage, these cells are shifted to a new culture medium to induce stress for enhanced cellular lipid accumulation [19,40]. Based on stress stimuli, two-stage cultivation strategies are divided into five categories: inducer addition by two-stage strategy, starvation-based two-stage strategy, metabolic switch by two-stage strategy, and irradiation-based two-stage strategy [96]. In a two-stage cultivation system, the average increase in biomass production was reported to

be higher than the non-hybrid strategies, 12.5% greater than photobioreactors, and 46–74% more than open ponds [96]. Mujtaba et al. (2012) successfully increased lipid productivity in *Chlorella vulgaris* using a nitrogen starvation-based two-stage strategy. In their study, lipid productivity was significantly increased from 31.5 mg $L^{-1}d^{-1}$ to 71 mg $L^{-1}d^{-1}$ [98]. In another study, supplementation of a high concentration of NaCl at late log phase enhanced lipid productivity during the two-stage cultivation of *Monoraphidium dybowskii* LB50 [99]

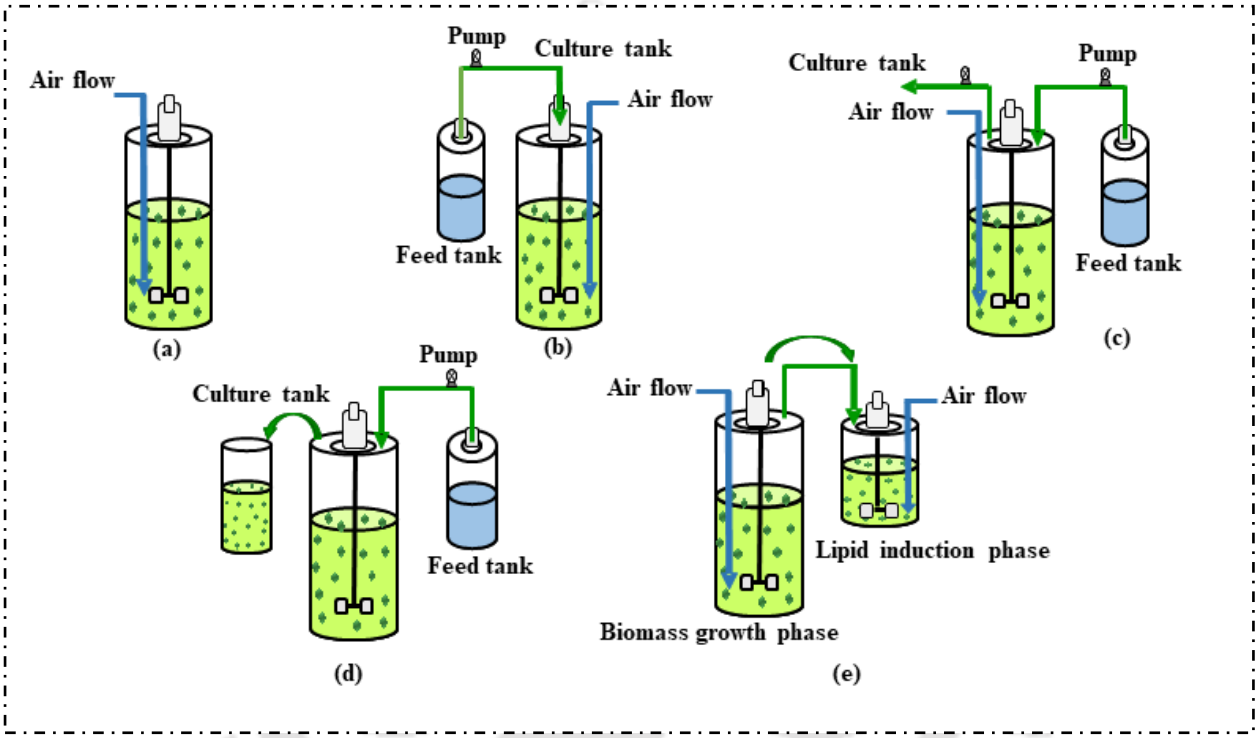

Figure 2.1. Diagram of the five microalgae cultivation strategies: (a) batch, (b) fed-batch, (c) continuous, (d) semi-continuous, and (e) two-stage cultivation strategies.

2.3 Microalgae Biochemical Composition

The feasibility of a microalgae-based biofuel system is primarily determined by its biochemical composition. The biochemical composition of microalgae comprises proteins, carbohydrates, nucleic acids, and lipids in varying proportions based on microalgal species. Lipid (37.6 kJ g^{-1}) is the most energy-rich compound, followed by proteins (16.7 kJ g^{-1}) and carbohydrates (15.7 kJ g^{-1}) [100]. Microalgal lipids are divided into polar and nonpolar lipids based on their structures. Polar lipids such as glycolipids and phospholipids are structural

components of organelle membranes. These lipids are amphiphilic in nature, with a hydrophilic head and a hydrophobic tail [101]. Nonpolar (neutral) lipids are storage lipids such as acylglycerols, sterols, free fatty acids, wax, and steryl esters [102].

Microalgae produce carbohydrates during the dark stage of photosynthesis. During photosynthesis, carbon dioxide is reduced to carbohydrates through the Calvin cycle [100]. Carbohydrates also comprise structural and storage components. Structural components such as pectin, cellulose, and sulfated polysaccharides are generally present in the cell wall, whereas storage components such as starch accumulate either inside or outside the chloroplast. The metabolism and composition of carbohydrates vary among microalgal species [103]. Generally, microalgae have a total carbohydrate content of about 20% dry weight [104]. Protein synthesis is the most intricate mechanism in all cells. Microalgal protein contains a number of different amino acids, such as arginine and leucine. Protein content in microalgae is believed to be proportional to the lipid content. Microalgae typically possess 20%-60% (dry cell weight) of protein [105].

2.4 Lipids in Microalgae

Microalgal lipids mainly consist of triacylglycerol (TAG) and diacylglycerol (DAG), which are desirable for commercial-scale biodiesel production [105]. It has been reported that during the exponential phase of growth, microalgae accumulate very little TAG, with the majority of TAG being accumulated during the stationary phase [100,106]. TAG is easily catabolized to provide energy for metabolic processes. TAG is primarily synthesized in the presence of light, stored in cytosolic lipid bodies, and then utilized for polar lipid synthesis when light is absent [107]. The lipid content of microalgae is usually in the range of 20% – 50% of the dry cell weight and can be as high as 80% under certain conditions [108]. However, the growth rate of high lipid-containing strains is reported to be lower than low lipid-containing strains [109].

The amount and ratio of saturated and unsaturated fatty acid determine the suitability of microalgae as a biofuel feedstock. Microalgal lipid is generally composed of unsaturated fatty acids such as palmitoleic (16:1), oleic (18:1), linoleic (18:2), linolenic acid (18:3), and saturated fatty acids such as palmitic (16:0) and a small portion of stearic acid (18:0). The fatty acid composition of lipids in microalgae significantly affects the biofuel properties. Microalgal lipid containing a low amount of saturated fatty acid exhibits better cold flow properties as long-chain saturated fatty esters increase the pour and cloud point of biodiesel [100]. However,

biodiesel with a high amount of unsaturated fatty acids is oxidized at a faster rate than conventional diesel, resulting in insoluble sediments that interfere with engine operation. Therefore, microalgae with the potential to generate a high quantity and quality of lipid should be selected for producing biodiesel efficiently.

2.5 Environmental Stresses affecting Microalgal Lipid Content and Composition

The biochemical composition of microalgae varies with the physiochemical changes in its culture environment. Numerous studies have employed environmental stresses such as light stress, temperature stress, nutrient stress, pH stress, and salt stress to improve the lipid content and composition of microalgae (Table 2.1).

2.5.1 Nutrient stress

Nutrient manipulation changes the metabolic strategies and biochemical composition of microalgae. Microalgal sensitivity to nutrient modification is typically considered through three levels of limitation: starvation, limitation, and depletion. The nutrient-starved condition involves growing microalgae in a nutrient-replete environment first, and then the cells are harvested and shifted to a media lacking specific nutrient/s. Nutrient starvation induces a sharp biological shock causing an accumulation of high-energy rich compounds such as lipids. During the nutrient-limited condition, cells are grown under continuous mode in a medium where all nutrients are available in excess except one particular nutrient that limits maximum biomass production and causes a physiological reaction to the limiting nutrient. Nutrient deficient growth is carried out in batch cultures where cells are grown in an environment replete with required nutrients. The growth rate increases with cell density until the nutrients are depleted. Then, the cell growth rate potentially reduces while the amount of high-energy storage compounds increase due to changes in metabolic processes [100]. Thus, increased production of targeted biofuels can be achieved by manipulating nutrient conditions.

2.5.1.1 Nitrogen

Nitrogen is an essential element required for protein biosynthesis. Under nitrogen-limited conditions, the majority of the carbon fixed in photosynthesis is utilized for lipid or carbohydrate synthesis rather than proteins. Nitrogen is considered to be an essential nutrient influencing the lipid metabolism in microalgae. Cellular nitrogen is found to be inversely related to lipid content in microalgae [100]. Nitrogen limitation causes three changes in the

species: decreases the cellular content of the thylakoid membrane, activates acyl hydrolase, and stimulates phospholipid hydrolysis. These changes might enhance the intracellular content of fatty acid acyl-CoA. Meanwhile, nitrogen deficiency may activate diacylglycerol acyltransferase, an enzyme that converts acyl-CoA to triacylglycerol. Therefore, nitrogen limitation can induce both lipid and TAG synthesis in microalgal cells [110].

Generally, lipid content in microalgae is increased by 2- to 3-fold when cultured for 4-9 days under nitrogen-limited conditions. Lipid content in *Neochloris oleoabundans* and *Nannochloropsis* sp. was found to increase by 2-fold and 1-fold, respectively, under nitrogen-starved conditions [111,112]. However, Rathinasabapathi et al. (2018) observed lipid accumulation in *chlorella* sp. just hours after the cells were nitrogen starved [100]. In another study, about 1.2-fold increase in lipid content was observed when *A. dimorphus* was nitrogen starved for 2 days [19]. The saturated fatty acid (palmitic acid, stearic acid) content in lipids of *A. falcatus* was found to increase when cultured under nitrogen stress conditions. The increase in percentage composition of saturated fatty acid and a simultaneous decrease in polyunsaturated fatty acid under nitrogen-limited conditions could be due to the oxidative damage of unsaturated fatty acids [113]. A high percentage of saturated fatty acids in lipids improves the oxidative stability and cetane number of the biodiesel produced. In another study, Ordog et al. (2013) reported that under nitrogen-stressed conditions, *Scenedesmus* strains had a more suitable FA profile with higher amounts of SFAs and MUFAs and a smaller PUFA component compared to *Chlorella* strains, which had a larger PUFA component [114].

2.5.1.2 Phosphorous

Phosphorus is another crucial nutrient for microalgal growth as it is involved in cellular metabolic activities such as signal transduction, energy transfer, and photosynthesis [100]. It has been reported that phosphorous limitation resulted in lipid accumulation, mainly TAG, in *Dunaliella parva*, *Chlorella* sp., *Scenedesmus* sp., *Monodus subterraneus* [115–118]. Xin et al. (2010) reported that under phosphorus limiting conditions *Scenedesmus* sp. accumulated about 53% lipid, whereas it accumulated only 25% - 28% of lipid under phosphorus-replete conditions [117]. Phosphorus limitation results in substantial changes in the biosynthesis process and thus in lipid composition. For instance, Yang et al. (2018) reported that phosphorus limitation reduced PUFA and increased SFA content from 35.9% to 38.7% in *Scenedesmus* sp., making it a suitable candidate for biodiesel production [119]. However, in another study, the fatty acid profile of *Picochlorum* Sp. was dominated by MUFA and PUFA under phosphorous starvation, making it unfit for biodiesel production [120]. Anne-Marie et al. (2020)

reported that PUFA content of lipid in *M. gracile* was significantly increased by approximately 2-fold in phosphate-replete and -excess cultures, whereas the MUFA content was slightly increased under limited phosphate concentration. Excess phosphate concentration also slightly increased the SFA content in *M. gracile* [121].

2.5.1.3 Carbon

Microalgae are efficient biological factories capable of capturing zero-energy forms of carbon, synthesizing, and then storing it in the form of natural oils or as a polymer of carbohydrates [100]. Various sources and amounts of carbon have shown significant effects on the growth kinetics, content, and composition of lipids in microalgae cells [122]. Some microalgae are capable of utilizing organic carbon instead of carbon dioxide as the carbon source for heterotrophic growth. For instance, Miao and Wu (year) reported that under heterotrophic conditions, *chlorella* cells were able to accumulate more lipid (55%) as compared to autotrophically grown cells [123]. Several studies have reported that high carbon dioxide concentration induces the accumulation of SFA, whereas a low concentration of carbon dioxide promotes the production of UFA [124,125].

2.5.1.4 Trace mineral nutrients

Trace mineral nutrients are essential for the growth and accumulation of lipids and carbohydrates in microalgae. According to numerous studies, the efficiency of these trace mineral compounds is dependent on their concentration in the media, their interactive synergistic or antagonistic effects with other environmental factors, and the species type [100]. Iron is one of the most crucial trace minerals, as ferric ions are involved in fundamental enzymatic reactions of photosynthesis. It has been reported that an increase in iron concentration resulted in a simultaneous increase in the growth rate and lipid content of *Botryococcus braunii* KMITL 2 [126]. In another study, Praveenkumar et al. (2012) reported that iron deprivation caused a slight decrease in biomass with no significant increase in lipid content of *Chlorella* sp. [127]. An increase in iron concentration in the culture media results in an increase in SFA content and a decrease in UFA content [100].

2.5.2 Salinity stress

Salinity influences microalgal metabolism by altering respiration rate, nutritional assimilation, and carbon uptake from the surrounding environment [128]. Most microalgae regulate lipid biosynthesis as a physiological resistance strategy to salt stress. High salt concentration can damage microalgal cells due to high extracellular osmotic pressure, but

optimal salt stress can induce lipid production. Salinity stress has been reported to intensify lipid accumulation by 40% and 44% in *Chlorella* CG12 and *Desmodesmus* GS12, respectively [129]. The degree of fatty acid unsaturation was found to increase with the increase in salt concentration from 10 to 20 g L^{-1} but decreased at a salt concentration of 30 g L^{-1} in *Nitzschia laevis* [130]. Changes in lipid and fatty acid composition under salinity stress suggested a decrease in membrane permeability and fluidity, which might have helped microalgae acclimatize to the salinity stress.

2.5.3 pH stress

The hydrogen ion concentration (pH) in the culture media is another stress factor that influences the growth and lipid composition of microalgae. Most microalgae exhibit optimal growth when the pH is within 7–9, and deviations from this range can inhibit growth, alter lipid content and composition, or even cause cell death [131]. Paliwal et al. (2017) reported that alkaline pH stress stimulated the accumulation of TAG and decreased the membrane lipid content of *Chlorella* sp. [132]. In another study, although the highest lipid content was obtained at pH 8 but the highest biomass production was observed at pH 7 [133]. Generally, in most microalgae, alkali pH stress has been reported to induce lipid accumulation with higher saturated fatty acids [100].

2.5.4 Temperature stress

Temperature is one of the most important cultural elements for the growth and physiology of microalgae since it directly effects photosynthesis, biochemical composition, and many other physiological processes [134]. Although most microalgal species are able to perform cell division and photosynthesis over a wide range of temperatures (15 °C - 30 °C), the optimum temperature range varies from species to species [100]. The increase in temperature from 20 °C to 25 °C was found to double the lipid production of *Nannochloropsis oculata* at the expense of a lower growth rate [135]. However, it has been observed that in the case of most microalgal species, lower temperature induces stress in favor of higher lipid accumulation [100]. At lower growth temperature, microalgae accumulate high lipid with a higher percentage of UFA, which helps in maintaining membrane fluidity under low temperatures [136]. However, these results are inconsistent, as in the case of *Nannochloropsis oculata* and *Chlorella vulgaris*, an increase in temperature beyond optimum temperature resulted in an increase of UFA [135].

2.5.5 Light stress

Microalgae are autotrophic microorganisms; thus, light is essential to carry out their photosynthetic activity. Microalgae exhibit remarkable changes in their biochemical composition under different light intensities. Red light irradiation induces biomass production, whereas blue and far-red light wavelengths induce lipid accumulation in microalgae, as light-harvesting pigments (chlorophyll a and b) are sensitive to these wavelengths. Wahidin et al. (2013) reported that maximum cell density, specific growth rate, and lipid yield were obtained by changing the light-dark cycle from 12:12–18:06 h at a light intensity of 100 μmol m^{-2} s^{-1} [137]. Generally, low light conditions induce the accumulation of PUFA, whereas the percentage of SFA and MUFA are increased under high light conditions [122]. As a high percentage of SFA and MUFA are desirable for obtaining high-quality biodiesel, therefore high light intensities are preferable for microalgal growth.

Table 2.1. The effect of environmental stress on microalgae lipid, biomass concentration and biomass productivity

Microalgae Species	Stress	Biomass concentration (mg L^{-1})		Biomass productivity (mg L^{-1} day^{-1})		Lipid content (%)		Ref.
		Before stress	After stress	Before stress	After stress	Before stress	After stress	
Acutodesmus dimorphus	High temperature	248.61	391.09	14.03	23.53	23.12	22.7	[134]
Ankistrodesmus falcatus	Nitrogen deficiency	-		252.8	124.29	23.33	59.6	[113]
Chlorella vulgaris	High salinity	380.8	456.9	18.7	23.8	12.7	24.5	[138]
Scenedesmus sp.	High salinity	460.15	404.18	22.74	19.01	18.98	33.13	[139]
Scenedesmus sp.	Nitrogen limitation	481.42	426.61	-		18.87	27.93	[140]
Nannochloropsis salina	pH					21.8	24.75	[141]
Scenedesmus obliquus	High light	-		441	841	16	38	[142]
N. oculata	High temperature	-		-		7.9	14.9	[135]
Chlorella sp.	pH	50	167.5			15	33	[143]
Ankistrodesmus falcatus	Phosphorus			0.175	0.124	31.31	59.6	[113]
Chlorella sp.	Phosphorus limitation			1.9	2.2	14	23.6	[116]
Scenedesmus obliquus	High carbon dioxide	50	400			4.2	33.14	[144]
Chlorella minutissima	High glucose	5500	8980			6	10.10	[145]

2.6 Possible Link between ROS Generation and Lipid Accumulation

According to several experimental reports, intracellular ROS seem to be mediator of lipid accumulation in microalgae [134,146]. A number of studies have shown that stress-induced lipid accumulation is invariably associated with increased antioxidant defenses (e.g., oxidative-stress response proteins) or increased intracellular ROS levels [146,147]. Zhang et al. (2019) reported that the cellular lipid content of *C. pyrenoidosa* increased under nitrogen, phosphorus, or sulfur-starved conditions. Moreover, the SOD, CAT, APX activity, and MDA content also increased under these nutrient-starved conditions suggesting the existence of high intracellular ROS content [38]. Shi et al. (2017) reported that ROS might be the second messenger of numerous stress factors that govern cellular responses to extracellular stress [45]. In another study, Pancha et al. (2015) reported that salinity-induced oxidative stress in *Scenedesmus* sp. resulted in highest lipid (24.77%) and neutral lipid (74.87%) accumulation, thereby suggesting oxidative stress as a vital inducer for neutral lipid accumulation. Moreover, high H_2O_2, MDA, APX, and proline contents in *Scenedesmus* sp. under salinity stress suggested a correlation between ROS and lipid accumulation [139]. Similar results were reported by Chokshi et al. (2015) where temperature-induced oxidative stress increased lipid content (22.7%) and neutral lipid (59%) accumulation in *A. dimorphus* [134]. However, only a few putative mechanisms of ROS-mediated lipid accumulation have been identified, and there is currently no direct experimental evidence.

2.7 Physical Properties of Microalgae

Microalgae are found in different shapes and forms: spherical, elongated or filamentous, and their cell size ranges from 0.5 μm - 200 μm. *Scenedesmus* species generally manifest long spines in the colonies of two or four-cell coenobia [148]. Whereas some species such as *Chlamydomonas reinhardtii* are found to be flagellated and mobile within the medium. This wide range of physical characteristics exhibited by microalgae disturbs harvesting efficiency. For instance, flagellated cells evade flocculation by swimming out of flocs, and the cells get easily damaged when the mechanical harvesting method is used [149]. The cell surface charge or Zeta potential of microalgae is negative, and it plays a vital role in the downstream processing. Gerardo et al. (2015) reported that the zeta potential of microalgal cells can vary from − 2 mV to − 75 mV under the influence of chemical functional groups present in the cell surface, which changes with culture conditions and cell age [150]. Moreover, ionization of certain chemical functional groups on the microalgal cell surface, such as the amino and

carboxyl groups, is involved in the charge and stabilization of microalgae suspensions [149]. The ionization of amino and carboxyl groups is greatly dependent on pH, and these ionized functional groups influence the physicochemical features of microalgal cells [151].

The cell density of diatoms and green algae is reported to vary from 1070 kg m^{-3} to 1140 kg m^{-3}, respectively [152]. Sedimentation, a gravity-based separation process, is highly influenced by the difference in solid-liquid/algae-medium density. The diameter of algal cells plays a crucial role in the sedimentation process, as the size of the cell affects the drag of the algal cells in the medium. Rapid settling can be observed if the effective cell size is enlarged by algal cell flocculation. Microalgal cells containing high lipid and gas vesicles do not settle under the influence of any gravitational force, thus, increasing the complexity of the harvesting process [149].

2.8 Microalgae Harvesting Techniques

Generally, microalgal harvesting involves two concentration steps. During the primary harvesting, a thickening procedure is applied where the microalgal slurry is concentrated to around 2% - 7% of total suspended solids (TSS). This can be attained by applying either flotation, sedimentation, flocculation, or a combination of flotation and sedimentation processes [150]. The thickening procedure is followed by a secondary dewatering procedure that results in the formation of an algal cake with 15% - 25% TSS, which can be attained by using centrifugation or filtration [60]. However, a secondary dewatering procedure requires more energy as compared to primary thickening procedures. Currently, microalgal cells are harvested either by physical, chemical, biological, electrical, or magnet-based methods. Some researchers have combined two or more of the above methods to harvest maximum microalgal biomass. Table 2.2 shows a comparison of various harvesting techniques.

Table 2.2. Comparison of various harvesting techniques.

Harvesting techniques	Recovery efficiency	Cell damage	Process time	Species specific	Energy consumption	Operational cost	Toxicity	Reusability of medium	Large scale application	Ref
Sedimentation	Low	No	Long	Yes	Low	Low	No toxicity	Possible	Suitable	[153–156]
Centrifugation	High	Yes	Short	No	High	High	AOM and EOM released cause toxicity	Possible	Unsuitable	[54,155–157]
Flotation	Medium	No	Short	No	Low	Medium	Surfactant may be toxic	Limited	Suitable	[54,156,158]
Filtration	High	No	Short	Unfeasible for very small size microalgae	Low	High	No toxicity	Possible	Unsuitable	[156,159,160]
Flocculation	High	No	Short	No	Low	Medium	Metal contamination	Limited	Suitable	[52,151,156]
Autoflocculation	High	No	Medium	Yes	Low	Low	No toxicity	Possible	Suitable	[156,161,162]
Bioflocculation	High	No	Short	No	Low	Medium	Microbial contamination	Limited	Suitable	[156,163,164]
Electroflocculation	High	Yes	Short	No	High	High	Metal contamination	-	Unsuitable	[156,165–167]
Magnetic particle assisted harvesting	High	No	Short	No	Low	High	Metal contamination	Limited	Unsuitable	[54,156,168]

2.8.1 Physical methods

Sedimentation, centrifugation, flotation, and filtration are the physical methods employed for harvesting microalgal biomass.

2.8.1.1 Sedimentation

In the process of sedimentation, gravitational forces entail the settling of the suspended algal cells from the medium of different densities. However, if the particle size or density difference is small, the separation process may be reduced [26]. Studies have shown the possibility of harvesting colonial algae such as *Micractinium* and *Scenedesmus* (with a cluster diameter of approximately 60 μm) via sedimentation. However, sedimentation is not possible for smaller microalgae such as *Chlorella* and motile algae such as *Euglena* and *Chlorogonium*. The sedimentation rate not only varies among microalgae species but also varies within the same species. Studies found that settling rates might vary with light intensity [169] and nutrient content [170]. However, older cells (senescent cells) [171] and spore-forming cells have high sinking rates [170]. It has been reported that lipid-rich microalgae have low density, and hence the settling rate is less. The sedimentation process has not been extensively used for settling microalgae [165] as the sedimentation rate of 4 μm - 5 μm sized microalgae in the large scale is very small [169]. In the case of microalgal settling, cell recovery is meagre, i.e., 60%-65% [172]. A large land area is required for constructing settling ponds and tanks [173]. Generally, a lamella-type settling tank consumes 0.1 kWh m^{-3} for obtaining 0.1%-1.5% dry microalgal biomass [153].

2.8.1.2 Centrifugation

The harvesting of biomass through centrifugation is based on the application of centrifugal force to enhance the settling rate. The efficiency of harvesting depends on the microalgae cell size and density difference between the microalgae biomass and the medium. Centrifuges of various designs are available; the characteristics of the feed and the end-product requirement determine the selection between sedimentation centrifuges or filtration centrifuges. Usually, to procure clarified liquid sedimentation, centrifuges are used, while filtration centrifuges are utilized to obtain dry cake [149]. Harvesting of microalgae biomass through centrifugation is much advantageous as compared to other methods. Flocculants and chemicals-free biomass can be obtained through centrifugation. Harvesting of microalgae biomass through centrifugation is applicable to all types of microalgae strains [174]. Harvesting through this process ensures a high recovery rate.

A study evaluated the cell viability and harvesting efficiency of various microalgae species using three different centrifugation techniques: bottle centrifuge, which operates at 1300 g-force, batch disc centrifuge, which operates at 6000 g-force and the tubular bowl centrifuge, which operates at 13,000 g-force. The tubular bowl centrifuge, being operated at the highest g-force could achieve a harvesting efficiency of nearly 100% for all species. However, some species such as *Chaetoceros muelleri* and *Isochrysis sp*. are found to be more sensitive to high g-force. The bottle centrifuge, being operated at the lowest g-force is less efficient. Nonetheless, this technique ensures 100% cell viability for all algal species that were evaluated. Depending on the type of algal species, the optimal centrifuge system is selected as high g-force may cause cell lysis [175]. Most large-scale centrifuges operate at 5000-10,000 g-force and are capable of achieving 95% harvesting efficiency under good operational conditions. The decanter type centrifuge is the optimal centrifuge for the mass harvesting of microalgae biomass, as it doesn't require to stop regularly and clean manually like the batch type centrifuges [154]. High solid fractions, along with the continuous discharge of the product can be achieved through decanter type centrifuges [176]. 22% of TSS is possible to obtain through decanter type centrifuge [154]. However, a study found that the decanter type centrifuge is not suitable for *Chlorella* sp, which is a commonly grown and commercially important species [176]. The microalgal cells are exposed to high shear and gravitational forces during centrifugation that may impair the cell structure, resulting in the loss of valuable materials. A study found that for a feed rate of 1 L min^{-1}, the energy consumed during microalgae harvesting through centrifugation is 8 kWh m^{-3} of microalgae suspension. However, energy consumption can be reduced by 10-fold if the feed rate is increased to 18 L min^{-1}, but this will result in low harvesting efficiency [177].

2.8.1.3 Flotation

The recovery of biomass via flotation is mainly dependent on the low density of microalgae, as the low density of microalgal cells facilitates them to float upwards more easily and rapidly than to sediment downwards [149]. Some cyanobacteria such as *Anabaena*, *Microcystis,* and *Spirulina* possess gas vesicles which facilitates them to float naturally [149]. Although some microalgae float naturally due to its low density or presence of gas vesicles, the incorporation of air bubbles in the medium can also help in promoting flotation [158]. Studies found that for most of the microalgal species, recovery of microalgal biomass through flotation is relatively fast in comparison to sedimentation [158]. In most cases, like the sedimentation process, flocculants are required to be added to make the flotation effective

[178]. A study found that large flocs produced by combining organic and inorganic polymers facilitated flotation of marine microalgae, *Isochrysis galbana* [179]. Flocculation flotation favours over sedimentation for the recovery of microalgal biomass because of the low density of microalgal flocs as compared to microalgal cells [180].

Based on the technique of bubble production, flotation processes are classified as froth flotation, dispersed air flotation, dissolved air flotation, and electrolytic flotation [154]. Froth flotation is a promising approach for commercial-scale harvesting of microalgae. However, all the surfactants employed for froth flotation are conventional monomeric surfactants containing a single similar hydrophobic group in the molecule, which leads to low harvesting efficiency. Dissolved air flotation (DAF) involves the generation of air bubbles that range in size from 10 µm to 100 µm with a mean size of 40 µm [178]. In countries such as the USA, usually, chemical coagulation is followed by dissolved air flotation for the purification of effluent instead of harvesting microalgal biomass [181]. It was reported in a study that a high quantity of alum (0.3 g L^{-1}) enables the recovery of microalgae from pig slurry [182]. Although the dissolved air flotation process is an efficient harvesting option, it requires high pressure making the process more energy-intensive [183].

The electro-flotation process is not considered as the optimum method for harvesting microalgae as the method is effective only at a bench scale, and moreover, the process is an energy-intensive one like the DAF [165]. Research suggested that electro-flotation process is more effective in marine water than freshwater [180]. Quantum Fracturing™ is a method developed by Origin Oil that applies pulsed electromagnetic fields and modified pH to fracture the microalgal cells and release the microalgal lipids to the surface, and letting the remains of microalgal biomass to settle out [184]. The University of Sheffield applied fluidic oscillation to develop an energy-efficient method for generating micro-bubbles [185]. Recently it has been seen that micro-bubbles produced by fluidic oscillation are being able to harvest microalgal biomass from growth medium effectively [183]. However, more research must be carried out to make it practically feasible to harvest large-scale microalgae through energy-efficient micro-bubbles [160]. Flotation of microalgal biomass with the aid of small bubbles requires high energy and operational costs. The cost involved in the flotation process in which the flocculant needs to be added may be the same as or greater than the cost involved during the centrifugation process [174]. Research still needs to be carried out to scale-up the low-energy flotation techniques and make the flotation process economically and technically feasible.

2.8.1.4 Filtration

The recovery of microalgal biomass by filtration involves a semi-permeable membrane that acts as a filter to separate solid from liquid. This semi-permeable filter is comprised of pores smaller than the cells being retained, allowing selective passage of substances smaller in size than the pores of the filter. Membrane filtration processes mainly involve two flow configurations: dead-end and tangential flow. In case of dead-end membrane filtration, the flow is perpendicular to the membrane surface. Dead-end filtration is generally a batch process, where cartridge filtration, vacuum drum filters, and horizontal filter press are the three common technologies that work in dead-end mode. In tangential membrane filtration, the flow is tangential to the membrane surface. Tangential flow filtration (TFF) consists of synthetic semi-permeable membranes with pore sizes ranging from a few Angstroms to a few Microns. Based on the pore size of the membrane, the membrane filtration is classified as microfiltration, ultrafiltration, nanofiltration, and reverse/forward osmosis [186].

Harvesting of microalgae through membrane filtration is usually carried out within the ultrafiltration-microfiltration range [187]. The forward osmosis membrane process is the optimum membrane filtration technique for the harvesting of microalgal biomass from dilute media as it also helps to reduce power consumption [188]. Membrane filtration follows a common rule of thumb, according to which a membrane filtration must have a pore size 10-20 times smaller than the cells that are to be retained [150]. Research by Rossi et al. (2004) found that ultrafiltration membrane performs better than microfiltration membranes at steady-state permeance [189]. On the other hand, some researchers concluded that applying an ultrafiltration membrane is pointless, as lower initial fluxes and higher operating pressures overshadow better performance [190]. Drawbacks of using membrane filtration include membrane pore blocking, cake formation, and adsorption of gel-flocculants such as EOM. Fouling can be reduced by back-flushing [191], membrane surface modification, addition of coagulants, dynamic filtration, and shear enhancement [192]. The PES/MWCNT-1/LiBr-5 membrane developed by thermally induced phase separation process exhibited high porosity and hydrophilic nature, which contributed to remarkable algae permeation and anti-fouling properties, respectively [193]. Polymeric and ceramic membranes are most commonly used to recover a wide variety of microalgae, although polymeric membranes are mostly preferred because of their low-cost. Filtration is a highly efficient and chemical-free process. The cell integrity remains undisturbed; hence, this harvesting technique is applicable for shear-sensitive species. Moreover, the process allows the reusability of the medium. The filtration process is

non-toxic and thus, is well suited for human and animal food applications. However, high operational costs due to pumping requirements and the high tendency of membrane fouling along with low membrane selectivity are the underlying weaknesses of this process [26].

2.8.2 Chemical method

Chemical method employs inorganic and organic flocculants to harvest microalgal biomass. In all the approaches of flocculation, small algal cells suspended in the growth medium are combined to form large aggregates followed by the accumulation of aggregates into bigger flocs [157]. Flocculation is usually used in combination with other harvesting techniques [21]. The settling rate can be enhanced through flocculation as it results in the aggregation of microalgal cells, thus increasing the size of the particles [25]. Flocculation being able to settle huge quantities and a wide range of microalgae becomes a superior technique to harvest algae [165]. Aggregation of microalgal cells require the negatively charged cell surface to be neutralized by the addition of flocculants [194]. Charge dispersion is the concept followed by the flocculation method [195]. This harvesting method specifically causes ionic interaction between cells and flocculants, and salts existing in the growth medium [196].

2.8.2.1 Inorganic flocculation

Inorganic chemicals possessing multivalent cations such as ferric chloride, ferric sulfate, and aluminum sulfate are the most widely used inorganic flocculants. The addition of iron or aluminum-based inorganic flocculants either reduces or neutralizes the negative charge attributed by the COOH terminal on the microalgal cell surface [60]. Dissolution of cationic salts in the growth medium releases its respective cations, which neutralizes or reduces the electrostatic force of repulsion between the algal cells, enabling the cells to form large flocs [195]. The flocculation efficiency of a flocculant is determined by its ionic strength. Therefore, ferric chloride and aluminum sulfate having trivalent cationic salts are the most widely used flocculant as compared to divalent cationic salts [181].

Chlorella cells were more efficiently flocculated by the addition of aluminum salts in comparison to ferric salts [197]. With respect to optimal flocculant dose, pH, and quality of the resultant medium, alum was found to be superior to ferric salt. The high solubility of chloride at a wide concentration range enables the salt to attain maximum flocculation efficiency as compared to sulfate salts [197]. Studies found that lower electronegativity of $CaSO_4$, $CaCl_2$, $MgSO_4$, $MgCl_2$, $(NH_4)_2SO_4$, and NH_4Cl salts resulted in lower harvesting efficiency [197].

Harvesting of biomass by inorganic flocculation is simple, fast, highly efficient, and economical as no energy is required. However, inorganic flocculants tend to have adverse effects on algal cells. It may also change the colour and modify the chemical composition of the algal growth medium, making it unsuitable for reuse [77]. Although inorganic flocculants such as iron and aluminum salts are relatively inexpensive compared to most synthetic organic flocculants, the higher concentration required to accomplish high flocculation efficiency ultimately increases the cost of harvesting. This also generates a huge quantity of sludge [48]. Inorganic flocculants work on specific microalgal species. Flocculation efficiency of inorganic flocculants is low in marine water, as it tends to coil in the high ionic environment; hence, inorganic flocculants are not suitable for harvesting marine microalgae [22].

2.8.2.2 Organic flocculation

Organic flocculants are natural or synthetic polymers that are either branched or linear and carrying cationic, anionic, or non-ionic charges [198]. However, as the microalgal cell surface is negatively charged, the role of anionic or non-ionic flocculants becomes insignificant [165]. Unlike inorganic flocculants, organic polymer flocculants with varying physicochemical properties are highly efficient even in low doses of a few milligrams per litre, and they generate smaller sludge volume without consumption of alkalinity [165]. Polymeric flocculants such as cationic polymers possess the dual ability of coagulation and flocculation. Coagulation is defined as a process by which a stabilized particle is destabilized by addition of a chemical compound, i.e., coagulant. On the contrary, flocculation is the coalescence of separate suspended microalgal cells into larger loosely attached conglomerates [161]. Cationic polymers neutralize the negative charge carried on the microalgal cell surface and simultaneously binds to the surface of two or more algal cells, thus, forming a bridge among the destabilized particles [199].

In contrast to natural polymeric flocculants, synthetic organic polymeric flocculants (e.g. Polyacrylamide and its derivatives) release very toxic monomers such as acrylamide and ethyleneimine, which may cause potent neurotoxic effects [200]. However, the overall efficacy of synthetic versus natural polymers depends on several factors such as pH, salinity, biomass concentration, and algal organic matter (AOM) [201]. In general, non-toxic and biodegradable natural polymeric flocculants such as starch, cellulose, and chitosan have received more interest as compared to synthetic flocculants [202]. It has been reported that 30 ppm of cationic locust bean gum biopolymer could successfully harvest 97.42% of *Scenedesmus* sp. [203]. One of the major drawbacks of polymeric flocculants is that they fail to flocculate marine algae.

The high salinity of the sea and brackish waters leads to the shrinking of the polymers to a smaller size, thus, failing to bridge the algal cells [204]. The high ionic strength of the marine environment attributes to the incompetence of polymeric flocculants to flocculate marine microalgae [165]. Cationic polymers are found to be effective in flocculating microalgae when the salinity of the medium is less than 5 g L^{-1} [157]. Chitosan is a natural polymeric flocculant with enhanced cationicity and is efficient in flocculating both fresh and marine microalgae at low pH without contaminating the microalgal biomass [151]. However, chitosan requires high dose (20 mg L^{-1}– 150 mg L^{-1}) as compared to other synthetic flocculants and is too expensive to be used for industrial-scale [60]. Chitosan is replaced by cationic starch, which is not too expensive and pH-dependent; however, it works at higher concentrations [205]. Thus, organic flocculants can harvest a huge amount of biomass easily and efficiently with no energy input. However, its commercial application is hampered due to the high cost of organic flocculants.

2.8.3 Biological methods

2.8.3.1 Autoflocculation

Among all the harvesting techniques, autoflocculation is the most inexpensive and eco-friendly method, also the process holds good for reusing the medium [162]. A study found that high pH, usually above pH 9 induces autoflocculation [206]. In the case of a high pH-induced autoflocculation, the cell wall interacts with divalent cations [207]. Calcium and phosphate ions in the culture medium get supersaturated with the increase of pH, causing the neutralization of the negatively charged microalgal cells by the positively charged calcium phosphate precipitate [181]. However, a prerequisite amount of phosphate (0.0031–0.0062 g L^{-1}) and calcium (0.06–0.1 g L^{-1}) is required to achieve autoflocculation at pH 8.5-9 [208]. Some researchers have reported achieving 80% flocculation efficiency by replacing calcium and phosphate by the addition of lime [209]. Knuckey et al. (2006) obtained 97±2% settling efficiency at pH 10 for *Scenedesmus*. He observed that at pH 10, the flocs lead to the formation of a robust structure due to which high settling efficiency was obtained [210]. However, it is not fit for industrial-scale harvesting, as it is time-consuming, unreliable, and suits only a few microalgae species [162,163,211].

2.8.3.2 Bioflocculation

Bioflocculation is a flocculation process where microalgal cells are flocculated with the assistance of flocculants that are of biological origins (plants, animals, microorganisms, etc.) [212]. Bioflocculants are macromolecular polymers produced by some species of higher plants (*Moringa oleifera*, *Strychnos potatorum*, *Plantago ovata*, *Moringa stepolata*, *Jatropha curcus*)

and microorganisms such as bacteria, fungi, and some microalgae or their metabolites [55]. These microorganisms produce flocculating agents at certain stages of growth in a liquid medium. Flocculant production by these microorganisms is influenced by media composition and environmental conditions (temperature and pH). The major constituents of most bioflocculants are carbohydrates/polysaccharides, proteins, nucleic acids, polyphenols, and glycoproteins. Bioflocculants have functional groups such as carboxylic (-COOH), hydroxyl (-OH), amino ($-NH_2$), methoxy ($ROCH_3$), and amide ($RCONR_2$) groups that enable them to react with and flocculate microalgae in solution [212]. Table 2.3 details various bioflocculants used for recovering microalgal biomass.

Table 2.3. Recovery of microalgal biomass by bio-flocculation.

Microalgae	Bioflocculant	Algal concentration	Flocculant dose	Process time	R(%)	Features	Ref.
Nannochloropsis sp.	Mung bean (Vigna radiata) protein extract	1.12 OD @540 nm	20 mL L^{-1}	2 h	>92 (pH 2)	Bioflocculant adds protein content in microalgal flocs	[62]
Chlorella vulgaris	*Aspergillus oryzae* (FSA)	-	1.2×10^4 spores mL^{-1}	-	92.2 (pH 4-5)	Chance of fungal contamination	[213]
Chlorella vulgaris	γ-PGA produced by *Bacillus subtilis*	1.2 g L^{-1}	20 mg L^{-1}	-	95	Affects microalgal cell integrity to some extent	[214]
Chlorella vulgaris	Bacteria in seafood wastewater effluent	20 mg L^{-1}	240.0×10^6 CFU mL^{-1}	-	92	Environment friendly	[215]
Pleurochrysis carterae	EPS produced by tap water bacterial inoculum	-	-	30 min	90-93	Reusability of the medium	[164]
Desmodesmus brasiliensis	γ-PGA produced by *Bacillus licheniformis*	0.5 g L^{-1}	2.5 mg L^{-1}	1 min	≥98	Biochemical composition of biomass remains intact	[63]
C. reinhardtii	Proteins extracted from *S. bayanus var. uvarum*	1 OD @660 nm	0.1 mg mL^{-1}	180 min	95 (pH 7.5)	Depends on extracted protein concentration	[216]
Chlorella sp.	*Moringa oleifera seed*	17×10^6 cells mL^{-1}	0.01 g L^{-1}	30 min	95 (pH 6.9-7.5)	Economically viable	[217]
Chlorella sp.	*Penicillium sp.* (FSA)	-	1.1×10^4 spores mL^{-1}	28 h	99 (pH 7)	Requires high glucose input	[218]
Chlorella sp.	*Pleurotus ostreatus* (FPA)	-	10 g (wet weight)	150 min	64.86	Harvested biomass can be used for feed or food production	[219]

Optical density (OD); Poly γ-glutamic acid (γ-PGA); Extracellular polymeric substances (EPS); Fungal spore-assisted (FSA); Fungal pellet-assisted (FPA)

Plant-Based Flocculants

The application of plant derivatives as bioflocculants is widely recognized for wastewater treatment [220]. Plant-based flocculants are currently gaining attention in microalgal harvesting owing to its low-cost, availability, non-toxicity, biodegradability, renewability, and environmental friendliness. Some plant species have bioactive coagulating agents in various sections such as seeds, leaves, and roots. These bioactive agents can be used as bioflocculant either in crude or purified form for harvesting microalgae. *M. oleifera* seed powder was able to flocculate 93.8% of *Nannochloropsis oculata* at a flocculant concentration of 4 g L^{-1} [221]. In a comparative study, Ali et al. (2019) compared the flocculation efficiency of four different seeds - de-oiled *Jatropha curcus*, *Azadrichta indica*, *M. oleifera*, and *Conocarpus erectus*, with a chemical flocculant (alum) for harvesting mixed microalgal species from domestic wastewater [222]. Among all the flocculants, powdered seeds of *Azadrichta indica* were able to achieve a maximum harvesting efficiency of 97.9% at a concentration of 0.1 g L^{-1}, mixing speed of 100 rpm, pH 9, and incubation period of 10 min. In another study, a constant dose (0.15 g L^{-1}) of *M. oleifera* seed powder was used to flocculate *Chlorella* sp. at three different pH values (9, 10, 11). Maximum flocculation efficiency was obtained at pH 11, suggesting that its efficacy is pH dependent [223]. The authors reported that at pH 11, the amino acid components of the flocculant were ionized into carboxylic and proton ions, which further reacted with negatively charged cell surfaces of *Chlorella* sp., thus resulting in flocculation.

Bacteria-based flocculants

In bacteria-mediated flocculation, microalgae flocculate with the help of the extracellular polysaccharides (EPS) and gamma glutamate that are secreted by bacteria [224]. Charge neutralization, electrostatic patching, or bridging are the mechanisms involved in bacteria-mediated bioflocculation, where the bioflocculants (EPS and gamma glutamate) with positively charged functional groups aggregate with the negatively charged microalgal cells [225]. The flocculation efficiency of bacteria-based flocculants depends on the quantity of EPS secreted by bacteria, attachment capacity between microalgae and polymers, and growth phase of the bacteria [157]. Uronic acids and pyruvic acids are the most commonly involved EPS during bioflocculation [226]. Poly γ-glutamic acid produced by *Bacillus licheniformis* CGMCC 2876 was successful in harvesting *Desmodesmus* sp. F51 with a

recovery efficiency of 92% [227]. *Bacillus subtilis* rich in poly γ-glutamic acid (19–22 mg L^{-1}) was successful in harvesting 95% and more than 90% of *C. vulgaris*, *C. protothecoides* and *N. oculata* LICME 002, *P. tricornutum*, respectively [214]. Thus, poly γ-glutamic acid facilitated bioflocculation proved to be an efficient harvesting method as it does not interfere with the cell integrity and the lipid content of the biomass. In another study, a bioflocculant FLC-hn06 extracted from the bacterium, *Streptomyces* sp. hsn06 showed a flocculation efficiency of 93% for *Chlorella vulgaris* at a concentration of 0.02 g L^{-1} [228]. Microorganisms involved in bioflocculation may even add on to the total lipid content [229]. Flocculants extracted from bacteria reduce the cost of harvesting to a great extent by eliminating the need for chemical flocculants. However, during bacteria mediated flocculation, there is a chance of bacterial contamination. Hence, the microalgal biomass harvested through this process is not safe for food applications.

Fungi-based flocculants

A symbiotic relationship was observed between microalgae and fungi. The fungi uptakes the nutrients especially exuded polysaccharides produced by microalgae during the photosynthetic process, and in return, the algae is protected from the external environment by the fungal filaments, which also holds the culture medium, thus, providing a large area for nutrients [230]. The self-pelletization process of filamentous fungal species can be elucidated by either coagulative or non-coagulative methods [231]. In coagulative process, the spores aggregate with microalgae to form pellets. *Aspergillus* sp., *Basidiomycete* sp. and *Phanerochaete* sp. flocculates microalgae through a coagulative method by forming dense spherical aggregates [231]. Whereas, in non-coagulative process, the hyphae germinated from the spores interlinks to form aggregates. The fungal strains such as *Rhizopus* sp., *Mucor* sp., and *Penicillium* sp. flocculates microalgae through a non-coagulative process [231]. These non-coagulative pellet strains have lower hydrophobicity, shorter germination period, and higher growth rate as compared to coagulative pellet strains. These properties of non-coagulative pellet strains retard the spore aggregation rate and time, thereby allowing the spores to germinate first and then form pellets [232,233]. It has been reported that *Rhizopus arrhizus* and *Mucor rouxii* spores germinate after 5 h of cultivation, whereas *A. niger* spores germinate after 8–10 h of cultivation [234–236]. Fungus-mediated flocculation does not require any additional energy or chemicals to be added, thus, making the harvesting process sustainable. However, this harvesting process is unreliable, as the process of flocculation is uncontrolled. High chances of fungal contamination stand as the major drawback of this harvesting

technique. Moreover, bioflocculation requires relatively high organic carbon source to cultivate autoflocculating microorganisms (such as algae, bacteria, and fungi) for flocculating microalgae.

2.8.3.3 Factors influencing microalgal flocculation

The characteristic of microalgal cell surfaces plays a key role in flocculation. Moreover, these characteristics of cell surfaces differ among the species and vary within a species based on culture conditions. Smaller algal cells require higher flocculant dosages to be harvested when compared to the larger cells of the same amount because the ratio of the microalgal cell surface to biomass decreases with increasing cell size [237]. Flocculation is also influenced by the varying biochemical composition of the algal cell surface [238]. The pH of the growth medium plays an important role in flocculation by not only altering the charge of an algal cell surface but also of chemical flocculants. Furthermore, a large amount of AOM consisting of proteins and polysaccharides is often excreted in the growth medium. These organic matters may interact with flocculants and thus, inhibit flocculation of algal cells [239]. The protein excreted in the medium forms complexes with the cationic ions of most chemical flocculants, whereas polysaccharides interact with the cationic flocculants, thus, making the flocculants unavailable for flocculating microalgal cells. The algal growth phase plays a leading role in flocculation as the pH of the culture medium, dissolved carbon dioxide, zeta potential, and algal cell size varies significantly throughout the growth period [157]. As these factors tend to vary with the algal growth, it is difficult to obtain the optimum flocculant dose. The polymer dosage plays a vital role in flocculation. Weak polymer bridging may result if the polymer dosage is less than the optimum amount, and the potential of bridging may be impaired due to electrostatic hindering if the dosage is too high [157]. Therefore, among all the growth phases, the stationary phase is found to be advantageous as the cellular metabolic activity, zeta potential, and cell mobility is lowered, and intercellular interactions are raised [53].

2.8.4 Electrical based harvesting techniques

Electro-flocculation is a physicochemical process where an anode such as iron or aluminum releases metal cations that induce coagulation [165]. In the process of electro-flocculation, flocculants are not required, and the only requirement is an electricity supply [240]. In this process, the electrodes are positioned vertically in the medium, the negatively charged microalgae move towards the positively charged anode, resulting in charge neutralization and enabling to form aggregates [166]. Electroflotation follows the same

principle as electroflocculation in which the anode is an active metal. Recently, electro-coagulation-flotation (ECF) process came to limelight as an alternative to the coagulation process, in which the hydrogen bubbles generated through water electrolysis at the anode are coupled with the electrocoagulation process at the cathode [241].

Electrical based harvesting technique applies two types of electrodes, sacrificial and non-sacrificial [165]. In the case of sacrificial electrodes, the metal ions are released from the active anode to the culture broth based on the current intensity of the electrolytic solution. The released cationic metal ions then destabilize and aggregate the anionic microalgal cells [165]. The cationic ions that are released from the anode are not toxic as compared to chemical coagulants [242]. However, in the case of non-sacrificial electrode, the negatively charged microalgal cells move towards the anode. Once the microalgal cells reach the anode, they destabilize and aggregate. The use of non-sacrificial electrodes leads to fouling. The material of the electrodes influences the efficiency of the electrical-based harvesting process. In this harvesting process, electrodes are most commonly made of aluminum and iron. As compared to aluminum electrodes, iron electrodes have lower current efficiency due to which iron electrodes dissociate to a lower extent resulting in lower harvesting efficiency [157]. Moreover, ferric electrode consumes more energy and ferric oxide formation results in browning of slurry. So, the aluminum electrodes have received more attention as compared to iron electrodes [157].

Current density is inversely proportional to the harvesting period and plays a key role in electroflocculation. With the increase in current density, more cationic metal ions are formed at the anode by oxidation, thus, improving the harvesting efficiency by decreasing the time required for harvesting [157]. However, energy consumption increases with the increase of current density. Gao et al. (2010) found that energy consumption increased from 0.2 kWh m^{-3} to 2.28 kWh m^{-3} when the current density was increased from 0.5 mA cm^{-2} to 5.0 mA cm^{-2} [241]. Thus, achieving efficient harvesting with a high current density is impractical without maintaining an equilibrium between current density and energy consumption [157]. Mixing and settling were carried out post electroflocculation to reduce energy consumption. Mixing increases the probability of cell contact and allows the cells to aggregate [157]. On the other hand, higher harvesting efficiency with lower settling time was achieved when flotation was carried out post electroflocculation [243]. With the rise of process temperature, cell collision and their transportation rate tend to increase [241]. In a harvesting experiment conducted by ECF technology, an increase in harvesting efficiency from 46% to 98% was observed with the rise in temperature from 18 °C to 36 °C [241]. An increase in process temperature also helps

in reducing the electrolysis time as it enhances the dissolution rate of metal ions [157]. Therefore, the reduction of electrolysis time helps to reduce the process energy consumption. As there is little chance of flocculant contamination, the harvested biomass is safe for the use of animal feed or food [166]. However, electroflocculation tends to contaminate the algal slurry with the residual metals released from metallic electrodes during the process. Since these trace metals may impair the value of the end products, further processing may be required [244]. The high power density involved in this harvesting process may impair cell integrity. There is also a high chance of cathode fouling. Thus, electro-flocculation being a power-induced process with high electrophoretic equipment cost, fails to be applicable for large-scale.

2.8.5 Magnetic particle assisted harvesting

In recent years, magnetophoretic separation of microalgae has gained much attention due to its potential over traditional harvesting techniques. Magnetic particles assisted harvesting is based on a simple separation method in which micro- or nano-sized magnetic particles are adsorbed by the suspended microalgal cells [245]. The magnetic particle tagged cells are recovered based on their intrinsic paramagnetic movement owing to the external magnetic force [246]. An ideal magnetic particle should be cost-effective, non-toxic, stable, reusable and must possess high adsorptive power for efficient harvesting.

Microalgal harvesting is generally carried out by two types of magnetic particles, naked and surface functionalized. In the case of naked magnetic particles, electrostatic interactions between the negatively charged algal cells and positively charged magnetic particles allow the microalgal cells to be harvested [247]. Naked magnetite synthesized by different methods was found to be successful in harvesting both marine and freshwater microalgal cells [245]. Among various magnetic nanoparticles, Fe_3O_4 particles were successfully used for recovering a wide range of microalgal strains owing to its specific surface area and super-paramagnetism [248]. Researchers found that up to 95% of harvesting efficiencies can be obtained for freshwater microalgal species *Botryococcus braunii* and *Chlorella ellipsoidea*, and the marine species *Nannochloropsis maritima* using Fe_3O_4 nanoparticles synthesized through chemical co-precipitation [248,249]. Relatively high harvesting efficiency was attained with naked iron oxide magnetic microparticles (IOMMs), as IOMMs releases cationic Fe ions from its surface, which acts as flocculant, thus, facilitating the harvesting process [247]. However, the chance of biomass contamination with the released metal ions is one of the major disadvantages of this harvesting process [168].

As the surface charge of uncoated magnetic particles is pH-dependent with an isoelectric point of around 7, the uncoated surface needs to be functionalized with cationic ions to enhance the harvesting efficiency [250]. In case of surface functionalized magnetite, there are two strategies for tagging polyelectrolyte, "attached-to" and "immobilized-on" strategy. In the "attached-to" approach, the surface of microalgal cells is coated with a polymer binder that helps attach with the magnetic particles. In case of "immobilized-on" strategy surface of the uncoated magnetic particles are functionalized with a polyelectrolyte that aids the binding with the algal cells [251]. A higher harvesting efficiency was attained with an equivalent dose of particles in the "immobilized-on" approach compared to the "attached-to" approach owing to the superior distribution and colloidal stability of the "immobilized-on" particles [252]. Thus, the "immobilized-on" strategy is widely used.

The "immobilized-on" approach based chitosan-Fe_3O_4 nanoparticle composites were able to harvest 99% of *Chlorella* sp. KR-1 without altering the culture medium pH. Moreover, this magnetophoretic process showed the potential for reducing the cost of algal fuel production by recycling the harvested medium without any adverse effects on algal cell growth [253]. In another study, recyclable aminoclay-nanoscale zero-valent iron (nZVI) composite was able to harvest ~100% *Chlorella* sp. KR-1 within a short time of 3 min at a > 20 g L^{-1} loading of the composite under an external magnetic field [125]. Similarly, $BaFe_{12}O_{19}$ particles functionalized by (3-aminopropyl)triethoxysilane (APTES) harvested 99% of *Chlorella* sp. KR-1 and after harvesting, the detachment efficiency of $BaFe_{12}O_{19}$ particles from algae-particle conglomerates was found to increase proportionally with the size of magnetic particles [254].

This harvesting approach is highly efficient, eco-friendly, requires low energy, and enables the medium along with the nanoparticles to be reused. However, the process requires a high dose of magnetic nanoparticles. These nanoparticles are expensive and require special equipment for recycling them.

2.9 Biomass as a Precursor for Carbon-Based Catalyst

A huge amount of biomass residues are generated following human agricultural activities such as harvesting and oil extraction. These residues usually have a poor commercial value, and their potential is often being ignored. In recent years, several researchers have been exploiting low-cost biomass by converting it into value-added products through various post-processing processes. Biomass waste is a sustainable source that can be converted into a porous carbonaceous material for catalyst synthesis. Biomass-based catalysts are non-toxic,

biodegradable, and possess a higher surface area than conventional catalysts [87]. Shu et al. (2009) were among the first to use vegetable oil asphalt as the biomass source for producing carbon support [255]. Since then, many researchers have focused on developing high-performance biomass-based catalysts for a variety of applications, such as esterification and transesterification of vegetable oils for biodiesel production.

2.10 Biomass-Derived Heterogeneous Catalyst in Biodiesel Production

Conventional homogeneous acid and base catalysts used in biodiesel production industries consume a large amount of energy during the separation process and corrodes the processing equipment [87]. Heterogeneous catalysts exist in different phases than the reactants, generally as solid in aqueous reactants. Therefore, a heterogeneous catalyst is considered a better choice over a homogeneous catalyst because of its ease of separation and anti-corrosion properties. The synthesis routes of conventional heterogeneous catalysts involve several complicated synthesis steps and expensive raw materials. On the other hand, the synthesis routes of biomass-derived heterogeneous catalysts are sustainable, as it require very low-cost raw materials and involves low capital and operating cost [256]. Therefore, biomass waste serves as a sustainable alternative for the synthesis of a heterogeneous catalyst. The efficiency of the biomass-derived catalyst is influenced by the chemical and physical properties of the biomass, such as biomass composition and cell structures [257]. For instance, the presence of a large quantity of protein and nitrogen atoms in the biomass has been reported to interfere with the pore development in the carbon precursor during carbonization [258].

2.10.1 Transesterification reaction by heterogeneous base catalysts

Biomass is generally converted into a heterogeneous base catalyst for biodiesel production through two main pathways. Biomass can be directly converted into a base catalyst such as calcium oxide through thermal treatment [259,260]. Biomass can also be transformed into supporting material such as silica support or activated carbon for the attachment of basic active compounds such as CaO, alkali metals, KOH, NaOH, etc. [87,261,262]. Alkaline earth metal oxide, especially CaO, possesses high basic strength and exhibits a high catalytic activity for biodiesel production. The CaO catalyst can be synthesized through the calcination of calcium carbonate at a high temperature [87]. The decomposition reaction from $CaCO_3$ to CaO is shown in equation (1.1).

$$CaCO_3 \rightarrow CaO + CO_2 \quad (1.1)$$

2.10.1.1 Direct conversion of biomass into base catalyst

Mucino et al. (2014) synthesized CaO catalyst from $CaCO_3$ rich sea sand through calcination at 800 °C for 2 h. FAME yield of 95.4% was obtained from cooking oil using 7.5 wt.% of CaO catalyst [263]. CaO catalyst synthesized by calcination at 900 °C also resulted in biodiesel yield and conversion above 97% [87,259]. In general, the particle size of CaO derived catalyst varies in the micrometer range with a smaller surface area [87]. Teo et al. (2017) successfully synthesized waste eggshell-derived superbasic CaO nanocatalyst through surfactant assisted precipitation method. The surface area of the CaO nanocatalyst (22.31 m^2 g^{-1}) was found to be much higher than the commercial CaO (7.29 m^2 g^{-1}) [264].

A novel CaO catalyst derived from *Turbonilla striatula* waste shell doped with 1% of $BaCl_2$ solution achieved FAME conversion above 98% at 60 °C reaction temperature, 8 h reaction time, and 6:1 methanol to oil ratio. The study found that CaO catalyst doped with metal ions increased the basicity of catalyst from 0.1 mmol g^{-1} to 0.2375 mmol g^{-1} [265]. In another study, Mansir et al. (2018) achieved a FAME yield of 90% in 3 h using *Gallus domesticus* shells derived CaO catalyst doped with molybdenum and zirconium (Mo-Zr). Moreover, it was observed that the CaO catalyst doped with Mo-Zr oxides reduced the leaching of Ca^{+2} ions and improved the reusability of the catalyst [266].

2.10.1.2 Synthesis of biomass as supporting material for base catalyst

Direct conversion of biomass into base catalyst involves basic oxide synthesis, such as CaO catalyst derived from biomass through calcination. However, the standalone application of CaO catalyst has several limitations, such as low surface area and is easily deactivated by moisture [87]. To overcome these problems, ash and activated carbon have been widely used as supporting material for base catalyst. Ash is generally produced as a residue after the combustion of organic compounds. Rice husk ash and coal fly ash are the two most commonly used supporting materials for base catalyst [267,268]. Chen et al. (2015) developed low-cost catalyst support for CaO by calcining rice husk at 800 °C to produce rice husk ash. Meanwhile, the CaO was produced from the calcination of the eggshell at 400 °C for 4 h. A maximum FAME yield of 91.5% was achieved using rice husk ash-supported CaO catalyst at 7 wt.% catalyst loading, 9:1 methanol to oil ratio, 65 °C, and 4 h reaction time [267].

In addition to supporting material for CaO, ashes are also widely used as catalyst support for alkali metals. Hindryawati et al. (2014) used silica-rich rice husk as support for alkali metals such as lithium (Li), sodium (Na), and potassium (K). The inert property, along

with the ability to create better dispersion of active sites, makes amorphous silica a good supporting material. The process was able to transesterify used cooking oil to FAME in the range of 96.5–98.2% in 1 h for all three Li, Na, and K silicate catalysts [262]. In another study, Buasri et al. (2011) produced activated carbon from palm shell and used as alkali earth metal support. However, the supported alkali earth metal catalyst resulted in a slightly lower FAME yield as compared to commercial CaO catalyst with the same catalyst amount (10.5 wt.%) [269]. One of the major drawbacks of base catalyst is that it is not suitable for simultaneously esterification and transesterification reaction of oils with high free fatty acids. Table 2.4 summarizes the base catalyst synthesized from different biomass sources and their respective optimum biodiesel production reaction conditions.

Table 2.4. Transesterification reaction by using biomass-derived heterogeneous base catalyst in biodiesel production.

Biomass	Type of CaO-based catalyst	Oil feedstock	Temperature (°C)	Alcohol to oil molar ratio	Reaction time (h)	Catalyst Loading (wt.%)	Yield (Y)/Conversion (C) (%)	Reusability (cycles)	Ref
Obtuse horn shell	Waste CaO	Refined Palm Oil	-	12:1	6	5	Y= 86.75	3	[260]
Barnacle	Waste CaO	Waste catfish fat	65	12:1	3	4	C= 97.20	4	[270]
Chicken manure	Waste CaO	Waste cooking oil	65	15:1	6	7.5	Y= 90.80	2	[271]
Eggshell	Doped CaO	*Mesua Ferrea L.* seed oil	65	10:1	4	5	C= 94.00	2	[272]
Snail shell	Waste CaO	Waste soybean oil	60	6.03:1	8	2	Y= 87.28 C= 99.58	-	[273]
Quail eggshell	Waste CaO	Sunflower oil	60	10.5: 1	2	2	Y= 99.00	3	[274]
Mud clam shell	Waste CaO	Crude Castor Oil	60	14:1	2	3	Y= 96.70	5	[275]
Meretrix venus shell	Waste CaO	Palm oil	60	12:1	2	10	Y= 92.30	-	[276]
Rice husk ash, egg shell	Rice husk ash supported CaO	Palm Oil	65	9:1	4	7	Y= 91.5	8	[267]
Flamboyant pods	Activated carbon supported KOH	Rubber seed oil	55	15:1	1	3.5	Y= 89.81	-	[261]

2.10.2 Transesterification reaction by heterogeneous acid catalysts

Activated carbon prepared from various carbon sources has been widely used to synthesize sulfonated carbon-based catalysts through the direct sulfonation method. Direct sulfonation using concentrated H_2SO_4 is the most simplest and commonly used sulfonation method among all the existing acid catalyst preparation techniques. The direct sulfonation method does not require any complicated pretreatment, thereby making the process economical [277]. Ezebor et al. (2014) synthesized heterogeneous acid catalysts by partial carbonization and sulfonation of sugarcane bagasse and oil palm trunk for biodiesel production. The FTIR bands at about 1160 cm^{-1} and 1030 cm^{-1} indicated the stretching vibrations of $–SO_3H$ and S=O, respectively, which confirmed the successful attachment of SO_3H. FAME yield of 94.34% and 93.36% was obtained for palm trunk and bagasse-derived catalysts, respectively. The study reported that the catalytic activity of palm trunk and bagasse-derived catalysts were comparable with the conventional sulfated zirconia catalyst which produced a 90% yield of methyl palmitate under the esterification reaction between methanol and palmitic acid [256]. Zong et al. (2007) reported that the catalytic activity of the sulfonated carbon-based catalyst for biodiesel production is much higher than that of sulfonated zirconia, as the former possess higher acid site densities [278]. In another study, Zeng et al. (2014) obtained a highest FFA conversion of 90.2% using a strong solid acid catalyst synthesized through partial carbonization and sulfonation of agricultural bio-waste peanut shells [279]. The carbonization and sulfonation processes are reported to be rapid and energy-efficient for low molecular weight biomass such as corn straw, yellow horn hulls, and bagasse as compared to complex molecular weight biomass such as peanut shell, jatropha hulls, biochar, cassava stillage residue, and corncob residues [277].

Ezebor et al. (2014) studied the effect of sulfonation time on the catalytic activity of palm trunk and bagasse-derived catalysts. The total acid density of catalysts and biodiesel yield was found to increase with the increase in sulfonation time from 2 h to 6 h. However, a marginal effect on sulfonic acid density was observed on increasing the sulfonation time beyond 6 h [256]. Zhou et al. (2006) on the other hand, obtained a maximum FAME conversion of 98.4% using carbon-based heterogeneous acid catalyst derived from bamboo with only 2 h sulfonation time. However, the process required a higher esterification temperature (90 °C) to maximize the FAME yield [280].

Apart from direct sulfonation using concentrated H_2SO_4, some special sulfonating agents such as fuming sulfuric acid, 4-benzene diazoniumsulfonate (4-BDS), p-tolunesulfonic

acid (PTSA), sulfur trioxide, and chlorosulfonic acid can also sulfonate carbonaceous materials [87]. Liu et al. (2013) had successfully synthesized solid acid catalyst by sulfonating carbonized corn straw with fuming sulfuric acid (50 wt.% SO_3). They obtained a FAME yield of 92% at 60 °C reaction temperature for 4 h with methanol: oil molar ratio of 3 and catalyst concentration of 3 wt.% [78]. Katsner et al. (2012) achieved biodiesel conversion of 97% using wood chip-derived carbon-based solid acid catalyst, which was sulfonated using gaseous sulfur trioxide [281]. In another study, Wang et al. (2013) had functionalized the carbonized sawdust with p-toluenesulfonic acid (PTSA). The PTSA functionalized solid acid catalyst was able to esterify high acetic acid containing bio-oil with a conversion rate of 86.6% [282]. However, the carbonaceous materials need to be pretreated before adding a special sulfonating agent, making the process economically unsustainable in comparison to the direct sulfonation method using concentrated H_2SO_4 [277]. Table 2.5 summarizes the acid catalyst synthesized from different biomass sources and their respective optimum biodiesel production reaction conditions.

Table 2.5. Transesterification and esterification reaction by using biomass derived heterogeneous acid catalyst in the biodiesel production.

Biomass	Sulfonation method	Oil feedstock	Temperature (°C)	Alcohol to oil molar ratio	Reaction time (h)	Catalyst Loading (wt.%)	Yield (Y)/Conversion (C) (%)	Reusability (cycles)	Ref
Deoiled coconut meal	In situ partial carbonization with conc. H_2SO_4	Waste palm oil	65–70	12:1	12	5	Y= 92.70	4	[283]
Coffee residue	Direct sulfonation (conc. H_2SO_4)	Caprylic acid	60	3:1	4	5	Y= 71.5	5	[284]
Durian peel residue	Direct sulfonation (conc. H_2SO_4)	Yeast lipid	65	10:1	1	9	Y= 78.73	4	[285]
Corn straw	Direct sulfonation (fuming sulfuric acid)	Oleic acid	60	7:1	4	7	Y= 98	-	[78]
Oil palm trunk	Direct sulfonation (conc. H_2SO_4)	Waste Oil	130	1.17 mL min^{-1}	4	12	Y= 80.6	4	[256]
Waste yeast residue	Direct sulfonation (conc. H_2SO_4)	waste cooking oil	60	10:1	6	4	Y= 96.2	-	[74]
De-oiled waste cake	Arylation/4-benzene-diazonium sulfonate	Oleic acid	64	20:1	10	3	C= 97	-	[258]
Sawdust	Direct sulfonation (conc. H_2SO_4)	Pongamia pinnatta oil	85	1:9	2	2	Y= 95.6 C= 64.5	3	[84]
Coconut shell	Direct sulfonation (conc. H_2SO_4)	Palm oil	60	30:1	6	6	C= 88.25	-	[286]

2.11 Knowledge Gaps

The above literature survey showed that there are significant reports on environmental stress induced lipid accumulation in microalgae; however, at the cost of reduced biomass content. Moreover, there are scanty reports on the change in fatty acid compositions of microalgae in response to stress and the correlation between stress-induced ROS and lipid accumulation. Therefore, it is necessary to develop a process and optimize stress conditions for obtaining enhanced microalgal growth and lipid accumulation.

Cost-effectiveness plays a major role when a pilot scale experiment is upgraded for industrial scale applications. In the literature survey section, it was clearly observed that most of the harvesting techniques were quite a time taking processes and require high energy and operational cost, and does not support the reusability of the harvested medium. Therefore, it is necessary to develop a sustainable and efficient harvesting technique.

Besides the high catalytic activity of the catalyst, the cost of the catalyst plays a vital role in shaping the economy of the overall process. Hence, catalysts with sufficient activity and low-cost are two important parameters for the sustainability of a catalytic process. As mentioned earlier, the conventional heterogeneous catalysts involve several complicated synthesis steps and expensive raw materials; therefore, biomass-derived heterogeneous catalysts are considered as a potential alternative. Though some of the heterogeneous catalysts used were synthesized from natural resources; however, scanty reports are available on the application of the catalyst for transesterification of microalgal oil. Hence, finding low-cost active catalysts always remains an indispensable research area for researchers working on catalysis.

2.12 Objectives

The aim of the current research is to develop a sustainable microalgal biodiesel production system. Based on the above knowledge gaps the following objectives were selected.

1. Isolation, characterization, screening and identification of potential microalgal strain for biodiesel production.

2. Process development and optimization of nutrient starvation for enhanced microalgal growth and lipid accumulation.
3. Development of sustainable and efficient harvesting technique.
4. Development and characterization of low-cost and eco-friendly catalyst for microalgal lipid transesterification to biodiesel.

भारतीय प्रौद्योगिकी संस्थान गुवाहाटी
Indian Institute of Technology Guwahati

Chapter 3

Process Development and Optimization of Nutrient Starvation for Enhanced Microalgal Growth and Lipid Accumulation

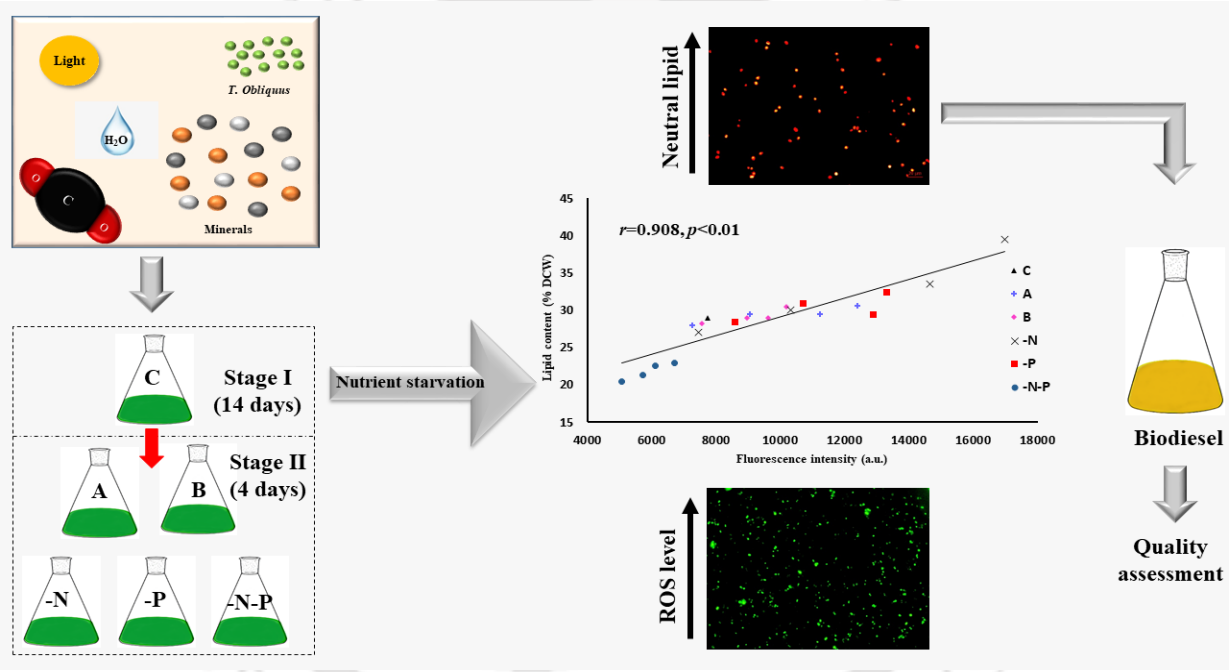

3.1 Overview

Microalgae accumulate a considerable amount of triacylglycerol when their cells are under nutrient-deficient conditions, making them one of the promising sustainable feedstock for biodiesel production. In this chapter, a novel microalgae, *Tetradesmus obliquus* KMC24 was isolated and exposed to nutrient stress (nitrogen and/or phosphorus) for a short period via two-stage cultivation to obtain maximum biomass and lipid. The effect of nutrient starvation on the morphology, biomass concentration, photosynthetic activity, and biochemical composition of *Tetradesmus obliquus* KMC24 was evaluated. Few recent reports suggested that oxidative stress-tolerant microalgae are highly efficient for biofuel production. To study the role of oxidative stress due to nutrient deficiency, responses of various stress biomarkers like reactive oxygen species (ROS), cellular enzymatic antioxidants such as catalase (CAT), ascorbate peroxidase (APX), and non-enzymatic scavengers such as polyphenols were also determined. Further, the correlation between stress-induced ROS and cellular lipid accumulation was investigated using these nutrient-starved cells. The influence of nutrient starvation on the fatty acid composition of *Tetradesmus obliquus* KMC24 and subsequently on the biodiesel quality was also studied.

3.2 Materials and Methods

3.2.1 Microalgae isolation and growth conditions

The water samples were collected from a drainage channel located in IIT Guwahati, Assam, India and inoculated in BG-11 medium. Individual microalgal strains were isolated through conventional serial dilution and plating methods [287]. The morphological identification of the strains was carried out by observing under a microscope (Axio Scope.A1, Zeiss, US). The pure algal culture was genetically identified via 28S rRNA gene partial sequencing (outsourced to Eurofins Genomics India Pvt. Ltd.) using the forward primer ITS1 (5′-TCCGTAGGTGAACCTGCGG-3′) and the reverse primer as ITS4 (5′-TCCTCCGCTTATTGATATGC-3′) [18]. NCBI BLAST (http://www.ncbi.nih.gov/BLAST) was used to carry out the homology studies of the partial 28S rRNA gene sequences of strain KMC24. Subsequently, the analyzed sequences were submitted to NCBI Nucleotide database using the BankIt sequence submission tool (www.ncbi.nlm.nih.gov/BankIt) and an accession number was obtained for the same. Furthermore, the phylogenetic tree was constructed using Neighbor-Joining method by using MEGA 7.0 software (Molecular Evolutionary Genetics

Analysis tool) [288]. The strain was cultured in a BG-11 (ATCC Medium 616) containing $NaNO_3$ (1.5 g L^{-1}), K_2HPO_4 (0.04 g L^{-1}), $MgSO_4 \cdot 7H_2O$ (0.075 g L^{-1}), $CaCl_2 \cdot 2H_2O$ (0.036 g L^{-1}), $C_6H_8O_7$ (0.006 g L^{-1}), $(NH_4)_5[Fe(C_6H_4O_7)_2]$ (0.006 g L^{-1}), EDTA (0.006 g L^{-1}), Na_2CO_3 (0.02 g L^{-1}), and 1 mL trace metal mix. The trace metal mixture was comprised of H_3BO_3 (2.86 g L^{-1}), $MnCl_2 \cdot 4H_2O$ (1.81 g L^{-1}), $ZnSO_4 \cdot 7H_2O$ (0.222 g L^{-1}), $NaMoO_4 \cdot 5H_2O$ (0.39 g L^{-1}), $CuSO_4 \cdot 5H_2O$ (0.079 g L^{-1}), $Co(NO_3)_2 \cdot 6H_2O$ (0.0494 g L^{-1}). All the experiments were performed at 25 ± 2 °C under a light intensity of 70 µmol photons m^{-2} s^{-1} (approx.), a light: dark period of 16: 08 h, and constant aeration with atmospheric air for uniform mixing of the cultures. The pH of the culture was maintained in the range of 7.0 - 7.5 by sparging CO_2 on-demand along with the airflow. The chemicals and CO_2 cylinder (purity 99.99%) were procured from HiMedia® and Assam Air Products Pvt. Ltd., India, respectively.

3.2.2 Experimental conditions

The experiments were carried out in batches in 500 mL flasks, which contained 300 mL of BG-11 culture medium. An inoculum (approximately 1×10^5 cells mL^{-1}) with 10% v/v of actively growing microalgal cells was used. After 14 days of cultivation (at the late log phase), cells were centrifuged at 10,000 rpm for 15 min, and the harvested biomass was washed three times with deionized water. Harvested biomass was re-inoculated in nitrogen-free (-N), phosphorus-free (-P), both nitrogen- and phosphorus-free (-N-P) BG-11 medium and cultured for the next one, two, three, and four days to deliver nitrogen, phosphorus, and combined nitrogen and phosphorus starvation for one, two, three and four days respectively. In a similar experiment, 14 days grown culture was inoculated in a modified BG-11 medium containing 0.5 g L^{-1} $NaNO_3$, 0.01 g L^{-1} $K_2HPO_4.3H_2O$ (A), and 0.25 g L^{-1} $NaNO_3$, 0.005 g L^{-1} $K_2HPO_4.3H_2O$ (B) to deliver partial nitrogen (1.5 g L^{-1} → 0.5 g L^{-1} → 0.25 g L^{-1} $NaNO_3$) and phosphorus (0.04 g L^{-1} → 0.01 g L^{-1} → 0.005 g L^{-1} $K_2HPO_4.3H_2O$) starvation. Microalgal cultures cultivated in the unmodified BG-11 medium (C) for 14 days were considered as control. A graphical scheme of the experimental procedure has been illustrated in Figure 3.1.

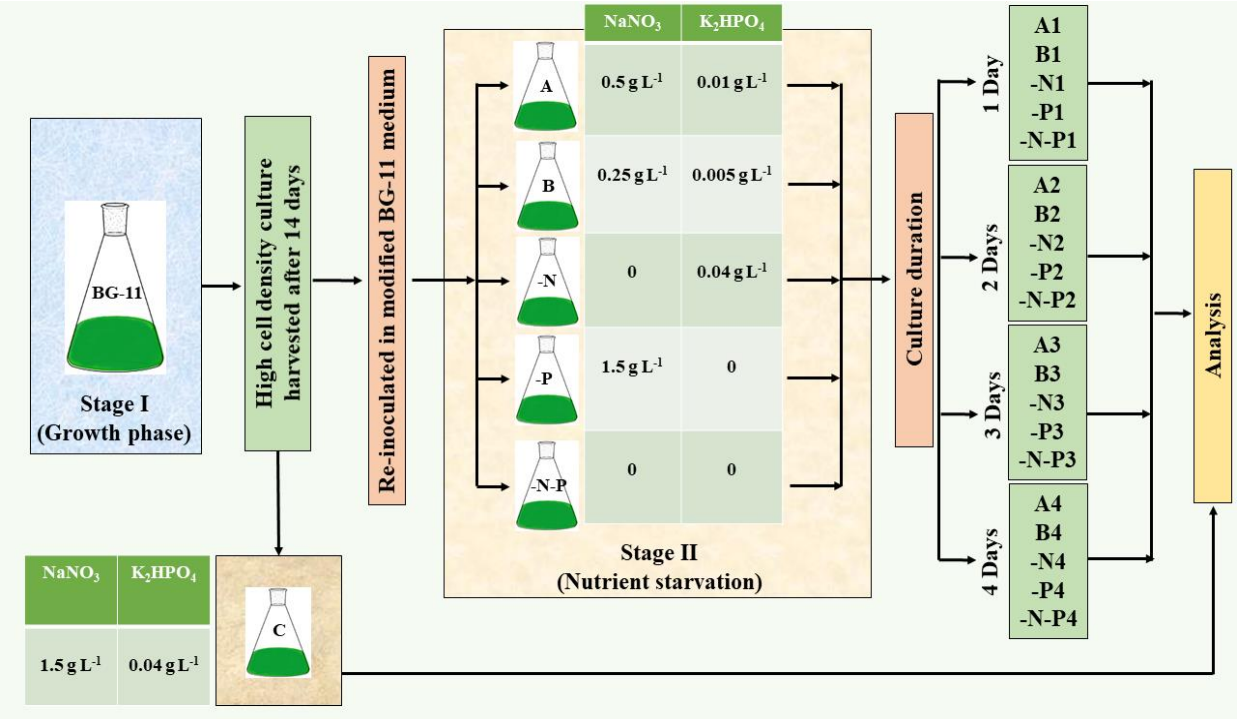

Figure 3.1. Schematic diagram depicting the experimental methodology.

3.2.3 Analytical procedures

3.2.3.1 Determination of microalgal growth

The growth of the microalgae was estimated by measuring the optical density (OD) of the cultures at regular intervals using a UV-visible spectrophotometer (Orion Aquamate 8000, Thermo Fisher Scientific, USA) at 750 nm. Dry cell weight (DCW) of the microalgal culture was determined by filtering a known volume of the cell suspension through a pre-weighed moisture free cellulose acetate membrane filter (0.45 µm). After filtration, the filter papers were dried in a hot air oven at 60 °C until an invariable weight was achieved and the final weight was recorded. The DCW was calculated by the difference in the weight of the blank filter paper, and the filter paper loaded with the microalgal culture and expressed in g L^{-1}. The biomass productivity ($P_{productivity}$, g L^{-1} day^{-1}) was calculated from the following equation [289].

$$P_{productivity} = \Delta X/\Delta t \quad (3.1)$$

where "ΔX" is the difference in biomass concentration (g L^{-1}) within a cultivation period of "Δt" (day).

3.2.3.2 Morphological identification

The field emission scanning electron microscopic (FESEM, Carl Zeiss SIGMA VP, Germany) analysis was carried out as reported by Kumar et al. [290]. The neutral lipid intensity within the microalgal cells was determined with a slight modification of the method described by Anand et al. [291]. Briefly, 1 mL of microalgal cell suspension was centrifuged at 10,000 rpm for 10 min, and the pellet was washed with Phosphate Buffer Saline (PBS). Subsequently, 330 µL of 25% (v/v) dimethyl sulfoxide (DMSO) was added to the pellet, and the mixture was vortexed for 1 min. The mixture was then ultrasonicated (PCi Analytics, 3.5 Lit, 50 Hz) for 1 min to facilitate penetration of Nile red by increasing the pore size of the cells. Following this, the cells were fixed with 10 µL of glutaraldehyde and stained with Nile red solution (15 µL of 0.1 mg mL^{-1}) for 10 min at 40 °C. The samples were observed under a Zeiss fluorescence microscope (40× magnification) containing a rhodamine filter.

3.2.3.3 Determination of photosynthetic activity

The pigment content and photosynthetic activity of *T. obliquus* KMC24 under various nutrient-starved conditions were measured spectrophotometrically by employing the protocol described by Lichtenthaler (1987). The calculated pigment contents were expressed as milligram per gram of DCW. The maximum quantum yield (F_v/F_m) of photosystem II (PS II) was estimated using a pulse-amplitude-modulated (PAM) fluorometer (AquaPen-C AP-C100, Photon System Instruments) by following the protocol reported by Kramer et al. [293]. The microalgal cells were dark-adapted for 20 mins prior to the experiment.

3.2.3.4 Biochemical characterization

Bligh and Dyer method was employed to determine the total lipid content in terms of dry cell weight [294]. Lipid content ($L_{content}$, %) was calculated using the following equation [295].

$$L_{content} = (W_{lipid}/W_{sample}) \times 100 \quad (3.2)$$

Further, the protocol described by Damiani et al. [296] was employed to fraction the total lipid into neutral lipids (NL), glycolipids (GL), and phospholipids (PL) using silica gel column chromatography. For the estimation of carbohydrate content, 50 mg of microalgal biomass was digested with 500 µL of 72% (w/v) H_2SO_4 for 1 h at room temperature. The concentration of the hydrolysate was reduced to 4% (w/v) by adding distilled water and was incubated at 121 °C for 1 h. After the solution was cooled to room temperature, the volume of

the content was made up to 50 mL with distilled water [297]. The solution was centrifuged, and the supernatant was analyzed for total sugar content by the phenol sulfuric acid method [298]. The total nitrogen content of microalgal biomass determined using CHNS (Perkin-Elmer Thermo Scientific Flash 2000) elemental analyzer was used to determine its crude protein content using the following equation:

$$\text{Total protein (\%)} = 6.25 \times \text{N (\%)} \quad (3.3)$$

3.2.3.5 Assessment of ROS and cell viability

The fluorometric probe, 2′, 7′-dichlorodihydrofluoresceine diacetate (DCFH-DA) (Sigma-Aldrich, USA) was used for determining the intracellular ROS content in *T. oliquus*. Briefly, 4 µg mL^{-1} microalgal cells were stained with 5 µM DCFH-DA and incubated for 1 h in dark conditions. The cells were then visualized using a Cytell Cell Imaging System (GE Healthcare Life Sciences) [299]. Quantitative analysis was conducted by spectrofluorimetry.

Flow cytometry (BD Calibur Flow Cytometer, BD Biosciences, USA) was performed to determine the viability of microalgal cells by measuring the fluorescence of propidium iodide-stained cells using the protocol as reported by [300]. Briefly, microalgal cells were collected through centrifugation (10,000 rpm, 10 min) and the pellet was washed thrice with phosphate buffer (10 mM, pH = 7.0). The cells were then stained with propidium iodide (10 mg L^{-1}) for 20 min in dark prior to flow cytometry analysis.

3.2.3.6 Measurement of enzymatic and non-enzymatic antioxidant scavengers

50 mg microalgal biomass was harvested through centrifugation and homogenized in 50 mM phosphate buffer (pH 7.0) containing 1 mM EDTA, 0.05% (v/v) Triton X-100, 2% (w/v) polyvinylpyrrolidone and 1 mM phenylmethylsulfonyl fluoride. The homogenate was centrifuged at 12,000 rpm for 25 min at 4 °C and the supernatant was used as crude extract. All enzyme activities were calculated based on the amount of protein in the crude extract and the total protein content was determined according to the Bradford method using bovine serum albumin as a standard [301].

For CAT activity analysis, 100 µL of the crude enzyme extract was mixed with 1.6 mL phosphate buffer (pH: 7.0), 100 µL EDTA (3mM) and 200 µL H_2O_2 (0.3%). Decrease in absorbance at 240 nm was recorded up to 150 s against a blank of same sample without H_2O_2. CAT activity was calculated using an extinction coefficient of 0.0436 mM^{-1} cm^{-1} [302]. One CAT unit was defined as the enzyme amount that transforms 1 µmol of H_2O_2 per minute. For

APX activity analysis, 100 µL of the crude extract was mixed with 1 mL phosphate buffer (pH 7), 100 µL EDTA (3 mM), 1 mL ascorbate (5 mM) and 200 µL H_2O_2 (0.3%). The reaction was followed for 3 min and the change in absorbance at 290 nm due to ascorbate oxidation was evaluated against a blank of same sample without H_2O_2. APX activity was calculated using an extinction coefficient of 2.8 mM^{-1} cm^{-1} [303]. One APX unit was defined as the enzyme amount that transforms 1 µmol of ascorbate per minute. The malondialdehyde (MDA) concentration in the microalgal cells was used to determine the lipid peroxidation using the protocol reported by Chokshi et al. [19]. Microalgal cells were harvested by centrifugation, homogenized in 2 ml of 80:20 (v:v) ethanol:water followed by centrifugation at 10,000 rpm for 10 min. An aliquot of 1 ml of the supernatant was mixed with 1 ml of thiobarbituric acid (TBA) solution comprising 20.0% (w/v) trichloroacetic acid (TCA), 0.01% butylated hydroxytoluene, and 0.65% TBA. Samples were then mixed vigorously, heated at 95 °C for 25 min, and cooled. The contents were centrifuged at 10,000 rpm for 10 min and absorbance of the supernatants was read at 450, 532, and 600 nm. The MDA content was calculated using the following formula and expressed on a fresh weight (FW) basis:

$$MDA\ (\mu mol\ g^{-1}\ FW) = \frac{[6.45\times(A_{532}-A_{600})]-[0.56\times A_{450}]}{FW} \quad (3.4)$$

The total polyphenol content in *T. obliquus* KMC24 was estimated spectrophotometrically by using the protocol reported by Chokshi et al. [19]. Microalgal cells were harvested by centrifugation and homogenized with 5 mL of 80% ethanol using a chilled mortar and pestle. The mixture was centrifuged at 10,000 rpm for 20 min and the supernatant was collected. The remaining residue was re-extracted, the supernatants were pooled and evaporated to dryness. The residue was dissolved in 5 mL of the distilled water. In a test tube, 1 mL of the aliquot was mixed with 0.5 mL of 1 N Folin–Ciocalteu's reagent and incubated for 3 min. Then 2 mL of 20% freshly prepared sodium carbonate solution was added to each tube and the content was thoroughly mixed. The solution was incubated at room temperature for 1 h in the dark, and the absorbance was measured at 650 nm. The concentrations of phenols in the samples were calculated from a calibration curve prepared using gallic acid as a standard.

3.2.3.7 Transesterification and Fatty Acid Methyl Esters (FAME) analysis

A two-step acid-base catalyzed transesterification reaction was carried out, as reported by Mishra and Mohanty [18]. The reaction was performed in a 25 mL round bottom flask in which approximately 200 mg of neutral lipid was allowed to react with methanol at 1:20 (molar ratio). The esterification reaction was carried out using H_2SO_4 (1 wt.% of lipid) as an acid catalyst, which was followed by a transesterification reaction using NaOH (1 wt.% of lipid) as a base catalyst. The reactions were performed at 70 ± 2 °C for two hours in a reflux setup. Subsequently, the product was washed repeatedly with distilled water in a separating funnel to recover FAME from catalyst and glycerol.

The FAME composition was analyzed on a GC (PerkinElmer, Clarus® 590, USA) system equipped with a cross bond polyethylene glycol elite-wax column (PerkinElmer, 30 m, 0.32 mm ID, and 0.25 µm df). The injector port and detector temperature were set at 250 °C and 260 °C respectively, and an injection volume of 1 µL was used with a split ratio of 20:1. The column temperature was set at 50 °C for 2 min, then ramped at a rate of 5 °C min^{-1} to 190 °C, hold for 2 min, followed by 5 °C min^{-1} ramp to 190 °C, hold for 2 min and then the temperature was ramped again at a rate of 5 °C min^{-1} to 240 °C, followed by 10 min holding.

3.2.3.8 Analysis of biodiesel properties based on FAME profiles

Properties such as viscosity (ɳ), saponification value (SV), iodine value (IV), cetane number (CN), highest heating value (HV), degree of unsaturation (DU), long-chain saturation factor (LCSF), and cold filter plugging property (CFPP) were estimated to determine the biodiesel quality using equations as reported by Kumar et al. [290] and Francisco et al. [304].

$$ɳ = 0.235W_C - 0.468W_{db} \quad (3.5)$$

$$SV = \Sigma(560 \times P_{FA})/MW \quad (3.6)$$

$$\mathrm{IV} = \Sigma(254 \times P_{FA} \times N_D)/MW \quad (3.7)$$

$$CN = 46.3 + \left(\frac{5458}{SV}\right) - (0.225 \times IV) \quad (3.8)$$

$$HV = 46.19 - \left(\frac{1794}{MW_i}\right) - 0.21 \times N_D \quad (3.9)$$

$$DU = (W_{MUFA}) + (2 \times W_{PUFA}) \quad (3.10)$$

$$Density = 0.8463 + \frac{4.9}{\Sigma \mathrm{MW}} + 0.0118 * \Sigma N_D \quad (3.11)$$

$$LCSF = (0.1 * C16) + (0.5 * C18) \quad (3.12)$$

$$CFPP = (3.417 * LCSF) - 16.477 \quad (3.13)$$

where, W_C represents the weighted-average number of carbon atoms in the fatty acids, W_{db} represents the weighted-average number of double bonds, P_{FA} denotes the fatty acid percentage, MW represents the molecular weight of fatty acid, N_D denotes number of double bonds, W_{MUFA} represents monounsaturated fatty acid (MUFA) in weight percentage, W_{PUFA} represents polyunsaturated fatty acid (PUFA) in weight percentage, MW_i denotes the molecular weight of the i^{th} FAME component.

3.2.4 Statistical analysis

All the experiments were analyzed on three biological replicates, and the results were expressed as mean values ± standard deviation. Normality test was performed for each data using the Shapiro-Wilk test. Data were further analyzed by one-way analysis of variance (ANOVA) using InfoStat, 2012. The mean values were compared with the LSD test, and a significant difference was considered at $P < 0.05$. The correlation between ROS and lipid content was determined using Pearson's correlation analysis.

3.3 Results and Discussion

3.3.1 Isolation and identification of microalgal strains

Axenic microalgal strains were isolated from the collected freshwater samples. Among the six isolated strains, maximum biomass (2.35 ± 0.02 g L^{-1}) and lipid yield (29.51 ± 0.26%) were obtained in the strain KMC24 (Figure 3.2). Thus, this strain was selected for further experiments. Morphological identification using a light microscope and FESEM revealed that KMC24 is a green unicellular microalga with globular cell morphology and measured about 4.35 µm in diameter. Based on the partial 28S rRNA gene sequence, the isolate KMC24 was identified as *T. obliquus* KMC24. The BLAST search in the GenBank database revealed that the obtained sequence was homologous to the 28S rRNA gene of *Scenedesmus obliquus* with 91% similarity. The sequence was deposited to GenBank (accession number MF661972). The genus *Tetradesmus* is a member of the family *Scenedesmaceae*. The phylogenetic tree (Figure 3.3) confirmed that the strain KMC24 had a close evolutionary relationship to the genus *Scenedesmus* and was similar to *S. obliquus* strains YSR17 (91%) and *Acutodesmus obliquus* KGE30 (86%).

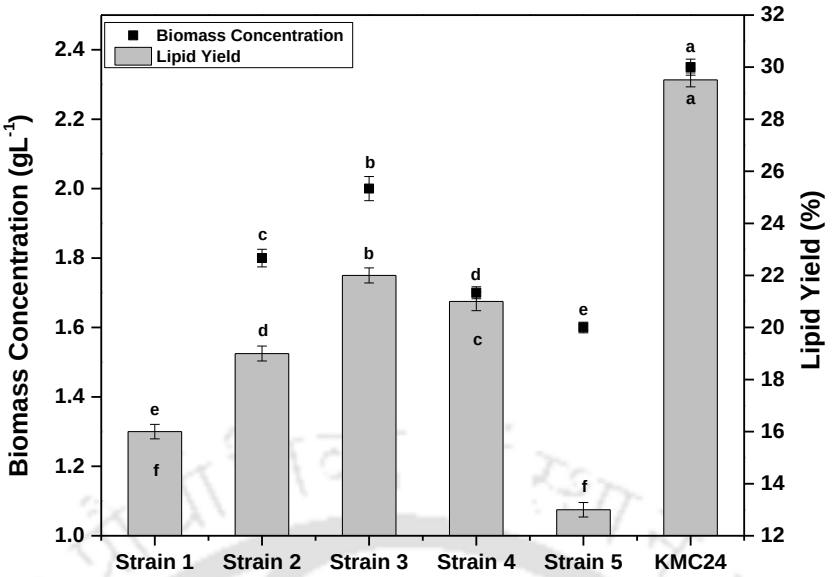

Figure 3.2. Biomass concentration and lipid yield for different strains cultivated in BG-11 media. Values are presented as the mean ± standard deviation (n = 3). Values with the different letters represent a significant difference ($P < 0.05$) between treatments (same letters are not significantly different). The alphabetical letters are denoted in the ascending order ("a" represents the highest value).

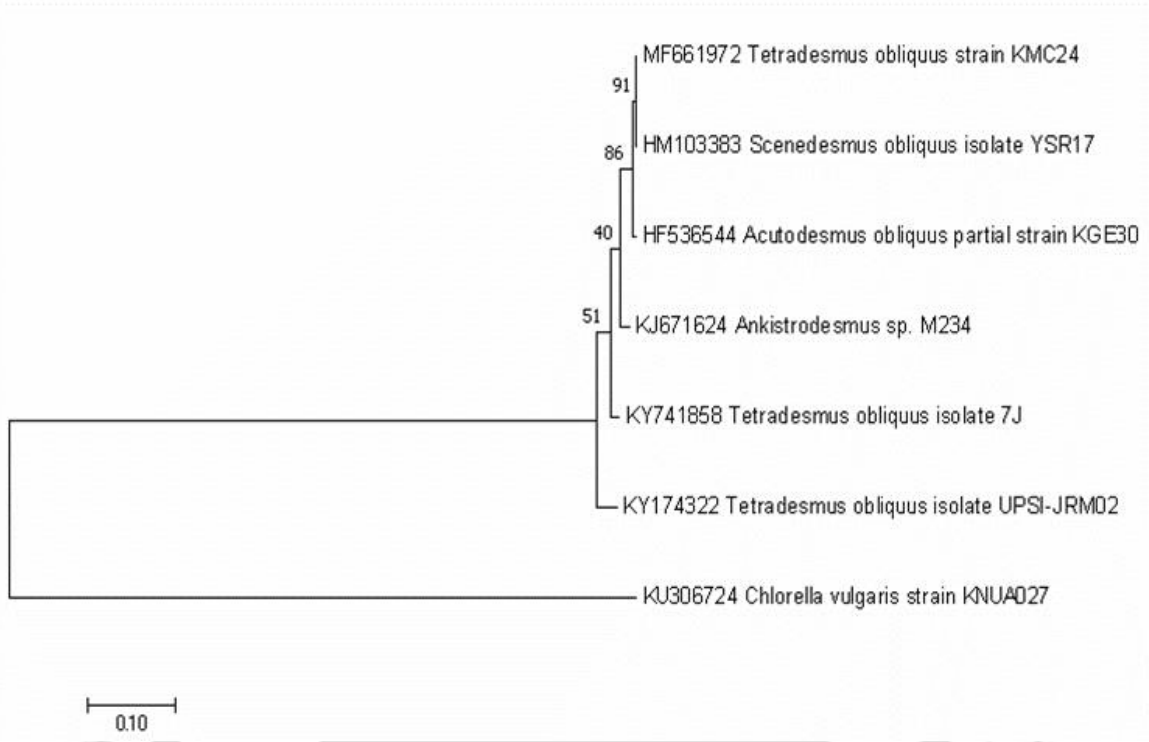

Figure 3.3. Phylogenetic analysis of *T. obliquus* KMC24 (GenBank accession no. MF661972). Dendrogram was generated using the neighbor-joining analysis based on 28S rRNA gene sequences. Bootstrap values are indicated at nodes. Scale bar (= 0.10) represents nucleotide substitution per 100 nucleotides. Representative sequences in the dendogram were obtained from GenBank.

3.3.2 Influence of nutrient starvation on biomass production

Nutrient starvation is one of the most prominent strategies for augmenting the desired biochemical constituent of microalgae, such as lipid. Although continuous nitrogen and phosphorus starvation play a positive role by increasing the lipid content of microalgae, it impairs their biomass productivity severely, as nitrogen is a crucial element of biological macromolecules like protein, chlorophyll, and DNA [39]. Likewise, phosphorus plays a vital role in biochemical pathways, such as ATP production, photosynthesis, biomass partitioning, and cellular processes [305]. Therefore, in this study, short-term nutrient starvation via two-stage cultivation was applied, where the maximum amount of biomass was harvested from the late log phase and re-inoculated in A, B, -N, -P, -N-P medium to apply short term starvation

for the next one (A1, B1, -N1, -P1, -N-P1), two (A2, B2, -N2, -P2, -N-P2), three (A3, B3, -N3, -P3, -N-P3) and four days (A4, B4, -N4, -P4, -N-P4).

To evaluate the influence of two-stage nutrient starvation on the growth of *T. obliquus* KMC24, DCW, and $P_{Productivity}$ were estimated. From Figure 3.4, it can be observed that the highest amount of DCW (2.35 ± 0.02 g L^{-1}) was obtained when the culture was grown in the control medium. This can be attributed to the optimum amount of nitrogen and phosphorus present in the control medium. No significant changes in DCW were observed when *T. obliquus* KMC24 cells were starved for two days in medium A (DCW: 2.15 ± 0.01 g L^{-1}), B (DCW: 2.15 ± 0.03 g L^{-1}), -N (DCW: 2.15 ± 0.04 g L^{-1}) and -P (DCW: 2.15 ± 0.03 g L^{-1}). These results demonstrated the ability of *T. obliquus* KMC24 cells to grow for the next two days with intracellular nitrogen and phosphorus as a substrate when the external nitrogen and phosphorus are limited or absent. However, after two days of starvation, a gradual decrease in DCW was observed in all the cases because of nutrient depletion. On the other hand, the DCW of the cells grown in medium -N-P decreased drastically from the first day of starvation. This impairment of cellular growth indicated that complete nitrogen and phosphorus starvation reduced the metabolic process and cell division in *T. obliquus* KMC24. The highest $P_{Productivity}$ (0.165 ± 0.0003g L^{-1} day^{-1}) was obtained when the culture was grown in the control medium. A gradual decrease in $P_{Productivity}$ was observed under all nutrient-starved conditions. As compared to control, approximately 15% reduction in $P_{Productivity}$ was observed when the cells were starved for one day in A, B, -N,-P medium. Similar types of results were witnessed in many microalgal species like *Chlorella vulgaris* [306], *Scenedesmus* sp. [140], *Chaetoceros muelleri*, and *Dunaliella salina* [40].

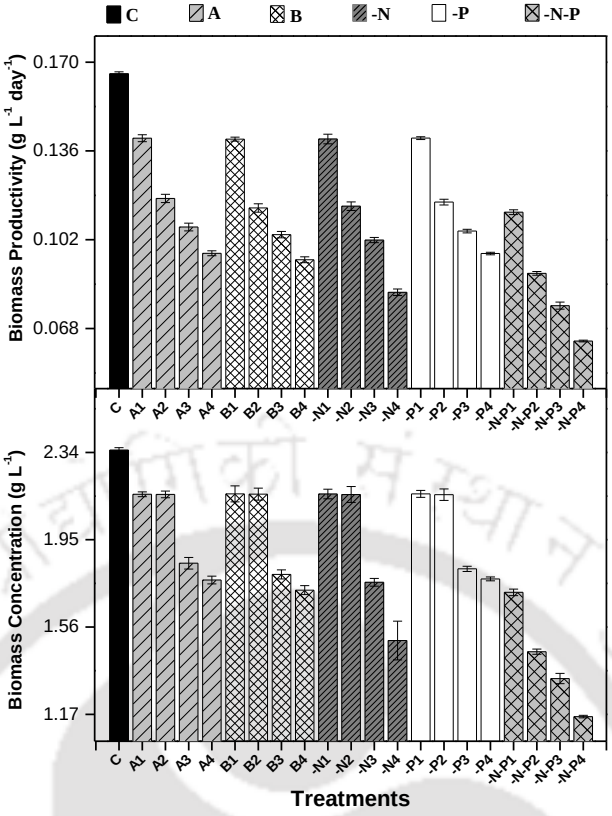

Figure 3.4. Biomass concentration and biomass productivity of *T. obliquus* KMC24 under various nutrient-starved conditions.Values are presented as the mean ± standard deviation (n = 3).

3.3.3 Morphological changes due to nutrient starvation

T. obliquus KMC24 is a member of *Scenedesmaceae* family, which exhibit pleomorphism by changing its morphology in response to various environmental conditions. The amount of energy stored in the cells is found to be directly proportional to the cell numbers in a colony [307]. In this study, significant morphological changes were not observed in the cells grown in A, B, -P and C medium. However, the cells grown in -N and -N-P medium changed their morphology from unicell to 2 and 4 celled coenobium with multiple spines at terminal cells. The cell length and number of spines increased with the duration of -N and -N-P starvation. The cell size was found to increase from 4.35 µm in control to approximately 6.17 µm in -N and -N-P starved cells. The FESEM and microscopic images of *T. obliquus* KMC 24 cells grown in control and –N media are shown in Figure 3.5. Massalski et al. suggested that the unfavorable growth conditions might have forced the cells to undergo repeated mitotic division without subsequent cytokinesis; thus, resulting in increased cell size [308]. The

increase in cell size and volume during nutrient starvation may indicate the accumulation of lipids, carbohydrates, and protein, probably due to delayed cell division. The spines at the terminals may act as a sensor to combat the stress conditions. These results were comparable with a similar study performed by Pancha et al. in which *Scenedesmus* sp. changed its morphology and size under nitrate-starved conditions [140].

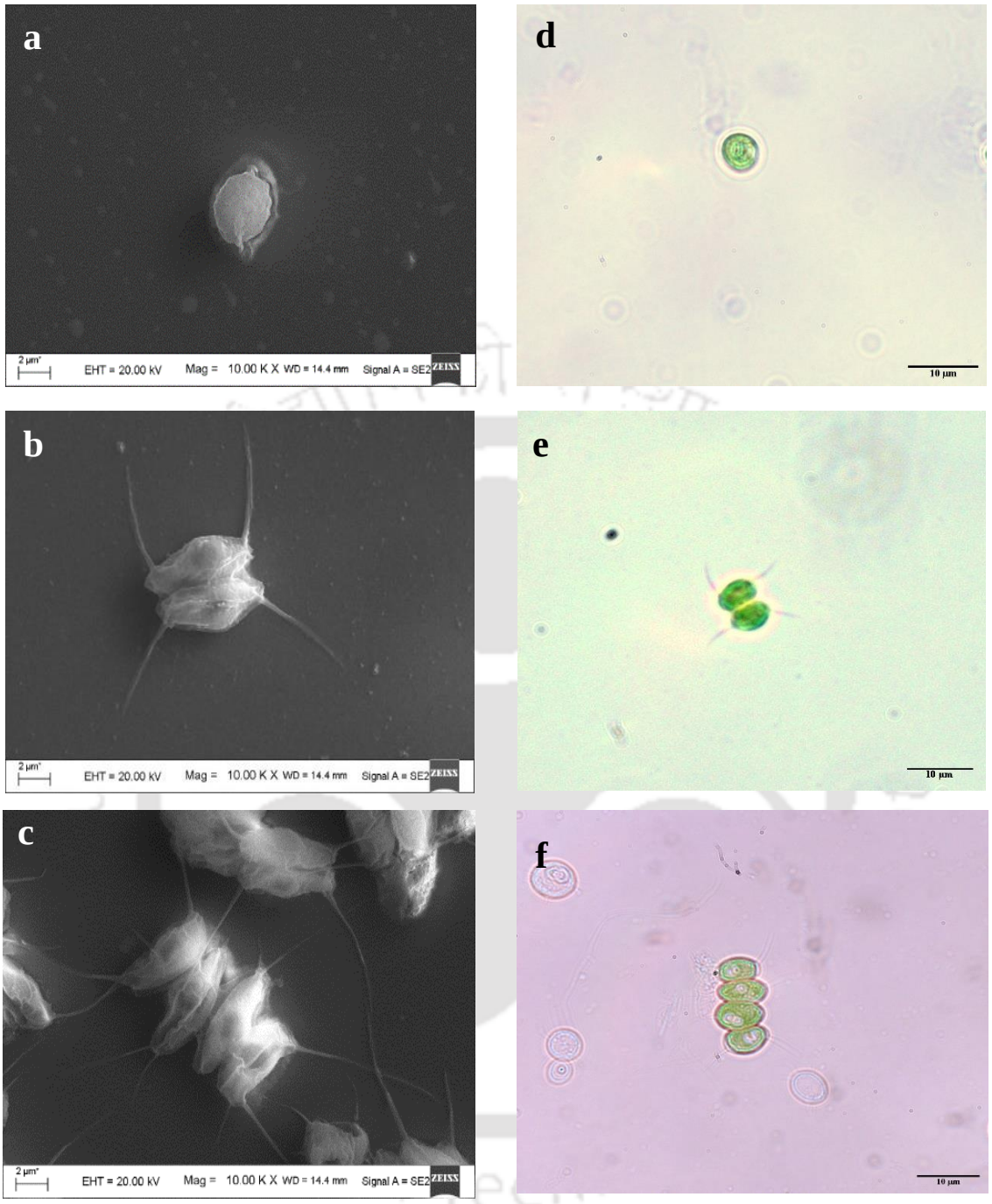

Figure 3.5. FESEM and microscopic images (40x) of *T. obliquus* KMC 24 (a, d: cells grown in control medium; b, c, e, f: cells grown in –N medium).

3.3.4 Influence of nutrient starvation on photosynthetic activity

The physiological indicators such as chlorophylls, carotenoids, and maximum quantum efficiency of PSII (F_V/F_m) helps to inspect the microalgal cell adaptation during nutrient-induced physiological stress. Nitrogen and phosphorus are consumed to a large extent during cell growth; thus, the algal cells tend to degrade the nitrogen-rich chlorophyll along with other photosynthetic machinery for their growth during -N and -P deficient conditions. Moreover, carotenoids play a protective role during oxidative stress in algal cells [19]. Nutrient limitation impairs the electron flow from the photosystems to the ETC (electron transport chain), resulting in ROS formation. Such impediment of the photosystem can be evaluated by the decrease in F_V/F_m [19].

As shown in Table 3.1, A4 and B4 cultures resulted in a 20.14% (Chl a+b =11.34 ± 0.06 mg g^{-1}) and 21.27% (Chl a+b =11.18 ± 0.11 mg g^{-1}) decrease in total chlorophyll content respectively, as compared to the control (Chl a+b =14.20 ± 0.14 mg g^{-1}). Further evidence of physiological stress was shown by the decrease in carotenoid content and maximum quantum efficiency (F_V/F_m). Nitrogen starvation for two days did not significantly affect the photosystem. However, nitrogen starvation beyond two days, i.e., on the third day, reduced the total chlorophyll and carotenoid content by 15.07% (Chl a+b: 12.06 ± 0.06 mg g^{-1}) and 16.81% (Caro: 3.86 ± 0.11 mg g^{-1}) respectively as compared to the control. The photosynthetic efficiency of three and four days nitrogen-starved cells was impaired due to a reduction in the chlorophyll and carotenoid content. Nitrogen starvation causes chloroplasts dismantling, which might have also contributed to the photosynthetic efficiency impairment [309]. Nitrogen starvation inhibits the cells from producing amino acids like glycine and glutamate, thereby restricting the synthesis of 5-Aminolevulinic acid, which consecutively lowers the chlorophyll content. The F_V/F_m value in two days nitrogen-starved cells was 0.61 ± 0.002, indicating healthy microalgal cells. However, the F_V/F_m value dropped to 0.49 ± 0.005 on the third day of starvation, indicating that the cells are under stressful conditions. This might be because -N starvation leads to remobilization of the nitrogen-rich metabolites such as chlorophyll to transitorily support their survival, which eventually slowed down the photosynthetic efficiency.

The photosynthetic apparatus was comparatively less affected during phosphorus starvation. However, a decrease in the total chlorophyll and carotenoid content by 12.11% (Chl a+b: 12.48 ± 0.36 mg g^{-1}) and 14.87% (Caro: 3.95 ± 0.18 mg g^{-1}) respectively, was observed on the fourth day of starvation. Phosphorus being the major constituent of DNA, RNA, and phospholipids, its limitation might have affected the photosynthetic apparatus on the fourth day

of phosphorous starvation. As compared to the control cultures (F_V/F_m: 0.69 ± 0.002), the parameter F_V/F_m remained nearly unaffected till the fourth day of phosphorus starvation (F_V/F_m: 0.60 ± 0.002), which indicated that phosphorus starvation had no severe impact on PSII in *T. obliquus* KMC24. Similar results were obtained by Huang et al., where F_V/F_m of *T. lutea* was least affected by phosphorus deprivation [310].

The cultures grown in -N-P medium faced the highest physiological stress where the total chlorophyll and carotenoid content was reduced by 12.04% (Chl a+b: 12.49 ± 0.33 mg g^{-1}) and 11.42% (Caro: 4.11 ± 0.04 mg g^{-1}) respectively, on the first day of starvation. Severe impairment of the photosystem was also illustrated by the decrease in F_V/F_m to 0.59 on the first day of starvation, which continued to decrease in the following days, indicating the negative influence on PSII.

Table 3.1. Effect of nutrient starvation on photosynthetic activity of *T. obliquus* KMC24. Values are presented as the mean ± standard deviation (n = 3). Values with the different letters represent a significant difference ($P < 0.05$) between treatments (same letters are not significantly different). The alphabetical letters are denoted in the ascending order ("a" represents the highest value).

Treatments	Chl-a (mg g^{-1})	Chl-b (mg g^{-1})	Chl a+b (mg g^{-1})	Caro (mg g^{-1})	F_V/F_m
C	10.30 ± 0.02^{a}	3.90 ± 0.12^{a}	14.20 ± 0.14^{a}	4.64 ± 0.03^{a}	0.69 ± 0.002^{a}
A1	10.17 ± 0.03^{a}	3.78 ± 0.08^{a}	13.95 ± 0.08^{a}	4.55 ± 0.24^{a}	0.68 ± 0.003^{a}
A2	9.49 ± 0.03^{b}	2.99 ± 0.07^{b}	12.48 ± 0.04^{b}	4.15 ± 0.16^{b}	0.67 ± 0.002^{a}
A3	9.29 ± 0.01^{b}	2.83 ± 0.11^{b}	12.12 ± 0.12^{b}	3.74 ± 0.04^{c}	0.56 ± 0.004^{b}
A4	9.09 ± 0.02^{b}	2.25 ± 0.04^{b}	11.34 ± 0.06^{c}	3.46 ± 0.03^{c}	0.52 ± 0.005^{b}
B1	10.14 ± 0.15^{a}	3.85 ± 0.17^{a}	13.99 ± 0.10^{a}	4.60 ± 0.07^{a}	0.68 ± 0.004^{a}
B2	9.36 ± 0.03^{b}	3.60 ± 0.06^{a}	12.96 ± 0.04^{b}	4.45 ± 0.01^{a}	0.66 ± 0.002^{a}
B3	9.28 ± 0.14^{b}	2.92 ± 0.03^{b}	12.20 ± 0.17^{b}	3.99 ± 0.08^{c}	0.64 ± 0.03^{a}
B4	9.03 ± 0.07^{b}	2.15 ± 0.04^{b}	11.18 ± 0.11^{c}	3.54 ± 0.01^{c}	0.53 ± 0.002^{b}
-N1	10.22 ± 0.04^{a}	3.77 ± 0.05^{a}	13.99 ± 0.08^{a}	4.52 ± 0.02^{a}	0.68 ± 0.002^{a}
-N2	9.88 ± 0.08^{b}	3.59 ± 0.03^{a}	13.47 ± 0.08^{a}	4.39 ± 0.01^{a}	0.61 ± 0.002^{a}
-N3	9.22 ± 0.06^{b}	2.84 ± 0.02^{b}	12.06 ± 0.06^{b}	3.86 ± 0.11^{c}	0.49 ± 0.005^{c}
-N4	9.13 ± 0.08^{b}	2.73 ± 0.05^{b}	11.86 ± 0.07^{c}	3.58 ± 0.04^{c}	0.42 ± 0.002^{c}
-P1	10.26 ± 0.03^{a}	3.82 ± 0.05^{a}	14.08 ± 0.06^{a}	4.60 ± 0.02^{a}	0.68 ± 0.003^{a}
-P2	10.13 ± 0.03^{a}	3.73 ± 0.12^{a}	13.86 ± 0.07^{a}	4.51 ± 0.01^{a}	0.65 ± 0.002^{a}
-P3	9.85 ± 0.13^{b}	3.23 ± 0.12^{a}	13.08 ± 0.25^{a}	4.25 ± 0.08^{b}	0.62 ± 0.002^{a}
-P4	9.51 ± 0.35^{b}	2.97 ± 0.03^{b}	12.48 ± 0.36^{b}	3.95 ± 0.18^{c}	0.60 ± 0.002^{a}
-N-P1	9.88 ± 0.35^{b}	3.61 ± 0.02^{a}	12.49 ± 0.33^{b}	4.11 ± 0.04^{b}	0.59 ± 0.002^{b}
-N-P2	9.43 ± 0.03^{b}	2.52 ± 0.02^{b}	11.95 ± 0.01^{c}	3.69 ± 0.02^{c}	0.55 ± 0.005^{b}
-N-P3	8.69 ± 0.03^{c}	1.64 ± 0.02^{c}	10.33 ± 0.01^{d}	3.28 ± 0.02^{d}	0.47 ± 0.002^{c}
-N-P4	8.02 ± 0.12^{c}	1.27 ± 0.04^{c}	9.29 ± 0.16^{e}	2.93 ± 0.02^{e}	0.42 ± 0.003^{c}

3.3.5 Influence of nutrient starvation on biochemical composition

As compared to the control, no significant difference in carbohydrate, lipid, and protein content was observed when the microalgal cells were cultivated in modified BG-11 medium A and B (Figure 3.6). Nitrogen being the most important component required for protein synthesis, a drastic drop in the protein content was observed with an increase in the duration of nitrogen starvation. The protein content of *T. obliquus* KMC24 was reduced as compared to the control (32.24 ± 0.75) by 9.65% (29.13 ± 0.72) and 36.01% (20.63 ± 0.46) on the first and fourth day of nitrogen starvation, respectively. A similar result was found by Pancha et al., where a reduction in the nitrate concentration from 247 mg L^{-1} to 0 mg L^{-1} decreased the protein content of *Scenedesmus* sp. by 60% [140]. Another possible reason for the decrease in protein content under nitrogen-starved conditions could be that the cells might have degraded the amino acid-rich proteins to maintain their cellular metabolic functions. Whereas the products of amino acid decarboxylation may further provide a precursor (acetyl-CoA) for fatty acid synthesis [310]. The distribution of photosynthetic carbon in microalgal cells is highly influenced by nitrogen starvation. It has been reported that the rate of carbon fixation in the microalgal cells during its early stage of nitrogen starvation surpasses the carbon demand, and surplus carbon is channeled into storage compounds like carbohydrates and neutral lipids (e.g., TAGs) [39]. Biomolecules such as lipids possess a highly reduced state and are efficiently packed in small compartments of the cells, thus favoring the storage of energy that can be used during stress conditions [311]. The highest lipid content was obtained in –N2 cultures (39.93 ± 0.64%), which was around 1.35-folds higher than the control (29.51 ± 0.26%). This clearly indicates that nitrogen starvation triggers the production of intracellular lipid. The possible explanations for the increase in lipid content under nitrogen starvation could be; (1) the microalgal cells under nitrogen starvation tends to degrade nitrogenous biomolecules such as chlorophylls and proteins, which further provides energy or carbon to the cells for lipid biosynthesis [39,310]; (2) nitrogen starvation triggers metabolic readjustments by re-routing the flux of carbon towards the biosynthesis of lipids rather than the accumulation of other biomass constituents [113]; (3) nitrogen starvation up-regulates malic enzyme (ME) producing NADPH, leading to lipid accumulation. The ME contributes to increase lipid accumulation by providing reducing power in the form of NADPH and also by supplying pyruvate, which in turn is converted by the pyruvate dehydrogenase complex into Acetyl-CoA, which is the precursor for fatty acids synthesis [312]. However, the lipid content was found to decrease when the cells were nitrogen-starved for more than two days. As compared to two days nitrogen-starved culture, the lipid content in three days nitrogen-starved culture was reduced

by 15.10% (33.93 ± 0.43%). The microalgal cells might have degraded their energy-rich lipids to sustain the stress condition, thereby causing a reduction in lipid content. The carbohydrate content in all the four nitrogen-starved cultures was significantly higher ($P < 0.05$) in comparison to the control. The carbohydrate content was maximum when the cells were nitrogen-starved for one day (31.83 ± 0.91%). A significant difference in the carbohydrate content was not found when the duration of nitrogen starvation was increased beyond two days. Whereas a simultaneous decrease in carbohydrate content and increase in lipid content in –N2 culture could be due to the shift of carbon fluxes from carbohydrate to lipid biosynthesis. Moreover, the findings in the present study are in accordance with the perception that lipid synthesis is also triggered when metabolic carbon exceeds carbohydrate biosynthesis capacity [313]. Thus, from the present study it can been seen that carbohydrate biosynthesis dominates over lipid accumulation.

As compared to nitrogen-starved cells, the cellular protein was comparatively less degraded during phosphorus starvation. However, the protein content was reduced compared to the control by 6.95% (30 ± 0.91) and 16.63% (26.88 ± 0.19) on the first and fourth day of phosphorus starvation, respectively. The decrease in protein content under phosphorus starvation could be because of the constraint on RNA and ATP biosynthesis. The carbohydrate content in all the four phosphorus-starved cultures was significantly higher ($P < 0.05$) than the control and was highest on the first and second day of starvation. Although the carbohydrate content in phosphorus-starved cells was higher than the control, it was comparatively lower than the nitrogen-starved cells. This suggests that energy metabolism in phosphorus-starved cells might be stimulated at the cost of carbohydrate accumulation. Under phosphorus starvation, a gradual increase in the lipid content was noted. The highest lipid content was obtained when the cells were starved for three days (32.93 ± 0.43). However, an increase in lipid content was observed with a gradual decrease in carbohydrate content. These results indicate that carbon flux might have shunted towards lipid biosynthesis from starch under phosphorus starvation.

A gradual decrease in carbohydrate, lipid, and protein content was observed when the microalgal cells were grown in -N-P medium. The carbohydrate, lipid, and protein content were reduced as compared to the control by 17.19% (19.80 ± 0.78), 22.06% (23 ± 0.57), and 20.37% (25.68 ± 0.16) respectively, on the first day of -N-P starvation, which continued to decrease in the following days. This can be attributed to the severe impairment of the photosystem due to stress.

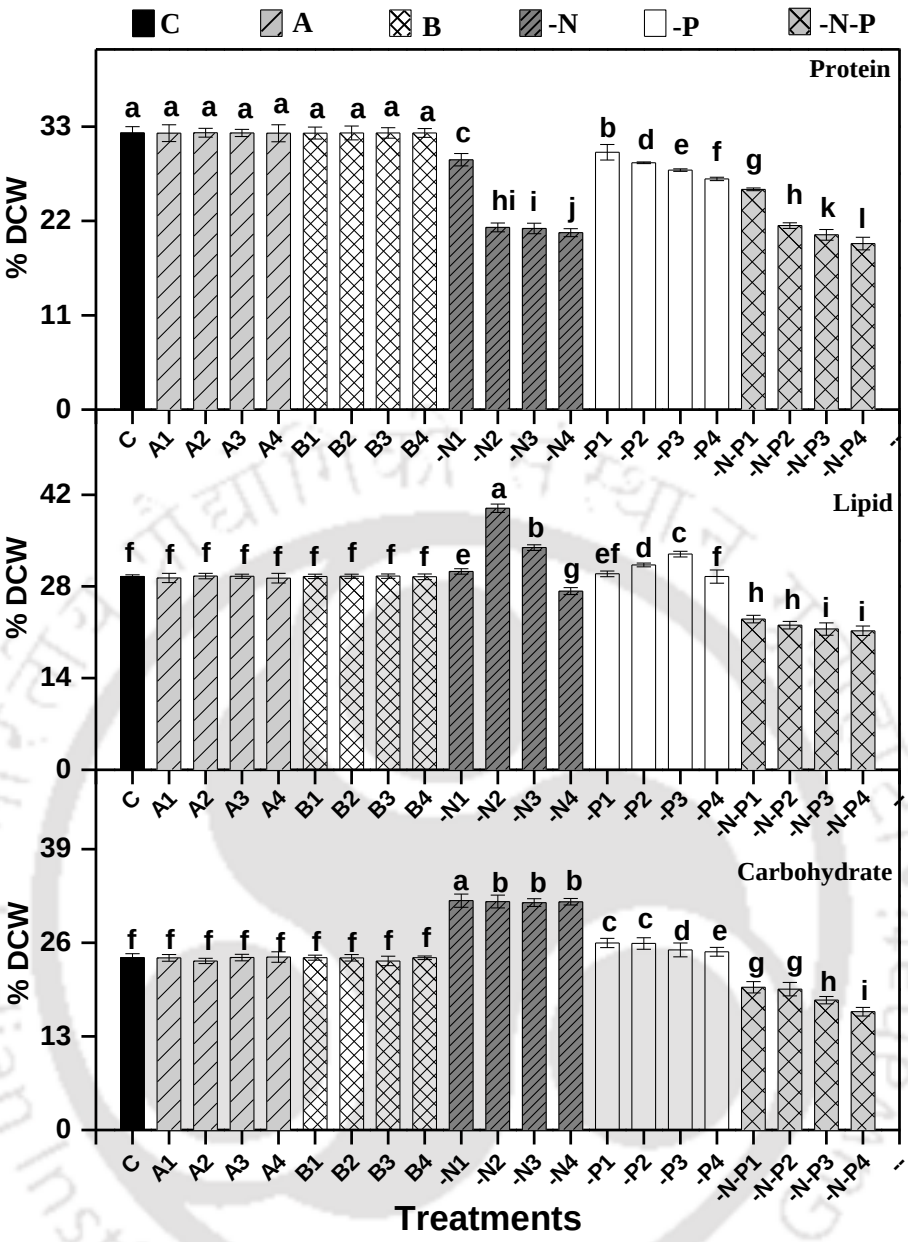

Figure 3.6. Biochemical composition of *T. obliquus* KMC24 under various nutrient-starved conditions. Values are presented as the mean ± standard deviation (n = 3). Values with the different letters represent a significant difference ($P < 0.05$) between treatments (same letters are not significantly different). The alphabetical letters are denoted in the ascending order ("a" represents the highest value).

3.3.6 Microalgal lipid composition

The impact of nutrient starvation on the lipid composition of *T. obliquus* KMC24 was investigated. The total lipids are constituted by several lipid classes, i.e., NL, GL, and PL. The

NL is primarily comprised of TAG that is essential for biodiesel production. Whereas PL and GL are primary constituents of the cell and intracellular organelle membranes. From Figure 3.7, it can be seen that under partial starvation (A and B medium) for up to four days, the accumulation of NL, PL, and GL was maintained with respect to the control.

The NL content of the nitrogen-starved cells increased with the duration of starvation. For one, two, three and four days nitrogen-starved cells, an increase in NL content (77.63 ± 0.29%, 84.95 ± 0.13%, 85.40 ± 0.09%, 85.84 ± 0.17%, respectively) was observed. The NL content in –N2 cultures were found to be almost similar to –N4 cultures with significantly higher ($P < 0.0001$) DCW. This suggested that two days of nitrogen starvation is a better approach for obtaining high biomass and NL content in *T. obliquus KMC24*.

Nile red, a lipophilic fluorescent dye, was used to determine the intracellular lipid bodies in nitrogen-starved cells through fluorescence microscopy (Figure 3.8). The intensity of neutral lipid droplets was found to be highest in two days nitrogen-starved cells. The results from the present study indicated that the increase in NL content of total lipid results in lipid accumulation during nitrogen starvation. The increase in NL content can be attributed to the accumulation of TAG, which is synthesized by two pathways; one from the Acyl-CoA dependent Kennedy pathway and another from the Acyl-CoA independent pathway [314]. A gradual increase in PL content from 6.52 ± 0.27% in control to 9.48 ± 0.21% in four days nitrogen-starved cultures was noted. Compared to the control, the GL content decreased with an increase in nitrogen starvation. The GL content in –N4 cells was about fivefold lower than the control (26.98 ± 0.27%). Thus, a gradual increase in NL and PL and a decrease in GL were observed with an increase in the duration of nitrogen starvation. However, Pancha et al. observed a decrease in both GL and PL when *Scenedesmus* sp. was nitrogen starved [140].

The NL content increased gradually from 68.96 ± 0.41% in control to 72.38 ± 0.07% in four days phosphorus-starved cells. Thus, the increase in NL content was more pronounced during nitrogen starvation. The PL content was reduced compared to the control by 43.54% (3.67 ± 0.23%) when the cells were phosphorus-starved for four days. Abida et al. proposed that phospholipids are secondary phosphorus-storage molecules, which break down during phosphorus starvation [315]. The decrease in PL content in phosphorus-starved cells coincided with a gradual increase in GL content. The NL content was found to increase when the cells were cultured in -N-P medium. A gradual decrease in PL and GL contents was observed when the *T. obliquus* KMC24 cells were cultured in -N-P medium for four days. The PL content

decreased from 6.52 ± 0.27% in control to 5.24 ± 0.26% and GL decreased from 26.98 ± 0.27% in control to 22.24 ± 0.25% in four days -N-P starved cells. These results indicate that each microalgal species undergo membrane remodeling in its own way to combat the stress conditions. In our study, the NL content of *T. obliquus* KMC24 cells was found to increase under all the stress conditions applied.

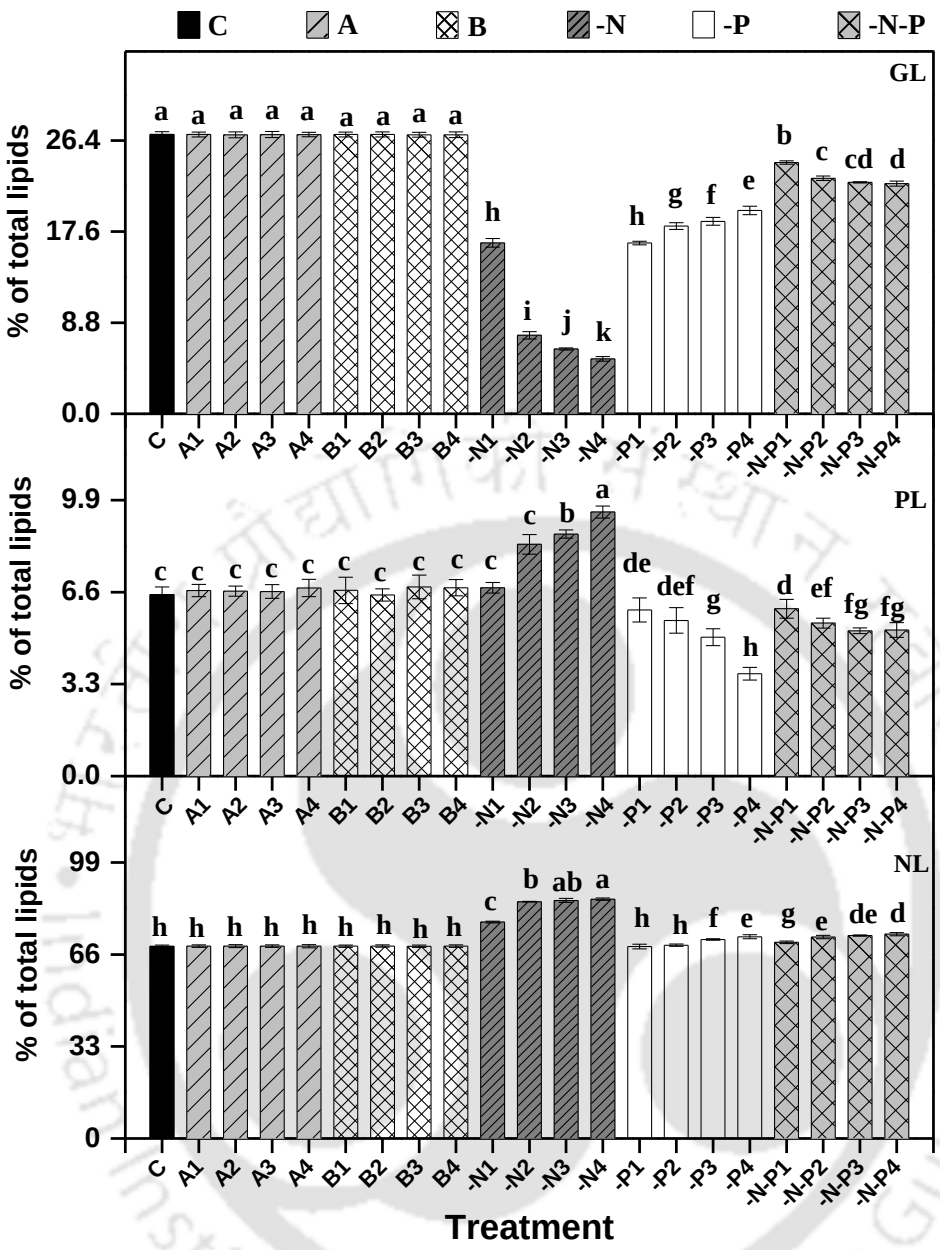

Figure 3.7. Lipid class composition of *T. obliquus* KMC24 under various nutrient-starved conditions. Values are presented as the mean ± standard deviation (n = 3). Values with the different letters represent a significant difference ($P < 0.05$) between treatments (same letters are not significantly different). The alphabetical letters are denoted in the ascending order ("a" represents the highest value).

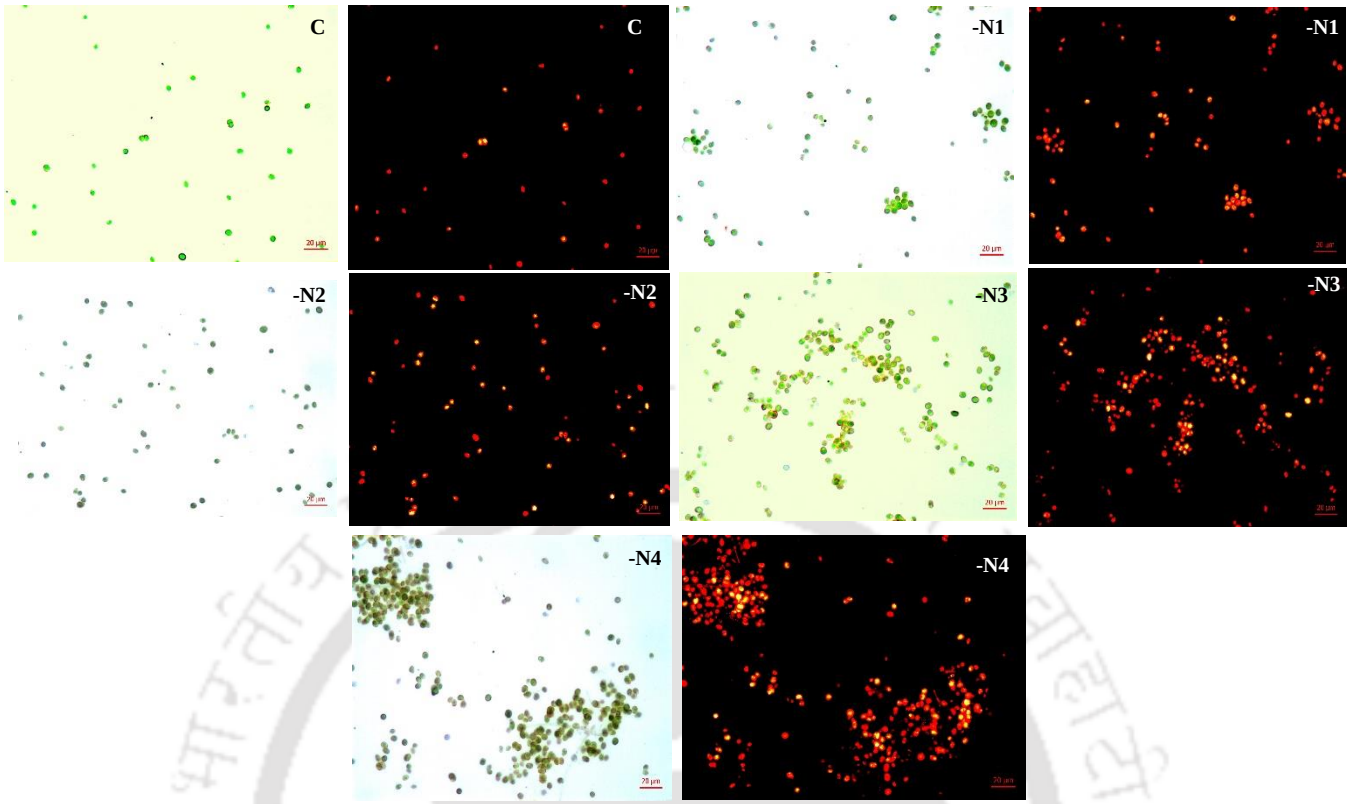

Figure 3.8. Nile Red images showing cellular neutral lipids in *T. obliquus* KMC24 cells (C: control cells, –N1 to –N4: one to four days nitrogen starved cells).

3.3.7 Cell viability

Cell death or a decrease in cell viability, whether due to senescence, acute stress, or aging, appears to be characterized by the loss of the cell's ability to retain homeostasis [34]. The viability of *T. obliquus* KMC24 cells under nutrient-starved conditions is represented in Fig. 6. 94.68 ± 2.01% to 91.95 ± 1.87% of the cells were live till the third day of starvation in A, B, -N, -P cultures. However, the cell viability was significantly reduced ($P < 0.0001$) on the fourth day of starvation from 99.72 ± 0.21% in control to 87.14 ± 1.01%, 84.50 ± 1.58%, 83.81 ± 1.12%, 83.88 ± 1.64% in A4, B4, -N4, -P4 cultures respectively. The cell viability was reduced as compared to the control by 15.95% (83.81 ± 3.94%) on the first day of –N-P starvation, which continued to decrease gradually in the following days. The gradual decrease in cell viability in all the cultures compared to control indicated the loss of membrane integrity under nutrient starvations.

3.3.8 ROS and MDA content under nutrient starvation

ROS are produced in different cellular compartments of microalgae under unfavorable growth conditions. Microalgal cells trigger several defense systems to scavenge these ROS. However, under stress conditions, the ROS production rate might exceed the scavenging rate of microalgal cells, thereby causing excess ROS accumulation. This excess ROS causes oxidative injury to the cells by damaging proteins, lipids, and DNA that ultimately causes cell death [19]. The effect of nutrient starvation on ROS fluorescence intensities is shown in Figure 3.9. The ROS fluorescence intensities in A1, A2, A3, B1, B2, B3, -N1, -N2, -N3, -P1, –P2, -P3, -P4 cultures increased significantly ($P < 0.034$) in comparison to control. This indicated that nutrient starvation was the environmental stress that led to ROS accumulation in the cells of *T. obliquus* KMC24. Zhang et al. observed similar results, where the ROS level increased significantly ($P < 0.0034$) in the nitrogen, phosphorus, and sulfur stressed cultures [38]. However, the fluorescence intensities in -N-P cultures were comparatively lower than the control. A gradual decrease in fluorescence intensities was observed with an increase in the duration of -N-P starvation. The dead cells do not possess ROS generating metabolic processes [316]. Therefore, a decrease in cell viability in -N-P cultures as assayed by flow cytometry could be the possible reason for reduced ROS fluorescence intensities. Also, a reduction in fluorescence intensities was observed from the third day of starvation in A, B, -N, -P cultures, probably due to the increase in dead cells with the duration of starvation. In our study, the highest ROS fluorescence intensity was observed in -N2 culture (17051.49 ± 93.15 a.u.).

MDA is a lipid peroxidation end product that is generally released as a stress indicator in microalgae. Hydroxyl radicals are highly reactive species that initiate membrane peroxidation, which results in the release of MDA as an end product [19]. In the present study, except for –N-P cultures, the MDA content was significantly increased ($P < 0.0001$) under all nutrient-starved conditions compared to the control culture (Fig. 7). The highest MDA content was observed in –N2 culture (3.81 ± 0.02 µM g^{-1} fresh weight), which was around 2.3-folds higher than the control culture (1.64 ± 0.01 µM g^{-1} fresh weight). The MDA content was consistent with the ROS level indicating that a linear correlation exists between ROS level and MDA content. Similar to our study, a simultaneous increase in ROS and MDA levels was reported in *D. salina* under nitrogen-limited conditions [146].

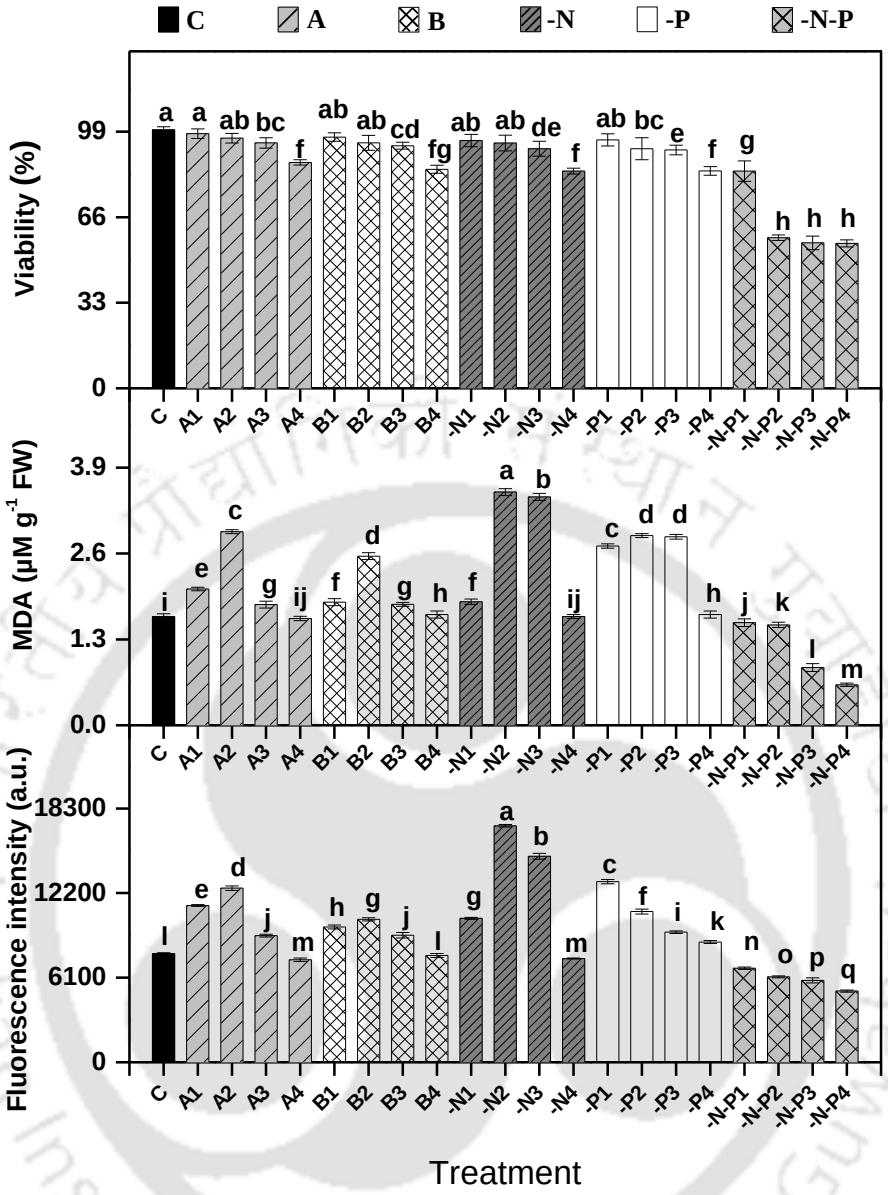

Figure 3.9. Effects of nutrient starvation on cell viability, malondialdehyde (MDA) content, and ROS fluorescence intensity of *T. obliquus* KMC24. Values are presented as the mean ± standard deviation (n = 3). Values with the different letters represent a significant difference ($P < 0.05$) between treatments (same letters are not significantly different). The alphabetical letters are denoted in the ascending order ("a" represents the highest value).

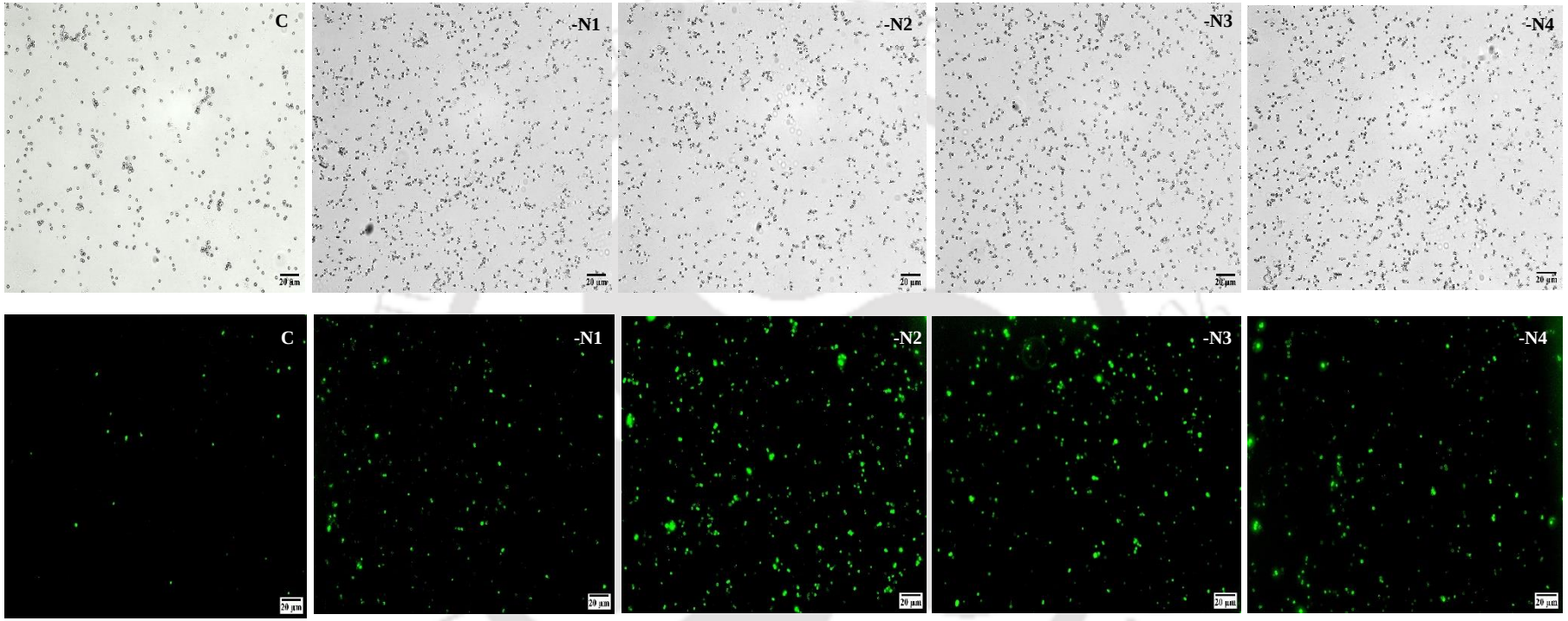

Figure 3.10. Fluorescence images of *T. obliquus* KMC24 cells stained with 2′, 7′-dichlorodihydrofluoresceine diacetate (DCFH-DA) probe showing the effect of nitrogen starvation in intracellular ROS formation (C: control cells, –N1 to –N4: one to four days nitrogen starved cells).

3.3.9 Correlation between lipid content and ROS level under nutrient starvation

The correlation between lipid content and ROS level under various nutrient-starved conditions was revealed using Pearson's correlation analysis (Figure 3.10). The ROS fluorescence intensity for all the nutrient stress conditions is represented on the x-axis, while the lipid content (%) is represented on the y-axis. The Pearson correlation coefficient was 0.908, indicating a high correlation between lipid content and ROS. In addition, a high correlation coefficient under individual nutrient stress conditions was obtained by plotting individual fluorescence intensities versus corresponding lipid content (Figure 3.11). These results further confirmed that the ROS levels were positively correlated with the lipid contents for all the nutrient-starved conditions. It has been reported that microalgal strains with high tolerance to oxidative stress are more efficient for producing biodiesel as compared to non-tolerant strains [317]. In the present study, the highest ROS fluorescent intensity and lipid content was observed in -N2 cultures. This indicated that *T. obliquus* KMC24 cells under two days of nitrogen starvation are highly oxidative stress tolerant with potential for biodiesel production. In a similar study, a positive linear correlation between ROS and lipid accumulation under different culture conditions was observed in *Chlorella pyrenoidosa* [38]. It has been reported that enhanced lipid production might be mediated by oxidative stress [146]. Recent evidence also indicated that ROS might act as a secondary messenger for various stress factors, which controls cellular responses to extracellular stress [318]. Some of the hypotheses on the mechanisms of ROS-mediated lipid accumulation are as follows:

- Lipids are highly reduced molecular entities. Therefore, NL overproduction necessitates significant amounts of NADPH, which is primarily obtained through the oxidative pentose phosphate (OPP) pathway. Oxidative stress causes the carbon metabolic flux to change from glycolysis to the OPP pathway through post-translational modification of glycolytic enzymes [318]. Hence, this could be a possible mechanism through which oxidative stress enhances NL accumulation.
- The stored NL bodies are accumulated within lipid droplets, and studies have reported that endoplasmic reticulum (ER) stress activates the production of lipid droplets [319]. As ROS stimulates ER stress, this could be another possible way through which ROS increases lipid droplets formation [318].

- ROS might function as a mediator for enhanced lipid accumulation through autophagy under unfavorable conditions. Suzuki et al. [320] reported that ROS accumulation triggers autophagy in eukaryotic cells, while Scott et al. [321] reported that ROS stimulates autophagy, thereby causing the cells to degrade macromolecules and shift large amounts of carbon to energy storage compounds, such as lipids. Zhao et al. reported that salinity stress induces ROS and activates cellular autophagy, which further regulates lipid synthesis [322]. Couso et al. suggested that autophagy is required for the synthesis of TAG in nitrogen or phosphate-starved cells of *Chlamydomonas* [323].
- Furthermore, ROS are also demonstrated to modulate cellular responses at the level of signal transduction pathways [324].

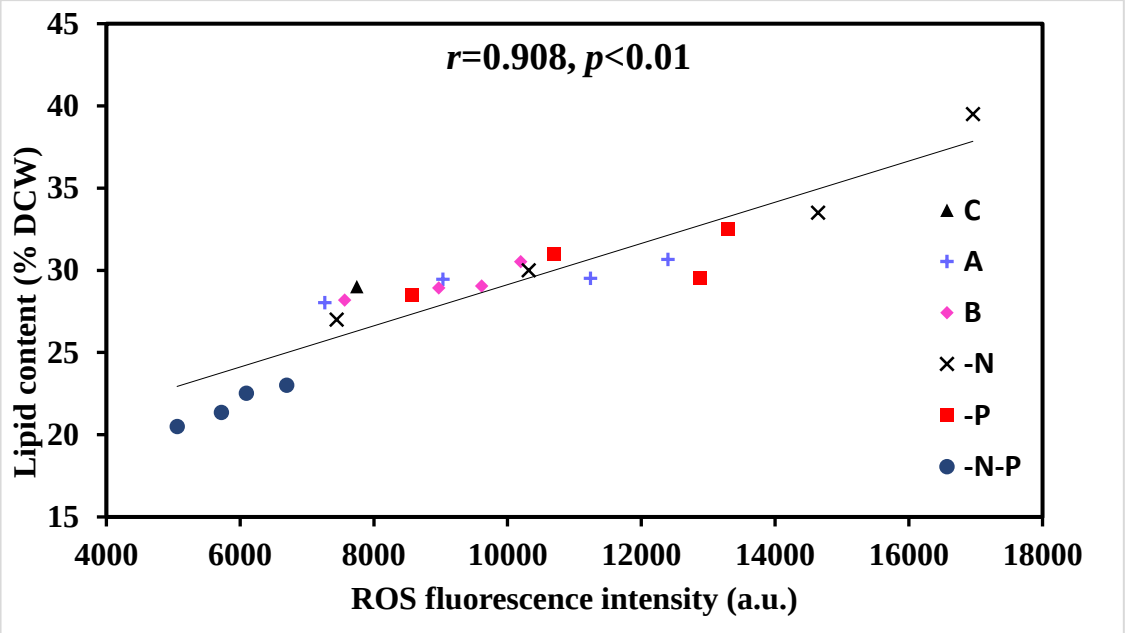

Figure 3.11. The correlation between lipid content and ROS level of *T. obliquus* KMC24 under various nutrient-starved conditions. Lines are linear fit with Pearson correlation coefficient (r).

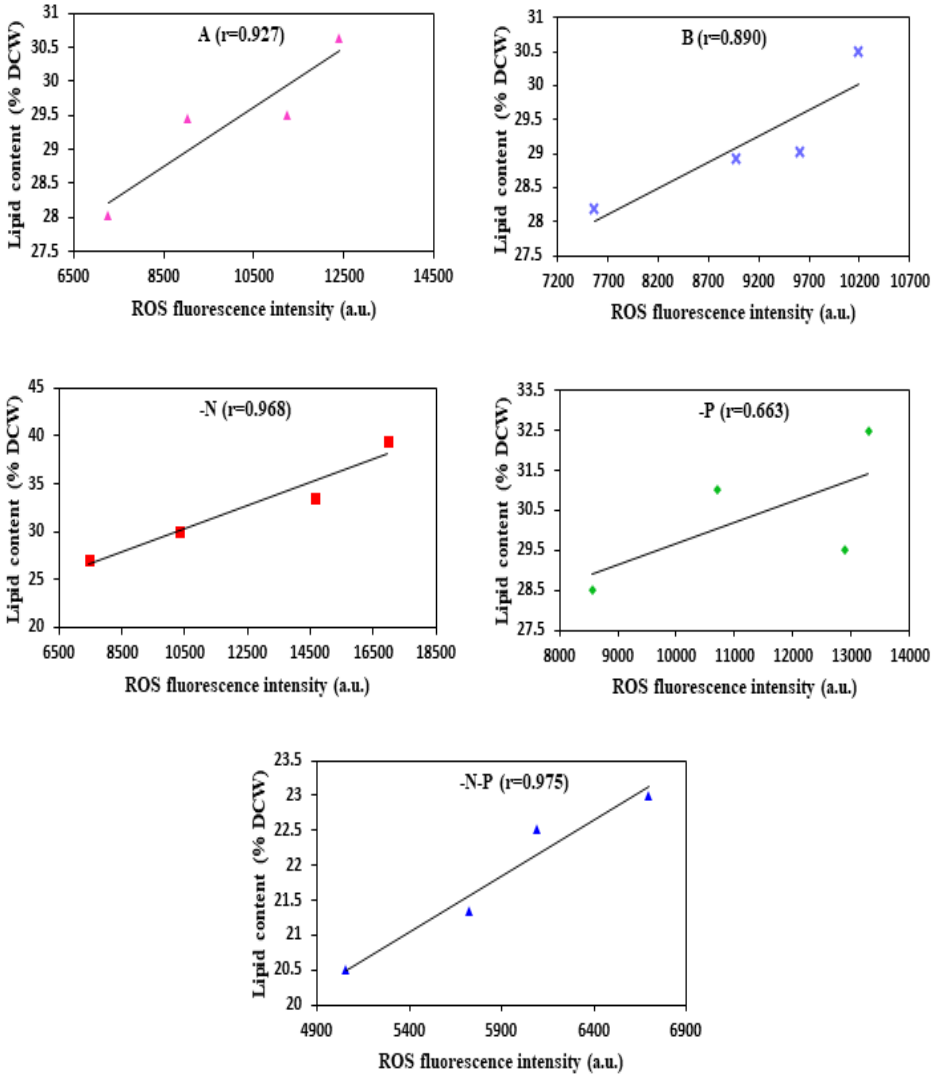

Figure 3.12. Relationship between the reactive oxygen species and corresponding lipid content (%) of *T. obliquus* KMC24 under individual culture condition. Lines are linear fit with Pearson correlation coefficient (r).

3.3.10 Responses of cellular antioxidants under nutrient starvation

Microalgal cells stimulate powerful intrinsic antioxidant systems such as enzymatic (CAT, APX) and non-enzymatic (polyphenols) metabolites to counter ROS toxicity. CAT is a heme-containing enzyme that allows the cell to remove H_2O_2 in an energy-efficient way by catalyzing the conversion of H_2O_2 into O_2 and H_2O [146]. CAT is absent in chloroplasts, so H_2O_2 is degraded in the chloroplast by APX. APX is an ascorbate-based antioxidative defense system that scavenges H_2O_2 [19]. The effect of nutrient starvation on the antioxidative defense system is illustrated in Figure 3.12. Except for –N-P cultures, the CAT and APX activity was significantly increased ($P < 0.0001$) under all nutrient-starved conditions, indicating a correlation with the corresponding H_2O_2 contents. The highest CAT and APX activity of 4.21 ± 0.05 U mg^{-1} protein and 2.79 ± 0.04 U mg^{-1} protein respectively was obtained in -N2 cultures, which were around 1.26- and 1.93-folds higher than those of control cultures (3.32 ± 0.07 U mg^{-1} protein and 1.44 ± 0.09 U mg^{-1} protein, respectively). The increase in the activities of CAT and APX strongly suggests that oxidative stress is induced under nutrient-starved conditions in *T. obliquus* KMC24 cells.

Polyphenols function as a substrate for the hydrogen peroxide-scavenging enzyme peroxidase and inhibit ROS dissemination by modifying peroxidation kinetics and reducing cell membrane fluidity [19]. However, limited studies are available on the impact of nutrient starvation on the polyphenol content of microalgae. In the present study, except for -N-P, A4, B4, and -N4 cultures, the total polyphenol content was enhanced under all nutrient-starved conditions compared to the control culture. The highest total polyphenol content was observed in -N2 culture (159.39 ± 2.82 µg g^{-1} FW), which was around 2.7-folds higher than the control culture (58.37 ± 0.69 µg g^{-1} FW). However, on increasing the duration of nutrient starvation (3 and 4 days), a decrease in both enzymatic and non-enzymatic activities was observed. Moreover, the responses of cellular antioxidants were significantly lower ($P < 0.0001$) than the control in –N-P cultures. A decrease in ROS accumulation could be the possible reason for the reduced activity of MDA, CAT, APX, and polyphenols in these cultures. Thus, it was observed that activities of CAT, APX, and polyphenols were consistent with lipid content suggesting a strong connection between oxidative stress and lipid accumulation.

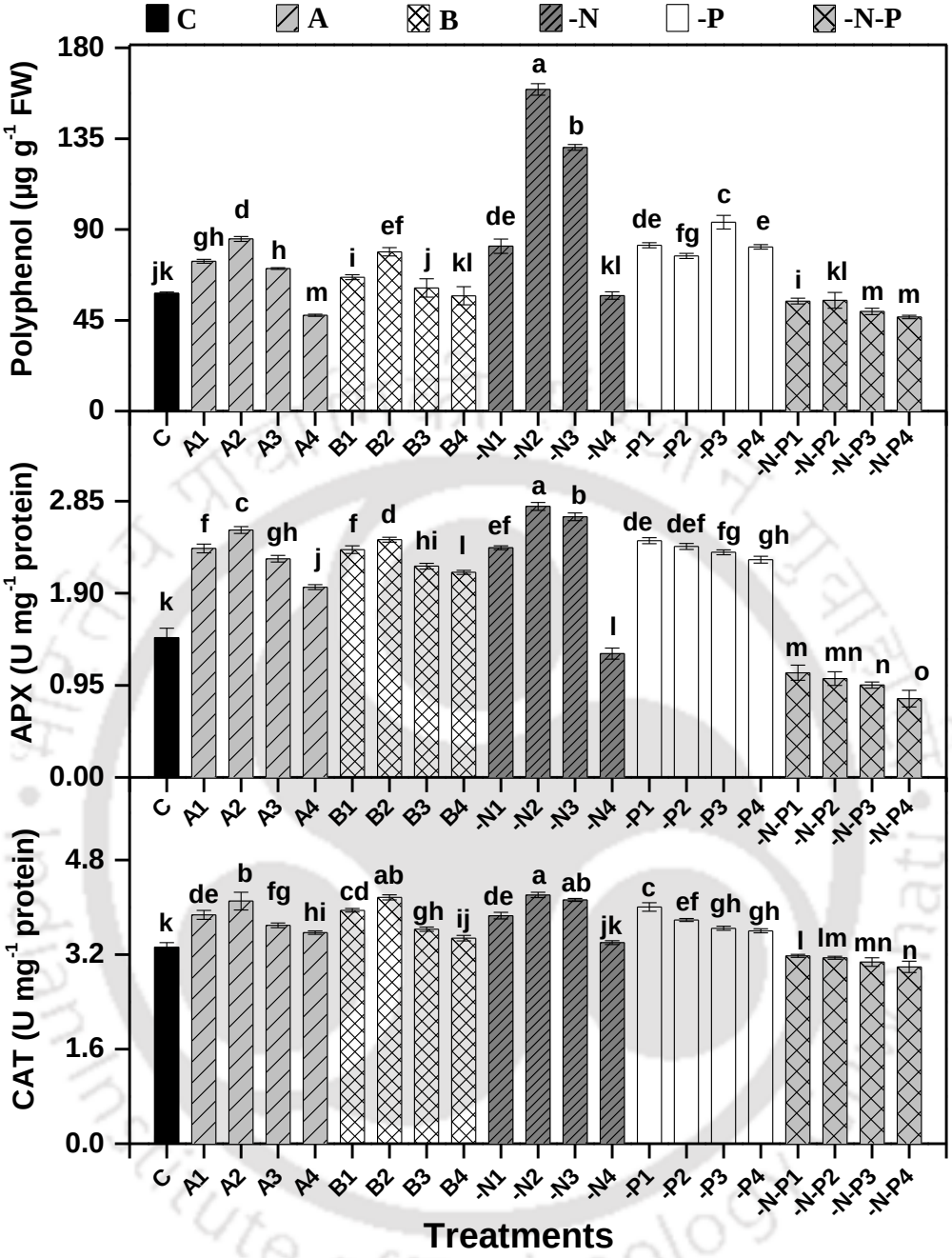

Figure 3.13. Activities of the enzymatic and non-enzymatic antioxidants of *T. obliquus* KMC24 under various nutrient-starved conditions. Values are presented as the mean ± standard deviation (n = 3). Values with the different letters represent a significant difference ($P < 0.05$) between treatments (same letters are not significantly different). The alphabetical letters are denoted in the ascending order ("a" represents the highest value).

3.3.11 Influence of nutrient starvation on fatty acid composition

The fatty acid compositions of *T. obliquus* KMC24 for all culture conditions are presented in Table 3.2. The major fatty acid components were palmitic acid (C16:0), palmitoleic acid (C16:1), oleic acid (C18:1n9c), elaidic acid (C18:1n9t), and arachidic acid (C20:0), accounting for about 97% of total FAME content for almost all nutrient stress conditions. A shift in monounsaturated fatty acid (MUFA) biosynthesis towards saturated fatty acid (SFA) production was observed when the cells were cultivated in A and B medium, where the SFA C16:0 and C20:0 were increased.

Interestingly, the accumulation of C16:0 increased with the duration of nitrogen starvation. The SFA content increased from 22.35% in control to 81.83% in –N4 cultures, whereas the MUFA content decreased from 75.36% in control to 18.83%. Nitrogen starvation for four days increased the SFA content by almost fourfold. However, the exact mechanism involved in the increase in SFA is still unknown. Fernandes et al. suggested that under nutrient deficiency, the ratio of carbon to mineral substrates (microalgal growth nutrients) increases, thereby increasing CO_2 availability, which may further improve SFA accumulation over unsaturated fatty acid (UFA) [325]. High content of SFA produces biodiesel with higher CN and superior oxidative stability [38]. High SFA content also mitigates the auto-oxidation of biodiesel, thereby improving its shelf life. Similar results were observed by Chandra et al., where nitrogen depletion and carbon supplementation, respectively, increased the degree of saturation of the total fatty acid pool [326]. PUFA are specifically sensitive to oxidation; thus, the reduction of UFA upon nitrogen starvation indicated oxidative damage [327,328]. Except for –P4 cultures, under all nutrient stress conditions, the value of C18:3 was found to be $\leqslant$12%, which is the permissible limit according to European standard EN 14214.

The production of polyunsaturated fatty acid (PUFA) was found to increase with the duration of phosphorus starvation. The PUFA content increased from 2.29% in control to 46.65% in –P4 cultures. However, the increase in PUFA production was coupled with a decline in SFA and MUFA content. SFA and MUFA are generated in the chloroplast, which serves as substrates for PUFA synthesis. As the duration of phosphorus starvation increased, a lower ratio of (SFA + MUFA)/PUFA was witnessed, which indicated a shift in SFA and MUFA biosynthesis towards PUFAs production. It has been reported that microalgae accumulate PUFA in mitochondrial membranes to protect the cell membranes from oxidative stress [329]. Combined nitrogen and phosphorus starvation significantly increased ($P < 0.05$) the MUFA content. The proportions of C16:1, C18:1n9c, C18:1n9t was found to increase gradually in -N-

P medium, while C16:0 content declined compared to the control. The MUFA content increased from 75.36% in control to 91.36% when the cells were starved for four days in -N-P medium.

Table 3.2. Fatty acid methyl esters (FAME) composition of *T. obliquus* KMC24 under various nutrient-starved conditions.

Treatments	Fatty acid (%)										SFA	MUFA	PUFA
	C16:0	C16:1	C18:1n9c	C18:1n9t	C18:2	C18:3	C20:0	C22:0	C22:1	C24:0	(%)	(%)	(%)
C	13.69	5.45	36.31	33.44	-	2.29	1.86	6.63	0.16	0.17	22.35	75.36	2.29
A1	16.74	6.95	32.10	28.43	-	0.08	-	10.02	2.72	2.96	29.72	70.2	0.08
A2	20.01	4.48	28.94	31.62	-	0.26	6.07	7.10	1.47	0.05	33.23	66.51	0.26
A3	24.60	12.50	50.40	-	-	1.1	6.64	2.16	2.34	0.26	33.66	65.24	1.1
A4	32.04	10.01	1.52	37.05	-	0.37	8.39	2.01	3.68	4.93	47.37	52.26	0.37
B1	24.67	5.35	22.40	15.94	-	2.03	22.06	0.78	4.04	2.73	50.24	47.73	2.03
B2	30.64	2.43	14.40	13.12	-	1.51	24.24	0.53	12.65	0.48	55.89	42.6	1.51
B3	33.47	2.56	11.19	11.49	-	0.84	29.08	0.35	6.25	4.77	67.67	31.49	0.84
B4	38.96	2.60	11.23	11.15	-	0.81	21.42	0.36	6.03	7.44	68.18	31.01	0.81
-N1	25.32	2.74	11.40	11.44	-	0.52	31.33	-	5.50	11.75	68.4	31.08	0.52
-N2	38.20	2.39	10.37	10.53	-	0.48	21.21	-	5.62	11.20	70.61	28.91	0.48
-N3	47.50	0.66	12.62	9.47	-	1.96	20.63	-	0.19	6.97	75.1	22.94	1.96
-N4	49.30	1.08	6.94	5.37	-	0.13	22.48	-	4.65	10.05	81.83	18.04	0.13
-P1	0.50	3.92	15.63	13.92	11.38	1.29	-	34.41	8.83	10.12	45.03	42.3	12.67
-P2	0.96	8.17	30.49		20.20	5.51	18.39	16.28	-	-	35.63	38.66	25.71
-P3	1.08	8.44	33.66	30.07	24.09	2.66	-	-	-	-	1.08	72.17	26.75
-P4	1.84	10.09	39.08	-	26.52	20.13	2.34	-	-	-	4.18	49.17	46.65
-N-P1	1.43	10.98	39.17	30.98	-	0.15	15.17	1.98	0.14	-	18.58	81.27	0.15
-N-P2	0.55	6.57	41.75	39.31	-	0.08	9.69	1.87	0.16	0.02	12.13	87.79	0.08
-N-P3	-	8.59	43.26	38.79	6.30	1.12	-	1.81	0.08	0.05	1.86	90.72	7.42
-N-P4	-	10.15	42.47	38.64	-	0.88	6.19	1.23	0.10	0.34	7.76	91.36	0.88

3.3.12 Influence of nutrient starvation on biodiesel properties

Based on the fatty acid composition, the biodiesel quality was assessed for all the growth conditions using the well-defined empirical equations (Table 3.3). Biodiesel with a high CN indicates improved ignition delay time and quality of combustion. The CN is positively related to the SFA content [38]. A high content of SFA under A, B, and -N growth conditions resulted in a higher CN. Owing to the lower SFA content under phosphorus starvation, comparatively a lower CN was obtained. Except for -P4, the CN for all other nutrient stress conditions was over 47, which is the permissible limit according to ASTM D6751. The DU and IV describes the oxidative stability of fuel, where a lower DU and IV favors better oxidation stability. As compared to all the nutrient stress conditions, *T. obliquus* KMC24 under nitrogen starved conditions possessed lower DU and IV. The viscosity defines the flow of fuel in an engine. Generally, lower viscosity results in good flow properties with high atomization quality and high biofuel penetration ability. Under all growth conditions, the kinematic viscosity was maintained in the range of 3.48 $mm^2 s^{-1}$ to 4.46 $mm^2 s^{-1}$. CFPP value predicts the flow performance of biofuel at low temperatures. Under all growth conditions, the CFPP value was comparatively lower than the ASTM D6751 and EN 14214 standards, thereby indicating excellent low temperature performance of biodiesel. Thus, it was observed that *T. obliquus* KMC24 under nitrogen starved conditions have high lipid content, combustion quality, low temperature performance and ignition delay time, thereby making *T. obliquus* KMC24 cells a potential factory for the biosynthesis of biodiesel.

Table 3.3. Biodiesel properties of *T. obliquus* KMC24 under various nutrient-starved conditions.

Treatments	Quality parameters of biodiesel						
	CN	η ($mm^2\ s^{-1}$)	SV (mg KOH g^{-1})	IV (g I_2 100 g^{-1} oil)	HV (MJ Kg^{-1})	DU	CFPP (°C)
C	57.46	3.86	196.30	73.96	40.20	79.94	-11.80
A1	60.23	3.97	193.79	63.17	40.13	70.36	-10.76
A2	60.64	3.93	195.37	60.43	40.19	67.03	-9.64
A3	58.19	3.83	197.93	61.69	40.27	67.44	-8.07
A4	63.54	3.96	195.02	47.77	40.19	53	-5.53
B1	64.04	4.04	191.61	47.74	40.19	51.79	-8.05
B2	66.13	4.11	189.16	40.09	40.19	45.62	-6.01
B3	68.61	4.18	188.54	29.51	40.19	33.17	-5.04
B4	68.53	4.15	189.78	29.04	40.19	32.63	-3.16
-N1	69.55	4.32	184.08	28.45	40.08	32.12	-7.83
-N2	69.38	4.22	188.13	26.35	40.08	29.87	-3.42
-N3	68.77	4.07	193.16	25.73	40.08	26.86	-0.25
-N4	71.53	4.20	189.63	15.78	40.08	18.3	0.37
-P1	64.06	4.46	175.08	59.64	40.08	53.72	-16.31
-P2	56.71	4.01	185.69	84.35	39.92	90.08	-16.15
-P3	48.39	3.63	197.10	113.78	39.54	95.6	-16.11
-P4	42.09	3.48	195.33	142.89	39.71	142.47	-15.85
-N-P1	57.71	3.91	194.59	73.96	40.03	50.59	-15.98
-N-P2	56.34	3.89	195.56	79.43	40.19	48.64	-16.29
-N-P3	52.35	3.74	197.77	95.75	40.15	66.77	-16.48
-N-P4	54.92	3.82	196.88	84.91	40.28	54.48	-16.48
Standard ASTM D6751/EN 14214	≥47	1.9–6.0	≤ 370	≤ 120	40	-	≤ +5

3.4 Conclusion

Short-term nitrogen starvation via a two-stage cultivation approach was the most effective strategy for enhancing the lipid content of *T. obliquus* KMC24 without affecting biomass concentration. The maximum carbohydrate (31.83 ± 0.11%) and lipid content (39.93 ± 0.44%) were obtained in –N1 and -N2 cultures, respectively. Compared to phosphorus starvation, the increase in NL content in *T. obliquus* KMC24 cells was more pronounced during nitrogen starvation. The combined nitrogen and phosphorus starvation (-N-P) was the most severe stress, which triggered cellular senescence. In contrast, a stepwise adaptive response was observed when the cells were grown in A, B, -N, and -P medium. The results suggested that stress-induced ROS generation is positively correlated with lipid accumulation. A fatty acid profile with high compatibility for biodiesel production was obtained under nitrogen-starved conditions.

भारतीय प्रौद्योगिकी संस्थान गुवाहाटी
Indian Institute of Technology Guwahati

Chapter 4

Development of a Sustainable and Efficient Harvesting Technique

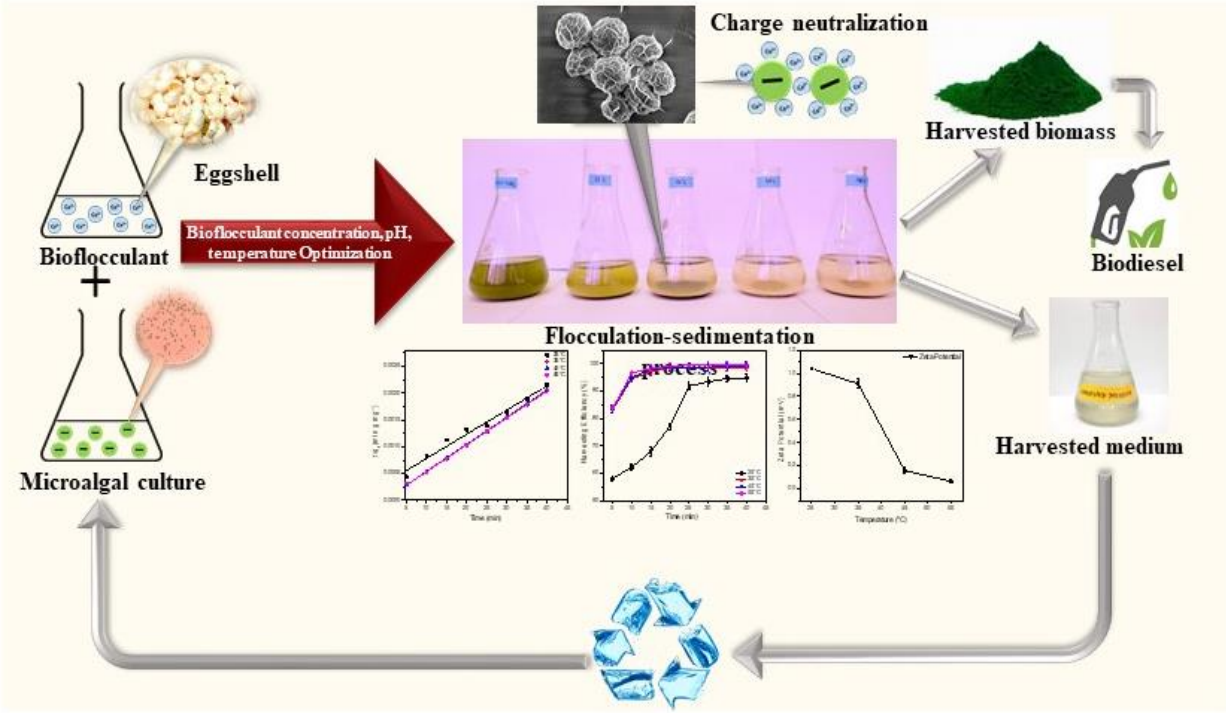

4.1 Overview

Food waste is a common solid waste produced from households and food industries in thousands of tons annually. These solid wastes may be detrimental to the environment when disposed without any pretreatments [330]. To manage these wastes, researchers have tried to valorize it as an adsorbent, catalyst, bio-template etc. [331]. Food waste is a renewable feedstock and a protagonist in the circular bioeconomy framework [332]. Recently, a few researchers have promoted the concept of green chemistry and circular bioeconomy by valorizing eggshell-derived bioflocculant [55,333]. Eggshell is a calcium-rich solid waste with a high density of cations and several functional groups such as –OH, -C=O, and $–PO_4$ [334]. These characteristic features of eggshell facilitate adsorption and destabilization of the negatively charged microalgal cells.

In this chapter, waste eggshells was valorized as a flocculating agent for harvesting *T. obliquus* KMC24. The possible mechanism involved during bioflocculation of microalgae was explored. The impact of several parameters such as temperature, bioflocculant concentration and, pH on the flocculation process was evaluated for achieving maximum harvesting efficiency. Kinetic and thermodynamic studies were also performed for evaluating the experimental data. Recyclability of the spent medium for subsequent cultivations were also studied. The effect of bioflocculant on biomass concentration, lipid yield and FAME composition was also determined.

4.2 Materials and Methods

4.2.1 Microalgae as an adsorbent

T. obliquus KMC24 was used as an adsorbent in this study. The microalgae culture was maintained in BG 11 medium. The biomass productivity was determined using the equation (3.1) as mentioned in the methodology section of chapter 3.

4.2.2 Eggshell-derived bioflocculant as an adsorbate

The waste eggshells (boiled and unboiled) were collected from the canteens of IIT Guwahati hostels and were dried in a hot air oven for 24 h at 60 °C after washing with distilled water several times. The dried eggshells were ground to fine powder using a mixer grinder. The powdered eggshell was then sieved manually using a 325-mesh sieve. The bioflocculant was extracted from the eggshell powder by using 10 mL of 0.1 mol L^{-1} HCl solution to dissolve 100 mg of the powder with continuous stirring for 35 min on a magnetic hot plate stirrer

(Tarsons digital spinot). The resulting solution was further filtered through a 0.2 μm PTFE syringe filter, and a final bioflocculant concentration of 1000 mg L^{-1} was obtained by diluting the filtrate to 100 mL with distilled water [333]. This flocculant extract was used as a stock solution for subsequent use in the experiments.

4.2.3 Optimization of bioflocculant concentration, pH, and temperature

Batch flocculation experiments were performed in 250 mL conical flasks containing 150 mL BG-11 medium. The microalgal cells were harvested in their early stationary phase, i.e., on the 14th day of cultivation, when the DCW (dry cell weight) was maximum, i.e., 2.35 g L^{-1}. Different concentrations of eggshell-derived bioflocculant solution (0–140 mg L^{-1}, at an increment of 20 mg L^{-1}) was applied to determine the influence of bioflocculant concentration on harvesting of microalgal biomass at room temperature 22°C and pH 7.

Harvesting efficiency was further enhanced by optimizing pH values (2, 4, 6, 8 and 10) of the culture medium at room temperature 22°C using optimal bioflocculant concentration. The pH values were maintained using 0.5 mol L^{-1} NaOH and 0.5 mol L^{-1} HCL. The effect of temperature on harvesting efficiency was also studied by varying the temperature (25°C, 35°C, 45°C, 55°C) of the culture medium. The temperature optimization experiment was carried out at an optimal pH value and bioflocculant concentration. The culture temperature was maintained using a shaking water bath (EQUITRON, MEDICA INSTRUMENT MFG. CO.). All the above studies were carried out within the variable contact time (0–40 min).

4.2.4 Harvesting efficiency of microalgal biomass

To determine the harvesting efficiency of the bioflocculant under various parameters, 2 mL of the supernatant was collected from the center of the algal suspension, and the optical density (OD) was measured in every 5 min of interval for 40 min. The optical density was determined at 750 nm by a UV-visible spectrophotometer. The harvesting efficiency (HE, %) of bioflocculant was calculated from the following equation [334]:

$$\mathrm{HE}(\%) = \frac{OD_{750}(t_0) - OD_{750}(t)}{OD_{750}(t_0)} \times 100\% \qquad (4.1)$$

where, $OD_{750}(t_0)$ and $OD_{750}(t)$ are the OD of microalgal cell suspension measured at time zero and t, respectively.

4.2.5 Analytical methods

Microscopic images of the treated (with bioflocculant) and untreated (without bioflocculant) microalgal cells were captured under optical microscope (Axio Scope.A1, Zeiss,

USA) to examine their morphological changes. The floc size of microalgae was considered as an evaluation mark for determining the flocculation efficacy of the bioflocculant. The bigger the size of the floc, higher the harvesting efficacy of the bioflocculant [334]. The morphology of the samples was determined by FESEM (Zeiss Sigma-300 Field Emission Scanning Electron Microscopy). Elemental components were determined by using energy dispersive spectroscopy (EDX) coupled with FESEM. The zeta potential values were recorded in triplicates using a Zeta potential analyzer (Malvern Zetasizer ZEN 3690), and the mean values were calculated in millivolts (mV) [334]. Soluble calcium concentration was determined by Systronics flame photometer (model no. 128).

The lipid content ($L_{content}$, %) of the dry biomass was determined by the protocol, as reported earlier [335]. Transesterification and FAME analysis were carried out using the protocol mentioned in the methodology section of chapter 3.

4.2.6 Determination of adsorption kinetics

The mechanism of flocculation-sedimentation process can be determined by estimating the adsorption rate. Kinetic models such as pseudo-first order equation (4), pseudo-second order equation (5) and intra-particle diffusion models equation (6) were used to study the adsorption kinetics of eggshell-derived bioflocculant by *T. obliquus* KMC24 cells. Many researchers have employed these kinetic models to evaluate the flocculation of microalgae by bioflocculants [56,334]. The high cationic charge density of eggshell enables it to be strongly adsorbed onto the negatively charged microalgal cells, which consequently causes them to flocculate due to charge neutralization.

Thus, flocculation of *T. obliquus* KMC24 by eggshell-derived bioflocculant can be considered as an adsorption process where bioflocculants are adsorbed over the microalgal cells. Therefore, these most commonly used kinetic models were employed to assess the binding of bioflocculants over microalgal cell surface with regard to time. The bioflocculant adsorption over microalgal cells q_t (mg g^{-1}) at time t, was determined from the following equation [336]:

$$q_t = \frac{(C_0 - C_t)V}{M} \quad (4.2)$$

where, q_t is the quantity of microalgal biomass (mg g^{-1}) flocculated at time t by the flocculant, C_0 (mg L^{-1}) and C_t (mg L^{-1}) are the microalgal cell concentration in the culture medium at time

zero and t respectively, V (L) is the volume of culture medium and M (g) is the mass of the bioflocculant.

$$\ln(q_e - q_t) = ln\, q_e - K_1\, t$$

(4.3)

$$\frac{t}{q_t} = \frac{1}{K_2 q_e^2} + \frac{1}{q_e} t$$

(4.4)

$$q_t = k_{int} t^{1/2} + C_i$$

(4.5)

where, q_t and q_e are the quantity of microalgal biomass (mg g^{-1}) flocculated at time t and equilibrium respectively, t (min) represents the contact time, while K_1 (min^{-1}), K_2 (g mg^{-1} min^{-1}) and k_{int} (mg g^{-1} $min^{-1/2}$) are the rate constants. C_i represents the intercept (mg g^{-1}).

4.2.7 Determination of adsorption thermodynamics

The spontaneity of the adsorption of eggshell-derived bioflocculant onto the microalgal cells was assessed using the Van't Hoff equation. The Gibbs free energy (ΔG) change is associated with the equilibrium constant (K_c) for biosorption of eggshell-derived bioflocculant over microalgal cells by the following relationship:

$$\Delta G° = -RT ln K_C$$

(4.6)

where, T is the absolute temperature in Kelvin and R is the gas constant (8.314 J mol^{-1} K^{-1}). The Gibbs' free energy equation is as follows:

$$\Delta G° = \Delta H° - T\Delta S°$$

(4.7)

where, ΔH and ΔS (J mol^{-1} K^{-1}) is the change in enthalpy and entropy respectively. Combining equation (7) and (8), we get:

$$ln K_C = -\frac{\Delta H°}{RT} + \frac{\Delta S°}{R}$$

(4.8)

A plot of $ln K_c$ vs $1/T$ is a linear graph, whose intercept and slope yields $\Delta S°/R$ and $\Delta H°/R$ respectively.

4.2.8 Activation energy analysis

The activation energy of the system was determined using the Arrhenius equation [337]. The activation energy was calculated to determine the minimum energy required for starting the chemical reaction once the bioflocculant is incorporated. Flocculation is expressed as a function of temperature in the pseudo-second order rate constant according to the Arrhenius equation (Equation 10) [56]:

$$k = Ae^{\frac{-E_a}{RT}} \tag{4.9}$$

where, E_a (J mol^{-1}) is the Arrhenius activation energy, K is the rate constant, T (Kelvin) is the absolute temperature, A is the pre-exponential factor and R is the universal gas constant.

Alternatively, the above equation can be expressed in its natural logarithm as

$$lnk = -\frac{E_a}{RT} + lnA \tag{4.10}$$

4.2.9 Recycling of harvested medium

The culture medium recovered after harvesting of microalgal cells using eggshell-derived bioflocculant was investigated for recyclability for the next cultivation cycle. After flocculation-sedimentation process, the spent medium was separated from the settled microalgal flocs by gravity. The pH of the harvested medium was neutralized, and the BG-11 medium was added before recycling the medium. The concentration of the inoculum was adjusted to have similar starting cell density in the recycled culture medium for the growth studies. The growth of *T. obliquus* KMC24 cells in the recycled culture medium was determined by recording the OD of the medium at 750 nm daily.

4.3 Results and Discussion

4.3.1 Microalgal growth

The growth curve of *T. obliquus* KMC24 in BG-11 medium was determined. From the growth pattern, it was observed that for the first 14 days, the microalgal growth was rapid before it attained the stationary phase. In this study, biomass productivity is demonstrated in terms of specific growth rate with 165 µg mL^{-1}day^{-1}. Zhu et al. (2013) obtained a biomass productivity of 0.296 µg mL^{-1}day^{-1} indicating that the specific growth rate obtained in our study was relatively higher as compared to the other reported literature [338]. A maximum biomass concentration of 2.35 g L^{-1} was achieved, which was higher than 2.25 g L^{-1} as reported by Choi et al. (2014) for *C. vulgaris* in Jaworski's Medium [339]. It has been observed that the

density of microalgal cells has a substantial part to play in its flocculation. For high-density microalgal cell cultures, a smaller portion of the cell surface area is exposed; thus, lower surface charge percentage needs to be neutralized. Whereas, low-density cell cultures require a high concentration of flocculant to neutralize the relatively bigger portion of the cell surface area, or else the cells are co-precipitated by phosphate present in the aqueous medium. Therefore, low density microalgal cultures should be pre-concentrated for achieving higher harvesting efficiency [55]. Thus, in the present study microalgal cultures were harvested on the 14th day when the culture density was maximum.

4.3.2 Effect of bioflocculant concentration

The flocculation efficiency of the bioflocculant on *T. obliquus* KMC24 from its culture medium was determined by using different concentrations (0 mg L^{-1} – 140 mg L^{-1}) with an increment of 20 mg L^{-1} for different time intervals (5 min – 40 min) at pH 7 and room temperature 22°C. The harvesting efficiency increased with increasing bioflocculant concentration and contact time (Figure 4.1a). Flocculation efficiency reached a maximum of 83 ± 1.45% when 120 mg L^{-1} of bioflocculant was used for 35 min (contact time). However, within the same contact time of 35 min, a minimum harvesting efficiency of 14.6 ± 1.3% was obtained in the control flask where no flocculant was added. On the other hand, as the concentration of bioflocculant was raised beyond 120 mg L^{-1}, the harvesting efficiency decreased to 66.65 ± 1.4%. It is reported that when the bioflocculant concentration is increased beyond the optimal dose, the microalgal culture system tends to re-stabilize instead of improving the flocculation-sedimentation process [340]. Moreover, the addition of excess bioflocculant results in agglomeration and reduction of active binding sites on microalgal cell wall; thus, impairing the flocculation efficiency [334].

The zeta potential value of the culture medium was measured to explain further the chemistry involved during bioflocculant based harvesting (Figure 4.1b). As the cell surface charge of *T. obliquus* KMC24 is found to be -16 mV, so a positively charged bioflocculant is required to neutralize the surface charges. The surface charge of eggshell was found to be positive for pH >11.4, neutral at pH =11.4 and negative for pH <11.4. The calcite surface complexes were responsible for the charge of the eggshell [341]. It has been reported that, bioflocculant extraction from eggshells using HCl acid as an extraction solvent results in the formation of CO_2, H_2O, and $CaCl_2$ as given in Equation (12)

$$CaCO_3 + 2HCl \rightarrow CO_2 + H_2O + CaCl_2 \quad (4.11)$$

This divalent cation calcium and mono-valent anion chloride significantly influence the zeta potential of the culture suspension. Elakneswaran et al. (2009) stated that for ground granulated blast furnace slag suspension an increase in the concentration of calcium ions increased the zeta potential [342]. The increase in bioflocculant concentration from 20 mg L^{-1} to 120 mg L^{-1} increased the zeta potential of the culture medium from -15.27 ± 0.49 mV to -4.99 ± 0.577 mV. This increase in zeta potential can be related to the increase in harvesting efficiency with the increase in bioflocculant concentration. However, when the bioflocculant concentration was raised to 140 mg L^{-1} from 120 mg L^{-1}, the zeta potential of the culture medium shifted from -4.99 ± 0.577 mV to +12.05 ± 0.99 mV. This sharp deviation from the isoelectric point with the increase in bioflocculant concentration to 140 mg L^{-1} may be the possible reason for the decrease in harvesting efficiency.

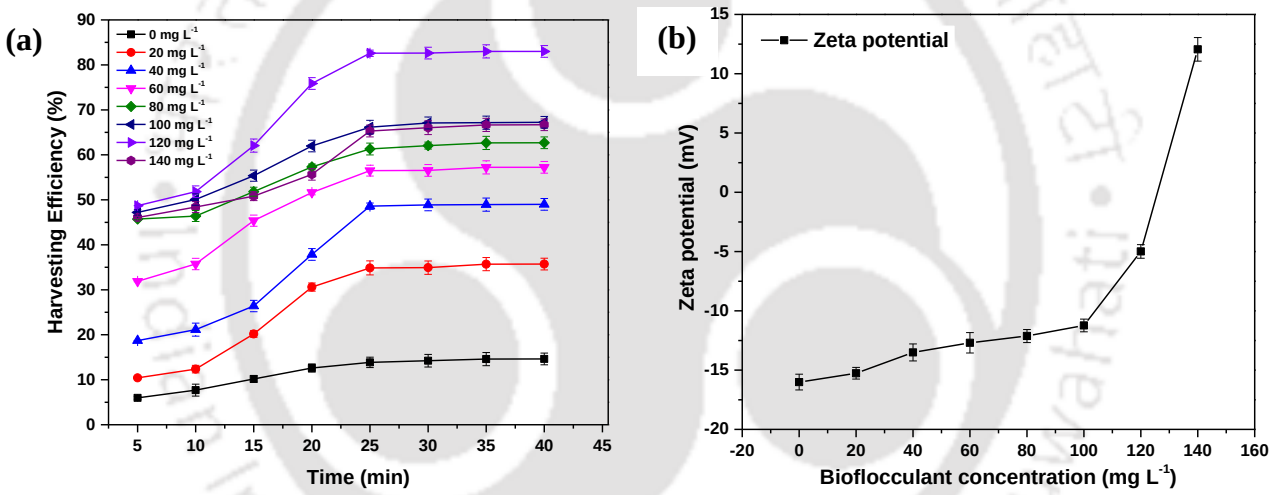

Figure 4.1. (a) Harvesting efficiency of *T. obliquus* KMC24 at various bioflocculant concentrations; (b) Relationship between bioflocculant concentration and zeta potential.

4.3.3 Effect of pH value

Another potential parameter, which influences the flocculation mechanisms, the zeta potential of microalgal cells, functional groups as well as the degree of ionization of bioflocculants is the pH of the culture medium [343]. Thus, the flocculation efficiency of eggshell-derived bioflocculant was enhanced by optimizing the pH of the culture medium (2.0, 4.0, 6.0, 8.0, 10.0) for different time intervals (5 min – 40 min) at room temperature 22°C and 120 mg L^{-1} bioflocculant concentration. In acidic conditions, the flocculation efficiency was found to be significantly high (Figure 4.2a). The highest harvesting efficiency of 94.72 ± 1.7%

was observed at pH 4.0 within 30 min of contact time, possibly because of the strong electrostatic attraction between the cationic bioflocculant and anionic microalgal cells at this particular pH. However, any further increase or decrease in pH from the optimum value resulted in a decrease of flocculation efficiency. Ali Zulfikar et al. (2012) reported that at extreme pH conditions, calcium-rich bioflocculant might get partially dissolved in the aqueous solution releasing cationic and anionic ions [344]. These ions may further get adsorbed onto the bioflocculant surface, resulting in the formation of an electrical double layer causing same species interference.

The flocculation efficiency of eggshell-derived bioflocculant at different pH values was further elucidated based on the zeta potential value of the culture medium (Figure 4.2b). At certain pH values, the colloidal particles in a solution become highly unstable and tend to coagulate. Moreover, it has been reported that as the pH of the medium drops, the H^+ concentration increases, causing cationic and anionic charges to bind. This leads to the collision of microalgal cells at a much faster rate [55]. At pH 4.0, the solution was near to the isoelectric point, representing the least stable colloidal system. Moreover, at pH 4.0, the zeta potential increased to 1.04 ± 0.35 mV thus, increasing the harvesting efficiency to 94.72 ± 1.7%. This zeta value (1.04 ± 0.35 mV) shows the highly unstable environment in algal cell suspension, which in turn intensifies the Brownian motion. From the above results, it can be concluded that the pH of the culture medium plays a significant role in harvesting *T. obliquus* KMC24.

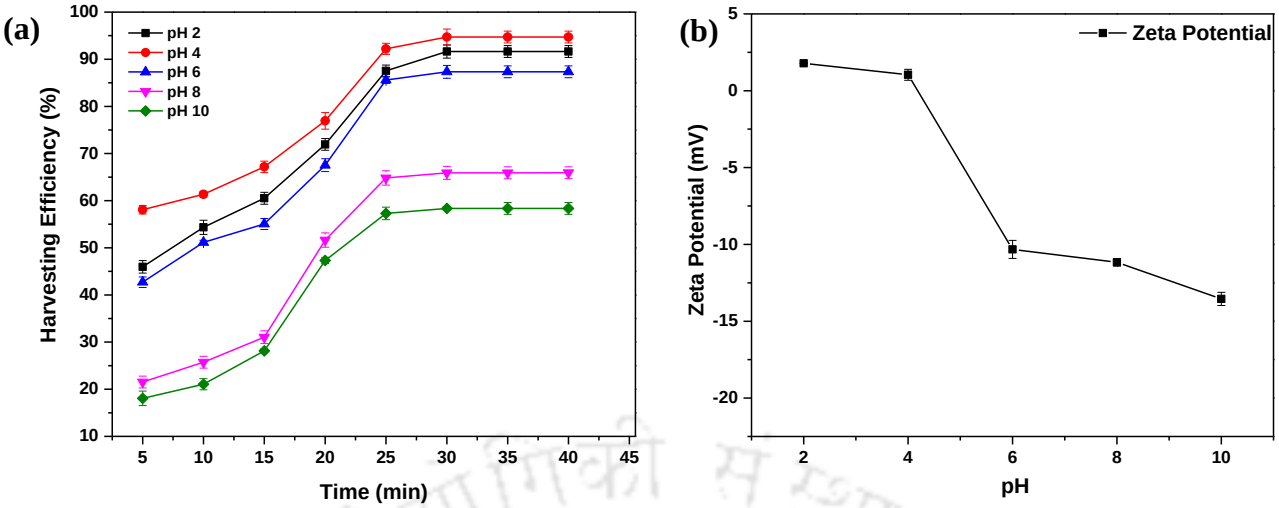

Figure 4.2. (a) Harvesting efficiency of *T. obliquus* KMC24 at various pH; (b) Relationship between pH and zeta potential.

4.3.4 Effect of temperature

Temperature plays an important role in the flocculation and settling phenomena [56]. Thus, the efficiency of the bioflocculant (120 mg L^{-1}, pH 4) to flocculate microalgal biomass over various temperatures (25 °C, 35 °C, 45 °C, 55 °C) and contact times (5 min – 40 min) was also investigated. With a contact time of 25 min, a maximum harvesting efficiency of 99.54±1.15% was achieved at a temperature of 55 °C (Figure 4.3a). The differences in flocculation efficacies were seemingly negligible for all the other studied temperatures. The increase in flocculation efficiency with the increase in temperature is probably because of the fact that higher temperature induces floc formations [345]. The acquired experimental data also revealed that harvesting time is inversely proportional to the rise in temperature. At 55 °C, the microalgal cells were flocculated within 25 min. Moreover, increased temperature accelerates floc formation by aiding the bioflocculants to attain an adequate amount of kinetic energy.

To understand temperature-influenced flocculation better, the zeta potential behavior of the culture medium under different temperature was evaluated (Figure 4.3b). The zeta potential of the culture medium was found to decrease from 1.04±0.01 mV to 0.065±0.01 mV as the temperature increased from 25 °C – 55 °C. When the zeta potential neared zero at 55 °C, the colloidal system was least stable, which resulted in floc formation. This is because at higher temperatures, the solubility of cationic Ca^{2+} ions from the calcite increases, which then binds with the anionic microalgal cells to neutralize the net surface charge [346].

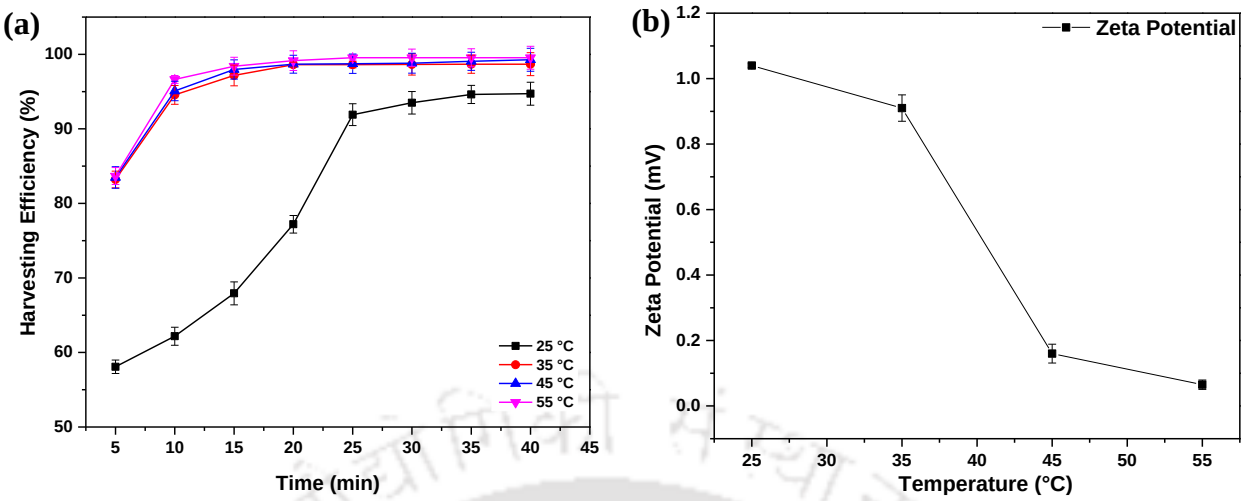

Figure 4.3. (a) Harvesting efficiency of *T. obliquus* KMC24 at various temperatures; (b) Relationship between temperature and zeta potential.

4.3.5 Microscopic, FESEM-EDX and flame photometer analysis

The microscopic and FESEM-EDX analysis of the microalgae recovered from control (without bioflocculant) and treated (with bioflocculant) medium were carried out to study the effect of bioflocculant on the morphology of *T. obliquus* KMC24 (Figure 4.4). Floc free scattered cells were observed in control, whereas, treated cells were closely associated with each other forming large dense flocs. The FESEM image of microalgal cells harvested under optimal conditions (120 mg L^{-1} bioflocculant concentration, pH 4, 35 °C temperature) did not have any structural deformation. However, microalgal cells flocculated at higher temperatures (> 35 °C) showed marked structural deformities. This is probably because the optimal temperature range for the growth of microalgal cells is 15 °C – 30 °C, beyond which the cells can tolerate a maximum temperature of up to 35 °C [347]. Therefore, based on the above facts, 35 °C was considered as the optimum temperature for flocculating microalgal cells. Harvesting efficiency of 98.62±0.43% was obtained within 25 min at 35 °C. The treated microalgal cells were somewhat whitened after flocculation experiments due to calcium deposition on the harvested biomass. This was further confirmed by performing the EDX analysis (Table 4.1).

Eggshell is mainly composed of calcium carbonate (94%), magnesium carbonate (1%), calcium phosphate (1%) and organic matter (4%) [348]. The concentration of calcium ions in the bioflocculant (120 mg L^{-1}) was found to be 34.75±1.17 ppm. Thus, the high concentration

of cationic calcium ions might have facilitated the charge neutralization of negatively charged microalgae. The possible mechanism of bioflocculation process is shown in Figure 4.5.

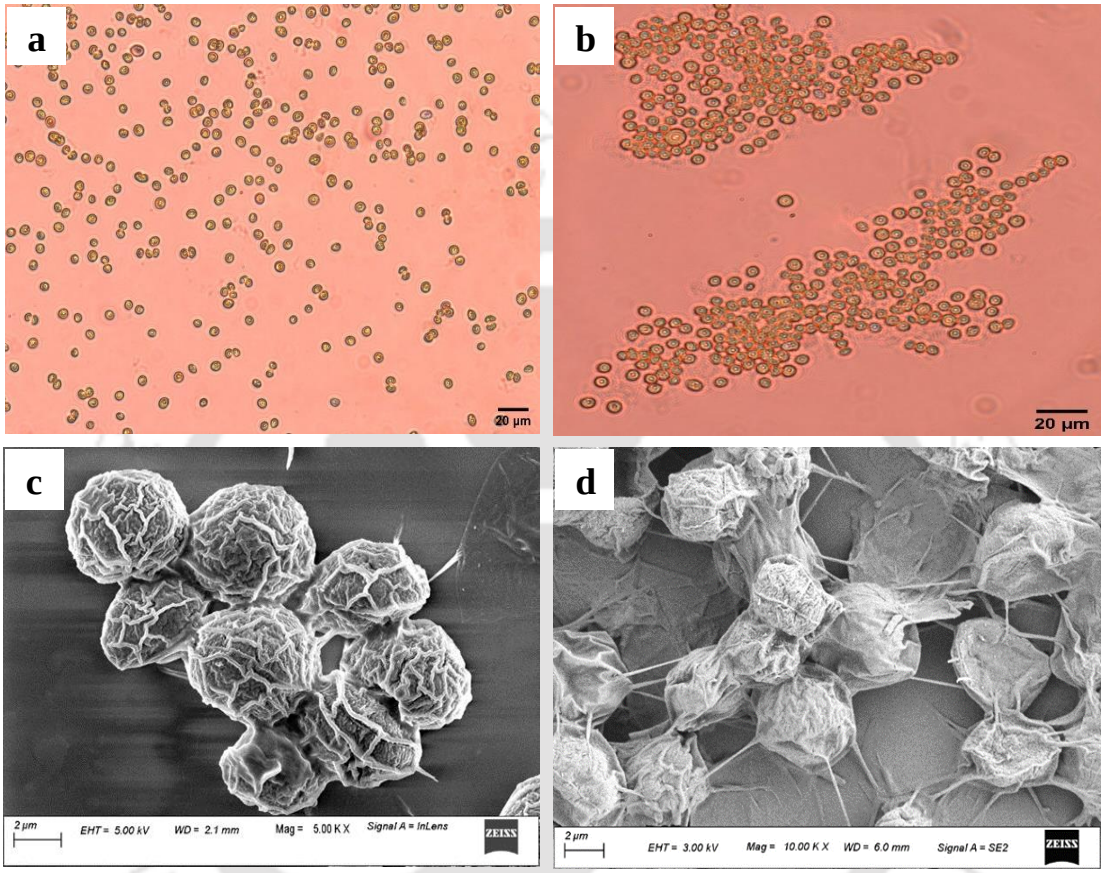

Figure 4.4. (a) Light microscopic image of *Tetradesmus obliquus* KMC 24 before adding bioflocculant (50X); (b) Light microscopic image of *Tetradesmus obliquus* KMC 24 after adding bioflocculant (50X); (c) FESEM image of *Tetradesmus obliquus* KMC 24 after harvesting at optimal conditions (120 mg L^{-1} bioflocculant concentration, pH 4, 35 °C temperature); (d) FESEM image of *Tetradesmus obliquus* KMC 24 harvested at >35 °C.

Table 4.1. Elemental composition of untreated (control) and treated (bioflocculant) *T. obliquus* KMC24 biomass.

Elements	C	O	Al	K	Na	Mg	P	Ca	Fe
Untreated	68.7	29.8	0.5	0.3	0.3	0.2	0.2	0.1	0.1
Treated	45.8	36.8	0.5	0.2	0.2	0.2	0.1	16.4	0.0

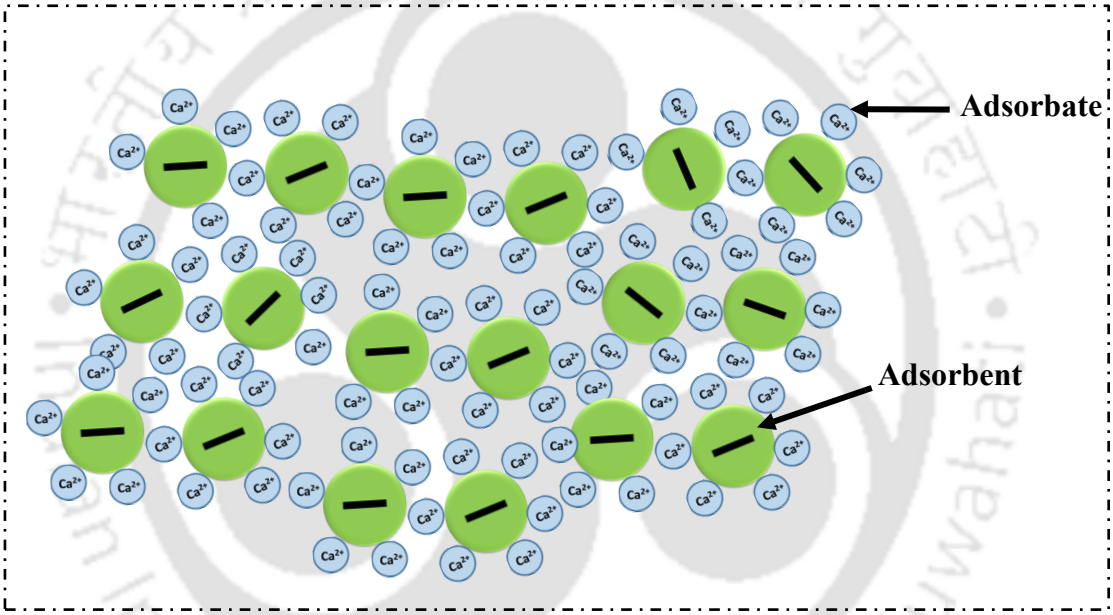

Figure 4.5. The possible mechnaism of bioflocculation process (charge neutralization).

4.3.6 Kinetic studies

Kinetic studies were carried out to gain insight into the flocculation process. From Table 4.2, it can be seen that pseudo-second order kinetic model fitted the experimental data for flocculating *T. obliquus* KMC24 with different temperatures quite well. For all temperature ranges, the plot of t/q vs t was found to be significant with high correlation (R^2>0.99) in comparison to the

pseudo-first order kinetic model (R^2<0.98) and intra-particle diffusion model (R^2<0.93) (Figure 4.6). Chemisorption is the rate limiting step in the flocculation process as per the

pseudo-second order kinetic model [343]. An increase in the rate constant (k_2) value with increase of temperature was indicated in the experimental data. This phenomenon indicates that the higher the temperature is, the better is the adsorption of bioflocculants over the microalgal cells. Thus, from a perspective of kinetics, this process of bioflocculation resembles a physical adsorption process, where, a rise in temperature speeds up the adsorption of eggshell-derived bioflocculant over the microalgal cell surface [56,336].

Table 4.2. Kinetic rate constants of various biosorption models.

Kinetic Models	Temperature			
	25 °C	35 °C	45 °C	55 °C
$q_{e,exp}$ (mg L^{-1})	18549	19325	19441	19493
Pseudo-first order kinetics				
$q_{e,cal}$ (mg g^{-1})	32991	14820	6653	28970
K_1 (min^{-1})	0.17	0.29	0.16	0.40
R^2	0.87	0.97	0.89	0.92
Pseudo-second order kinetics				
$q_{e,cal}$ (mg g^{-1})	20000	20000	20000	20000
K_2 (g mg^{-1} min^{-1})	0.000008	0.0000625	0.0000625	0.00008
R^2	0.98	0.99	0.99	0.99
Intra-particle diffusion model				
$C_{i,cal}$ (mg g^{-1})	6126	16051	16131	16303
K_{int} (mg g^{-1} $min^{-1/2}$)	2094.1	604.21	602.23	590.88
R^2	0.93	0.65	0.64	0.6

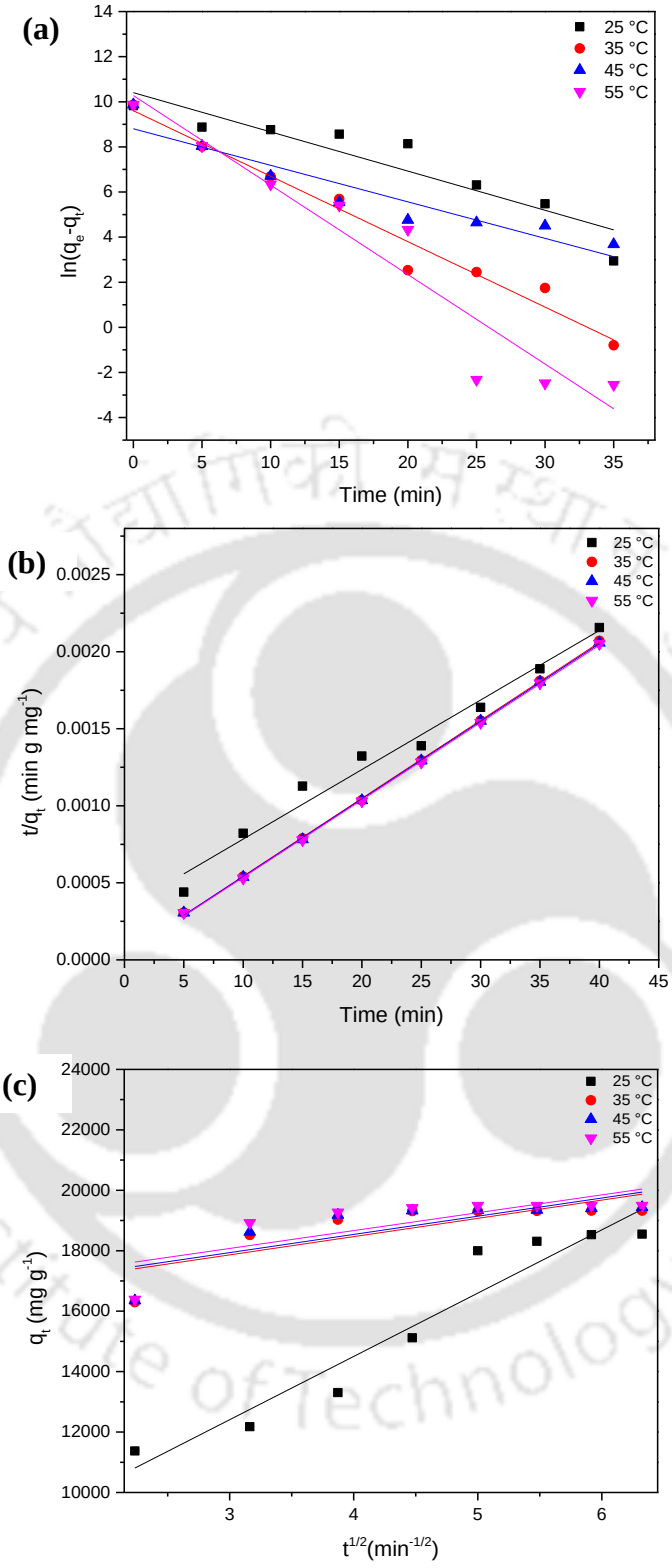

Figure 4.6. (a) First order rate constant at different temperatures; (b) Pseudo-second constant at different temperatures; (c) Intra-particle diffusion at different temperatures.

4.3.7 Thermodynamic studies

The influence of temperature on the adsorption of bioflocculant over the microalgal cell surface under various temperature ranges (298.15 K – 328.15 K) was evaluated. The values for thermodynamic functions such as entropy ($\Delta S°$), enthalpy ($\Delta H°$), Gibbs free energy ($\Delta G°$) and activation energy (E_a) are shown in Table 4.3. The negative value of $\Delta G°$ decreased gradually (-12.85 KJ mol^{-1}– -20.81 KJ mol^{-1}) with increasing temperature (298.15 K–328.15 K), indicating the spontaneity of the process, i.e. the bioflocculant adsorption over *T. obliquus* KMC24 cell surface is highly favorable and spontaneous in nature [349]. The positive value of $\Delta H°$ reveals that, the interaction between the bioflocculant and microalgal cells is endothermic in nature and there might be a probability of physical adsorption [350]. During physical adsorption process, adsorption capacity of the microalgal cells is enhanced to some extent with an increase in temperature [56]. The positive value of $\Delta S°$ indicates an increased disorder and randomness at the solid-solution interface during bioflocculant adsorption by the microalgal cells [349].

The rate of a chemical reaction can be determined from the activation energy of the system. The activation energy defines the minimum energy required for starting a chemical reaction. It has been reported that if the calculated activation energy is < 40 kJ mol^{-1} at room temperature 22 °C, the reaction rate is fast. While, the reaction rate is slower when the activation energy is >120 kJ mol^{-1} [337]. For the flocculation process, the Arrhenius activation energy was 57.11 kJ mol^{-1}, which indicated a slower adsorption process. Nonetheless, the obtained activation value in the present investigation was far superior when compared with similar studies by Kothari et al. (2017), who obtained relatively higher activation energy of 113.04 kJ mol^{-1} [56].

Table 4.3. Thermodynamic functions of *T. obliquus* KMC24 adsorption by bioflocculant.

Thermodynamic parameters		
Enthalpy, $\Delta H°$	66.15 KJ mol^{-1} K^{-1}	
Entropy, $\Delta S°$	0.265 KJ mol^{-1} K^{-1}	
Activation energy, E_a	57.11 kJ mol^{-1}	
Gibbs free energy, $\Delta G°$	Temperature (Kelvin)	$\Delta G°$(KJ mol^{-1})
	298.15	-12.85
	308.15	-15.51
	318.15	-18.16
	328.15	-20.81

4.3.8 Growth of *T. obliquus* KMC24 in the recycled medium

Spent medium recycling and reuse in microalgal cultivation can help in reducing the nutrients cost and water footprint. Ideally, spent medium after flocculation can be recycled for further cultivation. However, in many cases, the residual metal salts released from the flocculants in the aqueous medium tends to modify the medium composition causing adverse effects on microalgal cells. Eggshell-derived bioflocculant is free of metal salts and has no adverse impact on the cell structure and function. Thus, the spent medium recovered after flocculation process was recycled after neutralizing the pH and adding nutrients. Compared to the fresh culture medium, *T. obliquus* KMC24 showed relatively higher growth when cultivated in a recycled medium (Figure 4.7). The $CaCO_3$ present in the harvested medium might have acted as a carbon source for the growth of microalgae [351]. This relatively higher growth in the spent medium was observed even after three successive reuse cycles. In a similar study where alum was used as a flocculant, the recycled medium could not sustain microalgal growth, probably due to the toxicity of the residual alum [352]. Hence, the types of flocculants must be chosen wisely for successful reuse of the spent medium.

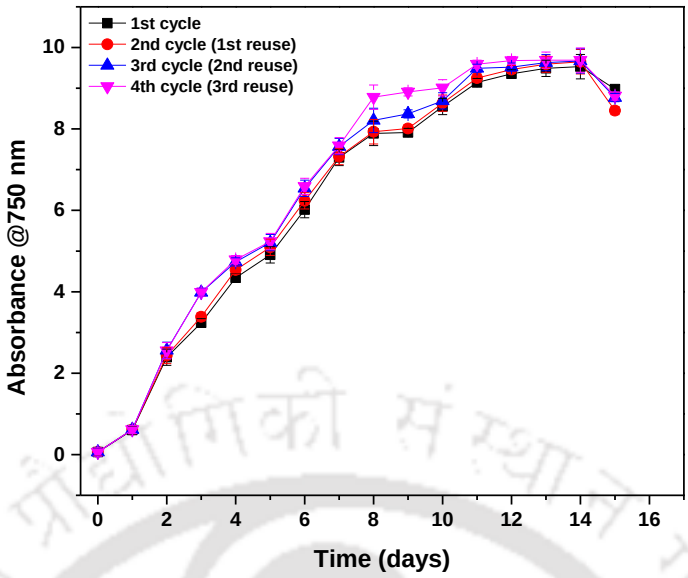

Figure 4.7. Growth of *T. obliquus* KMC24 in the recycled medium.

4.3.9 Biomass, lipid content and FAME analysis

Improved growth profiles in the recycled medium resulted in higher biomass (g L^{-1}) and lipid yield (%) (Figure 4.8). The residual calcium and magnesium ions in the spent medium might have served as micronutrients which indirectly resulted in higher biomass concentration of *T. obliquus* KMC24 [353]. Finally, the effect of bioflocculant on the fatty acid composition of lipid derived from *T. obliquus* KMC24 was investigated. The FAME composition of *T. obliquus* KMC24 cells harvested from control and treated medium exhibited similar fatty acid composition (Table 4.4). The FAME derived from the untreated (control) and treated (bioflocculant) biomass contained 22.35% and 23.37% of saturated fatty acids, respectively. A major fraction of the FAME was composed of unsaturated fatty acids.

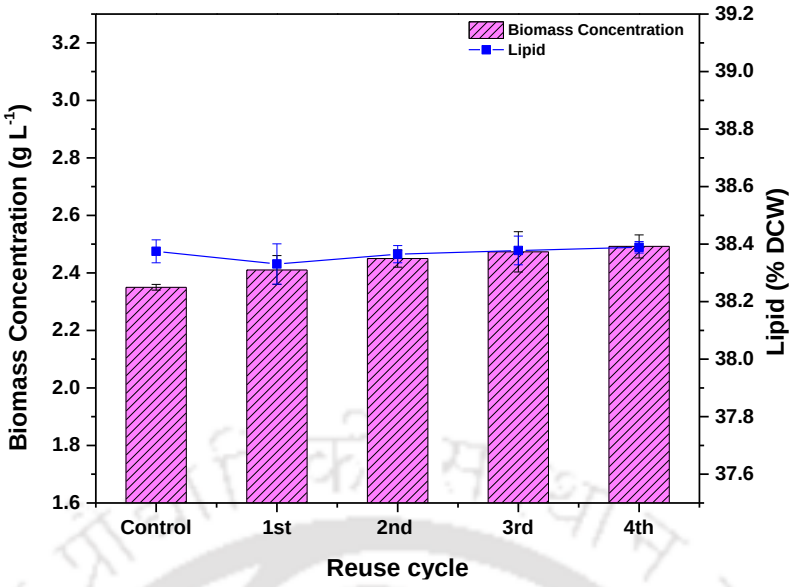

Figure 4.8. Biomass concentration and lipid content of *T. obliquus* KMC24 in recycled medium.

Table 4.4. FAME composition of untreated (control) and treated (bioflocculant) *T. obliquus* KMC24 biomass.

Samples	Fatty acid (%)								
	C16:0	C16:1	C18:1n9c	C18:1n9t	C18:3	C20:0	C22:0	C22:1	C24:0
Untreated	13.69	5.45	36.31	33.44	2.29	1.86	6.63	0.16	0.17
Treated	14.07	3.3	35.10	33.43	2.08	1.80	5.02	2.72	2.48

4.3.10 Eggshell-derived bioflocculant - A better alternative

As compared to the cultivation stages, the harvesting phase of microalgal biomass is more prone to contamination and involves high energy input. Hence, the sustainability of the harvesting process and the quality of the end product is greatly influenced by the harvesting method. Centrifugation process ensures a higher rate of recovery and cell viability but is not energy efficient for pilot scale systems. The cost of centrifugation is estimated to be about $ 4.52 L^{-1} of oil [177]. Flotation process requires positively charged chemical coagulant to overcome the repulsion between negatively charged microalgal cells and air bubbles. The estimated cost and energy involved during the flotation process is about $ 0.022 - 0.045 kg^{-1} and 0.16-0.44 kWh kg^{-1}, respectively [26]. Further, the process is species-specific and less sustainable for low-density microalgal culture. Filtration based harvesting processes involve high operational costs and often result in membrane fouling.

Chemical flocculants such as, a quaternary ammonium salt based cationic polymer and nano-Fe_3O_4 coated with polyethyleneimine was successful in harvesting 96.5% and $98.45 \pm 0.35\%$ of *Scenedesmus* sp. in 15 min respectively [354,355]. However, conventional chemical flocculation is a chemical dependent process, which produces huge quantities of sludge. Moreover, chemical flocculants are toxic that interferes with the cell properties and does not permit the reusability of the harvested medium. The residual aluminium salts (e.g., $AlCl_3$ and $Al_2(SO_4)_3$) affects the fatty acids methyl esters (FAME) composition, whereas, ferric salts (e.g., $FeCl_3$ and $Fe_2(SO_4)_3$) alter the quality of pigments [352]. The cost and energy input of flocculation with aluminium salt is about 1.8 \$ kg^{-1} and 14.81 kWh m^{-3} respectively [55]. Commercial polyelectrolyte flocculant such as Zetag 63 is a less toxic cationic flocculant, which is required in a dose of 10 mg L^{-1} to harvest 93% of *Chlorella stimatophora* [356]. In another study, Zou et al. (2018) harvested 83.77% of *Scenedesmus obliquus* using 30 mg L^{-1} of chitosan [357]. However, these polyelectrolyte flocculants require \$ 0.035 - 0.04 to harvest a kg of microalgal biomass [358].

To overcome these challenges, an increasing number of researchers have focused on bioflocculants due to their easy degradability with no secondary pollution. Polymeric bioflocculant isolated from *Streptomyces* sp. was able to harvest 99.18% of *Nannochloropsis* sp. in less than 10 min with 5000 mg L^{-1} of bioflocculant concentration [359]. A novel strain of *Pseudomonas* sp. was isolated which secretes a cellulase-free xylanase and simultaneously produce bioflocculants through directly converting untreated biomass [360]. However, these bioflocculation processes are unreliable, as the flocculation process is uncontrolled with high chances of microbial contamination.

Food industries and home kitchens generate several tons of eggshell as a solid waste [361]. As the bioflocculant used in this study is derived from solid waste, it lowers the cost of bioflocculant. The minimal preparation steps in this process involve relatively very less energy input. Moreover, bioflocculation being a chemical free process does not interfere with the quality of the end product and also support the reusability of the harvested medium. Further, there was no loss of biomass during the adsorption process, as the flocculant was not separated from the harvested biomass. Thus, the present study revealed that the eggshell-derived bioflocculant is a promising approach for harvesting biomass in a pilot scale as compared to the conventional harvesting techniques.

4.4 Conclusion

The present study supports valorization of waste eggshells to derive a flocculating agent for harvesting *T. obliquus* KMC24 and economically balances the microalgal biorefinery. Harvesting efficiency of 98.62±0.43% was achieved within 25 minutes under optimal conditions of 120 mg L^{-1} flocculant dose, pH 4.0 and a temperature of 35 °C. Zeta potential analysis confirmed charge neutralization as the flocculation mechanism. This process was spontaneous and endothermic in nature. The recycled medium did not impair the biomass concentration and lipid productivity. Therefore, this bioflocculant will reduce the shortcomings associated with downstream processing of biomass by cutting on the harvesting cost.

Chapter 5

Development and Characterization of Low-cost and Eco-friendly Catalyst for Microalgal Lipid Transesterification to Biodiesel

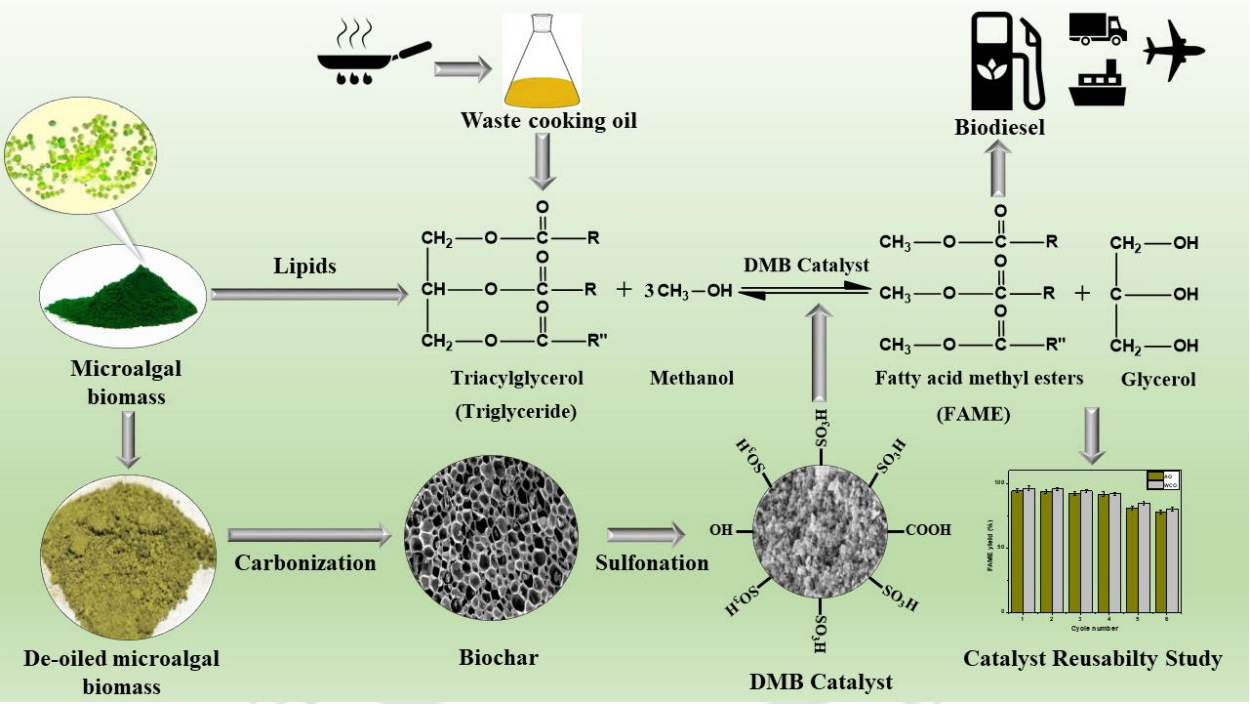

5.1 Overview

Biodiesel production from microalgal biomass generates a considerable amount of de-oiled microalgal biomass as a waste product [362]. It has been estimated that approximately 65% of the biomass remains as waste after lipid extraction [363]. These de-oiled microalgal biomass, which is a rich source of carbohydrate, protein, and mineral content can be valorized into value-added products in order to offset the biodiesel cost [364]. Therefore, in the present study, an integrated biorefinery concept was tried to establish by valorising de-oiled microalgal biomass as a solid acid catalyst for transesterification of microalgal oil. The de-oiled microalgal biomass-based (DMB) solid acid catalyst was developed through carbonization of the organic compounds followed by sulfonation. The effect of catalyst synthesis conditions such as pyrolysis temperature, sulfonation time, and H_2SO_4 concentration towards the surface acidity of the catalyst and free fatty acid (FFA) conversion was determined, and an optimized catalyst preparation condition was developed. The catalyst derived from de-oiled biomass was further characterized to evaluate its physicochemical properties. The DMB catalyst was used for the transesterification of microalgal oil (AO) and waste cooking oil (WCO). The influence of reaction parameters on the FAME yield was determined. Further, the catalyst reusability was investigated, and the possible mechanisms behind the reduction in catalytic activity with the number of reuses were explored. The impact of DMB catalyst on the FAME composition of AO and WCO was determined.

5.2 Materials and Methods

5.2.1 Materials

The de-oiled microalgal biomass was obtained from the previously isolated oleaginous microalgae *Tetradesmus obliquus* KMC24 after lipid extraction. The WCO was collected from the hostel of IIT Guwahati, Assam, India. All the chemicals and reagents were procured from HiMedia® and Sigma-Aldrich, India.

5.2.2 De-oiling of microalgal biomass

The *T. obliquus* KMC24 biomass (10 g) was de-oiled by extracting the lipid through the soxhlet extraction method employing n-hexane (200 mL) as a solvent [365]. Lipid, hexane,

and de-oiled biomass were recovered at the end of extraction. The de-oiled biomass was made solvent free through oven drying for carbon catalyst preparation.

5.2.3 Synthesis of DMB catalyst

The DMB catalyst was synthesized via a two-step process where carbonization of de-oiled microalgal biomass was followed by sulfonation of the carbonized biochar with sulphuric acid. In the first-step, 10g of de-oiled biomass was pyrolyzed in a tubular reactor at 400 °C-700 °C at a heating rate of 4 °C min^{-1} under a stream of Argon (100 mL min^{-1}) for 4 h to obtain biochar. The biochar yield was determined from the following equation:

$$Biochar\ yield = \frac{mass\ of\ biochar\ produced}{mass\ of\ biomass\ taken} \times 100\% \quad (5.1)$$

The biochar was ground to a fine powder using a mortar and pestle before sulfonation. 2g of biochar was sulfonated using (5, 10, 15, 20 mL) concentrated sulphuric acid for a reaction time of 2, 4, 6, and 8 h in a 500 mL glass beaker. The variable's ranges were selected based on the previously reported literature [366,367]. The reaction mixture was heated at 110 °C on a hot plate and was occasionally mixed with a glass rod. After the sulfonation process, the mixture was cooled and placed in deionized water. Later, the carbon catalyst was repetitively washed with hot deionized water until the washing solution was neutral in pH and free of sulfate ions. The synthesized solid acid catalyst was oven dried (110 °C) overnight and was stored in a vacuum desiccator for further study.

5.2.4 Characterization

The structural analysis of the catalyst was determined by X-ray diffraction (XRD) technique employing X-ray diffractometer (TTRAX III 18 kW; Rigaku Corporation, Japan) with Cu K_α radiation ($\lambda = 1.5406$ Å). Diffractograms were obtained in the 2θ range of 10° to 90°. The morphology of the samples was determined by FESEM (Zeiss Sigma-300 Field Emission Scanning Electron Microscopy). Elemental components were determined by using energy dispersive spectroscopy (EDX) coupled with FESEM. The KBr pellet technique was employed to record the Fourier transform-infrared (FT-IR) spectra over a wavenumber range of 4000 to 400 cm^{-1} by a spectrometer (Perkin Elmer Spectrum 2 FTIR). Raman spectra were recorded with a LabRAM HR Raman microscope (laser: 514 nm). Elemental analysis (C, H, N, S) of biochar, catalyst, and reused catalyst was carried out in a CHNS analyzer (Flash EA 1112 series, Thermo Finnigan, Italy). The BET (Brunauer-Emmett-Teller) surface area of the

samples was determined by N_2 adsorption-desorption measurements at 77.3 K using a TriStar II 3020, Micromeritics instrument. The hydrophilic and hydrophobic properties of the catalyst were determined by a drop shape analyzer. The thermal stability of the samples was determined using TGA (STA7200, Hitachi, Japan) under N_2 atmosphere. X-ray photoelectron spectroscopy (XPS) analysis on NEXSA; Thermo Scientific Instruments with a monochromatic Al Kα radiation was performed to analyze the chemical composition of the catalyst. The total acid density of the catalyst was determined by the titration method as reported in the literature [78]. The total acidity of the catalyst was also analyzed by temperature programmed desorption of ammonia (NH_3-TPD, MicrotracBEL BELCAT II). At first, degassing of the catalyst was carried out under He flow at 300 °C for 1 h. The degassed catalyst was then cooled to 40 °C by He gas at a flow rate of 50 mL min^{-1}. After cooling, a gas mixture of 10% NH_3/He was allowed to pass through the sample cell for 2 h. Subsequently, desorption of the physisorbed NH_3 was conducted from ambient temperature to 800 °C at the heating rate of 10 °C min^{-1} with a flow of He (30 mL min^{-1}). The desorbed NH_3 was detected using a TCD detector.

5.2.5 Reaction study

Catalyst synthesis conditions such as pyrolysis temperature, sulfonation time, and the amount of H_2SO_4 added during the sulfonation reaction were optimized by evaluating the percentage of FFA conversion during the esterification reaction. Esterification reaction of a known amount of oleic acid with methanol was conducted in a round-bottomed flask equipped with a refluxing condenser at 80 ^oC reaction temperature, methanol to oleic acid molar ratio of 10:1, a reaction time of 6 h, and catalyst concentration of 5 wt. %. At the end of the esterification process, the catalyst was retrieved via centrifugation, and the unreacted methanol was evaporated. Finally, the liquid product was analyzed for acid value and FFA conversion using the previously reported equations [368]. The percentage FFA was calculated by multiplying the factor 0.503 with the acid value [369].

Further, the catalytic activity of the DMB catalyst prepared under optimized conditions was tested for transesterification of lipid derived from *T. obliquus* biomass (AO) and WCO. The reaction parameters such as methanol/oil molar ratio, catalyst concentration, reaction temperature and time were optimized based on FAME yield in a round-bottomed flask equipped with a refluxing condenser. The variable's ranges of the reaction parameters were selected based on the previously reported literature [74]. At the end of the reaction, the product was shifted to an Eppendorf tube, where the catalyst was recovered through centrifugation.

Subsequently, hexane and warm distilled water were incorporated into the reaction mixture and vortexed. Finally, the mixture was centrifuged to separate the phases based on their density. The FAME was separated from the upper phase, and unreacted methanol was evaporated. The top layer consisting of hexane and FAME was collected. The hexane was vaporized, and the FAME yield (%) was determined using the following equation [74]:

$$FAME\ yield\ (\%) = \frac{FAME\ Obtained\ (g)}{Initial\ mass\ of\ oil\ (g)} \times 100 \quad (5.2)$$

The catalytic efficiency of the DMB catalyst was compared with the conventional acid-base catalyst. A two-step, acid-base (HCl-NaOH) transesterification reaction of AO and WCO was carried out under the optimized reaction conditions.

5.2.6 Catalyst reusability study

The stability of the DMB catalyst was evaluated by reusing it for consecutive cycles at the optimized reaction conditions. The catalyst recovered through centrifugation at the end of the experiment was rinsed with methanol, dried at 80 °C for 6 h, and was reused for the next experiment.

5.2.7 Analysis of FAME and biodiesel properties

The FAME composition and biodiesel properties were analysed using the protocol mentioned in the methodology section of chapter 3.

5.3 Results and Discussion

5.3.1 Optimization of catalyst synthesis conditions

The catalyst synthesis conditions such as pyrolysis temperature, sulfonation time, and the amount of H_2SO_4 added were optimized based on the surface acidity of the catalyst and FFA conversion (Figure 5.1). The pyrolysis temperature was optimized at a constant sulfonation time of 4 h and 10 mL of H_2SO_4. As shown in Figure 5.1 (a), the surface acidity of the DMB catalyst increased (0.5–1.5 mmol g^{-1}) on increasing the pyrolysis temperature from 400 °C to 600 °C. This indicates that at lower pyrolysis temperature, the degree of carbonization might be low, thereby making the product unsuitable as support for solid acid catalyst. Whereas, high pyrolysis temperature might have resulted in a higher degree of carbonization along with the formation of randomly orientated small aromatic carbon sheets preferable for bonding sulfonic groups during sulfonation [368]. However, the surface acidity of the catalyst was found to reduce on increasing the pyrolysis temperature beyond 600 °C; probably extreme high temperature caused the opposite effect on the surface acidity [367].

Similarly, an increase in pyrolysis temperature led to an increased FFA conversion, with a maximum (74.67%) conversion at 600 ^{o}C. The aromatic carbon structures formed during pyrolysis at high temperature (600 ^{o}C) might have provided large surfaces for the bonding of –SO_3H groups as active sites for esterification reactions. An increase in pyrolysis temperature from 400 °C to 600 °C resulted in a minimal reduction of biochar yield (37.50% to 36.68%). However, the biochar yield decreased to 27.15% on increasing the pyrolysis temperature to 700 °C. The reduction in biochar yield on increasing the pyrolysis temperature could be attributable to the thermal cracking of volatile components to lower molecular weight liquids and gases instead of biochar [84].

The sulfonation time was optimized at a constant pyrolysis temperature of 600 °C and 10 mL of H_2SO_4. The sulfonation process plays a crucial role during the synthesis of a carbon-based acid catalyst, as the process grafts the sulfonic groups on the activated carbon (AC) surface, thereby providing a platform for the reactions to take place. Therefore, during the sulfonation process, the optimization of sulfonation time is necessary for sufficient grafting of sulfonic groups on the carbon surface. Figure 5.1 (b) shows that the surface acidity of DMB catalyst and FFA conversion (%) increased with the duration of sulfonation time. Maximum surface acidity of 1.62 mmol g^{-1} and FFA conversion (%) of 80.62 % was achieved with 6 h sulfonation time. However, no significant changes in surface acidity and FFA conversion were observed when the sulfonation time was increased beyond 6 h. This indicates that 6 h sulfonation time is enough for sufficient grafting of sulfonic groups on the randomly oriented carbon surfaces. Moreover, a longer sulfonation time (6 h) saturates the AC surface with sulfonic groups until an equilibrium state is attained. Thus, increasing the sulfonation time beyond 6 h could no longer impact the quantity of sulfonic groups grafting on the AC surface due to the steric hindrance effect [368].

The amount of H_2SO_4 added was optimized at a constant pyrolysis temperature of 600 °C and sulfonation time of 6 h. The surface acidity of the DMB catalyst increased (1.22 mmol g^{-1}–1.73 mmol g^{-1}) with the increasing amount of H_2SO_4 (5 mL – 15 mL) (Figure 5.1c). This indicated that 15 mL of H_2SO_4 was necessary for the complete sulfonation reaction to occur. Significant changes in surface acidity were not observed when the amount of H_2SO_4 was increased beyond 15 mL. Similarly, an increase in H_2SO_4 concentration increased the FFA conversion with a maximum (83.61%) conversion when 15 mL H_2SO_4 was added. However, a slight reduction in FFA conversion was observed when the amount of H_2SO_4 was increased

beyond 15 mL. This may be attributed to the excessive amount of H_2SO_4 added that might have increased the acid concentration, thereby affecting the sulfonation process.

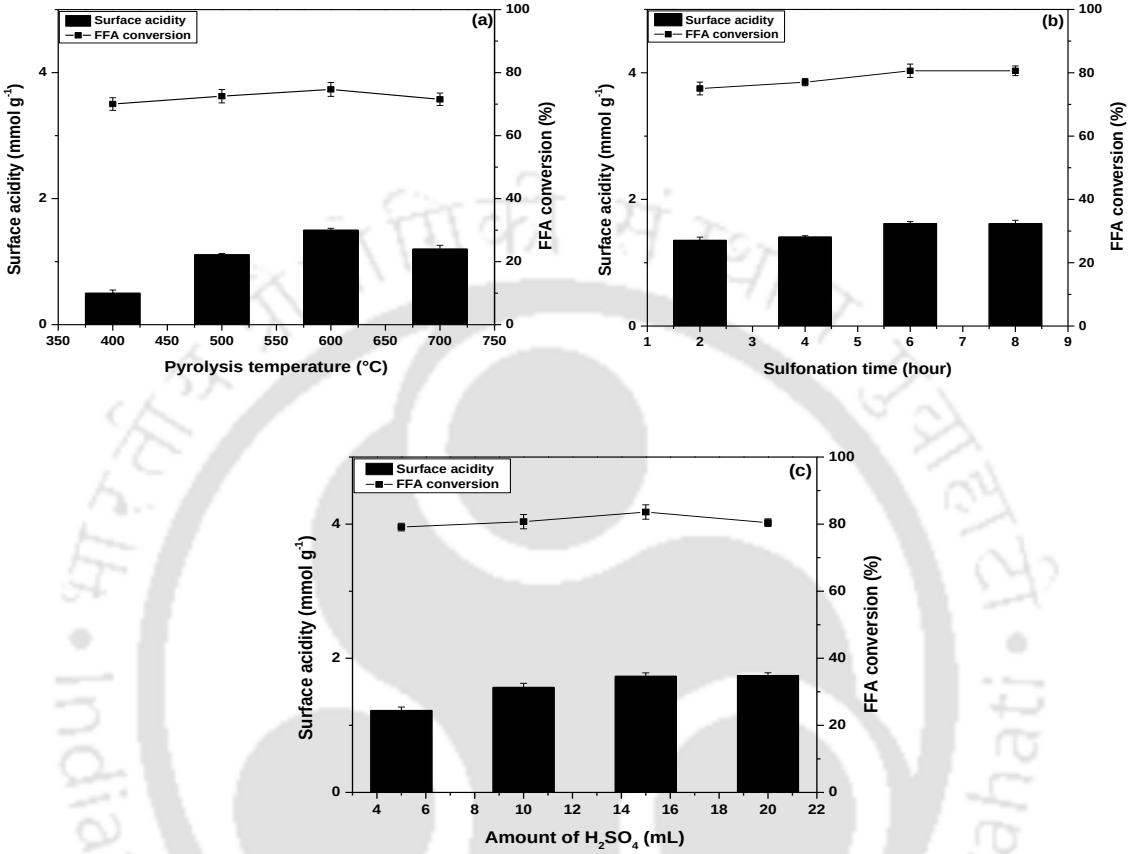

Figure 5.1. Effect of (a) pyrolysis temperature, (b) sulfonation time, and (c) H_2SO_4 concentration on surface acidity and FFA conversion.

5.3.2 Characterization of DMB catalyst

5.3.2.1 XRD analysis

The XRD patterns of the biochar and catalyst exhibited similar, one broad C(002) and weak C(001) diffraction peaks in the range of 2θ = 20°–30° and 2θ = 35°–50°, respectively (Figure 5.2). The peaks indicated that both the biochar and DMB catalyst were amorphous and possessed randomly oriented aromatic carbon sheets. Moreover, these amorphous structures are reported to favor the anchoring of sulfonic groups [370]. The narrowness of the C(002) peak in the case of the DMB catalyst is attributable to the presence of graphitic carbon structures. Upon sulfonation of the biochar, the intensity of the C(002) peak was found to

decrease. The reduction in peak intensity was due to the bonding of -SO_3H groups to the sp^2 carbon network [371].

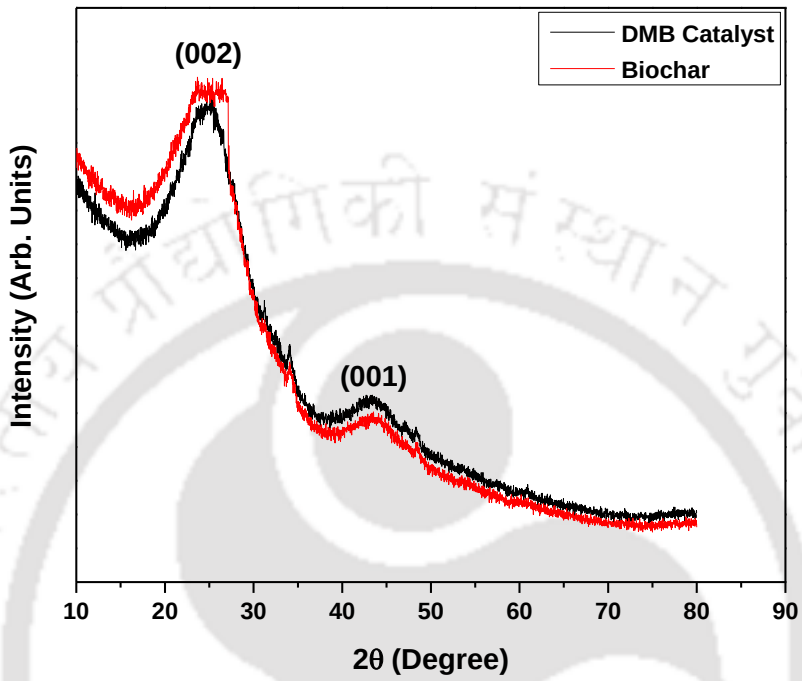

Figure 5.2. XRD analysis of biochar and DMB catalyst.

5.3.2.2 FTIR analysis

The functional groups present in the biochar and DMB catalyst are represented in Figure 5.3. The FTIR peaks at 3430 cm^{-1} were assigned to O–H stretching modes, indicating the presence of –COOH and phenolic –OH groups before and after sulfonation [370]. The vibration bands at 1600 cm^{-1} and 1376 cm^{-1} (C=C stretching mode) indicated the presence of polyaromatic compounds in both biochar and catalyst [372]. The peak intensity of C=C at 1376 cm^{-1} was relatively higher in all the acid treated catalyst than that of biochar. A similar observation was reported for sulfonated silica–carbon composites as a catalyst by Valle-Vigón et al. (2012). The FT-IR spectra of the catalyst showed the characteristic peaks corresponding to stretching vibrations of –SO_3H groups. The vibration bands at 1027 cm^{-1} and 1200 cm^{-1} confirmed the presence of –SO_3H groups in the catalyst [374]. The increase in relative intensity of bands at 1200 cm^{-1} indicated a greater presence of the sulfonic acid in the catalyst [375].

The FTIR spectra of catalyst also showed a peak at 1722 cm^{-1} which is ascribed to C=O stretching modes of the –COOH group [74]. The intensity of stretch C=O at 1722 cm^{-1} was increased due to partial oxidation of the C–O into C=O on –COOH groups, indicating that the sulfonation process favors the formation of –COOH groups on the catalyst surface due to the use of H_2SO_4, which is a strong oxidizing agent [376]. Thus, it was observed that after sulfonation, the peak intensities were increased. This indicated that new functionalities such as hydroxyl and aromatic structures formed due to carbonization of de-oiled microalgal biomass reacted with sulphuric acid, thereby forming –SO_3H functionalities on the catalyst surface.

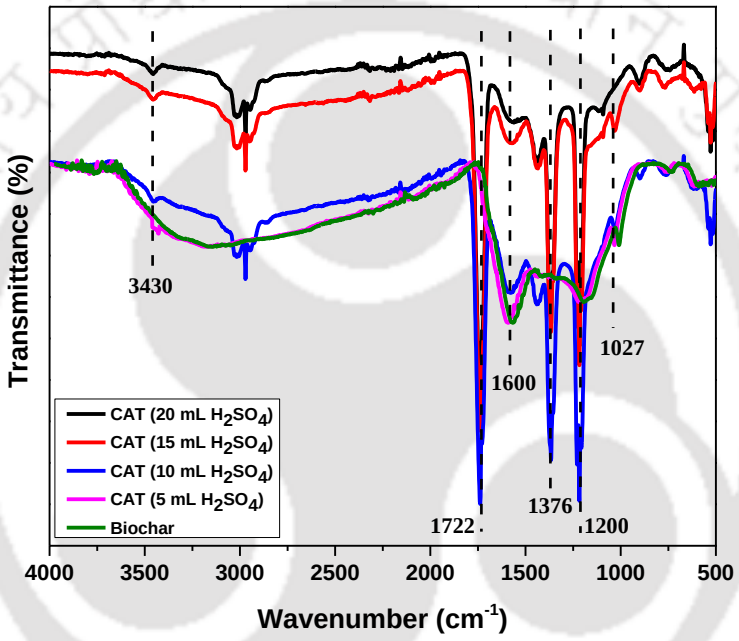

Figure 5.3. FTIR spectra of biochar and DMB catalyst.

5.3.2.3 FESEM analysis

The morphology of the de-oiled microalgal biomass, biochar, and DMB catalyst was studied using FESEM analysis (Figure 5.4). The non-porous structure was observed in de-oiled biomass before pyrolysis. On the other hand, biochar obtained after carbonization exhibited irregular and rough surface morphology with a well-defined porous structure. Carbonization of de-oiled biomass might have generated pores on the carbon surface during the escape of volatile compounds due to thermal treatment. Moreover, grains of different sizes blocked the large holes of biochar. Porous surfaces are known to provide a higher surface area, which is essential

for attaching sulfonic groups. Porous surfaces of the biochar facilitate sulphuric acid to access into the bulk of the carbon composites during sulfonation. Thereby, enhancing the concentration of covalently bonded $–SO_3H$ groups on the AC surface. The hydrophilicity of the $–SO_3H$ groups enables hydrophilic methanol molecules to incorporate into the carbon bulk and react with the hydrophobic reactants (FFA and triglyceride), thereby enhancing the bio-oil yield. After sulfonation of the biochar, globular structures were detected on the surface of the DMB catalyst that indicated bonding of $–SO_3H$ groups. The particle size of the DMB catalyst was reduced following sulfonation due to the breakdown of organic compounds by the action of H_2SO_4 [84]. It indicated that the smaller particle size (i.e., large surface area) could improve intraparticle diffusion of the reactants, thereby contributing to higher catalytic activities.

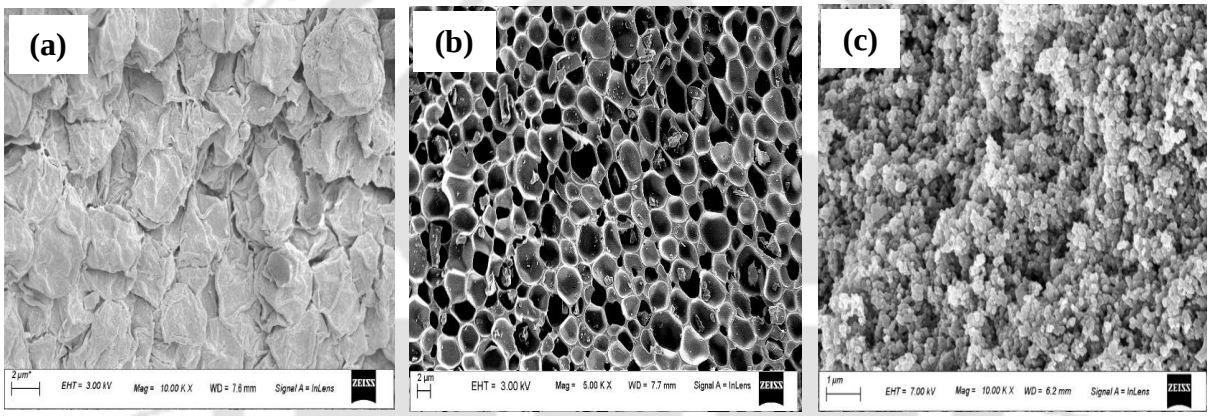

Figure 5.4. FESEM images of (a) de-oiled microalgal biomass, (b) biochar, and (c) DMB catalyst.

5.3.2.4 TGA analysis

The thermal stability of the DMB catalyst was determined through TGA analysis. Figure 5.5 represents the TGA curves of de-oiled microalgal biomass, biochar, and DMB catalyst. The decomposition process of de-oiled microalgal biomass can be partitioned into three phases for elucidation. In the first phase (30 °C to 200 °C) an initial mass loss of 8.5% occurred due to the release of moisture and volatile compounds through dehydration. The second phase (200 °C to 500 °C) involves the decomposition of organic compounds such as carbohydrates, proteins, and leftover lipids [377]. Therefore, in the second phase, a maximum weight loss of 64.5% was observed. During the third phase (500 °C to 700°C), the carbonaceous materials are gradually decomposed to biochar (27%). It was observed that the

weight loss of the DMB catalyst was comparatively more than the biochar. At 700 °C, the weight loss percentages of biochar and DMB catalyst were determined to be 7.53% and 15.91%, respectively. This indicated that sulfonation of biochar reduces its thermal stability. This is possibly due to the fact that sulfonation partially oxidizes the carbon surfaces and reduces the onset temperature for thermal decomposition.

The differential thermogravimetric (DTG) curve of de-oiled microalgal biomass, revealed two extensive peaks between 200 °C and 500 °C. The major peak between 250 °C and 350 °C is attributable to the decomposition of proteins and carbohydrates [378]. The second peak below 450 °C signifies the decomposition of leftover lipid [379]. From DTG results of biochar and DMB catalyst, it was established that the small peak arisen at a temperature of 50 °C is due to loss of moisture. In a similar study, yeast residue derived catalyst was thermally stable up to 150 °C. On increasing the temperature beyond 150 °C continuous weight loss was observed due to pyrolysis of organic groups, and the weight loss percentage of the catalyst was determined to be 94.7% at 640 °C [74]. In another study, de-oiled canola meal based catalyst was found to be thermally stable up to 250 °C [374]. Thus, the DMB catalyst prepared in the present study was comparatively thermally stable in comparison to previously reported literature.

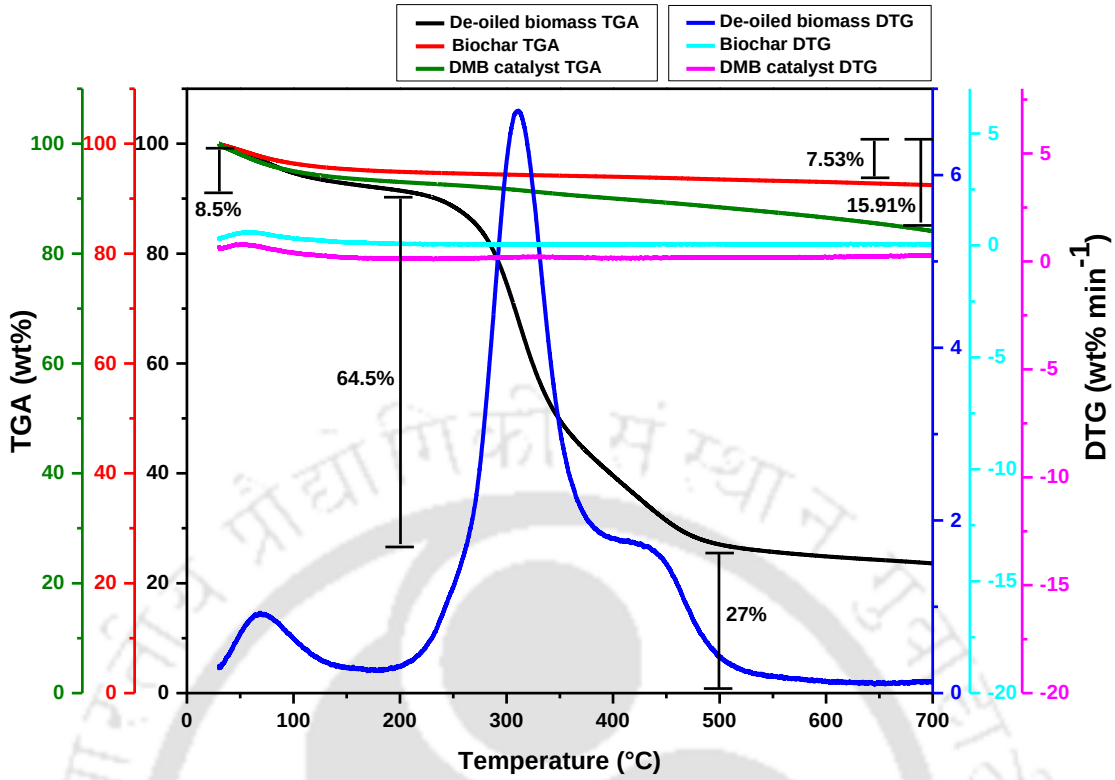

Figure 5.5. TG weight loss profile of de-oiled microalgal biomass, biochar, and DMB catalyst.

5.3.2.5 Raman analysis

Raman spectrum of biochar exhibited two distinct peaks at about 1330 cm^{-1} and 1600 cm^{-1} corresponding to the D (graphitic) and G (disorder) bands, respectively, which remained intact upon sulfonation in DMB catalyst (Figure 5.6). These peaks indicated the formation of graphene in the amorphous carbon [372]. The D/G band intensity ratio was about 0.83, which indicated that the average grapheme size in the amorphous carbon is ca. 1 nm. The Raman data also indicated that the minimum unit in both the samples is nano-graphene sheets comprising of around 10–20 six membered rings [370].

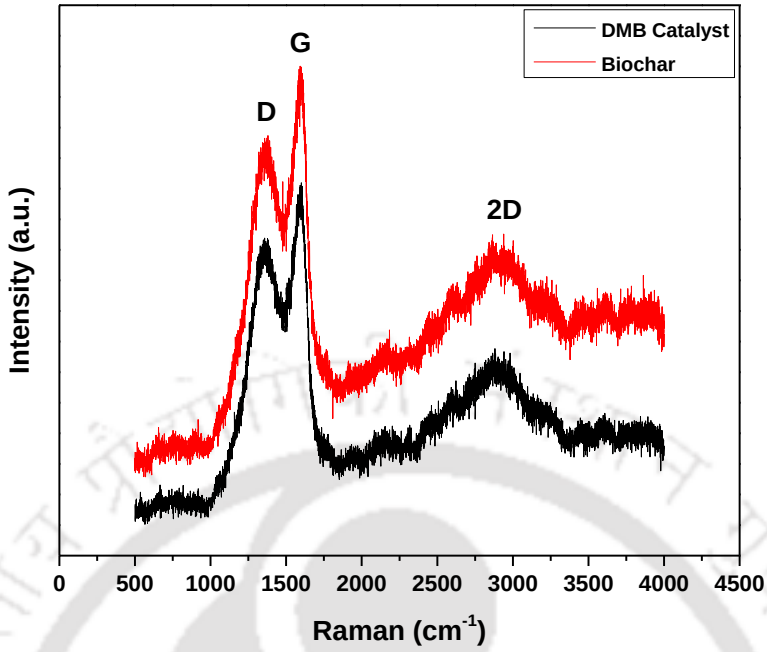

Figure 5.6. Raman spectrum of biochar and DMB catalyst.

5.3.2.6 XPS analysis

Chemical composition of the DMB catalyst was determined through XPS analysis (Figure 5.7). The XPS spectra of DMB catalyst produced peaks at 169.96 eV, 285.46 eV, and 533.03 eV corresponding to the S 2p, C 1s, and O 1s binding energy indicating that the catalyst is purely composed of –COOH and $–SO_3H$ groups [74]. The single S 2p peak produced at a binding energy of 169.96 eV confirmed that all the S atoms in the catalyst are attributed to $–SO_3H$ groups. The XPS spectra also confirmed that the high acid density of the DMB catalyst is ascribed to the –COOH groups produced during the carbonization and sulfonation process.

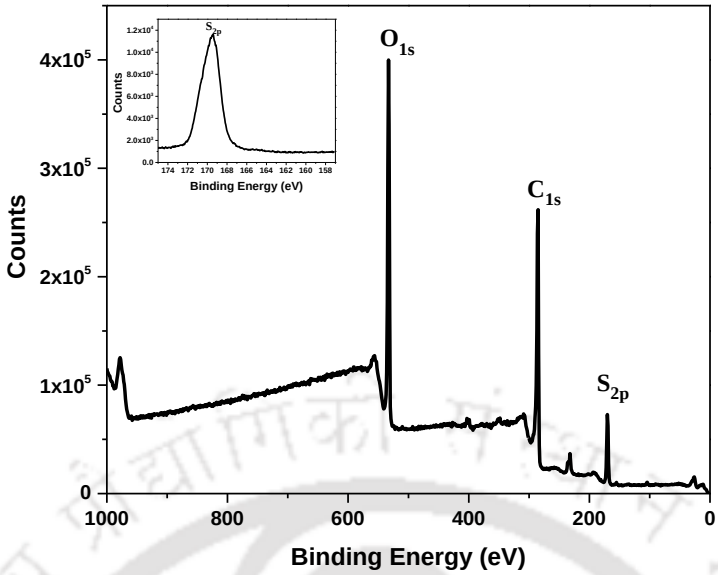

Figure 5.7. XPS analysis of DMB catalyst (the inset is the S_{2p} spectrum of the DMB catalyst).

5.3.2.7 Surface acidity analysis by NH_3-TPD

The total acidity of the DMB catalyst was determined through NH_3-TPD to analyze the acid catalyzed reactions (Figure 5.8). The amount of energy required for the desorption of NH_3 is designated by the relative position of the peak in the NH_3-TPD profile, and it is proportionate to the acidic strength of the catalyst. The NH_3-TPD profile of the DMB catalyst showed four well resolved peaks corresponding to weak, medium, strong and very strong acid sites at 130 °C, 270 °C, 350 °C, and 700 °C, respectively [380]. The desorption peaks at 130 °C and 270 °C is probably due to the interaction of $–NH_3$ with partially formed carbon sheets, whereas the desorption peaks at 350 °C and 700 °C could be attributed to the interaction of $–NH_3$ with sulfonic acid [380]. Thus, the strong acid sites in the sulfonated carbon-based catalyst correspond to the presence of the sulfonic group, and weak acid sites correspond to the presence of other –OH groups. The strong acid groups are known to react with weak acid groups such as carboxylic and phenolic groups, thereby imparting polarity to the catalyst [74]. These weak acid groups also enhance the weak acid sites and facilitate the adsorption of reactants on the catalyst surface. After deconvolution of the peaks, the density of weak, medium, strong, and very strong acid was determined as 0.257 mmol g^{-1}, 0.378 mmol g^{-1}, 0.459 mmol g^{-1}, and 2.155 mmol g^{-1}, respectively. Thus, the total acid density of the DMB catalyst was calculated as 3.249

mmol g^{-1}. Therefore, the presence of both weak and strong acid sites ensured that the DMB catalyst is chemically and thermally stable.

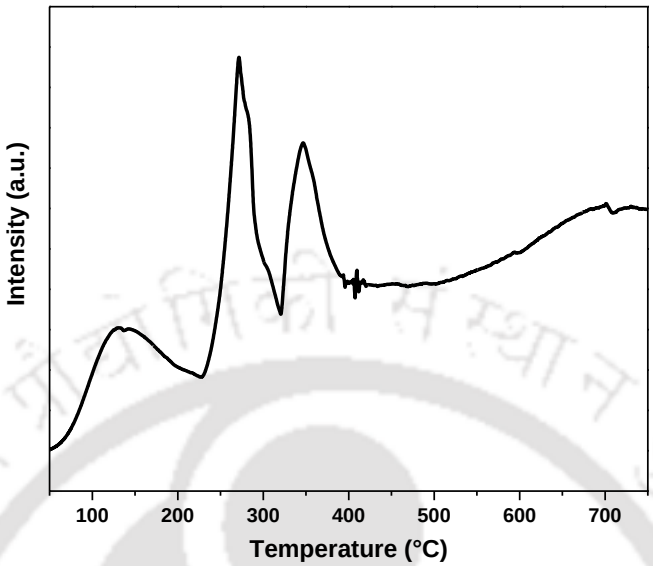

Figure 5.8. NH_3-TPD plot of the DMB catalyst.

5.3.2.8 BET analysis

The BET surface area, pore volume, and average pore size of the biochar and DMB catalyst are depicted in Table 5.1. The biochar exhibited a large BET surface area of 83.85 $m^2\ g^{-1}$, which was comparatively higher than the previously reported literature, where the surface area was less than 10 $m^2\ g^{-1}$ [374]. Biochar with a large surface area is favorable for grafting more $–SO_3H$ groups on the carbon matrix [368]. Small pore volume might correspond to pores with larger pore size. Cylindrical pore with an average pore size ≥ 2 nm is accessible by large molecular size reactants (FFA and triglyceride) without distortion. Thus, the catalytic efficiency of a catalyst is governed by its average pore size. The average pore size of the biochar and DMB catalyst was determined to be 2.42 nm and 2.63 nm, respectively, indicating that the reactants can easily pass through these pores. However, after sulfonation, the BET surface area of the DMB catalyst was significantly reduced to 68.13 $m^2\ g^{-1}$ as the $–SO_3H$ groups might have occupied the surface area. Moreover, the pore volume of the DMB catalyst was found to be comparatively smaller than the biochar as the $–SO_3H$ groups grafted on the catalyst surface might have partially filled the pores. Thus, these results further confirmed the successful

anchoring of $–SO_3H$ groups on the AC surface as active sites. Moreover, the BET surface area of the DMB catalyst was higher than the previously reported carbon-based catalysts [84,372].

Table 5.1. BET analysis of biochar and DMB catalyst.

Sample	BET Surface Area ($m^2\ g^{-1}$)	Pore Volume ($cm^3\ g^{-1}$)	Average Pore Size (nm)
Biochar	83.85	0.05	2.42
DMB catalyst	68.13	0.04	2.63

5.3.2.9 Hydrophobicity and hydrophilicity analysis

The water contact angle of the biochar was found to be 127°, indicating the hydrophobic nature of the biochar (Figure 5.9). The hydrophobic nature of the biochar can be attributed to the alkyl functional groups on its surface. High pyrolysis temperature produces biochar with lower aliphatic compounds, whereas low pyrolysis temperature results in biochar production with higher aliphatic compounds that improve its hydrophobicity. Hydrophobic carbon acts as potential support for sulfonated carbon catalysts as it prevents the −OH and $–SO_3H$ groups from being hydrated by the water generated during the esterification process. Hydrophobic support also repels the glycerol produced during the transesterification reactions from the active sites of the catalyst, making them solely available for the reactants [381]. Thus, hydrophobic carbon support maintains the stability and enhances the catalyst reusability. The water contact angle of the DMB catalyst was found to be 0°, indicating the hydrophilicity of the catalyst. The hydrophilic nature of the catalyst can be attributed to the hydrophilic functional groups ($–SO_3H$, –COOH, and –OH) attached to its surface. Hydrophilic functional groups also promote the catalytic activity, probably due to the strong affinity between the neutral –OH groups attached to the carbon matrix and the hydrophilic reactants, as well as by allowing the hydrophilic methanol molecules to access the acidic sites of the catalyst and react with the reactants (FFAs and triglycerides) [381]. Thus, it was observed that catalyst bearing both hydrophilic and hydrophobic groups aided the absorption of hydrophilic methanol and hydrophobic FFAs onto the active sites of the catalyst.

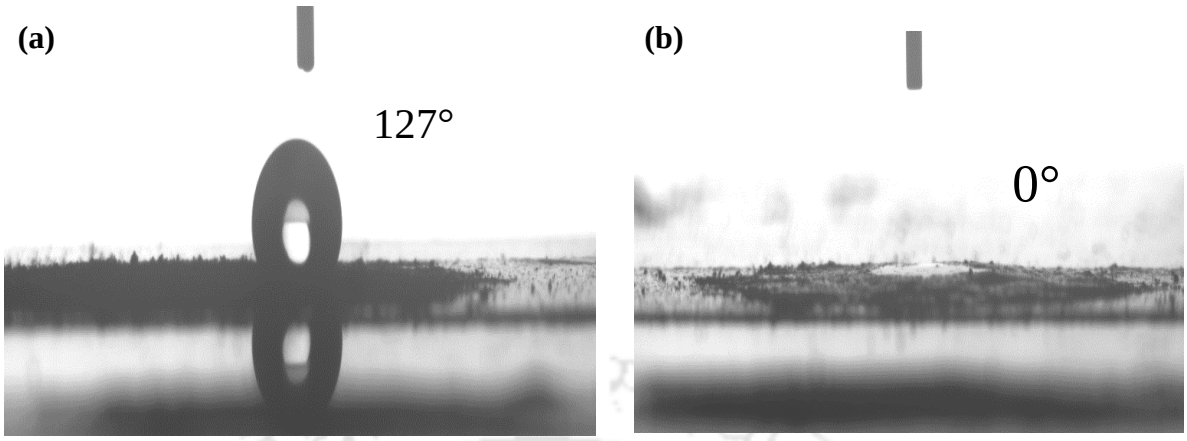

Figure 5.9. Contact angle of water droplet on the surface of (a) biochar and (b) DMB catalyst.

5.3.3 Optimization of FAME yield

FAME yield through transesterification reaction is influenced by numerous factors. Acid catalysts are recommended for better conversion of oil to esters at a relatively faster reaction rate when the moisture and FFA content of the oil is greater than 1% and 3%, respectively. The moisture and FFA content for AO was 1.52% and 38.5%, respectively, and for WCO was 1.32% and 16.94%, respectively, thereby suggesting the use of an acid catalyst. The acid values of AO and WCO were 76.54 mgKOH g^{-1} and 33.68 mgKOH g^{-1}, respectively. Thus, in our study, a heterogeneous DMB acid catalyst was simultaneously employed for the esterification and transesterification reaction of high FFA containing AO and WCO.

The optimal methanol/oil molar ratio favors the conversion of oil towards FAME. The methanol/oil molar ratio (8:1–13:1) was optimized at a constant reaction temperature of 60 °C, the reaction time of 6 h, and catalyst concentration of 3 wt.%. As illustrated in Figure 5.10 (a), the FAME yield for AO gradually increased from 68.23% to 81.67% on increasing the methanol/AO molar ratio from 8:1 to 11:1. However, increasing the methanol/AO molar ratio beyond 11:1, resulted in a reduction of FAME yield. A similar result was observed for WCO, where FAME yield was reduced on further increasing the methanol/WCO molar ratio beyond its optimal value (11:1). Thus, although a high methanol/oil molar ratio has a positive impact on FAME yield, excess methanol concentration dilutes the reaction system and floods the

active surface area of the catalyst. Moreover, excess methanol lowers the interaction between the triglyceride and catalyst, thereby hindering the fatty acid conversion to esters [382]. Hence, methanol/oil molar ratio of 11:1 was considered as the optimal value for further reactions.

A catalyst accelerates reaction by lowering the activation energy required for a reaction to occur. So, a higher catalyst concentration is expected to favor the reaction towards product formation. The catalyst concentration (1wt.%-6 wt.%) was optimized at a constant methanol/oil molar ratio of 11:1, reaction temperature of 60 °C, and reaction time of 6 h. The FAME yield for AO was 54.04% when 1 wt.% of the catalyst was employed, which gradually increased to 85.65% with the increase in catalyst concentration to 4 wt.% (Figure 5.10b). However, as the catalyst concentration was increased beyond 4 wt.%, the FAME yield decreased. Similarly, for WCO a maximum FAME yield of 86.03% was obtained when 3 wt.% of the catalyst was used, and it decreased on further increasing the catalyst concentration beyond its optimal value (3 wt.%). It has been reported that excessive catalyst aggravates mass transfer resistance by hindering the interaction between immiscible reactants (triglyceride and methanol), thereby resulting in phase separation [74]. This could be the possible reason for the decrease in FAME yield.

High reaction temperature enhances the reaction rate by reducing the viscosity of the reaction system and activating the substrate molecules. The reaction temperature (40 °C – 90 °C) was optimized at a constant methanol/oil molar ratio of 11:1, catalyst concentration of (4 wt.% for AO and 3 wt.% for WCO), and reaction time of 6 h (Figure 5.10c). A maximum FAME yield of 89.65% was achieved on increasing the temperature from 40 °C to 70 °C. However, a reduction in the FAME yield was observed on increasing the temperature beyond 70 °C. Similarly, for WCO, a maximum FAME yield of 91.03% was achieved at 60 °C reaction temperature, which decreased subsequently with the increase in temperature. During simultaneous esterification and transesterification reactions, the equilibrium is shifted towards product formation due to high reaction temperature. However, the accumulation of excess water as a product of the esterification reaction might reverse the reaction or even deactivate the catalyst [372]. Therefore, reaction temperatures of 70 °C for AO and 60 °C for WCO were considered optimum for subsequent experiments.

The reaction time (2, 4, 6, 8, 10, 12 h) was optimized at a constant methanol/oil molar ratio of 11:1, catalyst concentration of (4 wt.% for AO and 3 wt.% for WCO), and reaction temperature of (70 °C for AO and 60 °C for WCO) (Figure 5.10d). A maximum FAME yield

of 94.23% for AO and 96.25% for WCO was obtained after 8 h and 6 h of reactions, respectively. However, the FAME yield was significantly reduced as the reaction time was increased beyond the optimal value. Prolonged reaction time might have tend to reverse the reaction and deactivate the acidic hydroxyl groups. The excessive water accumulated during the esterification reaction deactivates the acidic hydroxyl groups by hydrating them, thereby reducing the FAME yield.

In this study, DMB catalyst gave a maximum FAME yield of 94.23% and 96.25% for AO and WCO, respectively, under optimized reaction conditions. A two-step, acid-base transesterification reaction of AO and WCO under the same optimized reaction conditions gave a FAME yield of 96.64% and 97.4%, respectively. Jain et al. (2011) obtained methyl ester yield of 90.6% during transesterification of WCO using conventional acid-base catalyst. In another study, a two-step acid–base catalysed transesterification of lipid extracted from *Chlorella thermophile* gave a FAME yield of 83.61% [335]. Thus, the catalytic activity of the DMB catalyst was comparable with the conventional acid-base catalyst.

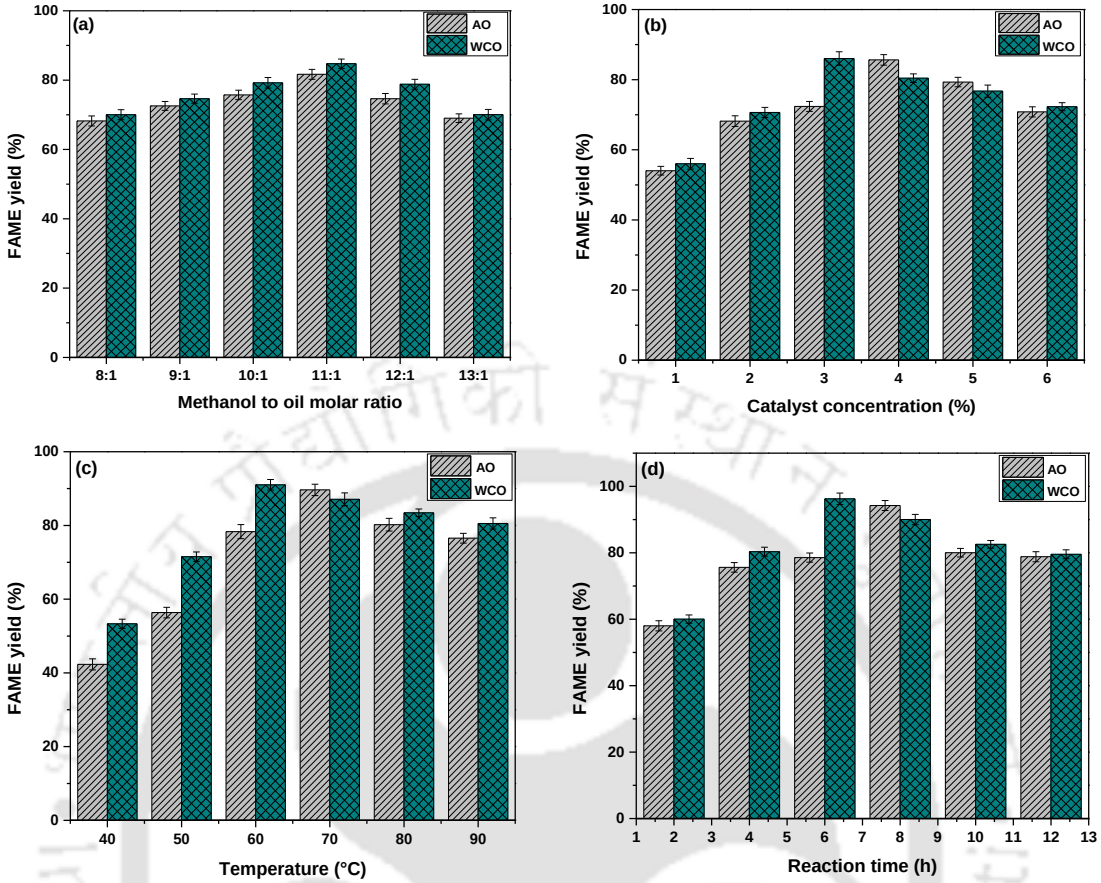

Figure 5.10. Effects of (a) methanol to oil molar ratio, (b) catalyst concentration, (c) reaction temperature, and (d) reaction time on the FAME yield (%) of AO and WCO.

5.3.4 Reusability study

The catalytic efficiency of a catalyst depends on its stability and reusability. Therefore, the stability of the DMB catalyst was estimated by reusing the catalyst for consecutive cycles at the optimized reaction conditions. As shown in Figure 5.11, for both AO and WCO, FAME yield >90% was obtained after four successive reuse cycles. However, the FAME yield decreased to 80.73% and 84.79% for AO and WCO, respectively, at the end of the fifth cycle. The stability of the DMB catalyst until the fourth cycle can be attributed to; (1) the hydrophobic nature of the carbon sheets that prevented –OH groups from being hydrated; (2) the hydrophilic $–SO_3H$ groups attached to the carbon sheets that improved the interaction between the reactants; and (3) the high surface acidity of the catalyst [382]. A gradual decline in the catalytic activity of the DMB catalyst after the fourth cycle was possibly due to the leaching of $–SO_3H$

groups from carbon sheets during the transesterification process. It has been reported that extensive methanol washing during the catalyst recovery process results in the leaching of the $–SO_3H$ groups as methanol reacts with the bonded $–SO_3H$ groups to form methyl sulphonate [384,385]. To further confirm the mechanisms behind the reduction in the catalytic activity, CHNS and FESEM-EDX analysis were carried out. As compared to the fresh catalyst, a significant reduction in the sulphur content was observed in the catalyst after the fourth cycle, which confirmed the leaching of $–SO_3H$ groups (Table 5.2).

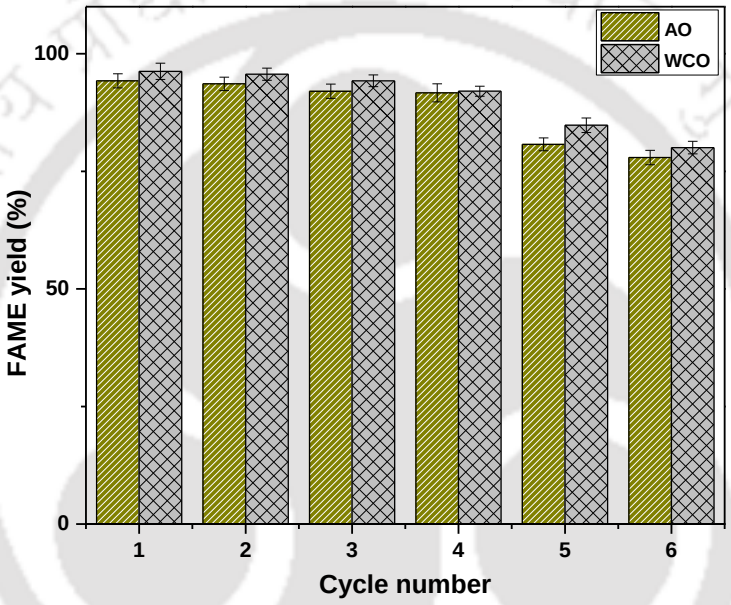

Figure 5.11. Stability study of DMB catalyst.

Table 5.2. Elemental composition of DMB catalyst and fourth used DMB catalyst.

CHNS elemental analysis (Atomic %)	DMB catalyst	Fourth used DMB catalyst
C	64.46	67.44
H	2.04	1.43
N	7.57	7.29
S	10.76	5.93
EDX elemental analysis (Atomic %)		
C	62.6	75.4
O	19.8	11.8
N	7.8	8.1
S	9.8	4.7

5.3.5 FAME composition analysis

The FAME profile of AO obtained after DMB catalyzed transesterification reaction was mostly composed of palmitic acid (40.96%), arachidic acid (22.39%), tetracosanoic acid (12.09%), palmitoleic acid (8.17%), oleic acid (7.28%), elaidic acid (5.48%), erucic acid (2.12%), behenic acid (1.62%), linolenic acid (1.51%) (Table 5.3). In comparison to the control, an increase in SFA content and a decrease in UFA content was observed in AO using DMB catalyst. Moreover, no significant changes in fatty acid composition were observed when the DMB catalyst was reused.

Table 5.3. FAME composition of AO using DMB catalyst and its comparison with conventional acid-base catalyst.

Fatty acid (%)	Acid-base catalyst (control)	DMB catalyst	DMB catalyst recycle			
			1	2	3	4
C16:0	13.69	40.96	40.61	40.08	40.55	40.78
C16:1	5.45	6.55	6.72	6.49	7.02	7.06
C18:1n9c	36.31	7.28	7.10	7.66	7.6	7.31
C18:1n9t	33.44	5.48	5.15	5.38	5.31	5.45
C18:3	2.29	1.51	1.12	1.44	1.03	1.29
C20:0	1.86	22.39	23.59	23.1	22.69	22.31
C22:0	6.63	1.62	1.58	1.60	1.55	1.57
C22:1	0.16	2.12	2.08	2.17	2.16	2.16
C24:0	0.17	12.09	12.05	12. 08	12.09	12.07

The fatty acid composition of WCO is illustrated in Table 5.4. It was observed that the major fraction of the FAME is composed of UFA as compared to SFA. The FAME profile of WCO obtained after DMB catalyzed transesterification reaction was mainly composed of oleic acid > erucic acid > linoleic acid > tetracosanoic acid > arachidic acid > behenic acid > linolenic acid. In comparison to conventional acid-base catalyzed transesterification reaction, an increase in SFA and MUFA content and a decrease in PUFA content was observed in WCO using DMB catalyst. The high MUFA content improves fuel storage stability, thereby enhancing the biodiesel quality [74]. Recycling of DMB catalyst did not have any significant impact on the fatty acid composition of WCO.

Table 5.4. FAME composition of WCO using DMB catalyst and its comparison with conventional acid-base catalyst.

Fatty acid (%)	Acid-base catalyst (control)	DMB catalyst	DMB catalyst recycle			
			1	2	3	4
C18:1	32.85	42.74	47.39	45.21	47.27	46.22
C18:2	46.21	12.65	17.38	12.25	13.75	12.01
C18:3	0.2	0.26	0.44	0.93	0.43	0.49
C20:0	5.21	7.00	7.12	7.07	7.07	7.16
C22:0	6.67	5.06	5.05	5.36	5.3	5.35
C22:1	3.46	23.52	15.49	20.98	17.98	20.54
C24:0	5.4	8.77	7.13	8.20	8.2	8.23

5.3.6 Biodiesel properties

The biodiesel properties of AO and WCO were determined based on their fatty acid compositions (Table 5.5 and 5.6). High content of SFA results in high cetane number [38]. The cetane number of biodiesel produced from AO and WCO using DMB catalyst was determined to be 57.46 and 61.53, respectively, indicating lower ignition delay time and better combustion quality. The lower degree of unsaturation and iodine value suggested better oxidative stability of the biodiesel derived from AO and WCO. The kinematic viscosity for both the AO and WCO derived biodiesel was within the permissible limit of ASTM D6751, indicating good biofuel flow properties and high penetration ability. The estimated CFPP was comparatively lower than the standard fuel parameters, thereby suggesting excellent low temperature performance of biodiesel. Thus, it was observed that all the biodiesel properties estimated were in agreement with the standard fuel parameters classified by EU 14214 and ASTM D6751, indicating its potential applications in internal combustion engines. However, the density and higher heating value of the biodiesel were slightly higher than the permissible limit. Moreover, no significant difference in biodiesel properties was observed when the DMB catalyst was recycled four times.

Table 5.5. Biodiesel properties estimated from FAMEs profile obtained from AO catalyzed by DMB catalyst.

Quality parameters of biodiesel	Standard fuel parameters	Acid-base catalyst (control)	DMB catalyst	DMB catalyst recycle			
	EU 14214/ ASTM D6751			1	2	3	4
Kinematic viscosity (mm^2s^{-1})	1.9-6.0	3.86	4.23	4.13	4.22	4.19	4.22
Density (g cm^{-3})	0.86–0.90	0.93	0.93	0.93	0.93	0.93	0.93
Saponification value (mg KOH)	≤ 370	196.30	166.64	172.63	168.62	169.74	168.76
Cetane number	≥47	57.46	61.53	58.81	60.82	60.39	61.01
Degree of unsaturation (% wt)	-	79.94	66.78	63.76	68.05	66.11	67.74
Cold filter plugging properties (°C)	≤ 5/ ≤ −20	-11.80	-16.47	-16.47	-16.47	-16.47	-16.47
Higher heating value (MJ Kg^{-1})	40	40.20	40.42	40.42	40.42	40.42	40.42
Iodine value (g I_2 100 g^{-1})	120 (max)	73.96	77.88	84.90	79.32	80.30	78.35

Table 5.6. Biodiesel quality parameters obtained from FAME profile of WCO using DMB catalyst.

Quality parameters of biodiesel	Standard fuel parameters	Acid-base catalyst (control)	DMB catalyst	DMB catalyst recycle			
	EU 14214/ ASTM D6751			1	2	3	4
Kinematic viscosity (mm^2s^{-1})	1.9-6.0	4.21	4.17	4.18	4.18	4.18	4.17
Density (g cm^{-3})	0.86–0.90	0.93	0.93	0.93	0.93	0.93	0.93
Saponification value (mg KOH)	≤ 370	188.13	189.50	189.22	189.21	189.44	189.56
Cetane number	≥47	69.38	69.55	69.90	69.59	69.72	69.57
Degree of unsaturation (% wt)	-	29.87	26.07	24.87	26.18	25.70	26.13
Cold filter plugging properties (°C)	≤ 5/ ≤ −20	-3.42	-2.48	-2.60	-2.78	-2.62	-2.54
Higher heating value (MJ Kg^{-1})	40	40.08	40.08	40.08	40.08	40.08	40.08
Iodine value (g I_2 100 g^{-1})	120 (max)	26.35	24.66	23.28	24.70	23.96	24.56

5.3.7 Comparative study of DMB catalyst with other bio-based solid acid catalyst

The catalytic activity of the DMB catalyst for FAME yield was compared with other reported bio-based solid acid catalysts (Table 7). Xiang et al. (2016) reported a FAME yield of 95.57% from WCO by using modified coal fly ash catalyst in the presence of ultrasound assisting system [386]. The methanol to WCO molar ratio, catalyst concentration, reaction temperature, and time were 10.71:1, 4.97 wt.%, 70 °C, and 1.41 min, respectively. Although the transesterification reaction was accomplished within 1.41 min, and a FAME yield of >90%

was obtained at the end of the eighth cycle, the extra cost of ultrasound treatment and the chemicals employed for modifying the catalyst makes the process economically unsustainable. Moreover, a relatively higher FAME yield (96.25%) was obtained in our study without any treatment. Kumar et al. (2020) obtained a FAME yield of ~84% by using immobilized *P. cepacia* lipase as a biocatalyst [387]. As compared to the DMB catalyst reported in this study, the relatively higher catalyst concentration, reaction time, along with the expensive jacketed packed bed bioreactor, might increase the overall production cost of biodiesel. Similarly, Arumugamurthy et al. (2019) performed sonochemical esterification of palm fatty acid distillate (PFAD) and obtained a FAME yield of 87.8% at 8 wt.% of catalyst, 21:1 methanol to PFAD molar ratio, 65 °C reaction temperature, and 3 h of reaction time [388]. The catalyst loading was high, and the FAME yield was relatively low as compared to the DMB catalyst. In another study, Vargas et al. (2019) obtained a FAME yield of 96% using biomass fly ashes catalyst at 10 wt.% catalyst concentration, 9:1 methanol to oil molar ratio, 60 °C reaction temperature, and 3 h of reaction time [389]. The catalyst concentration was relatively high in this study, and no catalyst reusability study was reported. Recently, Ngadi et al. (2016) employed cockle shell waste to develop a catalyst for the transesterification of palm oil [390]. The FAME yield (78.05%) obtained using cockle shell waste catalyst was relatively lower than our study; moreover, no catalyst stability study was reported.

Maniam et al. (2013) carried out ultrasound-aided transesterification of decanter cake using mill boiler ash catalyst [391]. The maximum FAME conversion (85.9%) obtained at optimized conditions was relatively lower than our study. Moreover, ultrasound-aided transesterification might increase the overall production cost. Rao et al. (2011) synthesized catalyst from de-oiled canola meal (DOCM) using the partial carbonization and sulfonation method [374]. A maximum FFA conversion of 93.8% was obtained under optimized reaction conditions. However, the DOCM catalyst's stability was relatively poor; the FFA conversion was reduced to 40.5% at the end of the fourth cycle due to leaching of the sulfonate groups. Pathak et al. (2018) obtained a maximum FAME yield of 98.95% using a green catalyst synthesized from banana peel ash [392]. Although a relatively high FAME yield was obtained by using banana peel ash catalyst, the stability of the catalyst was comparatively poor. The FAME yield was reduced to 52.16 % after the fourth cycle due to the significant reduction in the potassium and calcium concentration in the reused catalyst.

Table 5.7. Catalytic activity and stability comparison of DMB catalyst with other reported catalyst.

Catalyst	Feedstock	Methanol/oil molar ratio	Catalyst concentration (wt.%)	Reaction temperature (°C)	Reaction time (h)	FAME yield (%)	Catalyst reusability (FAME yield)	Ref.
Modified coal fly ash	Waste cooking oil	10.71:1	4.97	70	1.41 min	95.57	>90% obtained at 8th cycle	[386]
Immobilized *P. cepacia* li pase	Mixture of Karanja oil and Castor oil	5.93:1 (2-propanol to oil molar ratio)	9.46	49.7	24.32	~84	~70% obtained at 10th cycle	[387]
Brewer's spent yeast	Palm fatty acid distillate	21:1	8	65	3	87.8	>80% obtained at 4th cycle	[388]
Biomass fly ashes	Mixture of palm oil and waste cooking oil	9:1	10	60	3	96	Not reported	[389]
Cockle shell waste	Palm oil	9:1	10	50	1	78.05	Not reported	[390]
Mill boiler ash	Decanter cake	6:1	2.3	55	1	85.90	Not reported	[391]
Cocoa pod husk ash	Soybean oil	6:1	1	60	2	91.40	Not reported	[393]
De-oiled canola meal	Oleic acid and canola oil	60:1	7.5	65	24	93.8	40.5% obtained at 4th	[374]
Banana peel ash	Soybean oil	6:1	0.7	Room temperature	4	98.95	52.16 % obtained at 4th run	[392]
DMB	Microalgal oil	11:1	4	70	8	94.23	91.67% obtained at 4th run	Present study
DMB	Waste cooking oil	11:1	3	60	6	96.25	92.03% obtained at 4th run	Present study

5.4 Conclusion

De-oiled microalgal biomass was successfully valorized to a carbon-based solid acid catalyst for microalgae-based biodiesel production in an integrated biorefinery concept. The catalyst exhibited higher catalytic activity with a maximum FAME yield of 94.23% and 96.25% for AO and WCO, respectively. High catalyst activity (FAME yield >90%) was maintained until the fourth cycle. Moreover, most of the biodiesel properties obtained from the FAME profile of AO and WCO using DMB catalyst complied with the international fuel standards. Thus, the high catalytic efficiency of the DMB catalyst for the transesterification reaction process signifies its potential for sustainable biodiesel production.

Chapter 6

Overall Conclusion and Future Scope

6.1 Conclusions

The primary goal defined for the present study was to develop a sustainable way to produce biodiesel from microalgae. As a maiden step, potential microalgal strains were isolated based on biomass concentration and lipid yield. Among the six isolated strains, *Tetradesmus obliquus* KMC24 was considered the potential strain with maximum biomass (2.35 ± 0.02 g L^{-1}) and lipid yield ($29.51 \pm 0.26\%$). Further, *T. obliquus* KMC24 was exposed to nutrient stress (nitrogen and/or phosphorus) for a short period via two-stage cultivation to enhance the lipid content of the biomass without compromising the biomass concentration. Nitrogen starvation (-N) and combined nitrogen and phosphorous starvation (-N-P) changed the morphology of *T. obliquus* KMC24 from unicell to 2 and 4 celled coenobium with multiple spines at terminal cells. Compared to various nutrient starved conditions, the photosynthetic apparatus was comparatively less affected during phosphorus starvation. The highest lipid content of $39.93 \pm 0.64\%$ was obtained in –N2 cultures, which was around 1.35 folds higher than the control. This indicated that nitrogen starvation triggered the production of intracellular lipid. The NL content in –N2 cultures was almost similar to –N4 cultures with significantly higher ($P < 0.0001$) DCW, suggesting that two days of nitrogen starvation is a better approach for obtaining high biomass and NL content in *T. obliquus* KMC24. The highest ROS fluorescence intensity (17051.49 ± 93.15 a.u.) and MDA content (3.81 ± 0.02 µM g^{-1} fresh weight) were observed in -N2 cultures, which indicated that a linear correlation exists between ROS level and MDA content. Moreover, Pearson's correlation analysis revealed a positive linear correlation between ROS and lipid accumulation under all nutrient starved conditions. The activities of CAT, APX, and polyphenols were consistent with lipid content suggesting a strong connection between oxidative stress and lipid accumulation.

Nitrogen starvation for four days increased the degree of saturation of the total fatty acid pool by almost fourfold. Due to high SFA content in nitrogen starved cultures, biodiesel with higher CN, superior oxidative stability, and improved shelf life were obtained. Thus, it was observed that *T. obliquus* KMC24 cells under two days of nitrogen starvation possess a high potential for biodiesel production.

In the next part of the study, waste eggshell derived bioflocculant was successfully applied for harvesting *T. obliquus* KMC24. Harvesting efficiency of 98.62 ± 0.43% was achieved within 25 minutes under optimal conditions of 120 mg L^{-1} flocculant dose, pH 4.0, and a temperature of 35 °C. The bioflocculant consisting of a high concentration of cationic calcium ions significantly influenced the zeta potential of the culture suspension. Zeta potential analysis confirmed charge neutralization as the flocculation mechanism. FESEM analysis showed no structural deformations when the cells were harvested under optimal conditions. Pseudo-second order kinetic model was a suitable fit for the data obtained from the experiments, which indicated chemisorption as the probable mechanism. The thermodynamic parameters revealed that the sorption process was spontaneous and endothermic in nature. The spent medium was successfully recycled and reused to cultivate *T. obliquus* KMC24, thereby reducing the water footprint.

In the final phase of the current resarch, a sustainable catalyst using de-oiled microalgal biomass as carbon support was developed. The carbon-based solid acid catalyst was synthesized at an optimum pyrolysis temperature of 600 °C, sulfonation time of 6 h, and H_2SO_4 concentration of 15 mL. The amorphous DMB catalyst was predominantly composed of carboxylic, phenolic, and sulfonic acid groups. TGA and NH_3-TPD analysis confirmed that the DMB catalyst was thermally and chemically stable. Hydrophobic carbon acted as potential support for sulfonated carbon catalysts. A high FAME yield with improved fatty acid composition was obtained. Moreover, FAME yield >90% was obtained after four successive reuse cycles. Hydrophobic carbon support suppressed the leaching of −OH and $–SO_3H$ groups. Thus, the high catalytic efficiency of the DMB catalyst for the transesterification reaction process signified its potential for sustainable biodiesel production.

Therefore, the present study was able to accumulate a considerable amount of lipid in *T. obliquus* KMC24 under nitrogen starved conditions making it a promising

candidate for biodiesel production. A waste-to-wealth approach was successfully implemented by valorizing waste eggshell-derived bioflocculant. This low-cost and energy efficient harvesting technology was developed to attain net sustainability. Recyclability of the spent medium will certainly help to lower the water footprint of microalgal biodiesel production system. Moreover, the conversion of microalgal lipid to biodiesel and de-oiled microalgal biomass to catalyst will help to maximize the economic value of microalgae within a biorefinery concept, leading to a circular bioeconomy for biodiesel production from microalgae.

6.2 Future scope

The current research tried to address the various challenges faced during the upstream and downstream processes of biodiesel production from microalgae. However, the above study was limited to a lab-scale. Therefore, the research can be extended in the following mentioned areas to augment the work further.

- Optimization of nitrogen starvation for enhanced growth and lipid accumulation in *T. obliquus* KMC24 at the pilot-scale plant.
- Genetic engineering of *T. obliquus* KMC24 for enhanced biomass and lipid production.
- Process optimization and application of waste eggshell-derived bioflocculant for harvesting microalgae at the pilot-scale plant.
- Process optimization and application of DMB catalyst for transesterification at the pilot-scale plant.
- Leaching of active components is still an issue for the reported DMB catalyst, which needs further attention to reduce or eliminate them. It would help in enhancing the stability of the catalysts further.
- Techno-economic evaluation and life cycle analysis of the overall process need to be carried out to determine the sustainability of the system.

References

[1] J.L. Garcia-Moscoso, W. Obeid, S. Kumar, P.G. Hatcher, Flash hydrolysis of microalgae (Scenedesmus sp.) for protein extraction and production of biofuels intermediates, J. Supercrit. Fluids. 82 (2013) 183–190. doi:https://doi.org/10.1016/j.supflu.2013.07.012.

[2] S. Thapa, N. Indrawan, P.R. Bhoi, An overview on fuel properties and prospects of Jatropha biodiesel as fuel for engines, Environ. Technol. Innov. 9 (2018) 210–219.

[3] L. Tripathi, A.K. Mishra, A.K. Dubey, C.B. Tripathi, P. Baredar, Renewable energy: An overview on its contribution in current energy scenario of India, Renew. Sustain. Energy Rev. 60 (2016) 226–233. doi:https://doi.org/10.1016/j.rser.2016.01.047.

[4] S. Kesharvani, G. Dwivedi, Algae as a feedstock for biodiesel production in Indian perspective, Mater. Today Proc. (2021). doi:https://doi.org/10.1016/j.matpr.2021.04.295.

[5] W. Körbitz, Biodiesel production in Europe and North America, an encouraging prospect, Renew. Energy. 16 (1999) 1078–1083. doi:https://doi.org/10.1016/S0960-1481(98)00406-6.

[6] Y. Zhang, M.A. Dubé, D.D. McLean, M. Kates, Biodiesel production from waste cooking oil: 1. Process design and technological assessment, Bioresour. Technol. 89 (2003) 1–16. doi:https://doi.org/10.1016/S0960-8524(03)00040-3.

[7] S.C. Bhatia, 22 - Biodiesel, in: S.C. Bhatia (Ed.), Adv. Renew. Energy Syst., Woodhead Publishing India, 2014: pp. 573–626. doi:https://doi.org/10.1016/B978-1-78242-269-3.50022-X.

[8] H.H. Mardhiah, H.C. Ong, H.H. Masjuki, S. Lim, H. V Lee, A review on latest developments and future prospects of heterogeneous catalyst in biodiesel production from non-edible oils, Renew. Sustain. Energy Rev. 67 (2017) 1225–1236. doi:https://doi.org/10.1016/j.rser.2016.09.036.

[9] A. Galadima, O. Muraza, Waste materials for production of biodiesel catalysts: Technological status and prospects, J. Clean. Prod. 263 (2020) 121358. doi:https://doi.org/10.1016/j.jclepro.2020.121358.

[10] G. Saranya, T. V Ramachandra, Life cycle assessment of biodiesel from estuarine microalgae, Energy Convers. Manag. X. 8 (2020) 100065. doi:https://doi.org/10.1016/j.ecmx.2020.100065.

[11] A. Alagumalai, O. Mahian, F. Hollmann, W. Zhang, Environmentally benign solid catalysts for sustainable biodiesel production: A critical review, Sci. Total Environ. 768 (2021) 144856. doi:https://doi.org/10.1016/j.scitotenv.2020.144856.

[12] B. Changmai, C. Vanlalveni, A.P. Ingle, R. Bhagat, L. Rokhum, Widely used catalysts in biodiesel production: a review, RSC Adv. 10 (2020) 41625–41679.

[13] M.N. Bin Mohiddin, Y.H. Tan, Y.X. Seow, J. Kansedo, N.M. Mubarak, M.O. Abdullah, Y.S. Chan, M. Khalid, Evaluation on feedstock, technologies, catalyst and reactor for sustainable biodiesel production: A review, J. Ind. Eng. Chem. 98 (2021) 60–81. doi:https://doi.org/10.1016/j.jiec.2021.03.036.

[14] J.R. Ziolkowska, Chapter 1 - Biofuels technologies: An overview of feedstocks, processes, and technologies, in: J. Ren, A. Scipioni, A. Manzardo, H. Liang (Eds.), Biofuels a More Sustain. Futur., Elsevier, 2020: pp. 1–19. doi:https://doi.org/10.1016/B978-0-12-815581-3.00001-4.

[15] A. Mohr, S. Raman, Lessons from first generation biofuels and implications for the sustainability appraisal of second generation biofuels, Energy Policy. 63 (2013) 114–122. doi:https://doi.org/10.1016/j.enpol.2013.08.033.

[16] R.A. Lee, J.-M. Lavoie, From first- to third-generation biofuels: Challenges of producing a commodity from a biomass of increasing complexity, Anim. Front. 3 (2013) 6–11. doi:10.2527/af.2013-0010.

[17] F. Alam, S. Mobin, H. Chowdhury, Third Generation Biofuel from Algae, Procedia Eng. 105 (2015) 763–768. doi:https://doi.org/10.1016/j.proeng.2015.05.068.

[18] S. Mishra, K. Mohanty, Comprehensive characterization of microalgal isolates and lipid-extracted biomass as zero-waste bioenergy feedstock: An integrated bioremediation and biorefinery approach, Bioresour. Technol. 273 (2019) 177–184. doi:https://doi.org/10.1016/j.biortech.2018.11.012.

[19] K. Chokshi, I. Pancha, A. Ghosh, S. Mishra, Nitrogen starvation-induced cellular crosstalk of ROS-scavenging antioxidants and phytohormone enhanced the biofuel potential of green microalga Acutodesmus dimorphus , Biotechnol. Biofuels. 10 (2017) 60. doi:10.1186/s13068-017-0747-7.

[20] M.V.L. Chhandama, K.B. Satyan, B. Changmai, C. Vanlalveni, S.L. Rokhum, Microalgae as a feedstock for the production of biodiesel: A review, Bioresour. Technol. Reports. 15 (2021) 100771. doi:https://doi.org/10.1016/j.biteb.2021.100771.

[21] L. Brennan, P. Owende, Biofuels from microalgae-A review of technologies for production, processing, and extractions of biofuels and co-products, Renew. Sustain. Energy Rev. 14 (2010). doi:10.1016/j.rser.2009.10.009.

[22] A.H. Demirbas, Inexpensive oil and fats feedstocks for production of biodiesel, Energy Educ. Sci. Technol. Part A-Energy Sci. Res. 23 (2009) 1–13.

[23] A. Pugazhendhi, S. Nagappan, R.R. Bhosale, P.-C. Tsai, S. Natarajan, S. Devendran, L. Al-Haj, V.K. Ponnusamy, G. Kumar, Various potential techniques to reduce the water footprint of microalgal biomass production for biofuel—A review, Sci. Total Environ. 749 (2020) 142218. doi:https://doi.org/10.1016/j.scitotenv.2020.142218.

[24] J. Sen Tan, S.Y. Lee, K.W. Chew, M.K. Lam, J.W. Lim, S.-H. Ho, P.L. Show, A

review on microalgae cultivation and harvesting, and their biomass extraction processing using ionic liquids, Bioengineered. 11 (2020) 116–129. doi:10.1080/21655979.2020.1711626.

[25] T.M. Mata, A.A. Martins, N.S. Caetano, Microalgae for biodiesel production and other applications: A review, Renew. Sustain. Energy Rev. 14 (2010). doi:10.1016/j.rser.2009.07.020.

[26] M. Roy, K. Mohanty, A comprehensive review on microalgal harvesting strategies: Current status and future prospects, Algal Res. 44 (2019) 101683. doi:https://doi.org/10.1016/j.algal.2019.101683.

[27] K. Muylaert, L. Bastiaens, D. Vandamme, L. Gouveia, 5 - Harvesting of microalgae: Overview of process options and their strengths and drawbacks, in: C. Gonzalez-Fernandez, R. Muñoz (Eds.), Microalgae-Based Biofuels Bioprod., Woodhead Publishing, 2017: pp. 113–132. doi:https://doi.org/10.1016/B978-0-08-101023-5.00005-4.

[28] Li-Beisson, Yonghua, Peltier, Gilles, Third-generation biofuels: current and future research on microalgal lipid biotechnology, OCL. 20 (2013) D606. doi:10.1051/ocl/2013031.

[29] E.M. Grima, E.-H. Belarbi, F.G.A. Fernández, A.R. Medina, Y. Chisti, Recovery of microalgal biomass and metabolites: process options and economics, Biotechnol. Adv. 20 (2003) 491–515.

[30] F. Fasaei, J.H. Bitter, P.M. Slegers, A.J.B. van Boxtel, Techno-economic evaluation of microalgae harvesting and dewatering systems, Algal Res. 31 (2018) 347–362. doi:https://doi.org/10.1016/j.algal.2017.11.038.

[31] L. Amer, B. Adhikari, J. Pellegrino, Technoeconomic analysis of five microalgae-to-biofuels processes of varying complexity, Bioresour. Technol. 102 (2011) 9350–9359. doi:https://doi.org/10.1016/j.biortech.2011.08.010.

[32] S. White, A. Anandraj, F. Bux, PAM fluorometry as a tool to assess microalgal nutrient stress and monitor cellular neutral lipids, Bioresour. Technol. 102 (2011) 1675–1682. doi:https://doi.org/10.1016/j.biortech.2010.09.097.

[33] M. Power, Introduction, recovery in aquatic ecosystems: Considerations for definition and measurement, J. Aquat. Ecosyst. Stress Recover. 6 (1999) 179–180.

[34] M.A. Borowitzka, The 'stress' concept in microalgal biology—homeostasis, acclimation and adaptation, J. Appl. Phycol. 30 (2018) 2815–2825. doi:10.1007/s10811-018-1399-0.

[35] Y. Hong, H.-Y. Hu, F.-M. Li, Physiological and biochemical effects of allelochemical ethyl 2-methyl acetoacetate (EMA) on cyanobacterium Microcystis aeruginosa, Ecotoxicol. Environ. Saf. 71 (2008). doi:10.1016/j.ecoenv.2007.10.010.

[36] G.V. Subhash, M. V Rohit, M.P. Devi, Y. V Swamy, S.V. Mohan, Temperature induced stress influence on biodiesel productivity during mixotrophic microalgae cultivation with wastewater, Bioresour. Technol. 169 (2014) 789–793.

[37] S. Lin, R.W. Litaker, W.G. Sunda, Phosphorus physiological ecology and molecular mechanisms in marine phytoplankton, J. Phycol. 52 (2016) 10–36. doi:10.1111/jpy.12365.

[38] L. Zhang, N. Wang, M. Yang, K. Ding, Y.-Z. Wang, D. Huo, C. Hou, Lipid accumulation and biodiesel quality of Chlorella pyrenoidosa under oxidative stress induced by nutrient regimes, Renew. Energy. 143 (2019) 1782–1790. doi:https://doi.org/10.1016/j.renene.2019.05.081.

[39] C. Adams, V. Godfrey, B. Wahlen, L. Seefeldt, B. Bugbee, Understanding precision nitrogen stress to optimize the growth and lipid content tradeoff in oleaginous green microalgae, Bioresour. Technol. 131 (2013) 188–194.

[40] Y. Gao, M. Yang, C. Wang, Nutrient deprivation enhances lipid content in marine microalgae, Bioresour. Technol. 147 (2013) 484–491. doi:https://doi.org/10.1016/j.biortech.2013.08.066.

[41] K. Kawamura, K. Sumii, M. Matsumoto, D. Nakase, Y. Kosaki, M. Ishikawa, Determining the optimal cultivation strategy for microalgae for biodiesel production using flow cytometric monitoring and mathematical modeling, Biomass and Bioenergy. 117 (2018) 24–31.

[42] A. San Pedro, C. V González-López, F.G. Acién, E. Molina-Grima, Marine microalgae selection and culture conditions optimization for biodiesel production, Bioresour. Technol. 134 (2013) 353–361. doi:https://doi.org/10.1016/j.biortech.2013.02.032.

[43] Z.-K. Yang, Y.-H. Ma, J.-W. Zheng, W.-D. Yang, J.-S. Liu, H.-Y. Li, Proteomics to reveal metabolic network shifts towards lipid accumulation following nitrogen deprivation in the diatom Phaeodactylum tricornutum, J. Appl. Phycol. 26 (2014) 73–82. doi:10.1007/s10811-013-0050-3.

[44] X. Tang, X. Zan, L. Zhao, H. Chen, Y.Q. Chen, W. Chen, Y. Song, C. Ratledge, Proteomics analysis of high lipid-producing strain Mucor circinelloides WJ11: an explanation for the mechanism of lipid accumulation at the proteomic level, Microb. Cell Fact. 15 (2016) 1–16.

[45] K. Shi, Z. Gao, T.-Q. Shi, P. Song, L.-J. Ren, H. Huang, X.-J. Ji, Reactive Oxygen Species-Mediated Cellular Stress Response and Lipid Accumulation in Oleaginous Microorganisms: The State of the Art and Future Perspectives, Front. Microbiol. 8 (2017) 1–9. doi:10.3389/fmicb.2017.00793.

[46] S.B. Urbano, C. Di Capua, N. Cortez, M.E. Farías, H.M. Alvarez, Triacylglycerol accumulation and oxidative stress in Rhodococcus species: differential effects of pro-oxidants on lipid metabolism, Extremophiles. 18 (2014) 375–384.

[47] K. Yilancioglu, M. Cokol, I. Pastirmaci, B. Erman, S. Cetiner, Oxidative Stress Is a Mediator for Increased Lipid Accumulation in a Newly Isolated Dunaliella salina Strain, PLoS One. 9 (2014) 1–13. doi:10.1371/journal.pone.0091957.

[48] R.G. Alscher, J.L. Donahue, C.L. Cramer, Reactive oxygen species and antioxidants: Relationships in green cells, Physiol. Plant. 100 (1997) 224–233. doi:https://doi.org/10.1111/j.1399-3054.1997.tb04778.x.

[49] M. Montibus, L. Pinson-Gadais, F. Richard-Forget, C. Barreau, N. Ponts, Coupling of transcriptional response to oxidative stress and secondary metabolism regulation in filamentous fungi, Crit. Rev. Microbiol. 41 (2015) 295–308.

[50] N. Mallick, F.H. Mohn, Reactive oxygen species: Response of algal cells, J. Plant Physiol. 157 (2000) 183–193. doi:10.1016/S0176-1617(00)80189-3.

[51] V.I. Lushchak, Adaptive response to oxidative stress: Bacteria, fungi, plants and animals, Comp. Biochem. Physiol. Part C Toxicol. Pharmacol. 153 (2011) 175–190. doi:https://doi.org/10.1016/j.cbpc.2010.10.004.

[52] F. Fasaei, J.H. Bitter, P.M. Slegers, A.J.B. van Boxtel, Techno-economic evaluation of microalgae harvesting and dewatering systems, Algal Res. 31 (2018) 347–362. doi:10.1016/j.algal.2017.11.038.

[53] M.K. Danquah, L. Ang, N. Uduman, N. Moheimani, G.M. Forde, Dewatering of microalgal culture for biodiesel production: exploring polymer flocculation and tangential flow filtration, J. Chem. Technol. Biotechnol. 84 (2009) 1078–1083.

[54] T. Mathimani, N. Mallick, A comprehensive review on harvesting of microalgae for biodiesel – Key challenges and future directions, Renew. Sustain. Energy Rev. 91 (2018) 1103–1120. doi:https://doi.org/10.1016/j.rser.2018.04.083.

[55] A. Pandey, V. V Pathak, R. Kothari, P.N. Black, V. V Tyagi, Experimental studies on zeta potential of flocculants for harvesting of algae, J. Environ. Manage. 231 (2019) 562–569. doi:https://doi.org/10.1016/j.jenvman.2018.09.096.

[56] R. Kothari, V. V Pathak, A. Pandey, S. Ahmad, C. Srivastava, V. V Tyagi, A novel method to harvest Chlorella sp. via low cost bioflocculant: Influence of temperature with kinetic and thermodynamic functions, Bioresour. Technol. 225 (2017) 84–89. doi:https://doi.org/10.1016/j.biortech.2016.11.050.

[57] M. Shurair, F. Almomani, R. Bhosale, M. Khraisheh, H. Qiblawey, Harvesting of intact microalgae in single and sequential conditioning steps by chemical and biological based – flocculants: Effect on harvesting efficiency, water recovery and algal cell morphology, Bioresour. Technol. 281 (2019) 250–259. doi:https://doi.org/10.1016/j.biortech.2019.02.103.

[58] A. Lavoie, J. de la Noüe, J.B. Sérodes, Récupération de microalgues en eaux usées: étude comparative de divers agents floculants, Can. J. Civ. Eng. 11 (1984) 266–272.

[59] H. Jethani, U.H. Hebbar, Plant-based biopolymers: emerging bio-flocculants for microalgal biomass recovery, Rev. Environ. Sci. Bio/Technology. 20 (2021) 143–165. doi:10.1007/s11157-020-09561-x.

[60] C.Y. Chen, K.L. Yeh, R. Aisyah, D.J. Lee, J.S. Chang, Cultivation, photobioreactor design and harvesting of microalgae for biodiesel production: A critical review, Bioresour. Technol. 102 (2011) 71–81. doi:10.1016/j.biortech.2010.06.159.

[61] V. Ananthi, P. Balaji, R. Sindhu, S.-H. Kim, A. Pugazhendhi, A. Arun, A critical review on different harvesting techniques for algal based biodiesel production, Sci.

Total Environ. 780 (2021) 146467. doi:https://doi.org/10.1016/j.scitotenv.2021.146467.

[62] G. Kandasamy, S.R.M. Shaleh, Harvesting of the microalga Nannochloropsis sp. by bioflocculation with mung bean protein extract, Appl. Biochem. Biotechnol. 182 (2017) 586–597.

[63] T. Ndikubwimana, X. Zeng, T. Murwanashyaka, E. Manirafasha, N. He, W. Shao, Y. Lu, Harvesting of freshwater microalgae with microbial bioflocculant: a pilot-scale study, Biotechnol. Biofuels. 9 (2016) 47. doi:10.1186/s13068-016-0458-5.

[64] D.Y.C. Leung, X. Wu, M.K.H. Leung, A review on biodiesel production using catalyzed transesterification, Appl. Energy. 87 (2010) 1083–1095. doi:https://doi.org/10.1016/j.apenergy.2009.10.006.

[65] M.E. Borges, L. Díaz, Recent developments on heterogeneous catalysts for biodiesel production by oil esterification and transesterification reactions: A review, Renew. Sustain. Energy Rev. 16 (2012) 2839–2849. doi:https://doi.org/10.1016/j.rser.2012.01.071.

[66] M.K. Lam, K.T. Lee, A.R. Mohamed, Homogeneous, heterogeneous and enzymatic catalysis for transesterification of high free fatty acid oil (waste cooking oil) to biodiesel: a review, Biotechnol. Adv. 28 (2010) 500–518.

[67] L.C. Meher, D.V. Sagar, S.N. Naik, Technical aspects of biodiesel production by transesterification—a review, Renew. Sustain. Energy Rev. 10 (2006) 248–268.

[68] V. Kumar, M. Muthuraj, B. Palabhanvi, A.K. Ghoshal, D. Das, Evaluation and optimization of two stage sequential in situ transesterification process for fatty acid methyl ester quantification from microalgae, Renew. Energy. 68 (2014) 560–569. doi:10.1016/j.renene.2014.02.037.

[69] K.W. Chew, J.Y. Yap, P.L. Show, N.H. Suan, J.C. Juan, T.C. Ling, D.J. Lee, J.S. Chang, Microalgae biorefinery: High value products perspectives, Bioresour. Technol. 229 (2017) 53–62. doi:10.1016/j.biortech.2017.01.006.

[70] S. Mishra, N. Singh, A.K. Sarma, Assessment of a Novel Algal Strain Chlamydomonas debaryana NIREMACC03 for Mass Cultivation, Biofuels Production and Kinetic Studies., Appl. Biochem. Biotechnol. (2015) 2253–2266. doi:10.1007/s12010-015-1714-z.

[71] P.-L. Boey, G.P. Maniam, S.A. Hamid, Performance of calcium oxide as a heterogeneous catalyst in biodiesel production: A review, Chem. Eng. J. 168 (2011) 15–22. doi:https://doi.org/10.1016/j.cej.2011.01.009.

[72] A. Sánchez, R. Maceiras, A. Cancela, M. Rodríguez, Influence of n-hexane on in situ transesterification of marine macroalgae, Energies. 5 (2012) 243–257.

[73] K. Malins, V. Kampars, J. Brinks, I. Neibolte, R. Murnieks, Synthesis of activated carbon based heterogenous acid catalyst for biodiesel preparation, Appl. Catal. B Environ. 176–177 (2015) 553–558. doi:https://doi.org/10.1016/j.apcatb.2015.04.043.

[74] F. Deeba, B. Kumar, N. Arora, S. Singh, A. Kumar, S.S. Han, Y.S. Negi, Novel bio-based solid acid catalyst derived from waste yeast residue for biodiesel production, Renew. Energy. 159 (2020) 127–139. doi:https://doi.org/10.1016/j.renene.2020.05.029.

[75] A. MacArio, G. Giordano, L. Setti, A. Parise, J.M. Campelo, J.M. Marinas, D. Luna, Study of lipase immobilization on zeolitic support and transesterification reaction in a solvent free-system, Biocatal. Biotransformation. 25 (2007) 328–335. doi:10.1080/10242420701444256.

[76] S. Semwal, A.K. Arora, R.P. Badoni, D.K. Tuli, Biodiesel production using heterogeneous catalysts, Bioresour. Technol. 102 (2011) 2151–2161. doi:https://doi.org/10.1016/j.biortech.2010.10.080.

[77] M. Hamza, M. Ayoub, R. Bin Shamsuddin, A. Mukhtar, S. Saqib, I. Zahid, M. Ameen, S. Ullah, A.G. Al-Sehemi, M. Ibrahim, A review on the waste biomass derived catalysts for biodiesel production, Environ. Technol. Innov. 21 (2021) 101200. doi:https://doi.org/10.1016/j.eti.2020.101200.

[78] T. Liu, Z. Li, W. Li, C. Shi, Y. Wang, Preparation and characterization of biomass carbon-based solid acid catalyst for the esterification of oleic acid with methanol, Bioresour. Technol. 133 (2013) 618–621. doi:https://doi.org/10.1016/j.biortech.2013.01.163.

[79] Z. Zailan, M. Tahir, M. Jusoh, Z.Y. Zakaria, A review of sulfonic group bearing porous carbon catalyst for biodiesel production, Renew. Energy. 175 (2021) 430–452. doi:https://doi.org/10.1016/j.renene.2021.05.030.

[80] R.T. Yang, Adsorbents: fundamentals and applications, John Wiley & Sons, 2003.

[81] V. Boonamnuayvitaya, C. Chaiya, W. Tanthapanichakoon, The preparation and characterization of activated carbon from coffee residue, J. Chem. Eng. Japan. 37 (2004) 1504–1512.

[82] L.J. Konwar, J. Boro, D. Deka, Review on latest developments in biodiesel production using carbon-based catalysts, Renew. Sustain. Energy Rev. 29 (2014) 546–564.

[83] S.H.Y.S. Abdullah, N.H.M. Hanapi, A. Azid, R. Umar, H. Juahir, H. Khatoon, A. Endut, A review of biomass-derived heterogeneous catalyst for a sustainable biodiesel production, Renew. Sustain. Energy Rev. 70 (2017) 1040–1051.

[84] S. Chellappan, V. Nair, S. V., A. K., Synthesis, optimization and characterization of biochar based catalyst from sawdust for simultaneous esterification and transesterification, Chinese J. Chem. Eng. 26 (2018) 2654–2663. doi:https://doi.org/10.1016/j.cjche.2018.02.034.

[85] L. Geng, G. Yu, Y. Wang, Y. Zhu, Ph-SO3H-modified mesoporous carbon as an efficient catalyst for the esterification of oleic acid, Appl. Catal. A Gen. 427 (2012) 137–144.

[86] T. Wang, Y. Zhai, Y. Zhu, C. Li, G. Zeng, A review of the hydrothermal carbonization of biomass waste for hydrochar formation: Process conditions,

fundamentals, and physicochemical properties, Renew. Sustain. Energy Rev. 90 (2018) 223–247. doi:10.1016/j.rser.2018.03.071.

[87] Z.-E. Tang, S. Lim, Y.-L. Pang, H.-C. Ong, K.-T. Lee, Synthesis of biomass as heterogeneous catalyst for application in biodiesel production: State of the art and fundamental review, Renew. Sustain. Energy Rev. 92 (2018) 235–253.

[88] S. Nizamuddin, H.A. Baloch, G.J. Griffin, N.M. Mubarak, A.W. Bhutto, R. Abro, S.A. Mazari, B.S. Ali, An overview of effect of process parameters on hydrothermal carbonization of biomass, Renew. Sustain. Energy Rev. 73 (2017) 1289–1299. doi:10.1016/j.rser.2016.12.122.

[89] A. Shokrolahi, A. Zali, M.H. Keshavarz, Wet carbon-based solid acid/NaNO3 as a mild and efficient reagent for nitration of aromatic compound under solvent free conditions, Chinese Chem. Lett. 18 (2007) 1064–1066. doi:https://doi.org/10.1016/j.cclet.2007.06.031.

[90] J.J. Stephenson, A.K. Sadana, A.L. Higginbotham, J.M. Tour, Highly functionalized and soluble multiwalled carbon nanotubes by reductive alkylation and arylation: the billups reaction, Chem. Mater. 18 (2006) 4658–4661.

[91] T. Okuhara, Water-tolerant solid acid catalysts, Chem. Rev. 102 (2002) 3641–3666.

[92] M.A. Borowitzka, Species and Strain Selection, in: M.A. Borowitzka, N.R. Moheimani (Eds.), Algae for Biofuels and Energy, Springer Netherlands, Dordrecht, 2013: pp. 77–89. doi:10.1007/978-94-007-5479-9_4.

[93] S. Zhang, P. Liu, X. Yang, Z. Hao, L. Zhang, N. Luo, J. Shi, Isolation and identification by 18S rDNA sequence of high lipid potential microalgal species for fuel production in Hainan Dao, Biomass and Bioenergy. 66 (2014) 197–203. doi:https://doi.org/10.1016/j.biombioe.2014.01.015.

[94] A.K. Minhas, P. Hodgson, C.J. Barrow, B. Sashidhar, A. Adholeya, The isolation and identification of new microalgal strains producing oil and carotenoid simultaneously with biofuel potential, Bioresour. Technol. 211 (2016) 556–565. doi:https://doi.org/10.1016/j.biortech.2016.03.121.

[95] T. Fernandes, I. Fernandes, C.A.P. Andrade, N. Cordeiro, Assessing the impact of sulfur concentrations on growth and biochemical composition of three marine microalgae, J. Appl. Phycol. 32 (2020) 967–975. doi:10.1007/s10811-019-01946-y.

[96] M.M.A. Aziz, K.A. Kassim, Z. Shokravi, F.M. Jakarni, H.Y. Liu, N. Zaini, L.S. Tan, A.B.M.S. Islam, H. Shokravi, Two-stage cultivation strategy for simultaneous increases in growth rate and lipid content of microalgae: A review, Renew. Sustain. Energy Rev. 119 (2020) 109621. doi:https://doi.org/10.1016/j.rser.2019.109621.

[97] R. Poontawee, S. Limtong, Feeding Strategies of Two-Stage Fed-Batch Cultivation Processes for Microbial Lipid Production from Sugarcane Top Hydrolysate and Crude Glycerol by the Oleaginous Red Yeast Rhodosporidiobolus fluvialis, Microorganisms. 8 (2020) 151. doi:10.3390/microorganisms8020151.

[98] G. Mujtaba, W. Choi, C.-G. Lee, K. Lee, Lipid production by Chlorella vulgaris after a shift from nutrient-rich to nitrogen starvation conditions, Bioresour. Technol. 123 (2012) 279–283.

[99] H. Yang, Q. He, C. Hu, Lipid accumulation by NaCl induction at different growth stages and concentrations in photoautotrophic two-step cultivation of Monoraphidium dybowskii LB50, Bioresour. Technol. 187 (2015) 221–227.

[100] B. Sajjadi, W.-Y. Chen, A.A.A. Raman, S. Ibrahim, Microalgae lipid and biomass for biofuel production: A comprehensive review on lipid enhancement strategies and their effects on fatty acid composition, Renew. Sustain. Energy Rev. 97 (2018) 200–232. doi:https://doi.org/10.1016/j.rser.2018.07.050.

[101] Q. Hu, M. Sommerfeld, E. Jarvis, M. Ghirardi, M. Posewitz, M. Seibert, A. Darzins, Microalgal triacylglycerols as feedstocks for biofuel production: perspectives and advances, Plant J. 54 (2008) 621–639. doi:https://doi.org/10.1111/j.1365-313X.2008.03492.x.

[102] Z. Chen, L. Wang, S. Qiu, S. Ge, Determination of Microalgal Lipid Content and Fatty Acid for Biofuel Production, Biomed Res. Int. 2018 (2018) 1503126. doi:10.1155/2018/1503126.

[103] C.-Y. Chen, X.-Q. Zhao, H.-W. Yen, S.-H. Ho, C.-L. Cheng, D.-J. Lee, F.-W. Bai, J.-S. Chang, Microalgae-based carbohydrates for biofuel production, Biochem. Eng. J. 78 (2013) 1–10.

[104] D. Cheng, D. Li, Y. Yuan, L. Zhou, X. Li, T. Wu, L. Wang, Q. Zhao, W. Wei, Y. Sun, Improving carbohydrate and starch accumulation in Chlorella sp. AE10 by a novel two-stage process with cell dilution, Biotechnol. Biofuels. 10 (2017) 75. doi:10.1186/s13068-017-0753-9.

[105] M. Hashemian, H. Ahmadzadeh, M. Hosseini, S. Lyon, H.R. Pourianfar, Chapter 20 - Production of Microalgae-Derived High-Protein Biomass to Enhance Food for Animal Feedstock and Human Consumption, in: M. Hosseini (Ed.), Adv. Bioprocess. Altern. Fuels, Biobased Chem. Bioprod., Woodhead Publishing, 2019: pp. 393–405. doi:https://doi.org/10.1016/B978-0-12-817941-3.00020-6.

[106] T. Tonon, D. Harvey, T.R. Larson, I.A. Graham, Long chain polyunsaturated fatty acid production and partitioning to triacylglycerols in four microalgae, Phytochemistry. 61 (2002) 15–24.

[107] K.K. Sharma, H. Schuhmann, P.M. Schenk, High lipid induction in microalgae for biodiesel production, Energies. 5 (2012) 1532–1553. doi:10.3390/en5051532.

[108] X.-M. Sun, L.-J. Ren, Q.-Y. Zhao, X.-J. Ji, H. Huang, Microalgae for the production of lipid and carotenoids: a review with focus on stress regulation and adaptation, Biotechnol. Biofuels. 11 (2018) 272. doi:10.1186/s13068-018-1275-9.

[109] P.T. Vasudevan, M. Briggs, Biodiesel production—current state of the art and challenges, J. Ind. Microbiol. Biotechnol. 35 (2008) 421.

[110] M. Takagi, K. Watanabe, K. Yamaberi, T. Yoshida, Limited feeding of potassium nitrate for intracellular lipid and triglyceride accumulation of Nannochloris sp.

UTEX LB1999, Appl. Microbiol. Biotechnol. 54 (2000). doi:10.1007/s002530000333.

[111] Y. Li, M. Horsman, B. Wang, N. Wu, C.Q. Lan, Effects of nitrogen sources on cell growth and lipid accumulation of green alga Neochloris oleoabundans, Appl. Microbiol. Biotechnol. 81 (2008). doi:10.1007/s00253-008-1681-1.

[112] L. Rodolfi, G. Chini Zittelli, N. Bassi, G. Padovani, N. Biondi, G. Bonini, M.R. Tredici, Microalgae for oil: Strain selection, induction of lipid synthesis and outdoor mass cultivation in a low-cost photobioreactor, Biotechnol. Bioeng. 102 (2009) 100–112.

[113] P. Singh, A. Guldhe, S. Kumari, I. Rawat, F. Bux, Investigation of combined effect of nitrogen, phosphorus and iron on lipid productivity of microalgae Ankistrodesmus falcatus KJ671624 using response surface methodology, Biochem. Eng. J. 94 (2015) 22–29. doi:https://doi.org/10.1016/j.bej.2014.10.019.

[114] V. Ördög, W.A. Stirk, P. Bálint, C. Lovász, O. Pulz, J. van Staden, Lipid productivity and fatty acid composition in Chlorella and Scenepdesmus strains grown in nitrogen-stressed conditions, J. Appl. Phycol. 25 (2013) 233–243. doi:10.1007/s10811-012-9857-6.

[115] H.A. Said, Changes in levels of cellular constituents of Dunaliella parva associated with inorganic phosphate depletion, Middle-East J. Sci. Res. 4 (2009) 94–99.

[116] K. Liang, Q. Zhang, M. Gu, W. Cong, Effect of phosphorus on lipid accumulation in freshwater microalga Chlorella sp., J. Appl. Phycol. 25 (2013) 311–318.

[117] L. Xin, H. Hong-Ying, G. Ke, S. Ying-Xue, Effects of different nitrogen and phosphorus concentrations on the growth, nutrient uptake, and lipid accumulation of a freshwater microalga Scenedesmus sp., Bioresour. Technol. 101 (2010) 5494–5500.

[118] I. Khozin-Goldberg, Z. Cohen, The effect of phosphate starvation on the lipid and fatty acid composition of the fresh water eustigmatophyte Monodus subterraneus, Phytochemistry. 67 (2006). doi:10.1016/j.phytochem.2006.01.010.

[119] F. Yang, W. Xiang, T. Li, L. Long, Transcriptome analysis for phosphorus starvation-induced lipid accumulation in Scenedesmus sp, Sci. Rep. 8 (2018) 16420. doi:10.1038/s41598-018-34650-x.

[120] H.Y. El-Kassas, Growth and fatty acid profile of the marine microalga Picochlorum Sp. grown under nutrient stress conditions, Egypt. J. Aquat. Res. 39 (2013) 233–239. doi:https://doi.org/10.1016/j.ejar.2013.12.007.

[121] K. Anne-Marie, W. Yee, S.H. Loh, A. Aziz, T.S. Cha, Effects of Excess and Limited Phosphate on Biomass, Lipid and Fatty Acid Contents and the Expression of Four Fatty Acid Desaturase Genes in the Tropical Selenastraceaen Messastrum gracile SE-MC4, Appl. Biochem. Biotechnol. 190 (2020) 1438–1456. doi:10.1007/s12010-019-03182-z.

[122] D. Cheng, Q. He, Assessment of Environmental Stresses for Enhanced Microalgal Biofuel Production – An Overview, Front. Energy Res. 2 (2014) 26.

doi:10.3389/fenrg.2014.00026.

[123] X. Miao, Q. Wu, Biodiesel production from heterotrophic microalgal oil, Bioresour. Technol. 97 (2006) 841–846. doi:https://doi.org/10.1016/j.biortech.2005.04.008.

[124] U. Riebesell, A.T. Revill, D.G. Holdsworth, J.K. Volkman, The effects of varying CO<inf>2</inf> concentration on lipid composition and carbon isotope fractionation in Emiliania huxleyi, Geochim. Cosmochim. Acta. 64 (2000). doi:10.1016/S0016-7037(00)00474-9.

[125] H. Hu, K. Gao, Optimization of growth and fatty acid composition of a unicellular marine picoplankton, Nannochloropsis sp., with enriched carbon sources, Biotechnol. Lett. 25 (2003) 421–425. doi:10.1023/A:1022489108980.

[126] S. Ruangsomboon, Effect of light, nutrient, cultivation time and salinity on lipid production of newly isolated strain of the green microalga, Botryococcus braunii KMITL 2, Bioresour. Technol. 109 (2012). doi:10.1016/j.biortech.2011.07.025.

[127] R. Praveenkumar, K. Shameera, G. Mahalakshmi, M.A. Akbarsha, N. Thajuddin, Influence of nutrient deprivations on lipid accumulation in a dominant indigenous microalga Chlorella sp., BUM11008: Evaluation for biodiesel production, Biomass and Bioenergy. 37 (2012) 60–66. doi:https://doi.org/10.1016/j.biombioe.2011.12.035.

[128] P. Sudhir, S.D.S. Murthy, Effects of salt stress on basic processes of photosynthesis, Photosynthetica. 42 (2004) 481–486. doi:10.1007/S11099-005-0001-6.

[129] G. Srivastava, Nishchal, V. V Goud, Salinity induced lipid production in microalgae and cluster analysis (ICCB 16-BR_047), Bioresour. Technol. 242 (2017) 244–252. doi:https://doi.org/10.1016/j.biortech.2017.03.175.

[130] G.-Q. Chen, Y. Jiang, F. Chen, SALT-INDUCED ALTERATIONS IN LIPID COMPOSITION OF DIATOM NITZSCHIA LAEVIS (BACILLARIOPHYCEAE) UNDER HETEROTROPHIC CULTURE CONDITION1, J. Phycol. 44 (2008) 1309–1314. doi:https://doi.org/10.1111/j.1529-8817.2008.00565.x.

[131] A.W. Almutairi, A.E.-K.B. El-Sayed, M.M. Reda, Combined effect of salinity and pH on lipid content and fatty acid composition of Tisochrysis lutea, Saudi J. Biol. Sci. 27 (2020) 3553–3558. doi:https://doi.org/10.1016/j.sjbs.2020.07.027.

[132] C. Paliwal, M. Mitra, K. Bhayani, S.V.V. Bharadwaj, T. Ghosh, S. Dubey, S. Mishra, Abiotic stresses as tools for metabolites in microalgae, Bioresour. Technol. 244 (2017) 1216–1226.

[133] M.P. Rai, T. Gautom, N. Sharma, Effect of salinity, pH, light intensity on growth and lipid production of microalgae for bioenergy application, Online J. Biol. Sci. 15 (2015) 260.

[134] K. Chokshi, I. Pancha, K. Trivedi, B. George, R. Maurya, A. Ghosh, S. Mishra, Biofuel potential of the newly isolated microalgae Acutodesmus dimorphus under

temperature induced oxidative stress conditions, Bioresour. Technol. 180 (2015) 162–171. doi:10.1016/j.biortech.2014.12.102.

[135] A. Converti, A.A. Casazza, E.Y. Ortiz, P. Perego, M. Del Borghi, Effect of temperature and nitrogen concentration on the growth and lipid content of Nannochloropsis oculata and Chlorella vulgaris for biodiesel production, Chem. Eng. Process. Process Intensif. 48 (2009). doi:10.1016/j.cep.2009.03.006.

[136] Y. Wang, B. He, Z. Sun, Y.-F. Chen, Chemically enhanced lipid production from microalgae under low sub-optimal temperature, Algal Res. 16 (2016) 20–27.

[137] S. Wahidin, A. Idris, S.R.M. Shaleh, The influence of light intensity and photoperiod on the growth and lipid content of microalgae Nannochloropsis sp., Bioresour. Technol. 129 (2013) 7–11. doi:https://doi.org/10.1016/j.biortech.2012.11.032.

[138] C.-J. Yun, K.-O. Hwang, S.-S. Han, H.-G. Ri, The effect of salinity stress on the biofuel production potential of freshwater microalgae Chlorella vulgaris YH703, Biomass and Bioenergy. 127 (2019) 105277. doi:https://doi.org/10.1016/j.biombioe.2019.105277.

[139] I. Pancha, K. Chokshi, R. Maurya, K. Trivedi, S.K. Patidar, A. Ghosh, S. Mishra, Salinity induced oxidative stress enhanced biofuel production potential of microalgae Scenedesmus sp. CCNM 1077, Bioresour. Technol. 189 (2015) 341–348. doi:10.1016/j.biortech.2015.04.017.

[140] I. Pancha, K. Chokshi, B. George, T. Ghosh, C. Paliwal, R. Maurya, S. Mishra, Nitrogen stress triggered biochemical and morphological changes in the microalgae Scenedesmus sp. CCNM 1077, Bioresour. Technol. 156 (2014) 146–154. doi:https://doi.org/10.1016/j.biortech.2014.01.025.

[141] M.L. Bartley, W.J. Boeing, B.N. Dungan, F.O. Holguin, T. Schaub, pH effects on growth and lipid accumulation of the biofuel microalgae Nannochloropsis salina and invading organisms, J. Appl. Phycol. 26 (2014) 1431–1437. doi:10.1007/s10811-013-0177-2.

[142] S.-H. Ho, C.-Y. Chen, J.-S. Chang, Effect of light intensity and nitrogen starvation on CO2 fixation and lipid/carbohydrate production of an indigenous microalga Scenedesmus obliquus CNW-N, Bioresour. Technol. 113 (2012) 244–252. doi:https://doi.org/10.1016/j.biortech.2011.11.133.

[143] Q. Zhang, T. Wang, Y. Hong, Investigation of initial pH effects on growth of an oleaginous microalgae Chlorella sp. HQ for lipid production and nutrient uptake, Water Sci. Technol. 70 (2014) 712–719. doi:10.2166/wst.2014.285.

[144] H.H. Abd El Baky, G.S. El-Baroty, A. Bouaid, M. Martinez, J. Aracil, Enhancement of lipid accumulation in Scenedesmus obliquus by optimizing CO2 and Fe3+ levels for biodiesel production, Bioresour. Technol. 119 (2012) 429–432.

[145] J. Cao, H. Yuan, B. Li, J. Yang, Significance evaluation of the effects of environmental factors on the lipid accumulation of Chlorella minutissima UTEX 2341 under low-nutrition heterotrophic condition, Bioresour. Technol. 152 (2014). doi:10.1016/j.biortech.2013.10.084.

[146] K. Yilancioglu, M. Cokol, I. Pastirmaci, B. Erman, S. Cetiner, Oxidative stress is a mediator for increased lipid accumulation in a newly isolated Dunaliella salina strain, PLoS One. 9 (2014) e91957.

[147] Z.-K. Yang, Y.-F. Niu, Y.-H. Ma, J. Xue, M.-H. Zhang, W.-D. Yang, J.-S. Liu, S.-H. Lu, Y. Guan, H.-Y. Li, Molecular and cellular mechanisms of neutral lipid accumulation in diatom following nitrogen deprivation, Biotechnol. Biofuels. 6 (2013) 1–14.

[148] J.F. Sánchez, J.M. Fernández-Sevilla, F.G. Acién, M.C. Cerón, J. Pérez-Parra, E. Molina-Grima, Biomass and lutein productivity of Scenedesmus almeriensis: influence of irradiance, dilution rate and temperature, Appl. Microbiol. Biotechnol. 79 (2008) 719–729. doi:10.1007/s00253-008-1494-2.

[149] M.L. Gerardo, S. Van Den Hende, H. Vervaeren, T. Coward, S.C. Skill, Harvesting of microalgae within a biorefinery approach: A review of the developments and case studies from pilot-plants, Algal Res. 11 (2015) 248–262. doi:https://doi.org/10.1016/j.algal.2015.06.019.

[150] M.L. Gerardo, S. Van Den Hende, H. Vervaeren, T. Coward, S.C. Skill, Harvesting of microalgae within a biorefinery approach: A review of the developments and case studies from pilot-plants, Algal Res. 11 (2015) 248–262. doi:10.1016/j.algal.2015.06.019.

[151] D. Vandamme, I. Foubert, K. Muylaert, Flocculation as a low-cost method for harvesting microalgae for bulk biomass production., Trends Biotechnol. 31 (2013) 233–239. doi:10.1016/j.tibtech.2012.12.005.

[152] R. Henderson, S.A. Parsons, B. Jefferson, The impact of algal properties and pre-oxidation on solid–liquid separation of algae, Water Res. 42 (2008) 1827–1845. doi:https://doi.org/10.1016/j.watres.2007.11.039.

[153] S. Van Den Hende, H. Vervaeren, S. Desmet, N. Boon, Bioflocculation of microalgae and bacteria combined with flue gas to improve sewage treatment, N. Biotechnol. 29 (2011) 23–31. doi:https://doi.org/10.1016/j.nbt.2011.04.009.

[154] G. Shelef, A. Sukenik, M. Green, Microalgae harvesting and processing: a literature review, Technion Research and Development Foundation Ltd., Haifa (Israel), 1984.

[155] S.L. Pahl, A.K. Lee, T. Kalaitzidis, P.J. Ashman, S. Sathe, D.M. Lewis, Harvesting, Thickening and Dewatering Microalgae Biomass BT - Algae for Biofuels and Energy, in: M.A. Borowitzka, N.R. Moheimani (Eds.), Springer Netherlands, Dordrecht, 2013: pp. 165–185. doi:10.1007/978-94-007-5479-9_10.

[156] G. Singh, S.K. Patidar, Microalgae harvesting techniques: A review, J. Environ. Manage. 217 (2018) 499–508. doi:10.1016/j.jenvman.2018.04.010.

[157] A.I. Barros, A.L. Gonçalves, M. Simões, J.C.M. Pires, Harvesting techniques applied to microalgae: A review, Renew. Sustain. Energy Rev. 41 (2015) 1489–1500. doi:10.1016/j.rser.2014.09.037.

[158] A. Singh, P.S. Nigam, J.D. Murphy, Mechanism and challenges in

commercialisation of algal biofuels, Bioresour. Technol. 102 (2011) 26–34. doi:https://doi.org/10.1016/j.biortech.2010.06.057.

[159] I. Rawat, R. Ranjith Kumar, T. Mutanda, F. Bux, Biodiesel from microalgae: A critical evaluation from laboratory to large scale production, Appl. Energy. 103 (2013). doi:10.1016/j.apenergy.2012.10.004.

[160] J.J. Milledge, S. Heaven, A review of the harvesting of micro-algae for biofuel production, Rev. Environ. Sci. Biotechnol. 12 (2013) 165–178. doi:10.1007/s11157-012-9301-z.

[161] Z. Wu, Y. Zhu, W. Huang, C. Zhang, T. Li, Y. Zhang, A. Li, Evaluation of flocculation induced by pH increase for harvesting microalgae and reuse of flocculated medium, Bioresour. Technol. 110 (2012) 496–502. doi:https://doi.org/10.1016/j.biortech.2012.01.101.

[162] J.-I. Horiuchi, I. Ohba, K. Tada, M. Kobayashi, T. Kanno, M. Kishimoto, Effective cell harvesting of the halotolerant microalga Dunaliella tertiolecta with pH control, J. Biosci. Bioeng. 95 (2003) 412–415. doi:https://doi.org/10.1016/S1389-1723(03)80078-6.

[163] S. Salim, M.H. Vermuë, R.H. Wijffels, Ratio between autoflocculating and target microalgae affects the energy-efficient harvesting by bio-flocculation, Bioresour. Technol. 118 (2012) 49–55. doi:https://doi.org/10.1016/j.biortech.2012.05.007.

[164] A.K. Lee, D.M. Lewis, P.J. Ashman, Microbial flocculation, a potentially low-cost harvesting technique for marine microalgae for the production of biodiesel, J. Appl. Phycol. 21 (2009) 559–567. doi:10.1007/s10811-008-9391-8.

[165] N. Uduman, Y. Qi, M.K. Danquah, G.M. Forde, A. Hoadley, Dewatering of microalgal cultures: a major bottleneck to algae-based fuels, J. Renew. Sustain. Energy. 2 (2010) 12701.

[166] E. Poelman, N. De Pauw, B. Jeurissen, Potential of electrolytic flocculation for recovery of micro-algae, Resour. Conserv. Recycl. 19 (1997). doi:10.1016/S0921-3449(96)01156-1.

[167] M.Y.A. Mollah, P. Morkovsky, J.A.G. Gomes, M. Kesmez, J. Parga, D.L. Cocke, Fundamentals, present and future perspectives of electrocoagulation, J. Hazard. Mater. 114 (2004). doi:10.1016/j.jhazmat.2004.08.009.

[168] S.-K. Wang, A.R. Stiles, C. Guo, C.-Z. Liu, Harvesting microalgae by magnetic separation: A review, Algal Res. 9 (2015) 178–185. doi:https://doi.org/10.1016/j.algal.2015.03.005.

[169] A.M. Waite, P.A. Thompson, P.J. Harrison, Does energy control the sinking rates of marine diatoms?, Limnol. Oceanogr. 37 (1992) 468–477. doi:10.4319/lo.1992.37.3.0468.

[170] P.K. Bienfang, Sinking rates of heterogeneous, temperate phytoplankton populations, J. Plankton Res. 3 (1981) 235–253. doi:10.1093/plankt/3.2.235.

[171] T.J. SMAYDA, The suspension and sinking of phytoplankton in the sea, Ocean.

Mar. Biol. Ann. Rev. 8 (1970) 353–414.

[172] P. Collet, A. Hélias, L. Lardon, M. Ras, R.-A. Goy, J.-P. Steyer, Life-cycle assessment of microalgae culture coupled to biogas production, Bioresour. Technol. 102 (2011) 207–214. doi:https://doi.org/10.1016/j.biortech.2010.06.154.

[173] A. Singh, P.S. Nigam, J.D. Murphy, Renewable fuels from algae: an answer to debatable land based fuels, Bioresour. Technol. 102 (2011) 10–16.

[174] F.H. Mohn, Harvesting of micro-algal biomass, Micro-Algal Biotechnol. (1988) 395–414.

[175] M. Heasman, J. Diemar, W. O'connor, T. Sushames, L. Foulkes, Development of extended shelf-life microalgae concentrate diets harvested by centrifugation for bivalve molluscs–a summary, Aquac. Res. 31 (2000) 637–659.

[176] E.W. Becker, Microalgae: biotechnology and microbiology, Cambridge University Press, 1994.

[177] A.J. Dassey, C.S. Theegala, Harvesting economics and strategies using centrifugation for cost effective separation of microalgae cells for biodiesel applications, Bioresour. Technol. 128 (2013) 241–245.

[178] J.K. Edzwald, Algae, bubbles, coagulants, and dissolved air flotation, Water Sci. Technol. 27 (1993).

[179] G. Shelef, A. Sukenik, M. Green, Separation and harvesting of marine microalgal biomass, Algal Biomass Technol. J. Cramer, Color. (1984).

[180] W.J. Oswald, Large-scale algal culture systems (engineering aspects)., Micro-Algal Biotechnol. (1988) 357–394.

[181] L. Christenson, R. Sims, Production and harvesting of microalgae for wastewater treatment, biofuels, and bioproducts, Biotechnol. Adv. 29 (2011) 686–702. doi:10.1016/j.biotechadv.2011.05.015.

[182] A. Goh, Production of Microalgae Using Pig Waste as a Substrate: presented... at Algal Biomass Workshop, University of Colorado, Boulder, USA, 5-7 Apr. 1984, (1984).

[183] J. Hanotu, H.C. Bandulasena, W.B. Zimmerman, Microflotation performance for algal separation, Biotechnol. Bioeng. 109 (2012) 1663–1673.

[184] G. Luísa, SpringerBriefs in Microbiology, 2011. doi:10.1007/978-3-642-17997-6.

[185] W.B. Zimmerman, B.N. Hewakandamby, V. Tesař, H.C.H. Bandulasena, O.A. Omotowa, On the design and simulation of an airlift loop bioreactor with microbubble generation by fluidic oscillation, Food Bioprod. Process. 87 (2009) 215–227. doi:https://doi.org/10.1016/j.fbp.2009.03.006.

[186] M. Cheryan, Ultrafiltration and microfiltration handbook. 1998, Urbana, Illinois, USA Technomic Publ. Co. (n.d.) 245–267.

[187] M.L. Gerardo, D.L. Oatley-Radcliffe, R.W. Lovitt, Integration of membrane technology in microalgae biorefineries, J. Memb. Sci. 464 (2014) 86–99.

[188] S. Zou, Y. Gu, D. Xiao, C.Y. Tang, The role of physical and chemical parameters on forward osmosis membrane fouling during algae separation, J. Memb. Sci. 366 (2011) 356–362.

[189] N. Rossi, P. Jaouen, P. Legentilhomme, I. Petit, Harvesting of cyanobacterium Arthrospira platensis using organic filtration membranes, Food Bioprod. Process. 82 (2004) 244–250.

[190] R. Bhave, T. Kuritz, L. Powell, D. Adcock, Membrane-based energy efficient dewatering of microalgae in biofuels production and recovery of value added co-products, Environ. Sci. Technol. 46 (2012) 5599–5606.

[191] X. Zhang, Q. Hu, M. Sommerfeld, E. Puruhito, Y. Chen, Harvesting algal biomass for biofuels using ultrafiltration membranes, Bioresour. Technol. 101 (2010) 5297–5304.

[192] S.D. Ríos, J. Salvadó, X. Farriol, C. Torras, Antifouling microfiltration strategies to harvest microalgae for biofuel, Bioresour. Technol. 119 (2012) 406–418. doi:10.1016/j.biortech.2012.05.044.

[193] N.F.M. Khairuddin, A. Idris, L.W. Hock, Harvesting Nannochloropsis sp. using PES/MWCNT/LiBr membrane with good antifouling properties, Sep. Purif. Technol. 212 (2019) 1–11. doi:https://doi.org/10.1016/j.seppur.2018.11.013.

[194] C.-Y. Chen, K.-L. Yeh, R. Aisyah, D.-J. Lee, J.-S. Chang, Cultivation, photobioreactor design and harvesting of microalgae for biodiesel production: a critical review, Bioresour. Technol. 102 (2011) 71–81.

[195] I. Rawat, R.R. Kumar, T. Mutanda, F. Bux, Dual role of microalgae: Phycoremediation of domestic wastewater and biomass production for sustainable biofuels production, Appl. Energy. 88 (2011) 3411–3424. doi:https://doi.org/10.1016/j.apenergy.2010.11.025.

[196] N. Pragya, K.K. Pandey, P.K. Sahoo, A review on harvesting, oil extraction and biofuels production technologies from microalgae, Renew. Sustain. Energy Rev. 24 (2013) 159–171.

[197] A. Papazi, P. Makridis, P. Divanach, Harvesting Chlorella minutissima using cell coagulants, J. Appl. Phycol. 22 (2010) 349–355. doi:10.1007/s10811-009-9465-2.

[198] N. Rashid, M.S.U. Rehman, M. Sadiq, T. Mahmood, J.-I. Han, Current status, issues and developments in microalgae derived biodiesel production, Renew. Sustain. Energy Rev. 40 (2014) 760–778. doi:https://doi.org/10.1016/j.rser.2014.07.104.

[199] C.S. Lee, J. Robinson, M.F. Chong, A review on application of flocculants in wastewater treatment, Process Saf. Environ. Prot. 92 (2014) 489–508. doi:https://doi.org/10.1016/j.psep.2014.04.010.

[200] V.H. Dao, N.R. Cameron, K. Saito, Synthesis{,} properties and performance of organic polymers employed in flocculation applications, Polym. Chem. 7 (2016) 11–25. doi:10.1039/C5PY01572C.

[201] F. Roselet, D. Vandamme, M. Roselet, K. Muylaert, P.C. Abreu, Effects of pH, Salinity, Biomass Concentration, and Algal Organic Matter on Flocculant Efficiency of Synthetic Versus Natural Polymers for Harvesting Microalgae Biomass, BioEnergy Res. 10 (2017) 427–437. doi:10.1007/s12155-016-9806-3.

[202] K. Sievänen, J. Kavakka, P. Hirsilä, P. Vainio, K. Karisalmi, J. Fiskari, I. Kilpeläinen, Cationic cellulose betainate for wastewater treatment, Cellulose. 22 (2015) 1861–1872. doi:10.1007/s10570-015-0578-2.

[203] N. Kumar, C. Banerjee, N. Kumar, S. Jagadevan, A novel non-starch based cationic polymer as flocculant for harvesting microalgae, Bioresour. Technol. 271 (2019) 383–390. doi:https://doi.org/10.1016/j.biortech.2018.09.073.

[204] A. Schlesinger, D. Eisenstadt, A. Bar-Gil, H. Carmely, S. Einbinder, J. Gressel, Inexpensive non-toxic flocculation of microalgae contradicts theories; overcoming a major hurdle to bulk algal production, Biotechnol. Adv. 30 (2012) 1023–1030. doi:https://doi.org/10.1016/j.biotechadv.2012.01.011.

[205] K. Muylaert, D. Vandamme, B. Meesschaert, I. Foubert, Flocculation of microalgae using cationic starch, in: Phycologia, Int phycological soc, 2009: p. 63.

[206] K. Spilling, J. Seppälä, T. Tamminen, Inducing autoflocculation in the diatom Phaeodactylum tricornutum through CO2 regulation, J. Appl. Phycol. 23 (2011) 959–966.

[207] R. Munoz, B. Guieysse, Algal–bacterial processes for the treatment of hazardous contaminants: a review, Water Res. 40 (2006) 2799–2815.

[208] A. Sukenik, G. Shelef, Algal autoflocculation—verification and proposed mechanism, Biotechnol. Bioeng. 26 (1984). doi:10.1002/bit.260260206.

[209] Y. Nurdogan, W.J. Oswald, Enhanced nutrient removal in high-rate ponds, Water Sci. Technol. 31 (1995) 33–43. doi:https://doi.org/10.1016/0273-1223(95)00490-E.

[210] R.M. Knuckey, M.R. Brown, R. Robert, D.M.F. Frampton, Production of microalgal concentrates by flocculation and their assessment as aquaculture feeds, Aquac. Eng. 35 (2006). doi:10.1016/j.aquaeng.2006.04.001.

[211] S. Koley, S. Prasad, S.K. Bagchi, N. Mallick, Development of a harvesting technique for large-scale microalgal harvesting for biodiesel production, RSC Adv. 7 (2017) 7227–7237. doi:10.1039/C6RA27286J.

[212] C.N. Ogbonna, E.G. Nwoba, Bio-based flocculants for sustainable harvesting of microalgae for biofuel production. A review, Renew. Sustain. Energy Rev. 139 (2021) 110690. doi:https://doi.org/10.1016/j.rser.2020.110690.

[213] W. Zhou, M. Min, B. Hu, X. Ma, Y. Liu, Q. Wang, J. Shi, P. Chen, R. Ruan, Filamentous fungi assisted bio-flocculation: a novel alternative technique for harvesting heterotrophic and autotrophic microalgal cells, Sep. Purif. Technol. 107 (2013) 158–165.

[214] H. Zheng, Z. Gao, J. Yin, X. Tang, X. Ji, H. Huang, Harvesting of microalgae by

flocculation with poly (γ-glutamic acid), Bioresour. Technol. 112 (2012) 212–220. doi:https://doi.org/10.1016/j.biortech.2012.02.086.

[215] T.D.P. Nguyen, T.V.A. Le, P.L. Show, T.T. Nguyen, M.H. Tran, T.N.T. Tran, S.Y. Lee, Bioflocculation formation of microalgae-bacteria in enhancing microalgae harvesting and nutrient removal from wastewater effluent, Bioresour. Technol. 272 (2019) 34–39. doi:https://doi.org/10.1016/j.biortech.2018.09.146.

[216] E. Díaz-Santos, M. Vila, M. de la Vega, R. León, J. Vigara, Study of bioflocculation induced by Saccharomyces bayanus var. uvarum and flocculating protein factors in microalgae, Algal Res. 8 (2015) 23–29.

[217] S.H.A. Hamid, F. Lananan, W.N.S. Din, S.S. Lam, H. Khatoon, A. Endut, A. Jusoh, Harvesting microalgae, Chlorella sp. by bio-flocculation of Moringa oleifera seed derivatives from aquaculture wastewater phytoremediation, Int. Biodeterior. Biodegradation. 95 (2014) 270–275.

[218] J. Chen, L. Leng, C. Ye, Q. Lu, M. Addy, J. Wang, J. Liu, P. Chen, R. Ruan, W. Zhou, A comparative study between fungal pellet- and spore-assisted microalgae harvesting methods for algae bioflocculation, Bioresour. Technol. 259 (2018) 181–190. doi:10.1016/j.biortech.2018.03.040.

[219] S. Luo, X. Wu, H. Jiang, M. Yu, Y. Liu, A. Min, W. Li, R. Ruan, Edible fungi-assisted harvesting system for efficient microalgae bio-flocculation, Bioresour. Technol. 282 (2019) 325–330. doi:https://doi.org/10.1016/j.biortech.2019.03.033.

[220] M. Saleem, R.T. Bachmann, A contemporary review on plant-based coagulants for applications in water treatment, J. Ind. Eng. Chem. 72 (2019) 281–297.

[221] N. Baharuddin, N.S. Aziz, H.N. Sohif, W.A.A. Karim, J.R. Al-Obaidi, M. Basiran, Marine microalgae flocculation using plant: the case of Nannochloropsis oculata and Moringa oleifera, Pakistan J. Bot. 48 (2016) 831–842.

[222] M. Ali, A. Mustafa, M. Saleem, Comparative study between indigenous natural coagulants and alum for microalgae harvesting, Arab. J. Sci. Eng. 44 (2019) 6453–6463.

[223] W. Maghfiroh, G. Saefurahman, S. Hidayatuloh, M. Kawaroe, Harvesting effectiveness of Chlorella sp. biomass using different flocculation treatments of Moringa oleifera extract and pH conditions, in: IOP Conf. Ser. Earth Environ. Sci., IOP Publishing, 2018: p. 12014.

[224] J.A. Gerde, T. Wang, L. Yao, S. Jung, L.A. Johnson, B. Lamsal, Optimizing protein isolation from defatted and non-defatted Nannochloropsis microalgae biomass, Algal Res. 2 (2013) 145–153.

[225] C. Wan, X.-Q. Zhao, S.-L. Guo, M.A. Alam, F.-W. Bai, Bioflocculant production from Solibacillus silvestris W01 and its application in cost-effective harvest of marine microalga Nannochloropsis oceanica by flocculation, Bioresour. Technol. 135 (2013) 207–212. doi:https://doi.org/10.1016/j.biortech.2012.10.004.

[226] B. Frølund, R. Palmgren, K. Keiding, P.H. Nielsen, Extraction of extracellular polymers from activated sludge using a cation exchange resin, Water Res. 30

(1996) 1749–1758. doi:https://doi.org/10.1016/0043-1354(95)00323-1.

[227] T. Ndikubwimana, X. Zeng, Y. Liu, J.-S. Chang, Y. Lu, Harvesting of microalgae Desmodesmus sp. F51 by bioflocculation with bacterial bioflocculant, Algal Res. 6 (2014) 186–193. doi:https://doi.org/10.1016/j.algal.2014.09.004.

[228] Y. Li, Y. Xu, R. Song, C. Tian, L. Liu, T. Zheng, H. Wang, Flocculation characteristics of a bioflocculant produced by the actinomycete Streptomyces sp. hsn06 on microalgae biomass, BMC Biotechnol. 18 (2018) 1–10.

[229] F. Chen, Z. Liu, D. Li, C. Liu, P. Zheng, S. Chen, Using ammonia for algae harvesting and as nutrient in subsequent cultures, Bioresour. Technol. 121 (2012) 298–303.

[230] W. Zhou, Y. Cheng, Y. Li, Y. Wan, Y. Liu, X. Lin, R. Ruan, Novel Fungal Pelletization-Assisted Technology for Algae Harvesting and Wastewater Treatment, Appl. Biochem. Biotechnol. 167 (2012) 214–228. doi:10.1007/s12010-012-9667-y.

[231] S.O. Gultom, B. Hu, Review of Microalgae Harvesting via Co-Pelletization with Filamentous Fungus, Energies. 6 (2013) 5921–5939. doi:10.3390/en6115921.

[232] O.M.H. de Vries, M.P. Fekkes, H.A.B. Wösten, J.G.H. Wessels, Insoluble hydrophobin complexes in the walls of Schizophyllum commune and other filamentous fungi, Arch. Microbiol. 159 (1993) 330–335. doi:10.1007/BF00290915.

[233] A.P.J. Trinci, A study of the kinetics of hyphal extension and branch initiation of fungal mycelia, Microbiology. 81 (1974) 225–236.

[234] P.-J. Lin, L.H. Grimm, M. Wulkow, D.C. Hempel, R. Krull, Population balance modeling of the conidial aggregation of Aspergillus niger, Biotechnol. Bioeng. 99 (2008) 341–350. doi:10.1002/bit.21569.

[235] M.C. Morrin, Relationship between mycelial morphology, cell wall composition and product formation of Rhizopus arrhizus, (1989).

[236] S. Bartnicki-Garcia, N. Nelson, E. Cota-Robles, Electron microscopy of spore germination and cell wall formation in Mucor rouxii, Arch. Mikrobiol. 63 (1968) 242–255.

[237] P.M. Schenk, S.R. Thomas-Hall, E. Stephens, U.C. Marx, J.H. Mussgnug, C. Posten, O. Kruse, B. Hankamer, Second Generation Biofuels: High-Efficiency Microalgae for Biodiesel Production, BioEnergy Res. 1 (2008) 20–43. doi:10.1007/s12155-008-9008-8.

[238] R.K. Henderson, A. Baker, S.A. Parsons, B. Jefferson, Characterisation of algogenic organic matter extracted from cyanobacteria, green algae and diatoms, Water Res. 42 (2008) 3435–3445. doi:https://doi.org/10.1016/j.watres.2007.10.032.

[239] X. Zhang, P. Amendola, J.C. Hewson, M. Sommerfeld, Q. Hu, Influence of growth phase on harvesting of Chlorella zofingiensis by dissolved air flotation, Bioresour.

Technol. 116 (2012) 477–484.

[240] A.K. Patel, C. Laroche, A. Marcati, A.V. Ursu, S. Jubeau, L. Marchal, E. Petit, G. Djelveh, P. Michaud, Separation and fractionation of exopolysaccharides from Porphyridium cruentum, Bioresour. Technol. 145 (2013) 345–350.

[241] S. Gao, J. Yang, J. Tian, F. Ma, G. Tu, M. Du, Electro-coagulation–flotation process for algae removal, J. Hazard. Mater. 177 (2010) 336–343. doi:https://doi.org/10.1016/j.jhazmat.2009.12.037.

[242] A. Zenouzi, B. Ghobadian, M.A. Hejazi, P. Rahnemoon, Harvesting of Microalgae Dunaliella salina Using Electroflocculation, J. Agric. Sci. Technol. 15 (2013). http://journals.modares.ac.ir/article-23-4125-en.html.

[243] A.K. Lee, D.M. Lewis, P.J. Ashman, Harvesting of marine microalgae by electroflocculation: The energetics, plant design, and economics, Appl. Energy. 108 (2013) 45–53. doi:https://doi.org/10.1016/j.apenergy.2013.03.003.

[244] R. V Pearsall, R.L. Connelly, M.E. Fountain, C.S. Hearn, M.D. Werst, R.E. Hebner, E.F. Kelley, Electrically dewatering microalgae, IEEE Trans. Dielectr. Electr. Insul. 18 (2011) 1578–1583. doi:10.1109/TDEI.2011.6032827.

[245] S.K. Wang, A.R. Stiles, C. Guo, C.Z. Liu, Harvesting microalgae by magnetic separation: A review, Algal Res. 9 (2015) 178–185. doi:10.1016/j.algal.2015.03.005.

[246] M. Cerff, M. Morweiser, R. Dillschneider, A. Michel, K. Menzel, C. Posten, Harvesting fresh water and marine algae by magnetic separation: Screening of separation parameters and high gradient magnetic filtration, Bioresour. Technol. 118 (2012) 289–295. doi:https://doi.org/10.1016/j.biortech.2012.05.020.

[247] G. Prochazkova, I. Safarik, T. Branyik, Harvesting microalgae with microwave synthesized magnetic microparticles, Bioresour. Technol. 130 (2013) 472–477. doi:https://doi.org/10.1016/j.biortech.2012.12.060.

[248] Y.-R. Hu, F. Wang, S.-K. Wang, C.-Z. Liu, C. Guo, Efficient harvesting of marine microalgae Nannochloropsis maritima using magnetic nanoparticles, Bioresour. Technol. 138 (2013) 387–390. doi:https://doi.org/10.1016/j.biortech.2013.04.016.

[249] L. Xu, C. Guo, F. Wang, S. Zheng, C.-Z. Liu, A simple and rapid harvesting method for microalgae by in situ magnetic separation, Bioresour. Technol. 102 (2011) 10047–10051.

[250] A.E. Regazzoni, G.A. Urrutia, M.A. Blesa, A.J.G. Maroto, Some observations on the composition and morphology of synthetic magnetites obtained by different routes, J. Inorg. Nucl. Chem. 43 (1981) 1489–1493. doi:https://doi.org/10.1016/0022-1902(81)80322-3.

[251] P.Y. Toh, B.W. Ng, C.H. Chong, A.L. Ahmad, J.-W. Yang, C.J. Chieh Derek, J. Lim, Magnetophoretic separation of microalgae: the role of nanoparticles and polymer binder in harvesting biofuel, RSC Adv. 4 (2014) 4114–4121. doi:10.1039/C3RA46298F.

[252] L.J. Kang, C.D.C. Juinn, J.S. A., T.P. Yi, Y.N.H. Mat, N.B. Wah, A.A. Latif, Rapid Magnetophoretic Separation of Microalgae, Small. 8 (n.d.) 1683–1692. doi:10.1002/smll.201102400.

[253] K. Lee, S.Y. Lee, J.-G. Na, S.G. Jeon, R. Praveenkumar, D.-M. Kim, W.-S. Chang, Y.-K. Oh, Magnetophoretic harvesting of oleaginous Chlorella sp. by using biocompatible chitosan/magnetic nanoparticle composites, Bioresour. Technol. 149 (2013) 575–578. doi:https://doi.org/10.1016/j.biortech.2013.09.074.

[254] J.Y. Seo, K. Lee, S.Y. Lee, S.G. Jeon, J.-G. Na, Y.-K. Oh, S. Bin Park, Effect of barium ferrite particle size on detachment efficiency in magnetophoretic harvesting of oleaginous Chlorella sp., Bioresour. Technol. 152 (2014) 562–566. doi:https://doi.org/10.1016/j.biortech.2013.11.064.

[255] Q. Shu, Q. Zhang, G. Xu, Z. Nawaz, D. Wang, J. Wang, Synthesis of biodiesel from cottonseed oil and methanol using a carbon-based solid acid catalyst, Fuel Process. Technol. 90 (2009) 1002–1008.

[256] F. Ezebor, M. Khairuddean, A.Z. Abdullah, P.L. Boey, Esterification of oily-FFA and transesterification of high FFA waste oils using novel palm trunk and bagasse-derived catalysts, Energy Convers. Manag. 88 (2014) 1143–1150. doi:https://doi.org/10.1016/j.enconman.2014.04.062.

[257] T. Ji, L. Chen, L. Mu, R. Yuan, M. Knoblauch, F.S. Bao, Y. Shi, H. Wang, J. Zhu, Green processing of plant biomass into mesoporous carbon as catalyst support, Chem. Eng. J. 295 (2016) 301–308.

[258] L.J. Konwar, P. Mäki-Arvela, E. Salminen, N. Kumar, A.J. Thakur, J.-P. Mikkola, D. Deka, Towards carbon efficient biorefining: multifunctional mesoporous solid acids obtained from biodiesel production wastes for biomass conversion, Appl. Catal. B Environ. 176 (2015) 20–35.

[259] A. Piker, B. Tabah, N. Perkas, A. Gedanken, A green and low-cost room temperature biodiesel production method from waste oil using egg shells as catalyst, Fuel. 182 (2016) 34–41.

[260] S.L. Lee, Y.C. Wong, Y.P. Tan, S.Y. Yew, Transesterification of palm oil to biodiesel by using waste obtuse horn shell-derived CaO catalyst, Energy Convers. Manag. 93 (2015) 282–288.

[261] S.H. Dhawane, T. Kumar, G. Halder, Biodiesel synthesis from Hevea brasiliensis oil employing carbon supported heterogeneous catalyst: optimization by Taguchi method, Renew. Energy. 89 (2016) 506–514.

[262] N. Hindryawati, G.P. Maniam, M.R. Karim, K.F. Chong, Transesterification of used cooking oil over alkali metal (Li, Na, K) supported rice husk silica as potential solid base catalyst, Eng. Sci. Technol. an Int. J. 17 (2014) 95–103.

[263] G.G. Muciño, R. Romero, A. Ramírez, S.L. Martínez, R. Baeza-Jiménez, R. Natividad, Biodiesel production from used cooking oil and sea sand as heterogeneous catalyst, Fuel. 138 (2014) 143–148. doi:https://doi.org/10.1016/j.fuel.2014.07.053.

[264] S.H. Teo, A. Islam, H.R.F. Masoumi, Y.H. Taufiq-Yap, J. Janaun, E.-S. Chan, Effective synthesis of biodiesel from Jatropha curcas oil using betaine assisted nanoparticle heterogeneous catalyst from eggshell of Gallus domesticus, Renew. Energy. 111 (2017) 892–905.

[265] J. Boro, L.J. Konwar, A.J. Thakur, D. Deka, Ba doped CaO derived from waste shells of T striatula (TS-CaO) as heterogeneous catalyst for biodiesel production, Fuel. 129 (2014) 182–187. doi:https://doi.org/10.1016/j.fuel.2014.03.067.

[266] N. Mansir, S.H. Teo, U. Rashid, Y.H. Taufiq-Yap, Efficient waste Gallus domesticus shell derived calcium-based catalyst for biodiesel production, Fuel. 211 (2018) 67–75.

[267] G.-Y. Chen, R. Shan, J.-F. Shi, B.-B. Yan, Transesterification of palm oil to biodiesel using rice husk ash-based catalysts, Fuel Process. Technol. 133 (2015) 8–13.

[268] D. Jain, C. Khatri, A. Rani, Fly ash supported calcium oxide as recyclable solid base catalyst for Knoevenagel condensation reaction, Fuel Process. Technol. 91 (2010) 1015–1021.

[269] A. Buasri, N. Chaiyut, C. Nakweang, Preparing activated carbon from palm shell for biodiesel fuel production, Chiang Mai J. Sci. 38 (2011) 572–578.

[270] G.P. Maniam, N. Hindryawati, I. Nurfitri, I.S. Abd Manaf, N. Ramachandran, M.H.A. Rahim, Utilization of waste fat from catfish (Pangasius) in methyl esters preparation using CaO derived from waste marine barnacle and bivalve clam as solid catalysts, J. Taiwan Inst. Chem. Eng. 49 (2015) 58–66.

[271] T. Maneerung, S. Kawi, Y. Dai, C.-H. Wang, Sustainable biodiesel production via transesterification of waste cooking oil by using CaO catalysts prepared from chicken manure, Energy Convers. Manag. 123 (2016) 487–497.

[272] J. Boro, L.J. Konwar, D. Deka, Transesterification of non edible feedstock with lithium incorporated egg shell derived CaO for biodiesel production, Fuel Process. Technol. 122 (2014) 72–78.

[273] A. Birla, B. Singh, S.N. Upadhyay, Y.C. Sharma, Kinetics studies of synthesis of biodiesel from waste frying oil using a heterogeneous catalyst derived from snail shell, Bioresour. Technol. 106 (2012) 95–100.

[274] L. Marques Correia, J.A. Cecilia, E. Rodríguez-Castellón, C.L. Cavalcante, R.S. Vieira, Relevance of the physicochemical properties of calcined quail eggshell (CaO) as a catalyst for biodiesel production, J. Chem. 2017 (2017).

[275] S. Ismail, A.S. Ahmed, R. Anr, S. Hamdan, Biodiesel production from castor oil by using calcium oxide derived from mud clam shell, J. Renew. Energy. 2016 (2016).

[276] N. Viriya-Empikul, P. Krasae, W. Nualpaeng, B. Yoosuk, K. Faungnawakij, Biodiesel production over Ca-based solid catalysts derived from industrial wastes, Fuel. 92 (2012) 239–244.

[277] S. Pandian, A. Sakthi Saravanan, P. Sivanandi, M. Santra, V.K. Booramurthy, 4 - Application of heterogeneous acid catalyst derived from biomass for biodiesel process intensification: a comprehensive review, in: R.P. Kumar, E. Gnansounou, J.K. Raman, G. Baskar (Eds.), Refin. Biomass Residues Sustain. Energy Bioprod., Academic Press, 2020: pp. 87–109. doi:https://doi.org/10.1016/B978-0-12-818996-2.00004-1.

[278] M.-H. Zong, Z.-Q. Duan, W.-Y. Lou, T.J. Smith, H. Wu, Preparation of a sugar catalyst and its use for highly efficient production of biodiesel, Green Chem. 9 (2007) 434–437.

[279] D. Zeng, S. Liu, W. Gong, G. Wang, J. Qiu, H. Chen, Synthesis, characterization and acid catalysis of solid acid from peanut shell, Appl. Catal. A Gen. 469 (2014) 284–289. doi:https://doi.org/10.1016/j.apcata.2013.09.038.

[280] Y. Zhou, S. Niu, J. Li, Activity of the carbon-based heterogeneous acid catalyst derived from bamboo in esterification of oleic acid with ethanol, Energy Convers. Manag. 114 (2016) 188–196. doi:https://doi.org/10.1016/j.enconman.2016.02.027.

[281] J.R. Kastner, J. Miller, D.P. Geller, J. Locklin, L.H. Keith, T. Johnson, Catalytic esterification of fatty acids using solid acid catalysts generated from biochar and activated carbon, Catal. Today. 190 (2012) 122–132. doi:https://doi.org/10.1016/j.cattod.2012.02.006.

[282] C. Wang, Y. Hu, Q. Chen, C. Lv, S. Jia, Bio-oil upgrading by reactive distillation using p-toluene sulfonic acid catalyst loaded on biomass activated carbon, Biomass and Bioenergy. 56 (2013) 405–411.

[283] I. Thushari, S. Babel, Sustainable utilization of waste palm oil and sulfonated carbon catalyst derived from coconut meal residue for biodiesel production, Bioresour. Technol. 248 (2018) 199–203. doi:https://doi.org/10.1016/j.biortech.2017.06.106.

[284] K. Ngaosuwan, J.G. Goodwin, P. Prasertdham, A green sulfonated carbon-based catalyst derived from coffee residue for esterification, Renew. Energy. 86 (2016) 262–269. doi:https://doi.org/10.1016/j.renene.2015.08.010.

[285] R. Leesing, S. Siwina, K. Fiala, Yeast-based biodiesel production using sulfonated carbon-based solid acid catalyst by an integrated biorefinery of durian peel waste, Renew. Energy. 171 (2021) 647–657. doi:https://doi.org/10.1016/j.renene.2021.02.146.

[286] A. Endut, S.H.Y.S. Abdullah, N.H.M. Hanapi, S.H.A. Hamid, F. Lananan, M.K.A. Kamarudin, R. Umar, H. Juahir, H. Khatoon, Optimization of biodiesel production by solid acid catalyst derived from coconut shell via response surface methodology, Int. Biodeterior. Biodegradation. 124 (2017) 250–257.

[287] R.R.L. Guillard, Purification Methods for Microalgae, Algal Cult. Tech. (2005) 117.

[288] P. Varshney, J. Beardall, S. Bhattacharya, P.P. Wangikar, Isolation and biochemical characterisation of two thermophilic green algal species-Asterarcys

quadricellulare and Chlorella sorokiniana, which are tolerant to high levels of carbon dioxide and nitric oxide, Algal Res. 30 (2018) 28–37.

[289] S. Basu, A.S. Roy, K. Mohanty, A.K. Ghoshal, Enhanced CO2 sequestration by a novel microalga: Scenedesmus obliquus SA1 isolated from bio-diversity hotspot region of Assam, India, Bioresour. Technol. 143 (2013) 369–377. doi:https://doi.org/10.1016/j.biortech.2013.06.010.

[290] V. Kumar, M. Muthuraj, B. Palabhanvi, A.K. Ghoshal, D. Das, High cell density lipid rich cultivation of a novel microalgal isolate Chlorella sorokiniana FC6 IITG in a single-stage fed-batch mode under mixotrophic condition, Bioresour. Technol. 170 (2014) 115–124. doi:https://doi.org/10.1016/j.biortech.2014.07.066.

[291] V. Anand, M. Kashyap, K. Samadhiya, A. Ghosh, B. Kiran, Salinity driven stress to enhance lipid production in Scenedesmus vacuolatus: A biodiesel trigger?, Biomass and Bioenergy. 127 (2019) 105252. doi:https://doi.org/10.1016/j.biombioe.2019.05.021.

[292] H.K.B.T.-M. in E. Lichtenthaler, [34] Chlorophylls and carotenoids: Pigments of photosynthetic biomembranes, in: Plant Cell Membr., Academic Press, 1987: pp. 350–382. doi:https://doi.org/10.1016/0076-6879(87)48036-1.

[293] D.M. Kramer, G. Johnson, O. Kiirats, G.E. Edwards, New Fluorescence Parameters for the Determination of QA Redox State and Excitation Energy Fluxes, Photosynth. Res. 79 (2004) 209. doi:10.1023/B:PRES.0000015391.99477.0d.

[294] E.G. Bligh, W.J. Dyer, A rapid method of total lipid extraction and purification, Can. J. Biochem. Physiol. 37 (1959) 911–917.

[295] E. Neag, A.I. Török, O. Cadar, V.B.– Fuss, C. Roman, Enhancing lipid production of Synechocystis PCC 6803 for biofuels production, through environmental stress exposure, Renew. Energy. 143 (2019) 243–251. doi:https://doi.org/10.1016/j.renene.2019.05.005.

[296] M.C. Damiani, C.A. Popovich, D. Constenla, P.I. Leonardi, Lipid analysis in Haematococcuspluvialis to assess its potential use as a biodiesel feedstock, Bioresour. Technol. 101 (2010) 3801–3807.

[297] S. V Wychen, L.M.L. Laurens, Determination of total carbohydrates in algal biomass, Lab. Anal. Pro-Cedure Golden, CO, USA. (2013).

[298] M. Dubois, K.A. Gilles, J.K. Hamilton, P.A. t Rebers, F. Smith, Colorimetric method for determination of sugars and related substances, Anal. Chem. 28 (1956) 350–356.

[299] Y.-Y. He, D.-P. Häder, UV-B-induced formation of reactive oxygen species and oxidative damage of the cyanobacterium Anabaena sp.: protective effects of ascorbic acid and N-acetyl-L-cysteine, J. Photochem. Photobiol. B Biol. 66 (2002) 115–124.

[300] Y. Hu, F.-L. Meng, Y.-Y. Hu, N. Habibul, G.-P. Sheng, Concentration- and nutrient-dependent cellular responses of microalgae Chlorella pyrenoidosa to

perfluorooctanoic acid, Water Res. 185 (2020) 116248. doi:https://doi.org/10.1016/j.watres.2020.116248.

[301] M.M. Bradford, A rapid and sensitive method for the quantitation of microgram quantities of protein utilizing the principle of protein-dye binding, Anal. Biochem. 72 (1976) 248–254.

[302] H. Aebi, [13] Catalase in vitro, in: Oxyg. Radicals Biol. Syst., Academic Press, 1984: pp. 121–126. doi:https://doi.org/10.1016/S0076-6879(84)05016-3.

[303] Y. Nakano, K. Asada, Hydrogen Peroxide is Scavenged by Ascorbate-specific Peroxidase in Spinach Chloroplasts, Plant Cell Physiol. 22 (1981) 867–880. doi:10.1093/oxfordjournals.pcp.a076232.

[304] E.C. Francisco, D.B. Neves, E. Jacob-Lopes, T.T. Franco, Microalgae as feedstock for biodiesel production: carbon dioxide sequestration, lipid production and biofuel quality, J. Chem. Technol. Biotechnol. 85 (2010) 395–403.

[305] N. Chandra, P. Shukla, N. Mallick, Role of cultural variables in augmenting carbohydrate accumulation in the green microalga Scenedesmus acuminatus for bioethanol production, Biocatal. Agric. Biotechnol. 26 (2020) 101632. doi:https://doi.org/10.1016/j.bcab.2020.101632.

[306] A. Solovchenko, I. Khozin-Goldberg, I. Selyakh, L. Semenova, T. Ismagulova, A. Lukyanov, I. Mamedov, E. Vinogradova, O. Karpova, I. Konyukhov, S. Vasilieva, P. Mojzes, C. Dijkema, M. Vecherskaya, I. Zvyagin, L. Nedbal, O. Gorelova, Phosphorus starvation and luxury uptake in green microalgae revisited, Algal Res. 43 (2019) 101651. doi:https://doi.org/10.1016/j.algal.2019.101651.

[307] I. Šetlík, E. Berková, J. Doucha, Š. Kubín, J. Vendlová, V. Zachleder, The coupling of synthetic and reproduction processes in Scenedesmus quadricauda, Arch. Hydrobiol. Algol. Stud. 7 (1972) 172–217.

[308] A. Massalski, V.M. Laube, D.J. Kushner, Effects of cadmium and copper on the ultrastructure ofAnkistrodesmus braunii andAnabaena 7120, Microb. Ecol. 7 (1981) 183–193.

[309] C. Besagni, F. Kessler, A mechanism implicating plastoglobules in thylakoid disassembly during senescence and nitrogen starvation, Planta. 237 (2013) 463–470. doi:10.1007/s00425-012-1813-9.

[310] B. Huang, J. Marchand, S. Thiriet-Rupert, G. Carrier, B. Saint-Jean, E. Lukomska, B. Moreau, A. Morant-Manceau, G. Bougaran, V. Mimouni, Betaine lipid and neutral lipid production under nitrogen or phosphorus limitation in the marine microalga Tisochrysis lutea (Haptophyta), Algal Res. 40 (2019) 101506. doi:https://doi.org/10.1016/j.algal.2019.101506.

[311] N.M.D. Courchesne, A. Parisien, B. Wang, C.Q. Lan, Enhancement of lipid production using biochemical, genetic and transcription factor engineering approaches, J. Biotechnol. 141 (2009) 31–41.

[312] Y.-J. Liang, J.-G. Jiang, Characterization of malic enzyme and the regulation of its activity and metabolic engineering on lipid production, RSC Adv. 5 (2015) 45558–

45570. doi:10.1039/C5RA04635A.

[313] J. Fan, C. Yan, C. Andre, J. Shanklin, J. Schwender, C. Xu, Oil accumulation is controlled by carbon precursor supply for fatty acid synthesis in Chlamydomonas reinhardtii, Plant Cell Physiol. 53 (2012) 1380–1390.

[314] J.H. Janssen, J. Spoelder, J.J. Koehorst, P.J. Schaap, R.H. Wijffels, M.J. Barbosa, Time-dependent transcriptome profile of genes involved in triacylglycerol (TAG) and polyunsaturated fatty acid synthesis in Nannochloropsis gaditana during nitrogen starvation, J. Appl. Phycol. 32 (2020) 1153–1164. doi:10.1007/s10811-019-02021-2.

[315] H. Abida, L.-J. Dolch, C. Meï, V. Villanova, M. Conte, M.A. Block, G. Finazzi, O. Bastien, L. Tirichine, C. Bowler, Membrane glycerolipid remodeling triggered by nitrogen and phosphorus starvation in Phaeodactylum tricornutum, Plant Physiol. 167 (2015) 118–136.

[316] M.E. McBee, Y.H. Chionh, M.L. Sharaf, P. Ho, M.W.L. Cai, P.C. Dedon, Production of Superoxide in Bacteria Is Stress- and Cell State-Dependent: A Gating-Optimized Flow Cytometry Method that Minimizes ROS Measurement Artifacts with Fluorescent Dyes., Front. Microbiol. 8 (2017) 459. doi:10.3389/fmicb.2017.00459.

[317] O. Osundeko, H. Davies, J.K. Pittman, Oxidative stress-tolerant microalgae strains are highly efficient for biofuel feedstock production onwastewater, Biomass and Bioenergy. 56 (2013). doi:10.1016/j.biombioe.2013.05.027.

[318] K. Shi, Z. Gao, T.-Q. Shi, P. Song, L.-J. Ren, H. Huang, X.-J. Ji, Reactive oxygen species-mediated cellular stress response and lipid accumulation in oleaginous microorganisms: the state of the art and future perspectives, Front. Microbiol. 8 (2017) 793.

[319] N. Jacquier, V. Choudhary, M. Mari, A. Toulmay, F. Reggiori, R. Schneiter, Lipid droplets are functionally connected to the endoplasmic reticulum in Saccharomyces cerevisiae, J. Cell Sci. 124 (2011) 2424–2437.

[320] N. Suzuki, G. Miller, J. Morales, V. Shulaev, M.A. Torres, R. Mittler, Respiratory burst oxidases: the engines of ROS signaling, Curr. Opin. Plant Biol. 14 (2011) 691–699.

[321] S.A. Scott, M.P. Davey, J.S. Dennis, I. Horst, C.J. Howe, D.J. Lea-Smith, A.G. Smith, Biodiesel from algae: Challenges and prospects, Curr. Opin. Biotechnol. 21 (2010). doi:10.1016/j.copbio.2010.03.005.

[322] Y. Zhao, X. Song, P. Zhao, T. Li, J.-W. Xu, X. Yu, Role of melatonin in regulation of lipid accumulation, autophagy and salinity-induced oxidative stress in microalga Monoraphidium sp. QLY-1, Algal Res. 54 (2021) 102196. doi:https://doi.org/10.1016/j.algal.2021.102196.

[323] I. Couso, M.E. Pérez-Pérez, E. Martínez-Force, H.-S. Kim, Y. He, J.G. Umen, J.L. Crespo, Autophagic flux is required for the synthesis of triacylglycerols and ribosomal protein turnover in Chlamydomonas, J. Exp. Bot. 69 (2017) 1355–1367. doi:10.1093/jxb/erx372.

[324] K. Apel, H. Hirt, REACTIVE OXYGEN SPECIES: Metabolism, Oxidative Stress, and Signal Transduction, Annu. Rev. Plant Biol. 55 (2004) 373–399. doi:10.1146/annurev.arplant.55.031903.141701.

[325] T. Fernandes, I. Fernandes, C.A.P. Andrade, N. Cordeiro, Changes in fatty acid biosynthesis in marine microalgae as a response to medium nutrient availability, Algal Res. 18 (2016) 314–320.

[326] R. Chandra, M. V Rohit, Y. V Swamy, S. Venkata Mohan, Regulatory function of organic carbon supplementation on biodiesel production during growth and nutrient stress phases of mixotrophic microalgae cultivation, Bioresour. Technol. 165 (2014) 279–287. doi:https://doi.org/10.1016/j.biortech.2014.02.102.

[327] R. Pamplona, Membrane phospholipids, lipoxidative damage and molecular integrity: A causal role in aging and longevity, Biochim. Biophys. Acta - Bioenerg. 1777 (2008) 1249–1262. doi:https://doi.org/10.1016/j.bbabio.2008.07.003.

[328] W.S. Yang, K.J. Kim, M.M. Gaschler, M. Patel, M.S. Shchepinov, B.R. Stockwell, Peroxidation of polyunsaturated fatty acids by lipoxygenases drives ferroptosis, Proc. Natl. Acad. Sci. 113 (2016) E4966--E4975. doi:10.1073/pnas.1603244113.

[329] H. Matsui, K. Shiozaki, Y. Okumura, M. Ishikawa, V. Waqalevu, O. Hayasaka, A. Honda, T. Kotani, Effects of phosphorous deficiency of a microalga Nannochloropsis oculata on its fatty acid profiles and intracellular structure and the effectiveness in rotifer nutrition, Algal Res. 49 (2020) 101905. doi:https://doi.org/10.1016/j.algal.2020.101905.

[330] S. Dahiya, A.N. Kumar, J.S. Sravan, S. Chatterjee, O. Sarkar, S.V. Mohan, Food waste biorefinery: Sustainable strategy for circular bioeconomy, Bioresour. Technol. 248 (2018) 2–12. doi:https://doi.org/10.1016/j.biortech.2017.07.176.

[331] S. Mishra, M. Roy, K. Mohanty, Microalgal bioenergy production under zero-waste biorefinery approach: Recent advances and future perspectives, Bioresour. Technol. 292 (2019) 122008. doi:https://doi.org/10.1016/j.biortech.2019.122008.

[332] S.V. Mohan, S. Dahiya, K. Amulya, R. Katakojwala, T.K. Vanitha, Can circular bioeconomy be fueled by waste biorefineries — A closer look, Bioresour. Technol. Reports. 7 (2019) 100277. doi:https://doi.org/10.1016/j.biteb.2019.100277.

[333] H.J. Choi, Effect of eggshells for the harvesting of microalgae species, Biotechnol. Biotechnol. Equip. 29 (2015) 666–672. doi:10.1080/13102818.2015.1031177.

[334] U. Suparmaniam, M.K. Lam, Y. Uemura, S.H. Shuit, J.W. Lim, P.L. Show, K.T. Lee, Y. Matsumura, P.T.K. Le, Flocculation of Chlorella vulgaris by shell waste-derived bioflocculants for biodiesel production: Process optimization, characterization and kinetic studies, Sci. Total Environ. 702 (2020) 134995. doi:https://doi.org/10.1016/j.scitotenv.2019.134995.

[335] M. Gebremedhin, S. Mishra, K. Mohanty, Augmentation of native microalgae based biofuel production through statistical optimization of campus sewage wastewater as low-cost growth media, J. Environ. Chem. Eng. 6 (2018) 6623–6632. doi:https://doi.org/10.1016/j.jece.2018.08.061.

[336] R. Maurya, T. Ghosh, C. Paliwal, A. Shrivastav, K. Chokshi, I. Pancha, A. Ghosh, S. Mishra, Biosorption of Methylene Blue by De-Oiled Algal Biomass: Equilibrium, Kinetics and Artificial Neural Network Modelling, PLoS One. 9 (2014) e109545. https://doi.org/10.1371/journal.pone.0109545.

[337] F. Chen, C. Zhou, G. Li, F. Peng, Thermodynamics and kinetics of glyphosate adsorption on resin D301, Arab. J. Chem. 9 (2016) S1665–S1669. doi:https://doi.org/10.1016/j.arabjc.2012.04.014.

[338] L.D. Zhu, J. Takala, E. Hiltunen, Z.M. Wang, Recycling harvest water to cultivate Chlorella zofingiensis under nutrient limitation for biodiesel production, Bioresour. Technol. 144 (2013) 14–20. doi:https://doi.org/10.1016/j.biortech.2013.06.061.

[339] H.-J. Choi, Effect of optical panel distance in a photobioreactor for nutrient removal and cultivation of microalgae, World J. Microbiol. Biotechnol. 30 (2014) 2015–2023.

[340] F.H.M. Yunos, N.M. Nasir, H.H.W. Jusoh, H. Khatoon, S.S. Lam, A. Jusoh, Harvesting of microalgae (Chlorella sp.) from aquaculture bioflocs using an environmental-friendly chitosan-based bio-coagulant, Int. Biodeterior. Biodegradation. 124 (2017) 243–249. doi:https://doi.org/10.1016/j.ibiod.2017.07.016.

[341] J.V. Flores-Cano, R. Leyva-Ramos, J. Mendoza-Barron, R.M. Guerrero-Coronado, A. Aragón-Piña, G.J. Labrada-Delgado, Sorption mechanism of Cd(II) from water solution onto chicken eggshell, Appl. Surf. Sci. 276 (2013) 682–690. doi:https://doi.org/10.1016/j.apsusc.2013.03.153.

[342] Y. Elakneswaran, T. Nawa, K. Kurumisawa, Zeta potential study of paste blends with slag, Cem. Concr. Compos. 31 (2009) 72–76. doi:https://doi.org/10.1016/j.cemconcomp.2008.09.007.

[343] S.K. Bozbaş, Y. Boz, Low-cost biosorbent: Anadara inaequivalvis shells for removal of Pb(II) and Cu(II) from aqueous solution, Process Saf. Environ. Prot. 103 (2016) 144–152. doi:https://doi.org/10.1016/j.psep.2016.07.007.

[344] M. Ali Zulfikar, E.D. Mariske, S.D. Djajanti, Adsorption of lignosulfonate compounds using powdered eggshell., Songklanakarin J. Sci. Technol. 34 (2012).

[345] R.A. Joudah, Effect of temperature on floc formation process efficiency and subsequent removal in sedimentation process, J. Eng. Sustain. Dev. 18 (2014) 176–187.

[346] K. Rodríguez, M. Araujo, Temperature and pressure effects on zeta potential values of reservoir minerals, J. Colloid Interface Sci. 300 (2006) 788–794.

[347] L. Xin, H. Hong-Ying, Z. Yu-Ping, Growth and lipid accumulation properties of a freshwater microalga Scenedesmus sp. under different cultivation temperature, Bioresour. Technol. 102 (2011) 3098–3102.

[348] W.T. Tsai, J.M. Yang, C.W. Lai, Y.H. Cheng, C.C. Lin, C.W. Yeh, Characterization and adsorption properties of eggshells and eggshell membrane,

Bioresour. Technol. 97 (2006) 488–493. doi:https://doi.org/10.1016/j.biortech.2005.02.050.

[349] H.-J. Choi, Application of methyl-esterified sericite for harvesting microalgae species, J. Environ. Chem. Eng. 4 (2016) 3593–3600. doi:https://doi.org/10.1016/j.jece.2016.08.005.

[350] H.N. Tran, S.-J. You, H.-P. Chao, Thermodynamic parameters of cadmium adsorption onto orange peel calculated from various methods: a comparison study, J. Environ. Chem. Eng. 4 (2016) 2671–2682.

[351] J.-V. Pérez-Pazos, P. Fernández-Izquierdo, Synthesis of neutral lipids in Chlorella sp. under different light and carbonate conditions, CT&F-Ciencia, Tecnol. y Futur. 4 (2011) 47–58.

[352] C. Wan, M.A. Alam, X.Q. Zhao, X.Y. Zhang, S.L. Guo, S.H. Ho, J.S. Chang, F.W. Bai, Current progress and future prospect of microalgal biomass harvest using various flocculation technologies, Bioresour. Technol. 184 (2015) 251–257. doi:10.1016/j.biortech.2014.11.081.

[353] F. Hadj-Romdhane, X. Zheng, P. Jaouen, J. Pruvost, D. Grizeau, J.P. Croué, P. Bourseau, The culture of Chlorella vulgaris in a recycled supernatant: Effects on biomass production and medium quality, Bioresour. Technol. 132 (2013) 285–292. doi:https://doi.org/10.1016/j.biortech.2013.01.025.

[354] S.K. Gupta, N.M. Kumar, A. Guldhe, F.A. Ansari, I. Rawat, M. Nasr, F. Bux, Wastewater to biofuels: Comprehensive evaluation ofvarious flocculants on biochemical composition and yield of microalgae, Ecol. Eng. 117 (2018) 62–68. doi:https://doi.org/10.1016/j.ecoleng.2018.04.005.

[355] Y. Liu, W. Jin, X. Zhou, S.-F. Han, R. Tu, X. Feng, P.D. Jensen, Q. Wang, Efficient harvesting of Chlorella pyrenoidosa and Scenedesmus obliquus cultivated in urban sewage by magnetic flocculation using nano-Fe3O4 coated with polyethyleneimine, Bioresour. Technol. 290 (2019) 121771. doi:https://doi.org/10.1016/j.biortech.2019.121771.

[356] A. Pugazhendhi, S. Shobana, P. Bakonyi, N. Nemestóthy, A. Xia, R.B. J, G. Kumar, A review on chemical mechanism of microalgae flocculation via polymers, Biotechnol. Reports. 21 (2019) e00302. doi:https://doi.org/10.1016/j.btre.2018.e00302.

[357] X. Zou, Y. Li, K. Xu, H. Wen, Z. Shen, X. Ren, Microalgae harvesting by buoy-bead flotation process using Bioflocculant as alternative to chemical Flocculant, Algal Res. 32 (2018) 233–240. doi:https://doi.org/10.1016/j.algal.2018.04.010.

[358] L. Van Haver, S. Nayar, Polyelectrolyte flocculants in harvesting microalgal biomass for food and feed applications, Algal Res. 24 (2017) 167–180. doi:https://doi.org/10.1016/j.algal.2017.03.022.

[359] P. Sivasankar, S. Poongodi, A.O. Lobo, A. Pugazhendhi, Characterization of a novel polymeric bioflocculant from marine actinobacterium Streptomyces sp. and its application in recovery of microalgae, Int. Biodeterior. Biodegradation. 148 (2020) 104883. doi:https://doi.org/10.1016/j.ibiod.2020.104883.

[360] H. Guo, C. Hong, C. Zhang, B. Zheng, D. Jiang, W. Qin, Bioflocculants' production from a cellulase-free xylanase-producing Pseudomonas boreopolis G22 by degrading biomass and its application in cost-effective harvest of microalgae, Bioresour. Technol. 255 (2018) 171–179. doi:https://doi.org/10.1016/j.biortech.2018.01.082.

[361] H. Faridi, A. Arabhosseini, Application of eggshell wastes as valuable and utilizable products: A review, Res. Agric. Eng. 64 (2018) 104–114. doi:10.17221/6/2017-RAE.

[362] R. Maurya, K. Chokshi, T. Ghosh, K. Trivedi, I. Pancha, D. Kubavat, S. Mishra, A. Ghosh, Lipid extracted microalgal biomass residue as a fertilizer substitute for Zea mays L., Front. Plant Sci. 6 (2016) 1266.

[363] M. Nayak, D.K. Swain, R. Sen, Strategic valorization of de-oiled microalgal biomass waste as biofertilizer for sustainable and improved agriculture of rice (Oryza sativa L.) crop, Sci. Total Environ. 682 (2019) 475–484. doi:https://doi.org/10.1016/j.scitotenv.2019.05.123.

[364] R. Maurya, C. Paliwal, K. Chokshi, I. Pancha, T. Ghosh, G.G. Satpati, R. Pal, A. Ghosh, S. Mishra, Hydrolysate of lipid extracted microalgal biomass residue: An algal growth promoter and enhancer, Bioresour. Technol. 207 (2016) 197–204. doi:https://doi.org/10.1016/j.biortech.2016.02.018.

[365] F.D. AOCS, Official methods and recommended practices of the American Oil Chemists' Society, AOCS. 5 (1998) 2–93.

[366] X. Xiong, I.K.M. Yu, L. Cao, D.C.W. Tsang, S. Zhang, Y.S. Ok, A review of biochar-based catalysts for chemical synthesis, biofuel production, and pollution control, Bioresour. Technol. 246 (2017) 254–270. doi:https://doi.org/10.1016/j.biortech.2017.06.163.

[367] M.J. Jiménez Toro, X. Dou, I. Ajewole, J. Wang, K. Chong, N. Ai, G. Zeng, T. Chen, Preparation and Optimization of Macroalgae-Derived Solid Acid Catalysts, Waste and Biomass Valorization. 10 (2019) 805–816. doi:10.1007/s12649-017-0101-0.

[368] Z.-E. Tang, S. Lim, Y.-L. Pang, S.-H. Shuit, H.-C. Ong, Utilisation of biomass wastes based activated carbon supported heterogeneous acid catalyst for biodiesel production, Renew. Energy. 158 (2020) 91–102. doi:https://doi.org/10.1016/j.renene.2020.05.119.

[369] E. Kardash, Y.I. Tur'yan, Acid value determination in vegetable oils by indirect titration in aqueous-alcohol media, Croat. Chem. Acta. 78 (2005) 99–103.

[370] X. Fu, D. Li, J. Chen, Y. Zhang, W. Huang, Y. Zhu, J. Yang, C. Zhang, A microalgae residue based carbon solid acid catalyst for biodiesel production, Bioresour. Technol. 146 (2013) 767–770. doi:https://doi.org/10.1016/j.biortech.2013.07.117.

[371] L.J. Konwar, R. Das, A.J. Thakur, E. Salminen, P. Mäki-Arvela, N. Kumar, J.-P. Mikkola, D. Deka, Biodiesel production from acid oils using sulfonated carbon catalyst derived from oil-cake waste, J. Mol. Catal. A Chem. 388–389 (2014) 167–

176. doi:https://doi.org/10.1016/j.molcata.2013.09.031.

[372] F.A. Dawodu, O. Ayodele, J. Xin, S. Zhang, D. Yan, Effective conversion of non-edible oil with high free fatty acid into biodiesel by sulphonated carbon catalyst, Appl. Energy. 114 (2014) 819–826. doi:https://doi.org/10.1016/j.apenergy.2013.10.004.

[373] P. Valle-Vigón, M. Sevilla, A.B. Fuertes, Sulfonated mesoporous silica–carbon composites and their use as solid acid catalysts, Appl. Surf. Sci. 261 (2012) 574–583. doi:https://doi.org/10.1016/j.apsusc.2012.08.059.

[374] B. Rao, K.C. Mouli, N. Rambabu, A.K. Dalai, R.B.N. Prasad, Carbon-based solid acid catalyst from de-oiled canola meal for biodiesel production, Catal. Commun. 14 (2011) 20–26.

[375] M. Ayadi, S. Awad, A. Villot, M. Abderrabba, M. Tazerout, Heterogeneous acid catalyst preparation from olive pomace and its use for olive pomace oil esterification, Renew. Energy. 165 (2021) 1–13. doi:https://doi.org/10.1016/j.renene.2020.11.031.

[376] R.R.C. Bastos, A.P. da Luz Corrêa, P.T.S. da Luz, G.N. da Rocha Filho, J.R. Zamian, L.R.V. da Conceição, Optimization of biodiesel production using sulfonated carbon-based catalyst from an amazon agro-industrial waste, Energy Convers. Manag. 205 (2020) 112457. doi:https://doi.org/10.1016/j.enconman.2019.112457.

[377] H.-H. Bui, K.-Q. Tran, W.-H. Chen, Pyrolysis of microalgae residues – A kinetic study, Bioresour. Technol. 199 (2016) 362–366. doi:https://doi.org/10.1016/j.biortech.2015.08.069.

[378] S.-S. Kim, H.V. Ly, J. Kim, E.Y. Lee, H.C. Woo, Pyrolysis of microalgae residual biomass derived from Dunaliella tertiolecta after lipid extraction and carbohydrate saccharification, Chem. Eng. J. 263 (2015) 194–199. doi:https://doi.org/10.1016/j.cej.2014.11.045.

[379] L. Sanchez-Silva, D. López-González, J. Villaseñor, P. Sánchez, J.L. Valverde, Thermogravimetric–mass spectrometric analysis of lignocellulosic and marine biomass pyrolysis, Bioresour. Technol. 109 (2012) 163–172. doi:https://doi.org/10.1016/j.biortech.2012.01.001.

[380] D. Liu, P. Yuan, H. Liu, J. Cai, D. Tan, H. He, J. Zhu, T. Chen, Quantitative characterization of the solid acidity of montmorillonite using combined FTIR and TPD based on the NH3 adsorption system, Appl. Clay Sci. 80–81 (2013) 407–412. doi:https://doi.org/10.1016/j.clay.2013.07.006.

[381] S.H. Dhawane, T. Kumar, G. Halder, Recent advancement and prospective of heterogeneous carbonaceous catalysts in chemical and enzymatic transformation of biodiesel, Energy Convers. Manag. 167 (2018) 176–202. doi:https://doi.org/10.1016/j.enconman.2018.04.073.

[382] Q. Shu, J. Gao, Z. Nawaz, Y. Liao, D. Wang, J. Wang, Synthesis of biodiesel from waste vegetable oil with large amounts of free fatty acids using a carbon-based solid acid catalyst, Appl. Energy. 87 (2010) 2589–2596.

[383] S. Jain, M.P. Sharma, S. Rajvanshi, Acid base catalyzed transesterification kinetics of waste cooking oil, Fuel Process. Technol. 92 (2011) 32–38. doi:https://doi.org/10.1016/j.fuproc.2010.08.017.

[384] G. Chen, B. Fang, Preparation of solid acid catalyst from glucose–starch mixture for biodiesel production, Bioresour. Technol. 102 (2011) 2635–2640. doi:https://doi.org/10.1016/j.biortech.2010.10.099.

[385] M. Hara, Biodiesel production by amorphous carbon bearing SO 3 H, COOH and phenolic OH groups, a solid Brønsted acid catalyst, Top. Catal. 53 (2010) 805–810.

[386] Y. Xiang, L. Wang, Y. Jiao, Ultrasound strengthened biodiesel production from waste cooking oil using modified coal fly ash as catalyst, J. Environ. Chem. Eng. 4 (2016) 818–824. doi:https://doi.org/10.1016/j.jece.2015.12.031.

[387] D. Kumar, T. Das, B.S. Giri, B. Verma, Optimization of biodiesel synthesis from nonedible oil using immobilized bio-support catalysts in jacketed packed bed bioreactor by response surface methodology, J. Clean. Prod. 244 (2020) 118700. doi:https://doi.org/10.1016/j.jclepro.2019.118700.

[388] S. Saravanan Arumugamurthy, P. Sivanandi, S. Pandian, H. Choksi, D. Subramanian, Conversion of a low value industrial waste into biodiesel using a catalyst derived from brewery waste: An activation and deactivation kinetic study, Waste Manag. 100 (2019) 318–326. doi:https://doi.org/10.1016/j.wasman.2019.09.030.

[389] E.M. Vargas, M.C. Neves, L.A.C. Tarelho, M.I. Nunes, Solid catalysts obtained from wastes for FAME production using mixtures of refined palm oil and waste cooking oils, Renew. Energy. 136 (2019) 873–883. doi:https://doi.org/10.1016/j.renene.2019.01.048.

[390] N. Ngadi, N.F. Hamdan, O. Hassan, R.P. Jaya, Production of biodiesel from palm oil using egg shell waste as heterogeneous catalyst, J. Teknol. 78 (2016).

[391] G.P. Maniam, N. Hindryawati, I. Nurfitri, R. Jose, M.H. Ab. Rahim, F.A. Dahalan, M. M. Yusoff, Decanter cake as a feedstock for biodiesel production: A first report, Energy Convers. Manag. 76 (2013) 527–532. doi:https://doi.org/10.1016/j.enconman.2013.07.077.

[392] G. Pathak, D. Das, K. Rajkumari, L. Rokhum, Exploiting waste: towards a sustainable production of biodiesel using Musa acuminata peel ash as a heterogeneous catalyst, Green Chem. 20 (2018) 2365–2373.

[393] C. Ofori-Boateng, K.T. Lee, The potential of using cocoa pod husks as green solid base catalysts for the transesterification of soybean oil into biodiesel: Effects of biodiesel on engine performance, Chem. Eng. J. 220 (2013) 395–401.

List of Publications

Journal:

1. **Roy, M.,** Bera, S., Mohanty, K., 2021. Nutrient starvation-induced oxidative stress-mediated lipid accumulation in *Tetradesmus obliquus* KMC24. J. Appl. Phycol. https://doi.org/10.1007/s10811-021-02614-w
2. **Roy, M.,** Mohanty, K., 2021. Valorization of de-oiled microalgal biomass as a carbon-based heterogeneous catalyst for a sustainable biodiesel production. Bioresour. Technol. 337, 125424. https://doi.org/https://doi.org/10.1016/j.biortech.2021.125424
3. **Roy, M.,** Mohanty, K., 2020. Valorization of waste eggshell-derived bioflocculant for harvesting T. obliquus: Process optimization, kinetic studies and recyclability of the spent medium for circular bioeconomy. Bioresour. Technol. 307, 123205. https://doi.org/https://doi.org/10.1016/j.biortech.2020.123205
4. **Roy, M.,** Mohanty, K., 2019. A comprehensive review on microalgal harvesting strategies: Current status and future prospects. Algal Res. 44, 101683. https://doi.org/https://doi.org/10.1016/j.algal.2019.101683
5. Mishra, S., **Roy, M*.,** Mohanty, K., 2019. Microalgal bioenergy production under zero-waste biorefinery approach: Recent advances and future perspectives. Bioresour. Technol. 292, 122008. https://doi.org/https://doi.org/10.1016/j.biortech.2019.122008. ***equal first author contribution.**

Book Chapter:

1. Byproducts of microalgal biorefinery as a resource for circular bioeconomy (Communicated).

Conference Presentations

1. **M. Roy,** K. Mohanty, A review on comparison of microalgal biomass harvesting strategies, Research Conclave, IIT Guwahati, India, 16-19 March,

2017.

2. **M. Roy,** K. Mohanty, Phosphorus starvation-induced cellular crosstalk of ROS-scavenging antioxidants and enhanced biofuel potential of green microalga *Tetradesmus obliquus* KMC24, Indo-Japan Bilateral Symposium on Future Perspective of Bioresource Utilization in North-East India, IIT Guwahati, India, 1-4 February, 2018.
3. **M. Roy,** K. Mohanty, Nitrogen starvation induced oxidative stress as a mediator for enhanced lipid production by a novel oleaginous microalga *Tetradesmus obliquus* KMC24, International Conference on Biotechnological Research and Innovation for Sustainable Development (BioSD), CSIR-Indian Institute of Chemical Technology, Hyderabad, India, 22-25 November, 2018.
4. **M. Roy,** K. Mohanty, Bio-flocculant facilitated microalgal harvesting, Research Conclave, IIT Guwahati, India, 14-17 March, 2019.
5. **M. Roy,** K. Mohanty, Eggshell facilitated bioflocculation of *Tetradesmus obliquus* KMC24, International Conference on New Horizons in Biotechnology, Thiruvananthapuram, Kerala, India, 20-24 November, 2019.
6. **M. Roy,** K. Mohanty, A solid waste-based heterogeneous catalyst for a sustainable biodiesel production, International Conference on Advances in Chemical, Biological and Environmental Engineering, Malaviya National Institute of Technology, Jaipur, India, 23-24 April, 2021.

Journal of Applied Phycology (2021) 33:3617–3635
https://doi.org/10.1007/s10811-021-02614-w

Nutrient starvation-induced oxidative stress-mediated lipid accumulation in *Tetradesmus obliquus* KMC24

Madonna Roy[1] · Sounak Bera[1] · Kaustubha Mohanty[1,2]

Received: 10 May 2021 / Revised: 22 September 2021 / Accepted: 22 September 2021 / Published online: 9 October 2021

Abstract
A two-stage cultivation approach was employed to investigate the effect of nitrogen and/or phosphorus starvation on the morphology, biomass yield, photosynthetic activity, biochemical, and fatty acid composition of *Tetradesmus obliquus* KMC24. A two-day nitrogen-starved cells (-N2) were able to accumulate the maximum amount of lipid (39.93 ± 0.44%) without affecting the biomass yield (2.15 ± 0.04 g L^{-1}). During nitrogen (-N) and phosphorus (-P) starvation, photosynthetically fixed carbon pool was diverted to lipid biosynthesis. Pearson's correlation analysis suggested that stress-induced lipid accumulation is associated with an increased intracellular reactive oxygen species (ROS) level. The ROS fluorescence intensity was highest in -N2 cultures (17,051.49 ± 93.15 a.u.), suggesting highly oxidative stress-tolerant cells. A high degree of fatty acid saturation was obtained under nitrogen starvation as compared to other culture conditions. Biodiesel properties such as cetane number, saponification number, and iodine value improved under nitrogen starvation.

Keywords Tetradesmus obliquus · Nutrient stress · Lipid yield · Reactive oxygen species · Biodiesel

Introduction

Oleaginous microalgae are deemed as cell biofactories for biodiesel production. However, the lower biomass and lipid productivity, along with the high cost of downstream processing such as harvesting and biodiesel production, makes microalgae-based biodiesel economically unviable (Pancha et al. 2014). Thus, to make biodiesel commercially feasible, various strategies such as selection of potential microalgal strain, modification of cultivation mode, optimization of culture conditions, low-cost harvesting, and lipid extraction techniques need to be employed. Various studies have reported that microalgae have the potential to produce a considerable amount of triacylglycerol (TAG) when their cells are under stress. Stress is defined as a deviation from normal growth conditions as long as homeostasis permits (Borowitzka 2018). Stress can be physical stimuli such as variations in temperature, light intensity, photoperiod, or chemical stimuli such as nutrient (nitrogen and phosphorous) starvation, salinity, and pH of the medium (Hu et al. 2008). These physical and chemical stimuli, be it adverse or favorable, influences the biochemical composition of microalgae severely.

Nitrogen (N) and phosphorus (P) are the primary sources of microalgal nutrients influencing carbon flux and cellular energy reorientation (Adams et al. 2013; Chandra et al. 2020). Nitrogen is a major component of essential biological molecules such as nucleic acids, proteins, and chlorophylls, which influences cell division and growth, whereas phosphorus is a major component of nucleic acids and phospholipids. Moreover, modulation of nutrient levels has been reported to influence lipid accumulation and composition (Zhang et al. 2019). On the other hand, nitrogen boosts neutral lipid accumulation, whereas phosphorus limitation stimulates intra- and interspecific variability in metabolic responses. During nutrient limitation, surplus energy and carbon pool accumulated due to the inhibition of amino acids synthesis are diverted to lipid synthesis. However, this condition results in low biomass productivity and poor enzyme activity as the protein synthesis is impaired (Adams et al. 2013). To deal with these problems, a two-stage cultivation approach is widely employed. In the first stage of cultivation, a nutrient-rich medium is used to grow microalgal cells to obtain a high

✉ Kaustubha Mohanty
kmohanty@iitg.ac.in

[1] School of Energy Science and Engineering, Indian Institute of Technology Guwahati, Guwahati 781039, India

[2] Department of Chemical Engineering, Indian Institute of Technology Guwahati, Guwahati 781039, India

Bioresource Technology 307 (2020) 123205

Contents lists available at ScienceDirect

Bioresource Technology

journal homepage: www.elsevier.com/locate/biortech

Valorization of waste eggshell-derived bioflocculant for harvesting *T. obliquus*: Process optimization, kinetic studies and recyclability of the spent medium for circular bioeconomy

Madonna Roy[a], Kaustubha Mohanty[a,b,*]

[a] Centre for Energy, Indian Institute of Technology Guwahati, Guwahati 781039, India
[b] Department of Chemical Engineering, Indian Institute of Technology Guwahati, Guwahati 781039, India

GRAPHICAL ABSTRACT

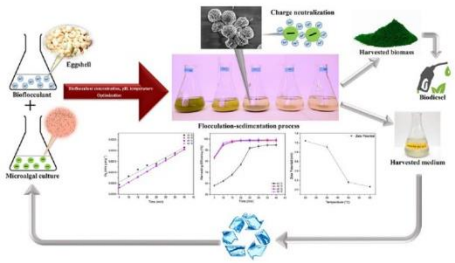

ARTICLE INFO

Keywords:
Microalgae
Bioflocculant
Valorization
Zeta potential
Adsorption kinetics

ABSTRACT

Waste eggshell-derived bioflocculant was used for harvesting *T. obliquus* in a circular bioeconomy approach. It was found that 120 mg L^{-1} bioflocculant can flocculate 98.62 ± 0.43% of *T. obliquus* cells within 25 min at optimal pH 4.0 and temperature 35 °C. The influence of bioflocculant concentration, pH and temperature on zeta potential was evaluated to understand the flocculation mechanism. Microscopic and FESEM-EDX images were analyzed to evaluate the microalgal structural changes. Adsorption mechanism of bioflocculant over the microalgal cells was determined by performing adsorption kinetic studies. Pseudo-second order kinetic model was a suitable fit for the data obtained from the experiments, which indicated chemisorption as the probable mechanism. The spent medium recovered after harvesting process was successfully recycled for subsequent cultivation of *T. obliquus*, thus reducing the dependency on fresh medium. The FAME composition of the biomass treated with bioflocculant was not altered.

1. Introduction

An upsurge in global energy demand is directly reflected in the ever increasing cost of fuels (Garcia-Moscoso et al., 2013). Moreover, this energy demand must be satiated for technological developments. The reliance on non-renewable energy resources which are mainly composed of fossil based fuels is not favorable as it produces a limited amount of energy and leads to emission of greenhouse gases

* Corresponding author at: Department of Chemical Engineering, Indian Institute of Technology Guwahati, Guwahati 781039, India.
E-mail address: kmohanty@iitg.ac.in (K. Mohanty).

https://doi.org/10.1016/j.biortech.2020.123205
Received 30 January 2020; Received in revised form 12 March 2020; Accepted 14 March 2020
Available online 23 March 2020
0960-8524/

Bioresource Technology 337 (2021) 125424

Contents lists available at ScienceDirect

Bioresource Technology

journal homepage: www.elsevier.com/locate/biortech

Valorization of de-oiled microalgal biomass as a carbon-based heterogeneous catalyst for a sustainable biodiesel production

Madonna Roy [a], Kaustubha Mohanty [a,b,*]

[a] School of Energy Science and Engineering, Indian Institute of Technology Guwahati, Guwahati 781039, India
[b] Department of Chemical Engineering, Indian Institute of Technology Guwahati, Guwahati 781039, India

HIGHLIGHTS

- Valorization of de-oiled microalgal biomass as heterogeneous acid catalyst.
- Hydrophobic carbon acts as potential support for sulfonated carbon catalysts.
- The catalyst exhibited high catalytic activity and stability.
- High FAME yield was obtained with improved fatty acid composition.
- FAME yield >90% was obtained after four successive reuse cycles.

GRAPHICAL ABSTRACT

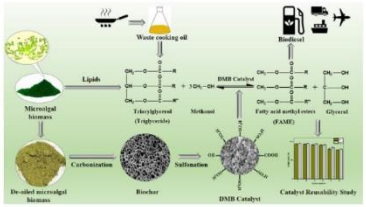

ARTICLE INFO

Keywords:
De-oiled microalgal biomass
Biodiesel
Valorization
Carbon-based solid acid catalyst
Transesterification

ABSTRACT

In this study, a novel carbon-based solid acid catalyst was synthesized by carbonization of de-oiled microalgal biomass followed by sulfonation. The effect of catalyst synthesis conditions such as carbonization temperature, sulfonation time, and H_2SO_4 concentration on the surface acidity of the catalyst and free fatty acid conversion was determined. The de-oiled microalgal biomass-based solid acid (DMB) catalyst was predominantly composed of carboxylic, phenolic, and sulfonic groups as indicated by the FTIR analysis and supported by the XPS analysis. The catalyst was further characterized by various methods to determine its physiochemical properties. A maximum fatty acid methyl ester (FAME) yield of 94.23% for microalgal oil (AO) and 96.25% for waste cooking oil (WCO) was obtained under optimized transesterification conditions. The catalyst exhibited high catalytic activity (FAME yield >90%) until the fourth cycle. Most of the biodiesel properties were within the permissible limit of EN 14,212 and ASTM D6751 standards.

1. Introduction

Currently, the global energy demand is satiated by non-renewable fossil fuels. The sole dependency on fossil resources is not sustainable due to its adverse environmental impacts. Biodiesel, which is composed of FAME, has the potential to substitute conventional non-renewable energy sources, as it is renewable, eco-friendly, and has low greenhouse gas (GHG) emission profiles (Deeba et al., 2020). However, the exorbitant costs for producing biodiesel in comparison to conventional fuels is a bottleneck in its commercialization. Therefore, researchers are trying to convert low-cost feedstock into biodiesel in an economical and environmentally benign approach.

Biodiesel is manufactured from oil bearing seeds (*Pongamia pinnata, Pongamia glabra Azadirachta indica, Jatropha curcas, Madhuca longifolia,*

* Corresponding author.
E-mail address: kmohanty@iitg.ac.in (K. Mohanty).

https://doi.org/10.1016/j.biortech.2021.125424
Received 30 April 2021; Received in revised form 11 June 2021; Accepted 12 June 2021
Available online 16 June 2021

Algal Research 44 (2019) 101683

Contents lists available at ScienceDirect

Algal Research

journal homepage: www.elsevier.com/locate/algal

Review article

A comprehensive review on microalgal harvesting strategies: Current status and future prospects

Madonna Roy[a], Kaustubha Mohanty[a,b,*]

[a] Centre for Energy, Indian Institute of Technology Guwahati, Guwahati 781 039, India
[b] Department of Chemical Engineering, Indian Institute of Technology Guwahati, Guwahati 781039, India

ARTICLE INFO

Keywords:
Microalgae
Harvesting
Review
Economic viability
Life cycle assessment
Technoeconomic analysis

ABSTRACT

Microalgae are considered as a potential and sustainable feedstock for the production of biofuels, fine chemicals, nutraceuticals, and cosmetics. This is accredited to their high lipid and carbohydrate content, fast growth and rapid CO_2 sequestration ability. However, large volumes of feedstock are required to extract and process biochemicals from microalgal biomass due to the small biomass to liquid ratio. This produces substantial challenges in attaining a sustainable energy balance in microalgae-based products process operations. Additionally, the small size of microalgal cells along with their negatively charged cell surface and cell density similar to the growth medium produces challenges in microalgae harvesting. The high cost associated with microalgae harvesting is a major bottleneck for commercialization of algae-based industrial products. Hence, microalgae harvesting is recognized as an area that needs to be explored and developed. This article aims to collate and present an overview of current harvesting strategies such as physical, chemical, biological, electrical and magnetic methods along with their future prospects. This review also highlights the evolution of microalgal harvesting and elucidates the fundamental phenomena of each technology in relation to key physical parameters such as morphology, size, density and surface charge. Besides throwing widespread light on various harvesting methods, this review article has also presented their advantages and disadvantages. Life cycle assessment (LCA) and technoeconomic analysis (TEA) was reviewed to assess the feasibility of various harvesting system for commercial application based on the environmental and technoeconomic impacts. Hence, the vital proposals provided in this review article would undeniably pave the way for choosing the appropriate harvesting strategy.

1. Introduction

The rapid growth of population and advancement in technology may lead to a rise in global energy consumption from 550 EJ in 2020 to 865 EJ by 2040 [1]. The need for energy must be satiated to maintain pace with technological development. Primary energy sources include both renewable as well as non-renewable sources. Fossil fuel, which is a non-renewable energy resource, is widely used to meet the global energy demand. But, fossil fuel provides a finite amount of energy, and a significant amount of impact is imposed on the environment during its exploration and use [2]. A major portion of the world's energy is produced and consumed by India. India, by producing 2.49% of the world's total annual energy ranks seventh in terms of energy production [3].

Research on microalgae as a feedstock for various products such as biofuels, chemicals, pharmaceutical, aquaculture feed, and cosmetics continues to increase because of the inherent advantages it holds over other traditional feedstock. From bioenergy perspective, microalgae possess the potential to generate a considerable amount of oil per acre as compared to other biofuel feedstock. Moreover, the land that is not suitable for crop cultivation can be used for growing microalgae [4]. Microalgae are unicellular photosynthetic microorganisms that grow very fast and has a thirst for carbon dioxide. The three key elements required for microalgal growth are light source (obtained from sun), nutrients (mainly nitrogen, phosphorus and trace metals) [5] and a carbon source (derived from CO_2). These are then stored in the cell tissues as carbohydrates, lipids, proteins and silica nanomaterials (in the case of diatom species) [6]. Microalgae biomass being rich in biochemical composition favours the production of a broad spectrum of marketable value-added products. The presence of triglycerides in microalgal lipids favours biodiesel production. A range of different industries can also use microalgal proteins and carbohydrates [7]. Products having high market value, such as β-carotene [8], PUFA such as eicosapentaenoic acid and docosahexaenoic acid [9], and astaxanthin [10] can be obtained in low volumes from microalgae. Besides having

* Corresponding author at: Centre for Energy, Indian Institute of Technology Guwahati, Guwahati 781 039, India
E-mail address: kmohanty@iitg.ac.in (K. Mohanty).

https://doi.org/10.1016/j.algal.2019.101683
Received 2 July 2019; Received in revised form 24 September 2019; Accepted 24 September 2019
Available online 29 October 2019

Bioresource Technology 292 (2019) 122008

Contents lists available at ScienceDirect

Bioresource Technology

journal homepage: www.elsevier.com/locate/biortech

Review

Microalgal bioenergy production under zero-waste biorefinery approach: Recent advances and future perspectives

Sanjeev Mishra[a,1], Madonna Roy[a,1], Kaustubha Mohanty[a,b,*]

[a] Centre for Energy, Indian Institute of Technology Guwahati, Guwahati 781039, India
[b] Department of Chemical Engineering, Indian Institute of Technology Guwahati, Guwahati 781039, India

GRAPHICAL ABSTRACT

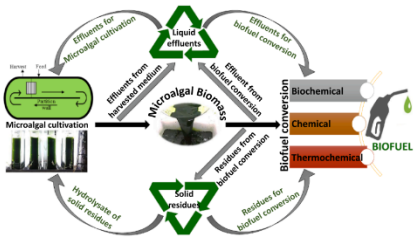

ARTICLE INFO

Keywords:
Microalgal biorefinery
Zero-waste
Circular economy
TEA
LCA

ABSTRACT

In view of the globalization and energy consumption, an economic and sustainable biorefinery model is essential to address the energy security and climate change. From this perspective, renewable biofuel production from microalgae along with a wide range of value-added co-products define its potential as a biorefinery feedstock. However, economic viability of microalgal biorefinery at its current state is not considered sustainable. Reduce, recycle, and reuse of waste derived from algal bioenergy conversion process will lead to an energy efficient and sustainable zero-waste microalgal biorefinery. This review focuses on three major aspects of zero-waste microalgal biorefinery approach; (1) recent advances on microalgal bioenergy conversion processes (chemical, biochemical and thermochemical); (2) mitigation and transformation of liquid and solid waste and (3) techno-economic analysis (TEA) and lifecycle assessment (LCA). In addition, the study also focuses on the challenges and future perspectives for an advanced microalgal biorefinery model.

1. Introduction

An ever-escalating global energy demand and global warming due to the burning of fossil fuels encourages the necessity for exploring and implementing alternate clean, green, and sustainable energy resources. Among several other renewable energy alternatives, bioenergy production from microalgae has acquired wide recognition over the last few years (Wijffels and Barbosa, 2010). However, commercialization of the process is a challenge considering current capital costs per unit of fuel production (Chandra et al., 2019). Given the background, high-value microalgal co-products should be explored for a sustainable biorefinery approach.

* Corresponding author at: Centre for Energy, Indian Institute of Technology Guwahati, Guwahati 781039, India.
E-mail address: kmohanty@iitg.ac.in (K. Mohanty).
[1] These authors contributed equally and should be regarded as co-first author.

https://doi.org/10.1016/j.biortech.2019.122008
Received 15 June 2019; Received in revised form 9 August 2019; Accepted 12 August 2019
Available online 16 August 2019
0960-8524/